AWARD NUMBER: W81XWH-17-1-0354

TITLE: **Cutaneous Human Papillomaviruses as Cofactors in Nonmelanoma Skin Cancer**

PRINCIPAL INVESTIGATOR: Nicholas A Wallace

CONTRACTING ORGANIZATION: Kansas State University, Manhattan, KS

REPORT DATE: **November 2021**

TYPE OF REPORT: **Final**

PREPARED FOR: U.S. Army Medical Research and Materiel Command
Fort Detrick, Maryland 21702-5012

REPORT DOCUMENTATION PAGE

Form Approved
OMB No. 0704-0188

1. REPORT DATE	2. REPORT TYPE	3. DATES COVERED
November 2021	Final	01Aug2017-31Jul2021

4. TITLE AND SUBTITLE

Cutaneous Human Papillomaviruses as Cofactors in Nonmelanoma Skin Cancer

5a. CONTRACT NUMBER
W81XWH-17-1-0354

5b. GRANT NUMBER

5c. PROGRAM ELEMENT NUMBER

6. AUTHOR(S)
Nicholas A. Wallace

E-Mail: nwallac@ksu.edu

5d. PROJECT NUMBER

5e. TASK NUMBER

5f. WORK UNIT NUMBER

7. PERFORMING ORGANIZATION NAME(S) AND ADDRESS(ES)

Kansas State University
1717 Claflin Road
Manhattan Ks, 66506

8. PERFORMING ORGANIZATION REPORT NUMBER

9. SPONSORING / MONITORING AGENCY NAME(S) AND ADDRESS(ES)

U.S. Army Medical Research and Materiel Command
Fort Detrick, Maryland 21702-5012

10. SPONSOR/MONITOR'S ACRONYM(S)

11. SPONSOR/MONITOR'S REPORT NUMBER(S)

12. DISTRIBUTION / AVAILABILITY STATEMENT

Approved for Public Release; Distribution Unlimited

13. SUPPLEMENTARY NOTES

14. ABSTRACT

We have made substantial strides in our efforts to better define β-HPV E6's ability to augment the mutagenic potential of genome destabilizing events. Our efforts have culminated in five peer reviewed manuscripts. All of the major tasks have been completed. We were granted a no cost extension on this grant due to disruptions caused by COVID-19. This additional time will allow us to complete the remaining work. Finally, we have been awarded two grants from the National Institutes of Health that will expand our work beyond the scope of this grant.

15. SUBJECT TERMS

Non-melanoma skin cancer, Cutaneous human papillomavirus infection, Ultraviolet irradiation, Ionizing radiation, DNA damage, Genome fidelity.

16. SECURITY CLASSIFICATION OF:			17. LIMITATION OF ABSTRACT	18. NUMBER OF PAGES	19a. NAME OF RESPONSIBLE PERSON
a. REPORT	b. ABSTRACT	c. THIS PAGE			USAMRMC
Unclassified	Unclassified	Unclassified	Unclassified	142	19b. TELEPHONE NUMBER *(include area code)*

TABLE OF CONTENTS

INTRODUCTION:

Genus β human papillomaviruses (β-HPVs) are believed to contribute to non-melanoma skin cancer by acting as a cofactor in UV-induced destabilization of the host genome. The purpose of this project is to test this hypothesis by measuring the ability of the E6 protein from β-HPV to disrupt cellular signaling in response to challenges to genome fidelity. We are examining non-homologous end joining, nucleotide excision repair, and the Hippo Pathway. Mechanistically, we are testing disruptions of this pathway that are either dependent or independent of β-HPV E6's degradation of p300, a cellular histone acetyltransferase.

1. KEYWORDS:

Non-melanoma skin cancer, Cutaneous human papillomavirus infection, Ultraviolet irradiation, Ionizing radiation, DNA damage, Genome fidelity.

2. ACCOMPLISHMENTS:

What were the major goals of the project? (next page)
What was accomplished under these goals?

Career Development Specific Tasks: During the first reporting period, I have made significant advancements toward my goal of establishing myself as a leader in the non-melanoma skin cancer research. This is will allow me to make continued contributions to the PRCRP topic area, "Melanoma and Other Skin Cancers

- **Career Development Specific Major Task 1:** Receive Career and Research Advice from Experts in Cancer Causing Viruses
  - **Projected Completion date** (from SOW): August 1, 2020
  - **Completion Percentage:** 100% (detailed in subsequent sections, calculated from percentage of milestones met)

Research Specific Tasks: My research continues to highlight the oncogenic risk of cutaneous human papillomavirus infection co-occurring with exposure to military relevant risk factors UV and ionizing radiation. My findings are consistent with β-HPV infections contributing to non-melanoma skin cancer in military personnel.

- **Specific Aim 1 Major Task 1:** Characterize β-HPV E6's attenuation of DNA crosslink repair.
  - **Projected Completion date** (from SOW): May 1, 2019
  - **Completion Percentage:** 100% (detailed in subsequent sections)
    - We have extended our efforts beyond the original task after completing the work proposed in the SOW.
- **Specific Aim 1 Major Task 2:** Determine the Extent to which β-HPV E6 Attenuates Non-Homologous End Joining Repair (NHEJ) of DNA Lesions
  - **Projected Completion date** (from SOW): August 1, 2021
  - **Completion Percentage:** 100% (detailed in subsequent sections)
- **Specific Aim 2 Major Task 1:** Defining β-HPV E6's inhibition of the Hippo Pathway (HP)
  - **Projected Completion date** (from SOW): February 1, 2019
  - **Completion Percentage:** 100% (detailed in subsequent sections)
- **Specific Aim 2 Major Task 2:** Determine the mechanism of β-HPV E6's inhibition of the HP.
  - **Projected Completion date** (from SOW): August 1, 2021
  - **Completion Percentage:** 100% (detailed in subsequent sections)
    - We have extended our efforts beyond the original task after completing the work proposed in the SOW.
- **Specific Aim 3 Major Task 1:** P300-Independent Disruption of DNA Crosslink Repair
  - **Projected Completion date** (from SOW): August 1, 2018
  - **Completion Percentage:** 100% (detailed in subsequent sections)
    - We have completed this task as much as possible and are currently examining the other p300-independent phenotypes that we identified during the completion of AIM2. This adheres with the theme of the proposal.
- **Specific Aim 3 Major Task 2:** Determine the mechanism of β-HPV E6's p300-independent inhibition of DNA crosslink repair.
  - **Projected Completion date** (from SOW): August 1, 2021
  - **Completion Percentage:** 100% (detailed in subsequent sections)
    - We have completed this task as much as possible and are currently examining β-HPV E6 in the context of a common mutation found in NMSC. This adheres with the theme of the proposal.

CAREER DEVELOPMENT-SPECIFIC TASKS

Major Task 1: Receive Career and Research Advice from Experts in Cancer Causing Viruses

Subtask 1: Present Research Annually to Drs. Laimonis and Giam's Research Teams

- First Reporting Period Summary: I met with Dr. Giam and Uniformed Services University Health Sciences Microbiology faculty in person. I also presented my research to Dr. Laimonis primarily via email and phone conversations.
- Second Reporting Period: I communicated with Dr. Giam about my progress via email. I met with Dr. Laimonis twice in person to discuss my work.
- Third Reporting Period: I communicated with Dr. Giam about my progress via email. I met with Dr. Laimonis twice in person to discuss my work. My third and fourth visits with Dr. Laimonis were cancelled due to COVID-19 restrictions. We have exchanged emails instead.
- Final Period: I communicated with Dr. Giam and Laimonis via zoom and email during this period. In person encounters were not possible due to COVID-19 restrictions.

Subtask 2: Attend and Present Research at Marquee HPV Research Conferences

- Last reporting Period Summary: I attended several regional conferences in between these meetings highlighted by 17th Annual Symposium in Virology hosted by the University of Nebraska's Center for Virology.
- Second Reporting Period: I attended the 2018 and 2019 DNA Tumor Virus Meetings and chaired a session in the 2018 meeting. I also presented at the 2019 International Papillomavirus Meeting. I also attended the 18th Annual Symposium in Virology hosted by the University of Nebraska's Center for Virology. In total, my lab and I presented work related to this project 4 times at international conferences and 3 times at a national conference.
- Third Reporting Period: I attended the 2019 Midwest Symposium on Papilloma and Polyom viruses. I presented at this meeting. My students presented at this meeting and at the American Society of Virology Meeting for a total of 3 international/national conference presentations. Several other speaking engagments were cancelled due to the pandemic.
- Final Period: I attended two regional conferences (Great Plains Infections Disease, University of Kansas Cancer Research Symposium. I also am currently attending the 2021 International Papillomavirus Meeting. The DNA Tumor Virus Meeting was cancelled due to COVID-19 restrictions. These conferences were a mix of in-person and remote.

Subtask 3: Monthly Discussion of Career Progress and Grant Submission Strategy with Dr. Laimonis.

Dr. Laimonis and I have discussed my career throughout the course of this support. This has included regular grant revisions and career guidance. These interactions have been incalculably helpful as I navigated my pre-tenure career. Thanks to his advice, support from

hard work from my lab members, I was able to achieve tenure early and will submit my tenure a year earlier than typical with overwhelming support (32 in favor and 1 opposed) from my colleagues. I have also obtained two grants funded by the National Institutes of Health.

Subtask 4: Discuss Scientific and Professional Progress with Dr. Clem (KSU Faculty Advisor).

With Dr. Clem's mentorship, I have seen my lab's output grow over the last year. My new lab's location near him continues to be beneficial.

Milestones Achieved:

(1) Presentation of project data at preeminent meetings annually, (12, 24 36 Months)
   a. Over the course of the support from this award, project data was presented 53 times at noteworthy regional, national, and international meetings. I also gave 16 invited lectures.
      i. At least 10 other presentations were cancelled due to the ongoing pandemic.

(2) Submit major grant proposal to extend project by the end of the second budget period (24 Months)
   a. In funding period 1 I submitted the two grants described below:
      i. A proposal to the American Cancer Center was resubmitted titled, "Genus Beta Human Papillomavirus E6 Impairs Genome Fidelity". This grant would provide support to expand the efforts funded by the CDMRP from 2019-2023. Notably, there is no overlap to the work supported by the CDMRP and this milestone was completed over 1 year earlier than projected.
         1. **Update: This grant was not funded, but its score improved and it was resubmitted during budget period 3.**
      ii. I am a junior investigator on a COBRE proposal (P20) resubmitted to the National Institute of General Medical Sciences. This work would also extend the efforts funded by the CDMRP with complimentary analysis of the oncogenic potential of cutaneous HPV infections. There is no overlap with the CDMRP funded project.
         1. **Update: This grant was funded during budget period 3.**
   b. I also submitted an R15 proposal to the National Institutes of Health entitled, "High Risk Genus Alpha HPV Oncogenes Dysregulate Translesion Synthesis". This grant received a favorable score but was not funded. There is no overlap with this CDMRP funded project.
      i. **Update: This grant was funded during budget period 3.**

(3) If necessary, revise and resubmit grant. (24, 36 Months)
   a. All three grants described above were resubmitted during budget period 2 and are awaiting review.
      i. **Since this time, two of the three grants listed above were funded and the third was not.**

(4) Publish Findings in Peer Reviewed Journal (24, 36 Months)
   a. **A total of 11 manuscripts have been published from our group during overall period of support from this grant. We expect 2-4 more manuscripts to be published after this report.**
   b. Three manuscripts were published ahead of schedule during the first funding period.
      i. Loss of Genome Fidelity: Beta HPVs and the DNA Damage Response. Wendel SO, Wallace NA Front. Microbiol. 2017 PMID:29187845 LINK
      ii. Characterizing DNA Repair Processes at Transient and Long-lasting Double-strand DNA Breaks by Immunofluorescence Microscopy. Murthy V, Dacus D, Gamez M, Hu C, Wendel SO, Snow J, Kahn A, Walterhouse SH, Wallace NA. 2018 PMID: 29939192 LINK
      iii. The Curious Case of APOBEC3 Activation by Cancer Associated Human Papillomaviruses. Wallace NA, Munger K. 2018 PMID: 29324878 LINK
   c. Two more manuscripts were published during the second budget period. References are listed below
      i. Cervical cancer cell lines are sensitive to sub-erthemal UV exposure. Gu W., Sun S., Kahn A., Dacus D., Wendel SO., McMillan N., Wallace NA. 2019 PMID: 30517878 LINK
      ii. mSphere of Influence: the Value of Simplicity in Experiments and Solidarity among Lab Members. Wallace NA. 2019. PMID: 31217299 LINK
   d. Six more manuscripts were published during the third budget period. References are listed below
      i. "Beta Human Papillomavirus 8E6 Attenuates Non-Homologous End Joining by Hindering DNA-PKcs Activity." Hu C, Bugbee T, Gamez M, Wallace NA. Cancers, 2020. PMID 32825402 LINK
      ii. Beta Human Papillomavirus 8E6 Attenuates LATS Phosphorylation after Failed Cytokinesis. D Dacus, C Cotton, TX McCallister, NA Wallace. 2020. PMID: 32238586. LINK

iii. β-HPV 8E6 combined with TERT expression promotes long-term proliferation and genome instability after cytokinesis failure. D Dacus, E Riforgiate, NA Wallace 2020 LINK
iv. DNA repair gene expression is increased in HPV positive head and neck squamous cell carcinomas. AJ Holcomb, L Brown, O Tawfik, R Madan, Y Shnayder, SM Thomas, NA Wallace 2020 LINK
v. β-HPV 8E6 Attenuates ATM and ATR Signaling in Response to UV Damage. JA Snow, V Murthy, D Dacus, C Hu, NA Wallace. 2019. PMID: 31779191 LINK
vi. Catching hpv in the homologous recombination cookie jar. NA Wallace. 2020. PMID: 31744663 LINK

(5) Gain career advice from experts in viral oncology
   a. I have had extensive interactions with my formal mentors and given talks at 6 different regional/national conferences (**Great Plains Infectious Disease, DNA Tumor Virus Meeting; Midwest Papillomavirus and Polyomavirus Symposium**; **Kansas IDEA Network of Biomedical Research Excellence's Annual Symposium; Kansas University Medical Center's Viral Pathogenesis Symposium; University of Nebraska's Center for Virology Fly Swat Meeting**).

RESEARCH-SPECIFIC TASKS

Specific Aim 1: To define the p300 inhibition of DNA repair by β-HPV E6

Major Task 1: Characterize β-HPV E6's attenuation of DNA crosslink repair.

A peer-reviewed manuscript (Snow et al; 2019) describing our data was published in the journal Pathogens during the third budget period.

Subtask 1: Obtain HRPO approval to isolate keratinocytes from neonatal foreskins and complete onboarding of Changkun Hu.

This was completed during the first budget period.

Subtask 2: Examine XPA phosphorylation and Stabilization using Immunoblot at representative time points following UV exposure. This will be done in vector control, β-HPV E6 and β-HPV ΔE6 expressing cells.

The work for this subtask was completed during budget period 3 and published after peer review in a special issue of the journal Pathogens. I have included the figure from the paper (Snow et al 2019) with data relevant to this subtask (Figure 1A-D). They demonstrate the β-HPV E6 (referred to as 8E6 in the paper and figure) reduce phosphorylation of XPA. In addition, we also found that β-HPV E6 also reduced expression of XPA (Figure 1B). This work as done in primary HFKs and TERT-immortalized HFKs. These data were also summarized more thoroughly in the report for the second budget period.

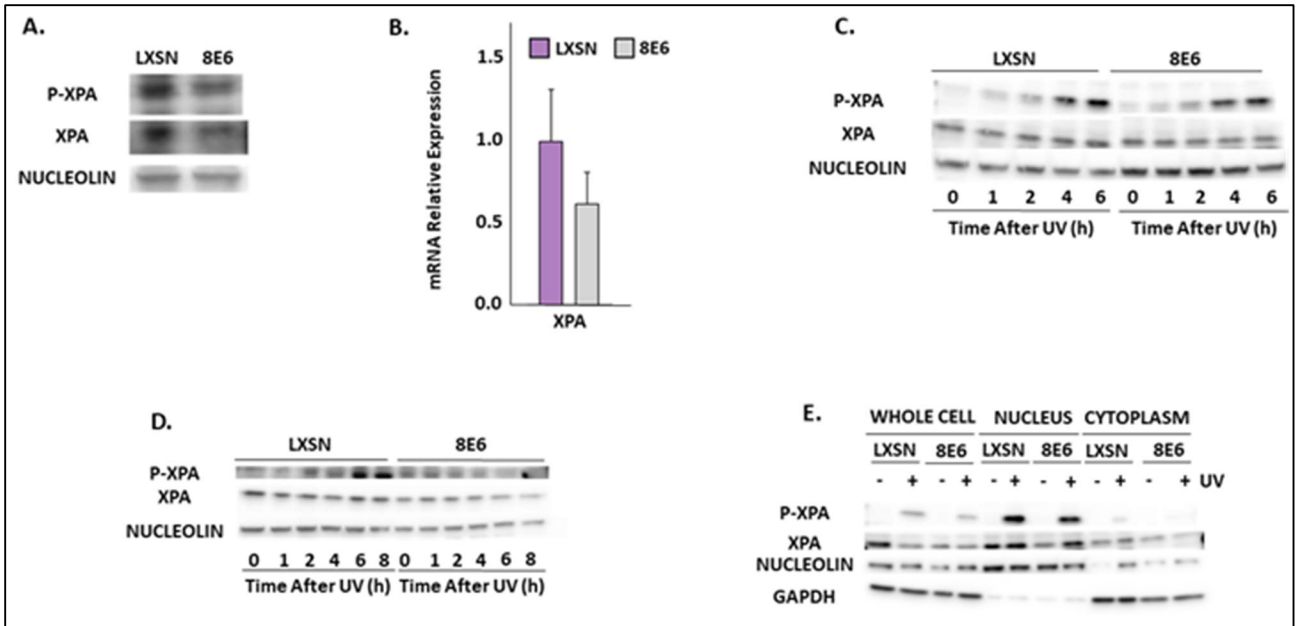

Figure 1: β-HPV E6 attenuates XPA phosphorylation. (A) Representative immunoblots of untreated hTERT HFKs with vector control (LXSN) and β-HPV 8E6 cell lines. Nucleolin was used as a loading control. (B) mRNA expression level of XPA in vector control (LXSN) and β-HPV 8E6 expressing primary HFKs as measured by RT-qPCR and normalized towards the expression level of β-actin. Data shown in figures are the means of ±SE of three independent experiments. (C) Representative immunoblots of hTERT HFKs with vector control (LXSN) and β-HPV 8E6 harvested 0–6 h post 5 mJ/cm2 UVR. Nucleolin was used as a loading control. (D) Representative immunoblots of primary HFKs with vector control (LXSN) and β-HPV 8E6 harvested 0–8 h post 5 mJ/cm2 UVR. Nucleolin was used as a loading control. (A,C,D) The numbers above bands represent quantification by densitometry. This is shown relative to untreated cells within the same cell line and normalized to the loading control. (E) Subcellular fractionation of hTERT HFKs with vector control (LXSN) and β-HPV 8E6 cell line lysates harvested 6 h post exposure to 5 mJ/cm2 UVR were observed via immunoblot. GAPDH was used as a cytoplasmic loading control and Nucleolin was used as a nuclear loading control.

Subtask 3: Determine if DNA crosslink repair is rescued by exogenous expression of XPA and ATR.

During budget period 2, our data suggested that excess ATR or XPA would not rescue crosslink repair. This was because β-HPV E6 blocked ATR activity. The data demonstrating this can be found in Figure 2 and in the previously mentioned manuscript.

As a result, we examined ATR phosphorylation targets. This demonstrated that β-HPV E6 has a broad but not universal ability to hinder ATR-mediated phosphorylation and is shown figure 3-4 and can also be found in Snow et al 2019. Notably, β-HVP E6 increased the frequency of cells in S-phase before and after UV (Figure 3F). This is expected to promote mutagenesis and HPV replication as genomes are more at risk during replication and HPV requires replicating cells for their proliferation. β-HPV E6 also decreases POLη expression and repair complexes formation. This extends the known signaling impact of β-HPV E6 to the translesion synthesis (TLS) pathway. TLS protects replication forks from collapsing until UV damage is repaired. This prevents replication forks from collapsing into double stranded DNA breaks (DSBs). Attenuation of the TLS pathway provides an explanation for our prior observation that β-HPV E6 makes UV-induced DSBs more likely. These data were also summarized more thoroughly in the report for the second budget period.

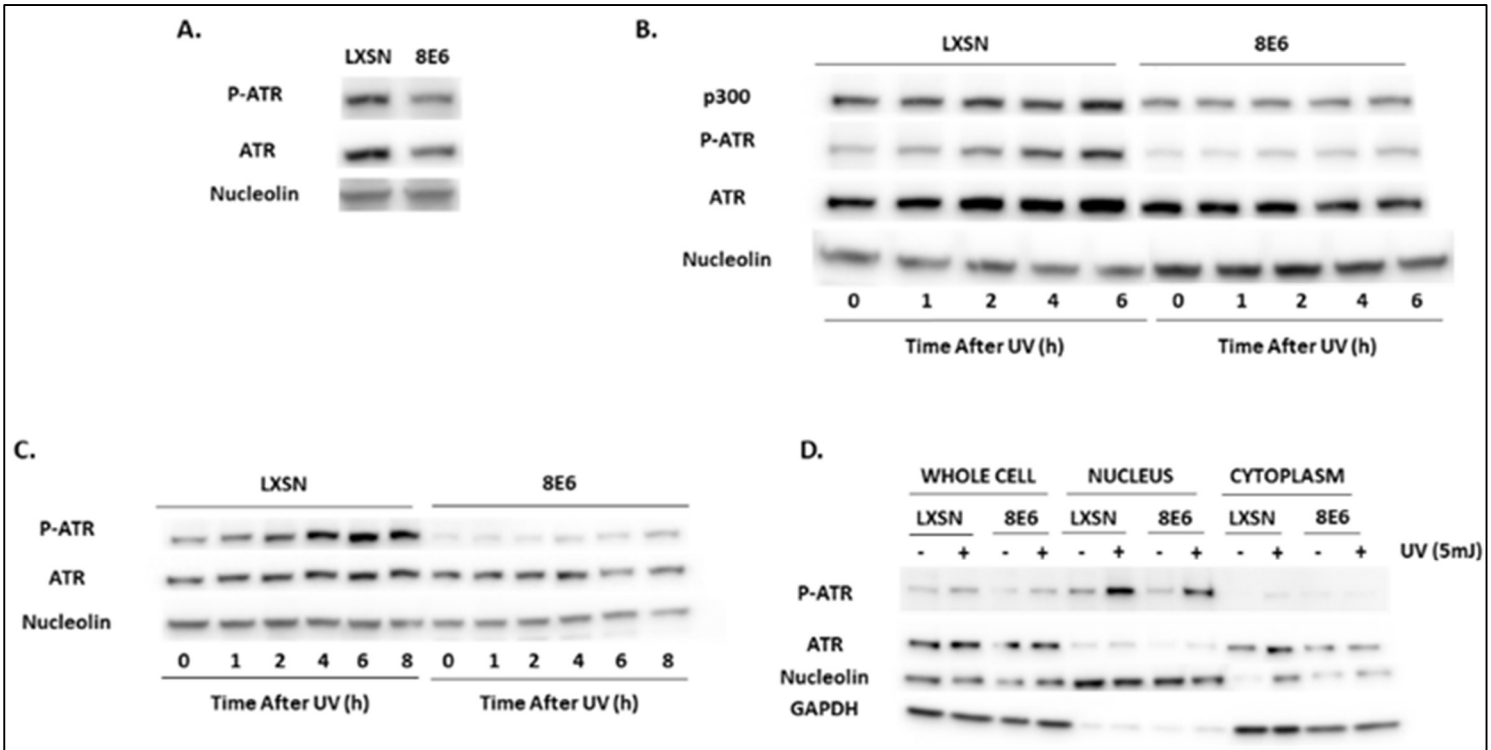

Figure 2: β-HPV 8E6 attenuates ATR activation. (A) Representative immunoblots of untreated hTERT HFKs with vector control (LXSN) and β-HPV 8E6 cell lines. Nucleolin was used as a loading control. (B) Representative immunoblots of hTERT HFKs with vector control (LXSN) and β-HPV 8E6 harvested 0–6 h post 5 mJ/cm2 UVR. Nucleolin was used as a loading control. (C) Representative immunoblots of primary HFKs with vector control (LXSN) and β-HPV 8E6 harvested 0–8 h post 5 mJ/cm2 UVR. Nucleolin was used as a loading control. (A–C) The numbers above bands represent quantification by densitometry. This is shown relative to untreated cells within the same cell line and normalized to the loading control. (D) Subcellular fractionation of hTERT HFKs with vector control (LXSN) and β-HPV 8E6 cell line lysates harvested 6 h post exposure to 5 mJ/cm2 UVR were observed via immunoblot. GAPDH was used as a cytoplasmic loading control and Nucleolin was used as a nuclear loading control.

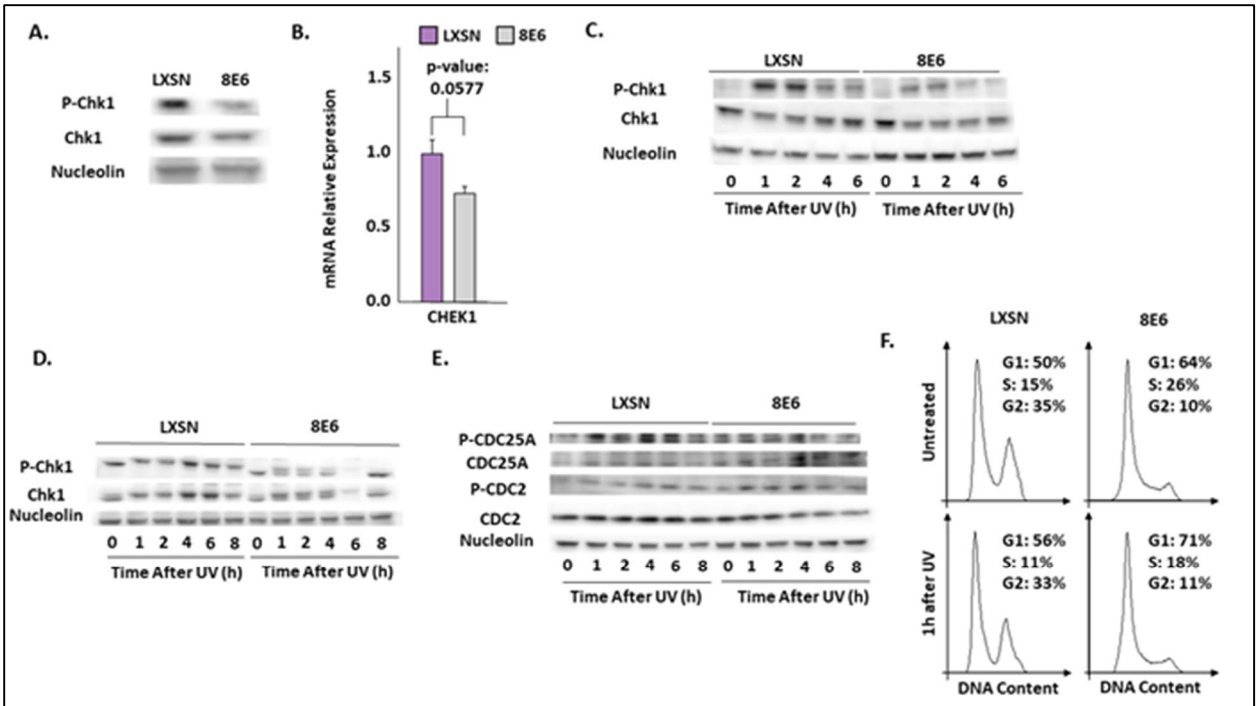

Figure 3: β-HPV 8E6 attenuates CHK1 phosphorylation. (A) Representative immunoblots of untreated hTERT HFKs with vector control (LXSN) and β-HPV 8E6 cell lines. Nucleolin was used as a loading control. (B) mRNA expression level of CHEK1 in vector control (LXSN) and β-HPV 8E6 expressing primary HFKs as measured by RT-qPCR and normalized towards the expression level of β-actin. Data shown in figures are the means of ±SE of three independent experiments. (C) Representative immunoblots of hTERT HFKs with vector control (LXSN) and β-HPV 8E6 harvested 0–6 h post 5mJ/cm2 UVR. Nucleolin was used as a loading control. (D) Representative immunoblots of primary HFKs with vector control (LXSN) and β-HPV 8E6 harvested 0–8 h post 5 mJ/cm2 UVR. Nucleolin was used as a loading control. (E) Representative immunoblots of hTERT HFKs with vector control (LXSN) and β-HPV 8E6 harvested 0–8 h post 5 mJ/cm2 UVR. Nucleolin was used as a loading control. (A, C–E) The numbers above bands represent quantification by densitometry. This is shown relative to untreated cells within the same cell line and normalized to the loading control. (F) Cell cycle analysis of hTERT HFKs with LXSN vector control and β-HPV 8E6 1 h post 5 mJ/cm2 UVR.

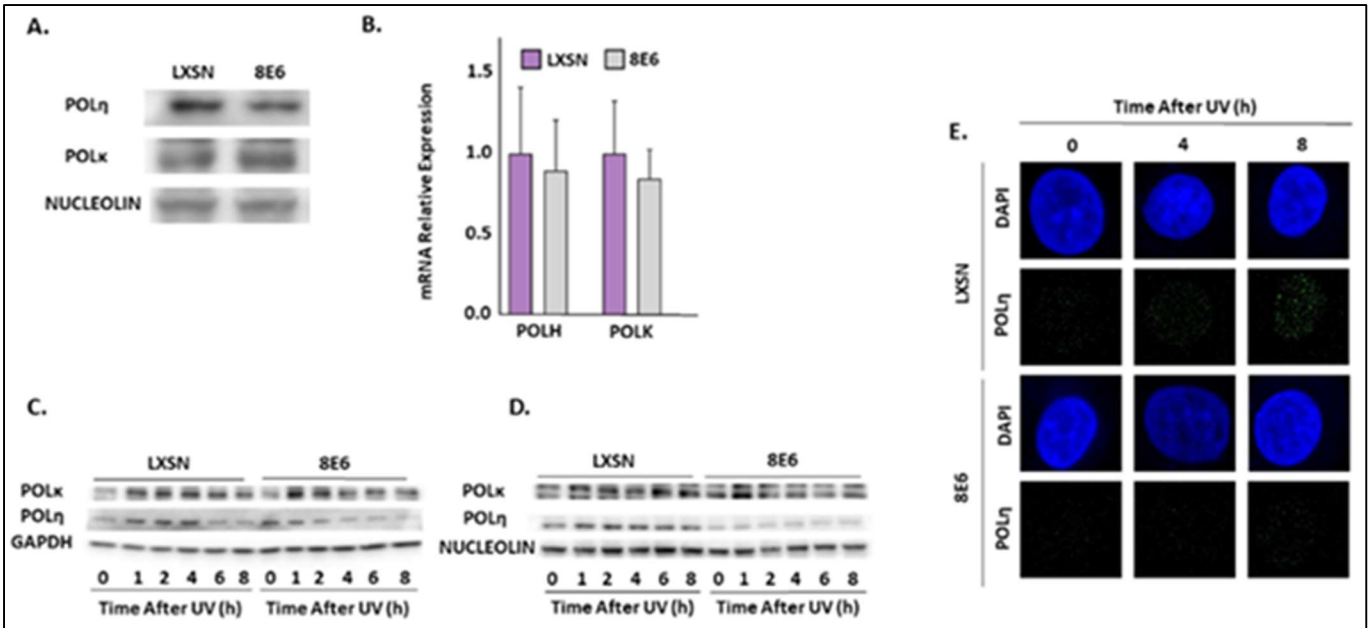

Figure 4: β-HPV 8E6 attenuates POLη abundance. (A) Representative immunoblots of untreated hTERT HFKs vector control (LXSN) and β-HPV 8E6 cell lines. Nucleolin was used as a loading control. (B) mRNA expression level of POLH and POLK in vector control (LXSN) and β-HPV 8E6 expressing primary HFKs as measured by RT-qPCR and normalized towards the expression level of β-actin. Data shown in figures are the means of ±SE of three independent experiments. (C) Representative immunoblots of hTERT HFKs with vector control (LXSN) and β-HPV 8E6 harvested 0–8 h post 5 mJ/cm2 UVR. GAPDH was used as a loading control. (D) Representative immunoblots of primary HFKs with vector control (LXSN) and β-HPV 8E6 harvested 0–8 h post 5 mJ/cm2 UVR. Nucleolin was used as a loading control. (A,C,D) The numbers above bands represent quantification by densitometry. This is shown relative to untreated cells within the same cell line and normalized to the loading control. (E) Representative immunofluorescence microscopy images of hTERT HFKs. POLη (green) and nuclei stained (blue) with DAPI.

Subtask 4: Define the subcellular localization of XPA using immunofluorescence microscopy and immunoblots, before and after UV.

We have shown that β-HPV E6 changes the subcellular localization of XPA by both microscopy and immunoblots of subcellular fractionations. These data were published in Snow et al 2019 and are summarized here in Figure 1E and Figure 5. They were also discussed in more detail in the report for budget period 1 and 2.

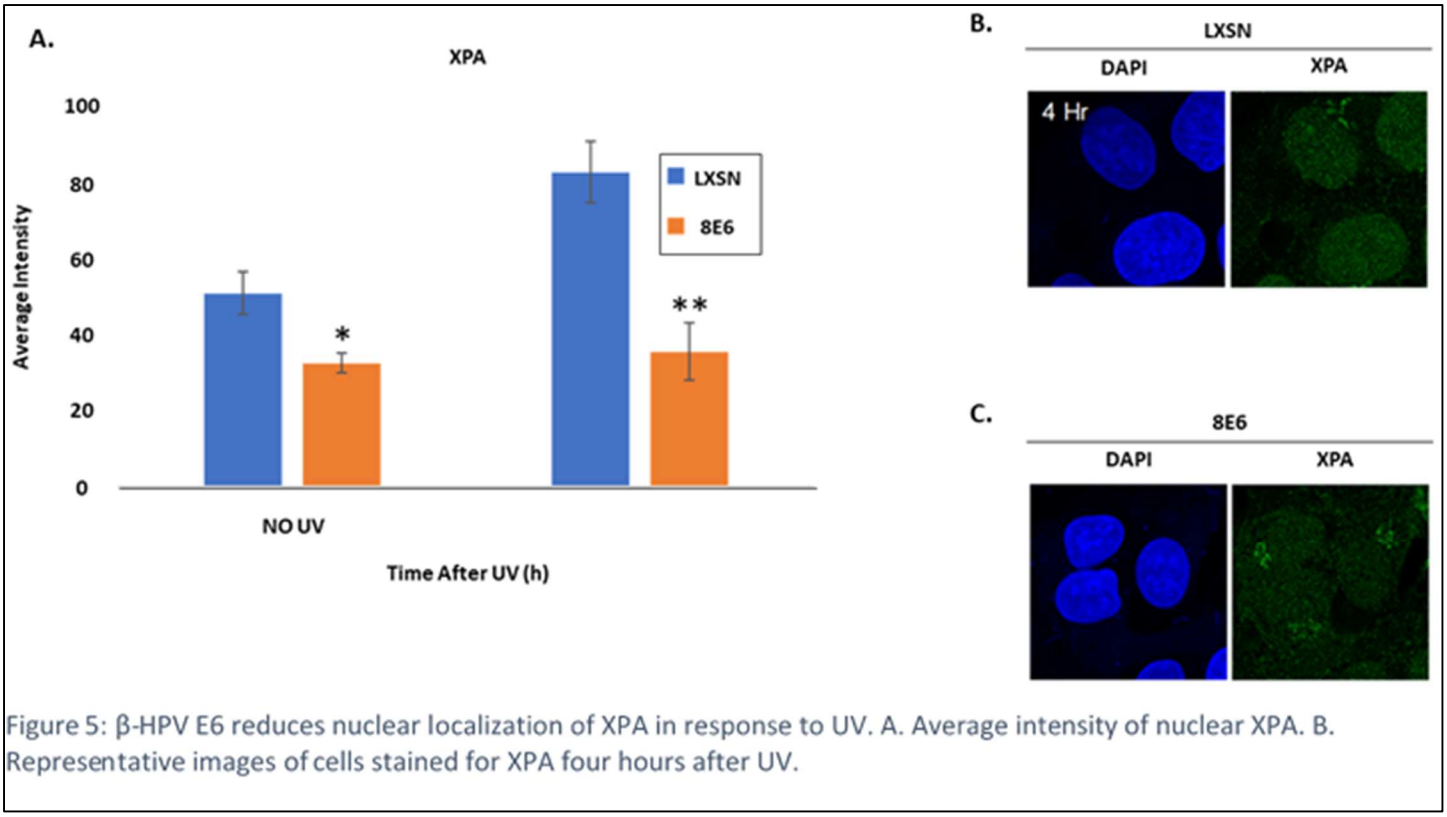

Figure 5: β-HPV E6 reduces nuclear localization of XPA in response to UV. A. Average intensity of nuclear XPA. B. Representative images of cells stained for XPA four hours after UV.

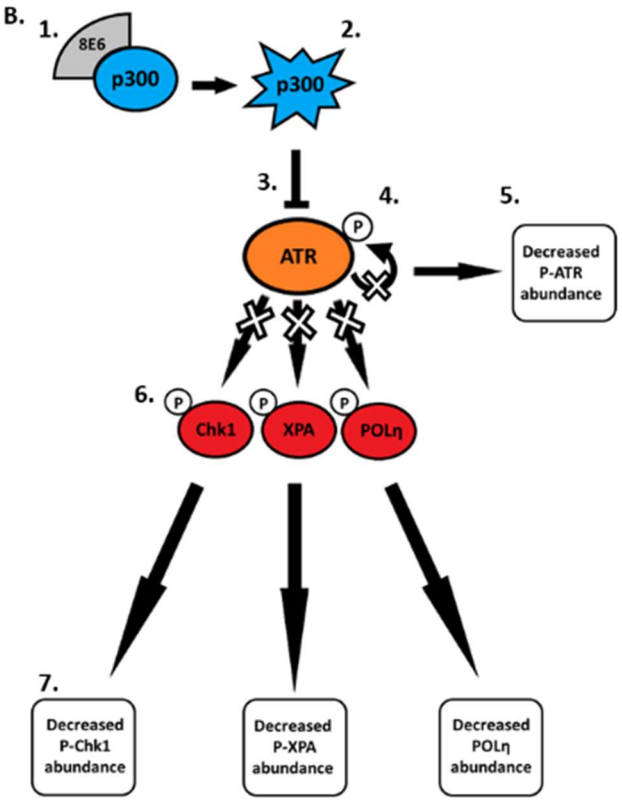

Figure 6: β-HPV 8E6 binds to p300 (1) causing p300 to become destabilized and subsequentially degraded (2). The decrease in p300 levels leads to less ATR transcription (3). This leads to a decrease in ATR autophosphorylation (4) resulting in less activated ATR available (5). Limited availability of activated ATR leads to a decrease in ATR-dependent phosphorylation of downstream proteins (6) causing changes in β-HPV 8E6 infected cells (7).

<u>Subtask 5: Determine if β-HPV E6 changes the abundance of other crosslink repair proteins using immunoblotting to detect the abundance of NER proteins before and after UV.</u>

This subtask was completed in budget period 2. We provide Figure 6 as a summary of the inhibition of ATR signaling discovered with the support from this grant.

Milestones Achieved: We will …

(1) obtain oversight from HRPO necessary to avoid unintentional or unethical mistreatment of the human subjects.

This was completed during the first budget period.

(2) get the staff necessary to complete this aim.

This was completed during the first budget period.

(3) *learn whether β-HPV E6 alters XPA phosphorylation and stabilization after UV and whether any changes are p300-dependent.*

This was completed and published in budget period 3.

(4) *learn whether β-HPV E6 acts through XPA- and ATR-dependent mechanisms to prevent crosslink repair.*

We found that β-HPV E6 inhibits ATR activation and expression meaning that it ultimately represses crosslink repair by decreasing ATR expression and activation. An extension of this observation is that β-HPV E6 acts indirectly through XPA.

(5) *learn whether β-HPV E6 changes the subcellular localization of XPA following UV and whether any changes are p300-dependent.*

This was completed and published in budget period 3.

(6) *learn if β-HPV E6 changes the abundance of NER proteins in cells with and without UV exposure.*

This was completed and published in budget period 3.

Major Task 2: Determine the Extent to which β-HPV E6 Attenuates Non-Homologous End Joining Repair (NHEJ) of DNA Lesions

Subtask 1: Define β-HPV E6's ability to disrupt DNApk expression and autophosphorylation by immunoblot.

Most of this subtask was completed during the first and second budget periods. We have shown that β-HPV E6 decreases DNApk autophosphorylation in response to DNA damage. These data are currently under-review at the peer-reviewed journal Cancer (Hu, Bugbee and Wallace 2020). They have been repeated in Keratinocytes (HFKs) and U2OS cells (Figure 7).

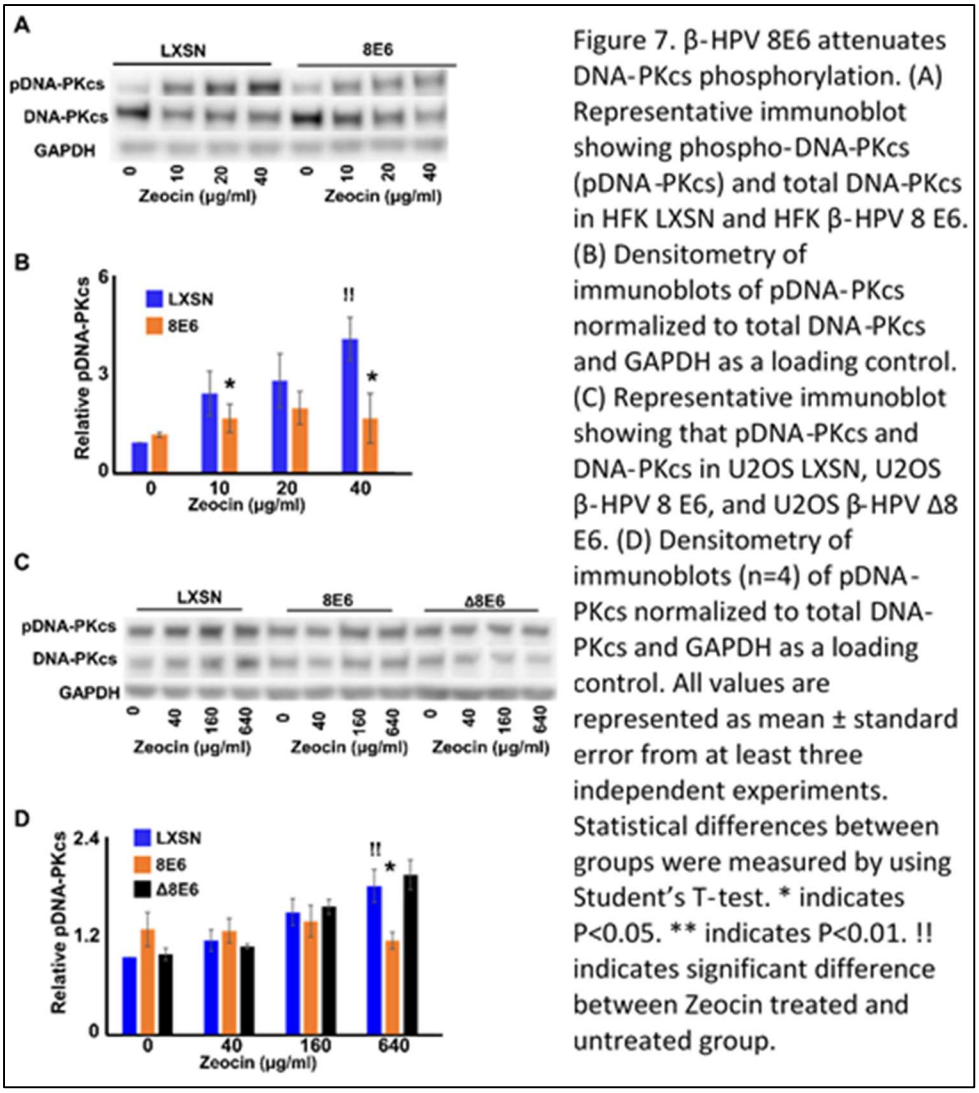

Figure 7. β-HPV 8E6 attenuates DNA-PKcs phosphorylation. (A) Representative immunoblot showing phospho-DNA-PKcs (pDNA-PKcs) and total DNA-PKcs in HFK LXSN and HFK β-HPV 8 E6. (B) Densitometry of immunoblots of pDNA-PKcs normalized to total DNA-PKcs and GAPDH as a loading control. (C) Representative immunoblot showing that pDNA-PKcs and DNA-PKcs in U2OS LXSN, U2OS β-HPV 8 E6, and U2OS β-HPV Δ8 E6. (D) Densitometry of immunoblots (n=4) of pDNA-PKcs normalized to total DNA-PKcs and GAPDH as a loading control. All values are represented as mean ± standard error from at least three independent experiments. Statistical differences between groups were measured by using Student's T-test. * indicates $P<0.05$. ** indicates $P<0.01$. !! indicates significant difference between Zeocin treated and untreated group.

Subtask 2: Determine the effect of β-HPV E6 on the expression of NHEJ proteins by immunoblot.

We have shown that β-HPV E6 does not decrease canonical NHEJ protein abundance by immunoblot. These data are also included in the submitted manuscript (Hu, Bugbee and Wallace 2020). See figure 8.

Subtask 3: Define the ability of β-HPV E6 to impair NHEJ using a fluorescence based reporter system (traffic light reporter assay).

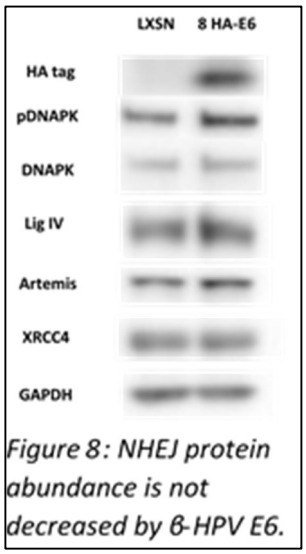

Figure 8: NHEJ protein abundance is not decreased by β-HPV E6.

We have taken two approaches to the previously reported problems with the broken flow cytometer at Kansas State University. First, we requested permission to buy a table top flow cytometer using funds from this grant. That request is currently being processed and evaluated. In the meantime, we converted a flow cytometry based assay for NHEJ to be detectable by immunoblot. Specifically, we use Cas9-directed endonucleases to make DSB cuts downstream of the GAPDH promoter and upstream of the CD4 open reading frame. When this is repaired by NHEJ, cells constitutively express CD4. We found this was detectable by immunoblot. To confirm that the CD4 expression was due to NHEJ, we used ATM and DNApk inhibitors (Ku55933 and NU7441, respectively). As expected, ATM inhibition increased NHEJ (determined by CD4 abundance), while DNApk inhibition abolished NHEJ. We then used this assay to demonstrate that β-HPV E6 decreased NHEJ in HFKs and U2OS cells. Further, at least some of this inhibitory effect was p300-independent. These data are also included in the previously mentioned manuscript. Please see Figure 10)

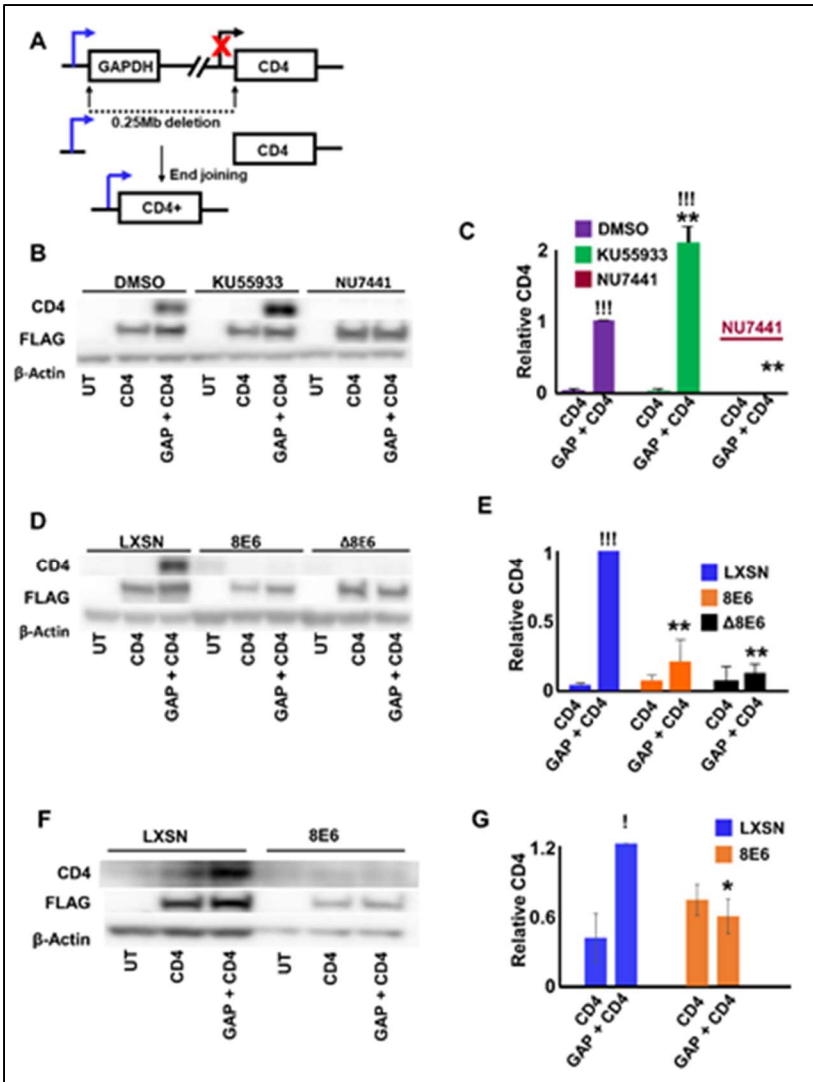

Figure 10. β-HPV 8E6 decreases NHEJ efficiency using CD4 expression as a readout. (A) Schematic of end-joining reporter assay. FLAG-tagged SgRNA-CAS9 induced double strand breaks in GAPDH and CD4 on chromosome 12 in U2OS cells. Rearrangement leads to CD4 expression driven by the promoter of GAPDH. Red "X" represents that CD4 expression is naturally inactivated. (B) Representative immunoblots showing CD4 expression in U2OS cells treated with control, ATM inhibitor (KU55933), and DNA-PK inhibitor (NU7441) after transfection with control (UT), FLAG-tagged SgRNA-CAS9 targeting CD4 (CD4), and FLAG-tagged SgRNA-CAS9 targeting GAPDH together with FLAG-tagged SgRNA-CAS9 targeting CD4 (GAP/CD4). (C) Densitometry of immunoblots (n=3) from panel B. CD4 was normalized to β-actin as a loading control. Transfection efficiency was accounted for using FLAG abundance. (D) Representative immunoblots showing CD4 expression in U2OS LXSN, β-HPV 8 E6, and β-HPV Δ8E6 after transfection with control (UT), FLAG-tagged SgRNA-CAS9 targeting CD4 (CD4), and FLAG-tagged SgRNA-CAS9 targeting GAPDH and FLAG-tagged SgRNA-CAS9 targeting CD4 (GAP/CD4). (E) Densitometry of immunoblots (n=3) from panel D. CD4 was normalized to β-actin as a loading control. Transfection efficiency was accounted for using FLAG abundance. (F) Representative immunoblots showing CD4 expression in HFK LXSN and HFK β-HPV 8 E6 after transfection with control (UT), FLAG-tagged SgRNA-CAS9 targeting CD4 (CD4), and FLAG-tagged SgRNA-CAS9 targeting GAPDH and FLAG-tagged SgRNA-CAS9 targeting CD4 (GAP/CD4). (G) Densitometry of immunoblots (n=3) from panel F. CD4 was normalized to β-actin as a loading control. Transfection efficiency was accounted for using FLAG abundance. All values are represented as mean ± standard error from at least three independent experiments. Statistical differences between groups were measured by using Student's T-test. * indicates P<0.05. ** indicates P<0.01. ! indicates significant difference between transfection with SgRNA-CAS9 targeting CD4 and co-transfection with SgRNA-CAS9 targeting CD4 and GAPDH.

Subtask 4: Determine the ability of β-HPV E6 to prevent NHEJ repair foci formation by immunofluorescence microscopy.

This subtask was completed during budget period 2. During the previous reporting period, we also reported that β-HPV E6 significantly increased the presence of pDNApk and RAD51 co-localization at DSBs. These co-localized foci are likely catastrophic for cells because NHEJ (indicated by pDNApk) removes the type of single strand overhangs that must occur for RAD51 foci to exist. This is predicted to result in large deletions. We are currently using the Cas9 technology described in Figure 10 to create a DSB at a known genomic location and using targeted deep sequencing to define the mutagenic consequences of β-HPV E6 expression at a DSB.

Finally, we found that β-HPV E6 attenuated ATM activation and phosphorylation of ATM target proteins in response to UV. These data were included in a recently accepted manuscript (Snow et al 2019) and are shown in Figure 11.

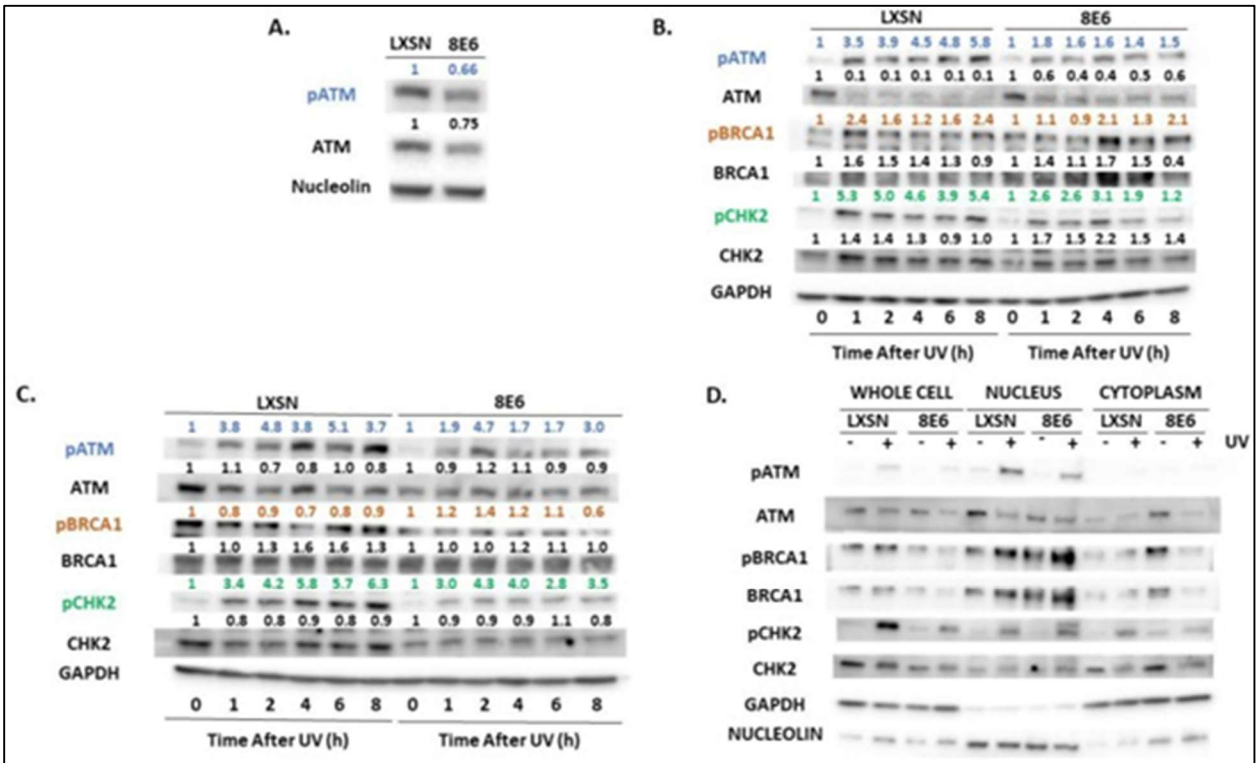

Figure 11: β-HPV 8E6 attenuates ATM activation. (**A**) Representative immunoblots of untreated hTERT HFKs with vector control (LXSN) and β-HPV 8E6 cell lines. Nucleolin was used as a loading control. (**B**) Representative immunoblots of hTERT HFKs with vector control (LXSN) and β-HPV 8E6 harvested 0–8 h post 5 mJ/cm^2 UVR. GAPDH was used as a loading control. (**C**) Representative immunoblots of primary HFKs with vector control (LXSN) and β-HPV 8E6 harvested 0–8 h post 5 mJ/cm^2 UVR. GAPDH was used as a loading control. (**A–C**) The numbers above bands represent quantification by densitometry. This is shown relative to untreated cells within the same cell line and normalized to the loading control. (**D**) Subcellular fractionation of hTERT HFKs with vector control (LXSN) and β-HPV 8E6 cell line lysates harvested 6 h post exposure to 5 mJ/cm^2 UVR were observed via immunoblot. GAPDH was used as a cytoplasmic loading control and Nucleolin was used as a nuclear loading control.

Milestones Achieved: We will…

(1) learn the extent to which β-HPV E6 prevents DNApk expression and activation as well as whether this phenotype is p300-dependent.

Thus this milestone was met and surpassed. We found p300-dependent attenuation of DNApk activation and p300-indpendent attenuation of NHEJ.

(2) learn whether β-HPV E6 decreases the abundance of NHEJ proteins and whether these changes are dependent on p300 degradation.

This milestone was achieved during the first budget period.

(3) learn whether β-HPV E6 inhibits the repair of double strand breaks by the non-homologous end joining pathway as well as the role of p300 in any inhibition.

This milestone has been reached and published in a peer reviewed journal.

(4) learn the extent to which β-HPV E6 prevents non-homologous end joining proteins from forming repair foci and the p300-dependence of any such phenotype.

This goal was met and surpassed. Further, relevant data has been published in a peer reviewed journal.

Specific Aim 2: Determine the breadth and mechanism of β-HPV E6's Hippo Pathway (HP) Inhibition

We are preparing a manuscript for submission to the Journal of Virology based on the data from Specific Aim 2. This is the highest ranked journal in virology. We expect to submit the manuscript in early Fall.

Major Task 1: Defining β-HPV E6's inhibition of the HP

Subtask 1: Obtain HRPO approval to isolate keratinocytes from neonatal foreskins.

This was completed during the first budget period.

Subtask 2: Determine the impact of β-HPV E6 on the phosphorylation of HP proteins by immunoblot.

This was completed during the first budget period.

Subtask 3: Define the subcellular localization of HP proteins in cells by immunofluorescence microscopy.

This was completed during the first budget period.

Subtask 4: Determine the extent to which β-HPV E6 promotes TEAD promoter activity by luciferase reporter assay.

This task was completed during the third budget period and published in the Journal of Virology (Dacus et al 2020) along with the data described in Subtasks 1-4. Relevant data for the other three subtasks was provided in the previous reporting period. Figure 12 contains the relevant data.

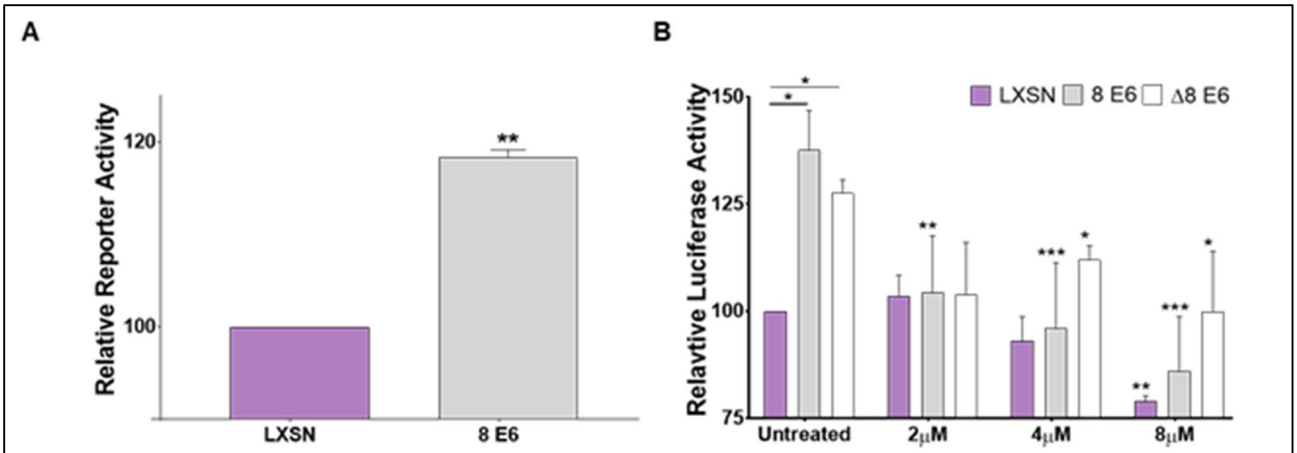

Figure 12: β-HPV E6 increases TEAD-reporter activity as measured by luciferase reporter assay. A. In untreated HFKs, β-HPV E6 increases TEAD-reporter activity. B. This is at least partially independent of its ability to degrade p300 as β-HPV ΔE6 also significantly increases TEAD-reporter activity. However, inducing failed cytokinesis with increasing concentrations of H2CB returns TEAD-reporter activity to vector control levels.

Subtask 5: Define the prevalence of multipolar mitosis and micronuclei formation in β-HPV E6 expressing cells by immunofluorescence microscopy.

As reported for budget period two, our data supports the idea that β-HPV E6 promotes multipolar mitosis and demonstrates that micronuclei are increased by β-HPV E6. We are currently limited in our ability to detect multipolar mitoses because of the less than ideal frequency of mitotic cells in vector control HFKs. To combat this restriction, we are actively working out the conditions to increase the frequency of cells in mitosis by employing a double thymidine block.

Milestones Achieved: We will…

(1) obtain oversight from HRPO necessary to avoid unintentional or unethical mistreatment of the human subjects.

This was completed during the first budget period.

(2) learn whether β-HPV E6 alters the phosphorylation of Hippo pathway proteins and if any such changes are p300-dependent.

This was completed during the first budget period.

learn whether β-HPV E6 prevents the subcellular localization of Hippo proteins induced by failed cytokinesis and if any such inhibition is p300-dependent

This was completed during the first budget period.

(3) learn whether β-HPV E6 increase TEAD promoter activity after failed cytokinesis and if they can whether or not it is a p300-dependent phenotype.

We completed this task, showing that TEAD promoter activity was increased in basal cells in a p300 dependent manner by β-HPV E6 however after failed cytokinesis TEAD promoter activity was decreased when β-HPV E6 was expressed. We have independently confirmed these results using rtPCR and an *in silico* screen.

(4) learn whether β-HPV E6 increases the likelihood of multipolar mitosis and micronuclei formation after failed cytokinesis as well as the role of p300-degradation in any such increases.

This milestone has been completed.

Major Task 2: Determine the mechanism of β-HPV E6's inhibition of the HP.

Subtask 1: Define the abundance of HP proteins by immunoblot. This will be done in vector control, β-HPV E6 and β-HPV ΔE6 expressing cells.

This was completed during the first budget period.

Subtask 2: Determine if p300 is involved in β-HPV E6-induced changes to the abundance of HP proteins using β-HPV ΔE6 mutant and immunoblot.

This was completed during the first budget period.

Subtask 3: Determine if p300 is present at HP gene promoters by chromatin immunoprecipitation and qPCR.

We completed the planned qPCR experiments but did not see any change in HP gene expression (Fiugre 22). As a result, we did not continue with the planned chromatin immunoprecipitation experiment.

Subtask 4: Perform an unbiased analysis of β-HPV E6's effect on the HP using HP PCR Array purchased from Qiagen and validated by qPCR as well as immunoblot.

This was completed during the first budget period.

Milestones Achieved: We will learn…

(1) whether β-HPV E6 changes the abundance of select HP proteins by destabilizing p300.

This was completed during the first budget period.

(2) whether p300 is at the promoters of HP genes and whether β-HPV E6 changes the abundance of p300 at these promoters.

Our rtPCR data demonstrate that HP gene expression is not decreased by β-HPV E6. As a result, there was no value in determining the mechanism of β-HPV E6's non-existent modification of HP expression. We do see an increase in LATS2 protein abundance suggesting an increase in protein stability.

(3) the comprehensive impact of β-HPV E6 on HP gene expression.

This was completed during the first budget period.

Specific Aim 3: Determine how β-HPV E6 induces p300-independent inhibition of DNA repair.

Major Task 1: P300-Independent Disruption of DNA Crosslink Repair

Subtask 1: Finish Onboarding for Dalton Dacus and obtain HRPO approval to isolate keratinocytes from neonatal foreskins.

This was completed during the first budget period.

Subtask 2: Define ICL-repair in HT1080 cells where β-HPV cannot degrade p300 by immunofluorescence microscopy using antibodies against UV-induced ICLs.

As discussed in the report for budget period 2, we have shifted the focus of this subtask to better characterizing the ability of β-HPV E6 to induce aneuploidy. This has been a very fruitful effort, leading to a recently accepted manuscript in the peer-reviewed journal, Virology (Dacus, Riforgiate and Wallace 2020). In this manuscript, we show that that β-HPV E6 becomes particularly capable of mitigating the long term anti-proliferative effects of failed cytokinesis when the viral gene is expressed in cells immortalized by telomerase activity. This does not affect β-HPV E6's ability to alter Hippo pathway signaling, but does allow cells to maintain longer term proliferation and accumulate aneuploidy. The relevant data for this work is provided in figures 13-17.

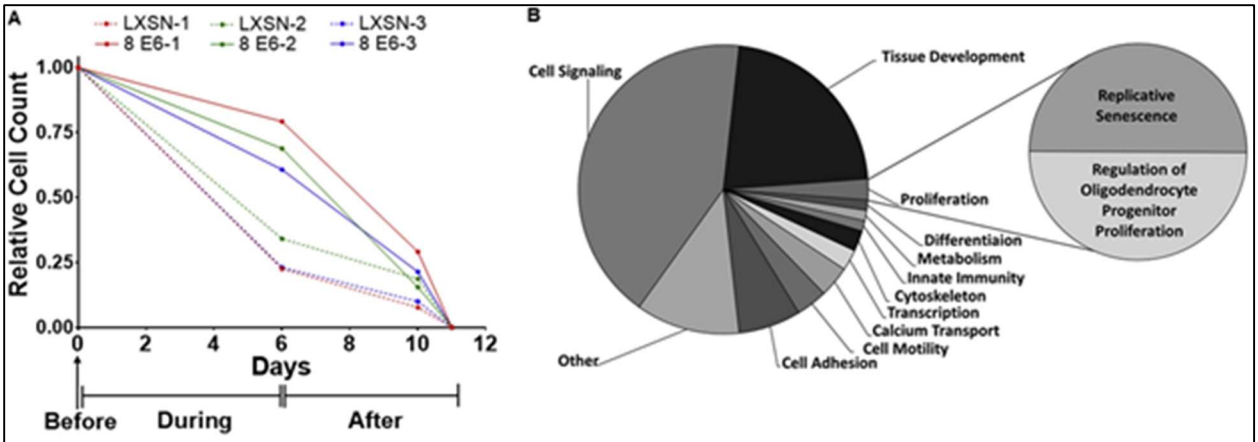

Fig. 13: H2CB-induced failed cytokinesis prevents long-term proliferation. (A) Three growth curves (biological replicates) comparing HFK LXSN and β-HPV 8E6 cells before, during, and after 6 days of H2CB exposure in 6-well tissue culture plates. HFK LXSN (dashed) and β-HPV 8E6 (solid) data with the same color and number (red, 1; green, 2; and blue, 3) were treated in parallel. (B) Two charts representing GO analysis of common mutations in cSCC. The larger chart on the left represents nodes of similar GO: biological process terms. The smaller chart represents the two GO: biological process terms within the "Proliferation" node. TERT expression allows β-HPV 8E6 HFKs growth after H2CB-induced failed cytokinesis.

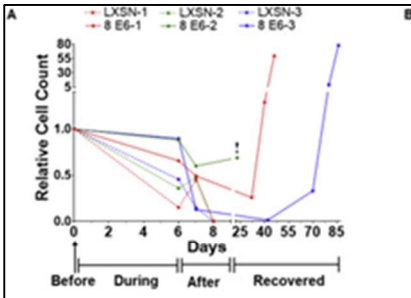

B

Cell Type	% Recovered
LXSN	0% (3/3)
8 E6	0% (3/3)
LXSN + *TERT*	~11% (1/9)
8 E6 + *TERT*	100% (9/9)

Fig. 14. TERT expression promotes recovery from failed cytokinesis. (A) Three growth curves (biological replicates) comparing TERT-HFK LXSN and β-HPV 8E6 cells before, during, after, and recovered from 6 days of H2CB exposure in 6-well tissue culture plates. LXSN (dashed) and β-HPV 8E6 (solid) data with the same color and number (red, 1; green, 2; and blue, 3) were treated in parallel. ! signifies the premature end of the long-term cultivation due to bacterial contamination. (B) Percent of HFK and TERT-HFK cells capable of long-term growth after 6 days in H2CB.

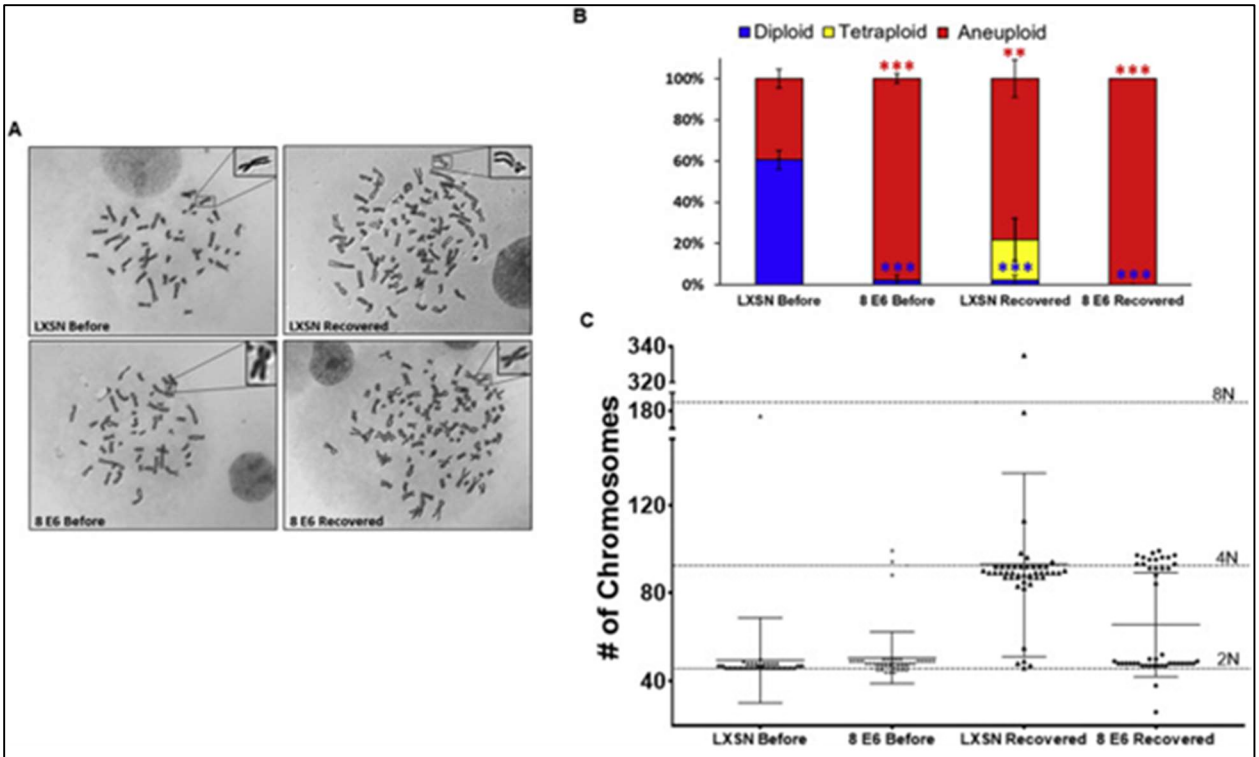

Fig. 15. β-HPV 8E6 and cytokinesis failure induce changes in ploidy. (A) Representative images of metaphase spreads. Insert on the top-right corner shows a magnified chromosome. (B) Relative frequency of diploidy (blue), tetraploidy (yellow), and aneuploidy (red) before H2CB treatment and once cells recovered. Red and blue asterisks denote a significant difference from 'LXSN Before' for aneuploidy and diploidy, respectively. (C) Graphical presentation of the distribution of the number of chromosomes among ≥ 45 cells analyzed by metaphase spreads (before or recovered from 6 days of H2CB exposure). Horizontal-dotted lines represent 46 (2 N), 92 (4 N), or 184 (8 N) chromosomes. ** denotes significant difference between indicated samples $p \leq 0.01$, *** denotes $p \leq 0.001$ (Student's t-test).

Subtask 3: Define ICL-repair when exogenous expression of degradation resistant p300 prevents β-HPV E6 from degrading p300 using immunofluorescence microscopy with antibodies against UV-induced ICLs.

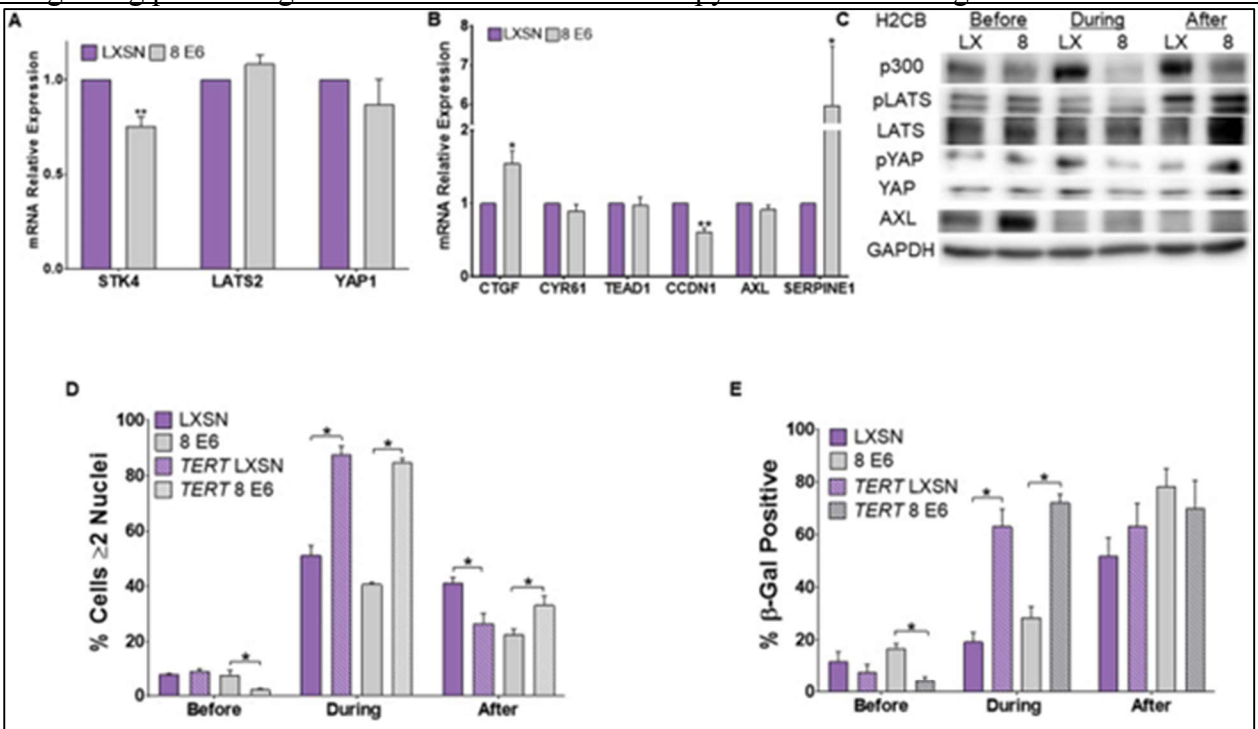

Fig. 16: Responses to H2CB-induced failed cytokinesis in TERT-HFK. Expression of (A) canonical HP genes and (B) TEAD-regulated genes in TERT-HFKs measured by RT-qPCR and normalized to β-actin mRNA. (C) Representative immunoblot of HP proteins in TERT-HFK cells before, during, and after H2CB exposure. (D) Quantification of cells with more than 1 nucleus before, during, and after H2CB exposure. (E) Quantification of SA β-Gal staining in HFK cells vs TERT-HFK before, during, and after H2CB treatment. Figures depict means ± standard error of the mean. n ≥ 3. * denotes significant difference between indicated samples * denotes $p \leq 0.05$, ** denotes $p \leq 0.01$. (Student's t-test).

As noted in the previous annual report and prior sections of this one, we are now the characterizing micronuclei found in cells expressing β-HPV E6. Specifically, we found that micronuclei caused by β-HPV E6 are on average smaller than those in control cells (Figure A). This is independent of p300 degradation and shared with between multiple β-HPV E6 proteins. In contrast, β-HPV E6 does not change the frequency of H2AX staining or the intensity of DAPI staining (Figure B and C). Finally, we determined if β-HPV E6 changed the frequency of

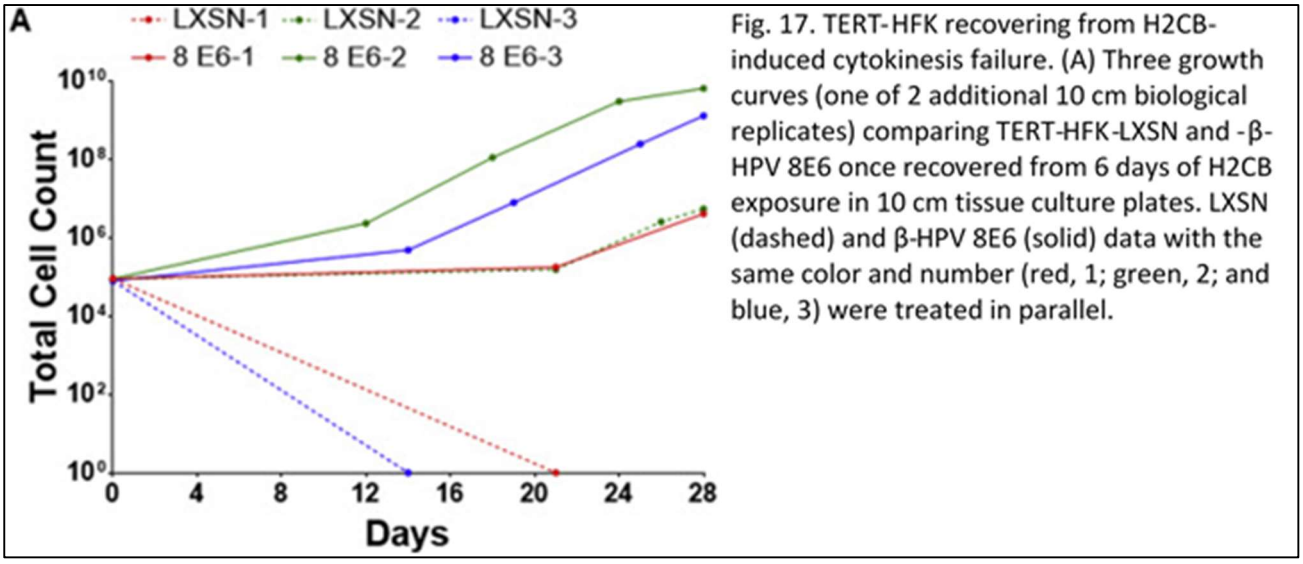

Fig. 17. TERT-HFK recovering from H2CB-induced cytokinesis failure. (A) Three growth curves (one of 2 additional 10 cm biological replicates) comparing TERT-HFK-LXSN and -β-HPV 8E6 once recovered from 6 days of H2CB exposure in 10 cm tissue culture plates. LXSN (dashed) and β-HPV 8E6 (solid) data with the same color and number (red, 1; green, 2; and blue, 3) were treated in parallel.

centromeres in micronuclei using cenpA as a marker for centromeres. There was a modest p300-dependent increase in centromere staining that accompanied β-HPV E6 expression (Figure D).

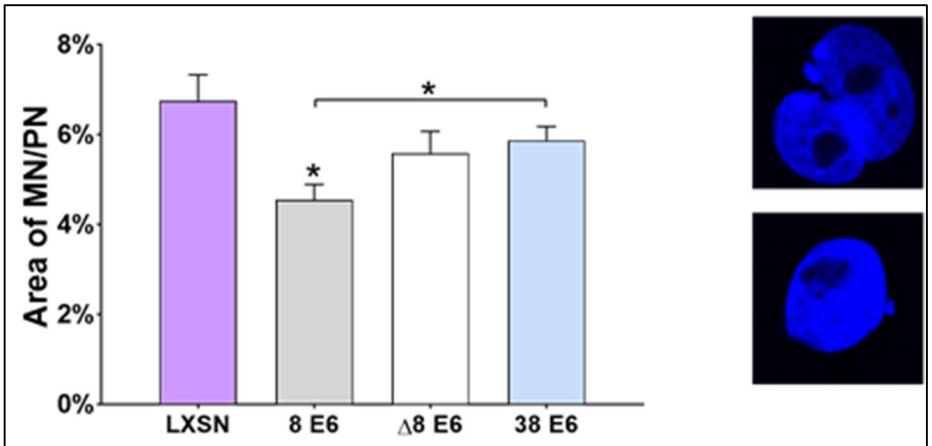

Figure A: Average micronuclei size compared to the area of the primary nucleus and representative images of small and large micronuclei.

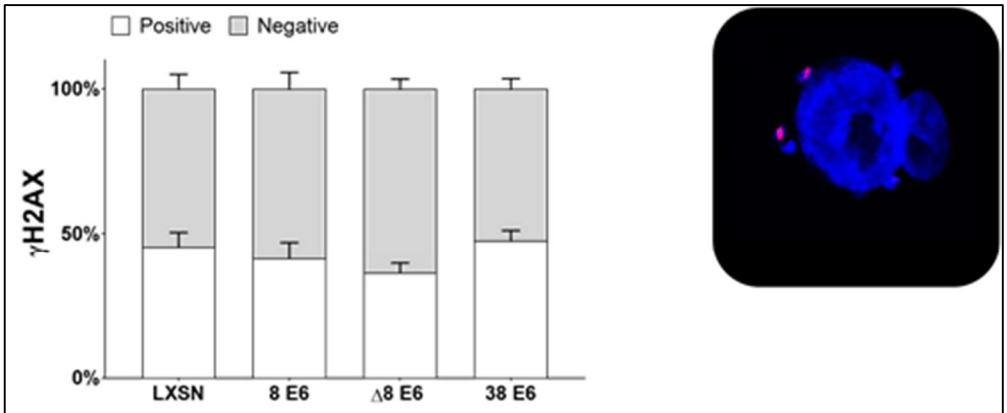

Figure B: Frequency of H2AX staining in micronuclei and representative image.

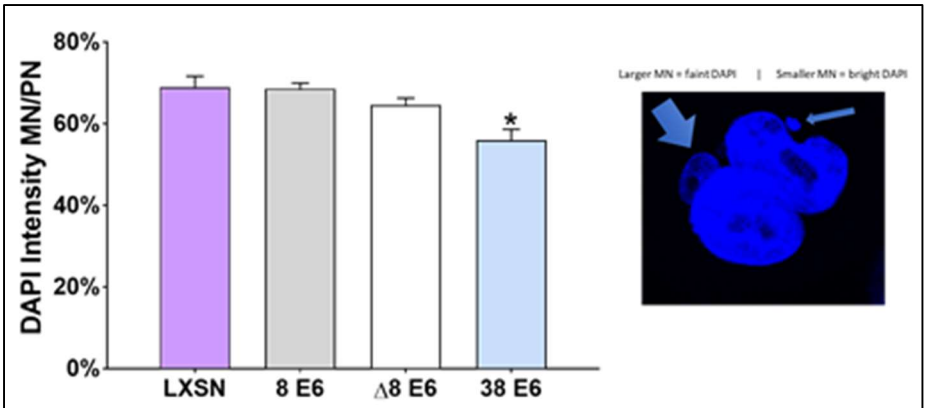

Figure C: Average DAPI Intensity in Micronuclei compared to primary nucleus and representative image.

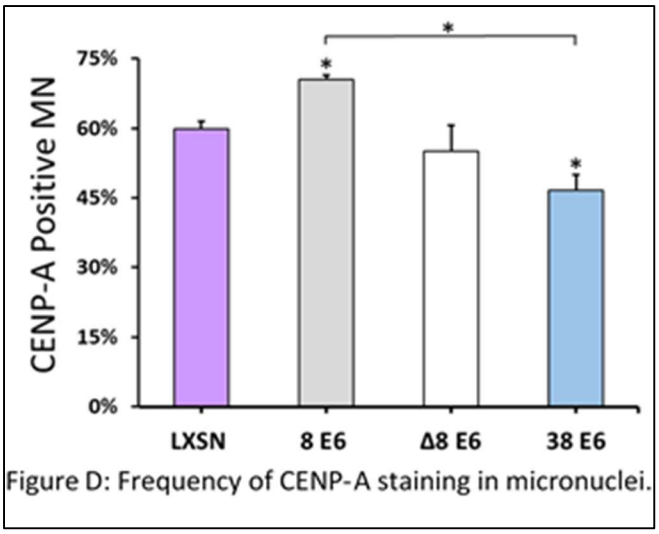

Figure D: Frequency of CENP-A staining in micronuclei.

Subtask 4: Determine if β-HPV E6 can further impede crosslink repair in cells where ATR and p300 are targeted for RNAi mediated degradation (Assayed by immunofluorescence microscopy).

We have completed and executed the MTA (Kansas State University and International Agency for Research on Cancer) that allowed us to obtain cells expressing other genes from other β-HPVs. The ongoing pandemic delayed this exchange but the cells were recently obtained and we have continued define aneuploidy and micronucleation in them. We also used whole generation sequencing to show that 8E6 causes chromothripsis (100s-1000s of mutations in a single chromosome over a single cell division). These data will be submitted for publication in the next 3 months.

Milestones Achieved: We will…

(1) obtain oversight from HRPO necessary to avoid unintentional or unethical mistreatment of the human subjects.

This was completed during the first budget period.

(2) get the staff necessary to complete this aim.

This was completed during the first budget period.

(3) learn the extent to which β-HPV E6 prevents ICL repair through p300-independent mechanisms.

Our shift in focus has been very fruitful, resulting in the manuscript described above. We consider ourselves to have achieved and surpassed this milestone.

(4) learn the extent to which β-HPV E6 prevents ICL repair through p300- and ATR-independent mechanisms.

Our shift towards focusing on micronuclei has identified p300 and ATR independent induction of micronuclei. These data will be published in a manuscript that we expect to submit in the next 3 months.

Major Task 2: Determine the mechanism of β-HPV E6's p300-independent inhibition of DNA crosslink repair.

As described above, we have refocused our attention. Remaining within the framework of our proposal, we have extending the efforts of AIM 2 by defining how β-HPV E6 expressing cells recover from failed cytokinesis. These data were combined with data from Major Task 1 and published in Dalton Riforgiate and Wallace 2020.

Subtask 1: Define the extent to which BCL6 inhibition prevents β-HPV E6 from preventing DNA crosslink repair by immunofluorescence microscopy and chemical inhibition and RNAi-mediated knockdown of BCL6.

We accomplished our goal of understand how β-HPV E6 expressing cells recovered from H2CB-induced failed cytokinesis and identified a common cellular mutation that acted synergistically with β-HPV E6 to promote recovery. These data have been described in preceding sections and as mentioned can be found in the peer-reviewed manuscript Dacus, Riforgiate and Wallace 2020. This was incorporated in Subtasks 1-4 of this Major task.

Subtask 2: Determine if β-HPV E6 interacts with ATR/ATRIP using Co-immunoprecipitation reactions.

See above

Subtask 3: Determine if BCL6 is acting as a transcriptional repressor of ATR expression using chromatin immunoprecipitation.

See above

Subtask 4: Define the impact of β-HPV E6 on BCL6 protein stability and transcription using immunoblots and qPCR.

See above

Subtask 5: Identify novel β-HPV E6 interacting proteins by mass spectrometry with validation by co-immunoprecipitation.

We have continued our efforts to understand p300-independent activities of β-HPV E6 with regard to DSB repair. Specifically building off of the observation that β-HPV ΔE6 attenuated, we have defined a p300-independent mechanism of NHEJ inhibition. β-HPV ΔE6 and β-HPV E6 both prevent the induction of a repair complex essential for NHEJ. Namely, XRCC4 foci are not induced by the DSBs created from zeocin exposure. These data are shown in figure 18 and are under-review in the journal Cancers. In this figure we also show that DNA-PK mediated phosphorylation is attenuated by β-HPV E6, but this phenotype was p300-dependent.

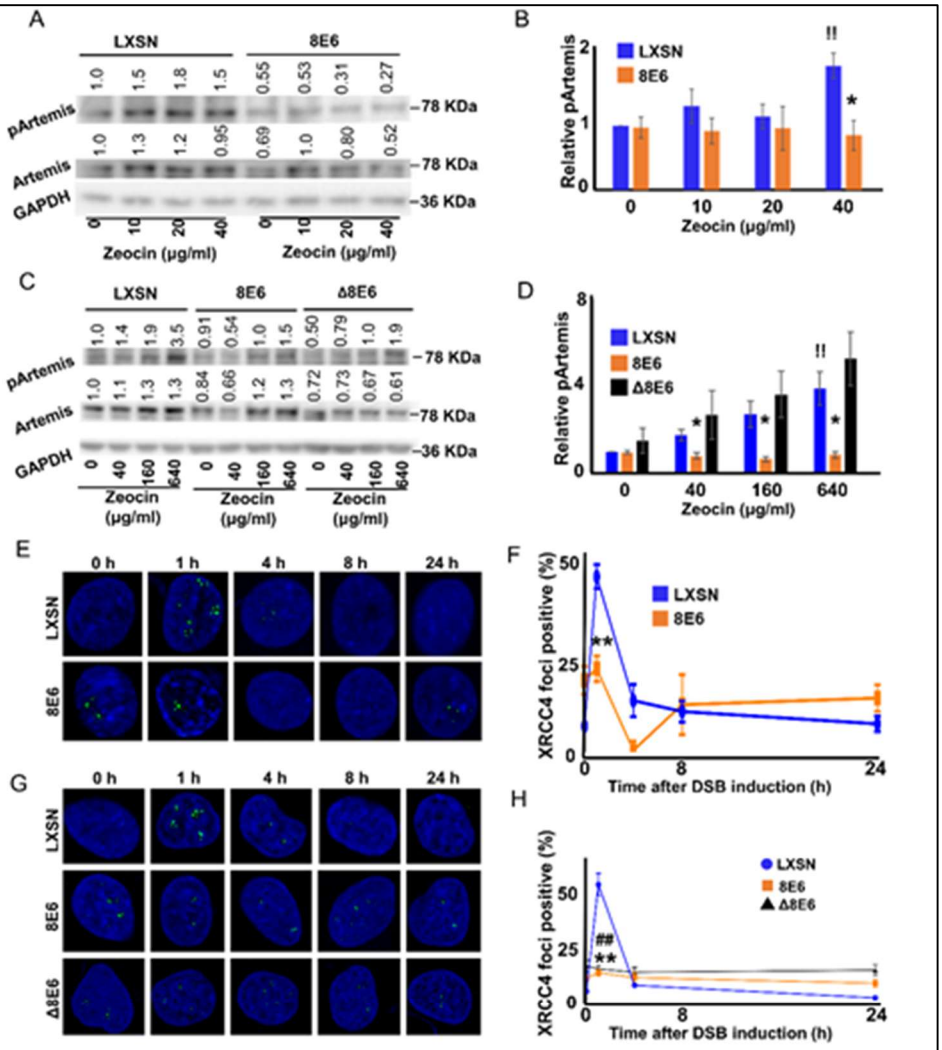

Figure 5. β-HPV 8E6 decreases pDNA-PKcs target proteins pArtemis abundance and XRCC4 foci formation. (A) Representative immunoblot showing pArtemis and total Artemis in HFK LXSN and HFK β-HPV 8 E6. (B) Densitometry of immunoblots (n=4) of pArtemis normalized to total Artemis and to GAPDH as a loading control. (C) Representative immunoblot showing that pArtemis and total Artemis in U2OS LXSN, U2OS β-HPV 8 E6, or U2OS β-HPV Δ8 E6. (D) Densitometry of immunoblots (n=4) of pArtemis normalized to total Artemis and to GAPDH as a loading control. (E) Representative images of XRCC4 foci in HFK cell lines 0-24 hours following Zeocin exposure. (F) Percentages of XRCC4 foci positive (>2) HFK cells following DSB induction. (G) Representative images of XRCC4 foci in U2OS cell lines 0-24 hours following Zeocin exposure. (H) Percentages of XRCC4 foci positive (>2) U2OS cells following DSB induction. All values are represented as mean ± standard error from at least three independent experiments. Statistical differences between groups were measured by using Student's T-test. * indicates P<0.05. ** indicates P<0.01. !! indicates significant difference between Zeocin treated and untreated group. ## indicates significant difference between U2OS β-HPV Δ8 E6 and control.

Milestone(s) Achieved: We will learn…

(1) whether β-HPV E6 inhibits ICL repair through BCL6 inhibition.

We have not been able to complete the originally proposed milestones, because our BCL6 result produced a phenotype that was too small/variable for further characterization. To honor our commitment to the award, we have instead extended our work in two ways to identify β-HPV E6's p300-dependent and -independent genome

destabilizing activity. We have published a manuscript describing how β-HPV E6 acts synergistically with telomerase activation to promote long term proliferation after failed cytokinesis. Second, we identified β-HPV E6's p300-independent ability to impair NHEJ and a mechanism for this attenuation (inhibition of XRCC4 foci formation).

(1) whether β-HPV E6 interacts with ATR/ATRIP.

See above.

(2) whether β-HPV E6 induced increases in BCL6 result in transcriptional repression of ATR.

See above.

(3) the extent to which β-HPV E6 chances BCL6 protein stability.

See above.

(4) the extent to which β-HPV E6 changes BCL6 transcription.

See above.

(6) the identity of novel β-HPV E6 interacting proteins.

See above.

What opportunities for training and professional development has the project provided?

- Both graduate students funded in this project have presented their work three times at a international conferences (DNA tumor virus meeting and international papillomavirus meeting). Dalton Dacus also presented his work at a virtual assembly of the American Society for Virology. The PI received significant mentoring from Drs. Laimins, Gao and Clem. Further, he was invited to give 18 seminars on his work at Universities across the country and internationally.

- **What do you plan to do during the next reporting period to accomplish the goals?**
  - **This is the final reporting period. Our efforts since the last reporting period are noted below. They allowed us to either complete all of the proposed work or additional data when our hypotheses were not validated.**
  - Dr. Wallace will continue his career development adapting to the realities presented by COVID-19. Specifically, we will engage with his mentors virtually and continue to grow his connections by presenting at virtual conferences.
  - We are in the process of implementing two next gen sequencing based experiments related to this grant but supported from outside sources of funding.
  - We expect to publish at least one additional paper from the work supported here.
  - We have resubmitted our application to the American Cancer Society and hope for positive news later this month. An R01 grant application to the National Institutes of Health will be submitted on topics relevant to the work funded here.

How were the results disseminated to communities of interest?

- **How were the results disseminated to communities of interest?**
  - Our group is highly engaged in the dissemination of our findings to the local regional and international communities of interest.
  - We have a very active twitter account (@wallacehpvlab) that we use to communicate our work to a network of followers.
  - We have engaged over 100 community members in hands-on tours of our lab during each reporting period, prior to COVID-19. These outreach activities are not available now. We have however continued our efforts to use our proximity to a US military base (Fort Riley) to facilitate engagement with the military health community.
  - Before COVID-19 limited our outreach efforts, we participated in events organized by the K-State Office for the Advancement of Women in Science and Engineering to promote the participation of women in science (Girls Reaching Our World and EXploring sCIence, Technology and Enginnering).
  - The PI also gave a public lecture as part of the local "Science on Tap" series.

What do you plan to do during the next reporting period to accomplish the goals?

Nothing to report (final report)

4. IMPACT:

What was the impact on the development of the principal discipline(s) of the project?

- β-HPV infections are believed to cause cancer by increasing the ability of sunlight and radiation to cause skin cancer. We have hypothesized that they do this by preventing the cells they infect from properly responding to damaged DNA. In this period, we have published five manuscripts (Three of these were relevant to this funding). The data presented in these papers support this idea by showing the proteins from this virus destabilize the host genome. These results are important for the military community in particular for two reasons. 1. Military service is a risk factor for skin cancers. 2. Military service is associated with increased sun and radiation exposure.

What was the impact on other disciplines?

- Our work has broad impacts as it helps clarify the role of p300 in signaling pathways known to suppress tumors. This includes investigators studying the Hippo Pathway, chromosome segregation and maintenance, double strand break repair, cell cycle regulation and crosslink repair.

What was the impact on technology transfer?

- *The overall goal of this project is to determine the oncogenic potential of β-HPV infections so that anti-viral drugs or vaccines can be developed. Our results remain supportive of this goal.*

What was the impact on society beyond science and technology?

- Efforts to prevent cancer will always have the potential to impact society at large. Our work remains impactful in this manner.
- Our outreach and engagement efforts also help grow lay knowledge of science and encourage participation in science by underrepresented members of society

5. CHANGES/PROBLEMS:

Changes in approach and reasons for change

- *We have continued and expanded the new course described in our report for budget period 2.*

Actual or anticipated problems or delays and actions or plans to resolve them

none

Changes that had a significant impact on expenditures

none

Significant changes in use or care of human subjects, vertebrate animals, biohazards, and/or select agents

Significant changes in use or care of human subjects

none

Significant changes in use or care of vertebrate animals

none

Significant changes in use of biohazards and/or select agents

none

6. PRODUCTS:

- **Publications, conference papers, and presentations**

Journal publications.

I believe all acknowledge the federal support.

- "Beta Human Papillomavirus 8E6 Attenuates Non-Homologous End Joining by Hindering DNA-PKcs Activity." Hu C, Bugbee T, Gamez M, Wallace NA. Cancers, 2020. PMID 32825402 LINK
- Beta Human Papillomavirus 8E6 Attenuates LATS Phosphorylation after Failed Cytokinesis. D Dacus, C Cotton, TX McCallister, NA Wallace. 2020. PMID: 32238586. LINK
- β-HPV 8E6 combined with TERT expression promotes long-term proliferation and genome instability after cytokinesis failure. D Dacus, E Riforgiate, NA Wallace 2020 LINK
- DNA repair gene expression is increased in HPV positive head and neck squamous cell carcinomas. AJ Holcomb, L Brown, O Tawfik, R Madan, Y Shnayder, SM Thomas, NA Wallace 2020 LINK
- β-HPV 8E6 Attenuates ATM and ATR Signaling in Response to UV Damage. JA Snow, V Murthy, D Dacus, C Hu, NA Wallace. 2019. PMID: 31779191 LINK
- Catching hpv in the homologous recombination cookie jar. NA Wallace. 2020. PMID: 31744663 LINK
- Cervical cancer cell lines are sensitive to sub-erthemal UV exposure. Gu W., Sun S., Kahn A., Dacus D., Wendel SO., McMillan N., Wallace NA. 2019 PMID: 30517878 LINK
- mSphere of Influence: the Value of Simplicity in Experiments and Solidarity among Lab Members. Wallace NA. 2019. PMID: 31217299 LINK
- Loss of Genome Fidelity: Beta HPVs and the DNA Damage Response. Wendel SO, Wallace NA Front. Microbiol. 2017 PMID:29187845 LINK
- Characterizing DNA Repair Processes at Transient and Long-lasting Double-strand DNA Breaks by Immunofluorescence Microscopy. Murthy V, Dacus D, Gamez M, Hu C, Wendel SO, Snow J, Kahn A, Walterhouse SH, Wallace NA. 2018 PMID: 29939192 LINK
- The Curious Case of APOBEC3 Activation by Cancer Associated Human Papillomaviruses. Wallace NA, Munger K. 2018 PMID: 29324878 LINK

***Bo*oks or other non-periodical, one-time publications.**

Nothing to report

Other publications, conference papers and presentations.

Invited Seminars by Nicholas A Wallace:

16. Kansas State University Department of Diagnostic Medicine and Pathobiology, (2021) “Human Papillomavirus Oncogenes Hinder DNA Repair”

15. Louisiana State University, Shreveport Health Science Center, (2020) “HPV Oncogenes Induce and Disrupt Translesion Synthesis”

14. University of Kansas Cancer Center (2019) “HPV Oncogenes Induce and Disrupt Translesion Synthesis”

13. Department of Microbiology, Molecular Genetics & Immunology, University of Kansas Medical Center (2019) “HPV Oncogenes Induce and Disrupt Translesion Synthesis”

12. Center for Molecular Medicine’s Symposium on the missing links in HPV-Biology: Focus on Head & Neck cancer and Skin Cancer, Cologne, Germany (2019) “Interference of HPV with DNA Damage and Repair Pathway”

11. Virginia Commonwealth University Philips Institute for Oral Health Research (2018) “HPV Oncogenes Induce and Disrupt Translesion Synthesis”

10. Wake Forest University School of Medicine Microbiology and Immunology (2018) “HPV Oncogenes Induce and Disrupt Translesion Synthesis”

9. University of Kansas, Lawrence, KS (2018) “HPV Oncogenes Induce and Disrupt Translesion Synthesis”

8. Griffith University, Gold Coast, Australia (2018) “Cutaneous HPV infections and Skin Cancer”

7. Uniformed Services University Health Science Center (2018) “HPV Oncogenes Induce and Disrupt Translesion Synthesis”

6. University of Kansas Cancer Center (2017) “HPV E6 and E7 Disrupt DNA Repair”

5. Tulane University Cancer Center (2017) “HPV E6 and E7 Disrupt DNA Repair.”

4. Department of Biochemistry & Molecular Biophysics, Kansas State University (2016) “HPV and Skin Cancer”

3. Stowers Institute for Medical Research, Kansas City, MO (2016) ”HPV and Skin Cancer”

2. Xavier University of Louisiana, New Orleans, LA (2016) “Wallace lab research and research/graduate school opportunities at Kansas State University”

1. Louisiana Cancer Research Consortium (2016) “HPV, DNA Damage Repair and Skin Cancer”

Conference and Meeting Oral Presentations by Nicholas A Wallace:

11. 19th Annual Great Plains Infectious Disease (2021) “A possible role of cutaneous HPV infections in non-melanoma skin cancer.” 2021

10. 6th Workshop on Emerging Issues in Oncogenic Virus Research. Manduria, Italy. (2020) “β-HPV E6 Attenuates UV Repair” (Abstract Accepted, Conference Cancelled)

9. Midwest HPV Conference, Indiana University School of Medicine (2019) “HPV Oncogenes and Genome Stability”

8. Designing Molecules Workshop and Conference. Japan Society for Promotion of Science and K-State Department of Chemistry. (2019) “HPV Oncogenes Induce and Disrupt Translesion Synthesis”

7. International Papillomavirus Society Conference. Cape Town, SA. (2017) “β-HPV E6 inhibits the Hippo pathway in a P300-Dependent Manner”

6. International Papillomavirus Society Conference. Cape Town, SA. (2017) “Carcinogenesis and Pathogenesis State of the Field/Where are the gaps” (Session Chair and Presenter)

5. DNA Tumor Virus Meeting. Birmingham UK. (2017) “HR-α Oncogenes Induce Aberrant Translesion Synthesis”.

4. Viral Pathogenesis Symposium. University of Kansas Medical Center, (2017) “HPV E6 and E7 Disrupt DNA Repair.”

3. Johnson Cancer Center Board Meeting. Kansas State University (2016) “How human papillomaviruses (HPV) cause cancer”

2. DNA Tumor Virus Meeting. Montreal, Canada (2016) "HR-α HPV E6 and E7 Block Homologous Recombination"

1. Intercampus Virology Meeting. University of Nebraska (2016) "β-HPV, DNA Damage and Skin Cancer"

Select Conference Oral Presentations by Wallace Lab Members

24. American Society for Virology 39th Annual Meeting. (2020) "β-HPV 8E6 dysregulates the Hippo Pathway After Failed Cytokinesis" Dalton Dacus, Nicholas A. Wallace.

23. 2019 Midwest HPV and PyV Research Symposium. (2019) "One is the Loneliest Number: β-HPV E6's Quest for More Micronuclei" Dalton Dacus, Nicholas A. Wallace.

22. Johnson Cancer Research Center Awards Banquet (2019) Keynote Speaker Jazmine Snow*

21. Annual Nebraska Center for Virology Meeting. (2019) "Translesion Synthesis Protein Abundance in HPV Transformed Cell Lines" Jazmine Snow*, Nicholas A. Wallace.

20. Annual Nebraska Center for Virology Meeting. (2019) "High Risk α-HPV Oncogenes Induce and Disrupt Translesion Synthesis" Sebastian O. Wendel, Nicholas A. Wallace.

19. KINBRE Symposium. (2019) "High Risk α-HPV Oncogenes Induce and Disrupt Translesion Synthesis" Sebastian O. Wendel, Nicholas A. Wallace.

18. Annual Nebraska Center for Virology Meeting. (2019) "β-HPV E6 Inhibits Hippo Pathway Activation Following Failed Cytokinesis" Dalton Dacus, Nicholas A. Wallace.

17. Annual Nebraska Center for Virology Meeting. (2019) "Beta Genus Human Papillomavirus E6 Attenuates DNAPK Phosphorylation and Foci Resolution" Changkun Hu, Nicholas A. Wallace.

16. DNA Tumor Virus Meeting (2019) "High Risk α-HPV Oncogenes Induce and Disrupt Translesion Synthesis" Sebastian O. Wendel, Nicholas A. Wallace.

15. DNA Tumor Virus Meeting (2019) "β-HPV E6 Inhibits Hippo Pathway Activation Following Failed Cytokinesis" Dalton Dacus, Nicholas A. Wallace.

14. 45th Annual Graduate Student Research Forum "β-HPV E6 Inhibits Hippo Pathway Activation Following Failed Cytokinesis" 2019. Dalton Dacus, Nicholas A. Wallace.

13. DNA Tumor Virus Meeting (2019) "β-HPV E6 Deregulates Double Strand Break Repair". Changkun Hu, Nicholas A. Wallace.

12. Intercampus Virology Meeting (2018) "Influence of High Risk Alpha-HPV Oncogenes on Translesion Synthesis" Sebastian Wendel, Monica Gamez, Andrew Kahn*, Nicholas A. Wallace

11. DNA Tumor Virus Meeting (2018) "High Risk α-HPV Oncogenes Induce and Disrupt Translesion Synthesis" Sebastian Wendel, Laura Brown, Daniel Neill, Tyler Bastian*, Jazmine Snow*, Vaibhav Murthy, Monica Gamez, Andrew Kahn*, Dalton Dacus, Kevin Ault, Ossama Tawfik, Cen Wu, Nicholas A. Wallace

10. Intercampus Virology Meeting (2018) "β-HPV E6 Inhibits Hippo Pathway Activation following Failed Cytokinesis" Dalton Dacus, Celeste Cotton*, Nicholas A. Wallace

9. Kansas State University Division of Biology 50th Anniversary Symposium (2018) "β-HPV E6 and the Hippo Pathway" Dalton Dacus, Celeste Cotton*, Nicholas A. Wallace

8. Kansas State University Division of Biology Graduate Research Forum (2018) "β-HPV E6 and the Hippo Pathway" Dalton Dacus, Celeste Cotton*, Nicholas A. Wallace

7. DNA Tumor Virus Meeting (2018) "β-HPV E6 Inhibits Hippo Pathway Activation following Failed Cytokinesis" Dalton Dacus, Celeste Cotton*, Tristan McCallister*, Nicholas A. Wallace

6. University of Nebraska, Lincoln SciComm Conference (2018) "HPV Vaccination Prevents Cancer" Andrew Kahn*, Nicholas A. Wallace

5. Intercampus Virology Meeting (2017) "β-HPV E6 inhibits non-homologous end joining", Monica Gamez, Nicholas A. Wallace

4. Intercampus Virology Meeting (2017) “Influence of High Risk Alpha-HPV Oncogenes on Translesion Synthesis” Sebastian Wendel, Monica Gamez, Andrew Kahn*, Nicholas A. Wallace

3. Intercampus Virology Meeting (2017) “β-HPV E6 inhibits the Hippo pathway in a P300-Dependent Manner”. Dalton Dacus, and Nicholas A. Wallace

2. SUROP Oral Presentations (2016) “LINE1 Retrotransposition: Cellular Variations” Michaela Smith*, Cecily Bennet DeFreece, Nicholas A. Wallace,

1. Kansas State University SUROP Symposium (2016) “The Effect of LINE-1 Retrotransposition on DNA Damage Repair” 2016 Manhattan KS. Michaela Smith* Cecily Defreece, Nicholas A. Wallace

<u>Select Conference Poster Presentations by Wallace Lab Members:</u>

19. Meeting of the College of American Pathologists (2018) “Immunohistochemical stains directed at DNA repair genes may be helpful in evaluating Human Papilloma Virus-associated cervical squamous intraepithelial lesions” Laura Brown, Daniel Neill, Nicholas A. Wallace, Kevin Ault, Ossama Tawfik

18. K-INBRE Symposium (2018) “Beta HPV and the Hippo Tumor Suppressor Pathway” Celeste Cotton*, Dalton Dacus, Nicholas A. Wallace

17. K-INBRE Symposium (2018) “Mechanistic action of dietary flavonoids in induction of apoptosis in cancer cell lines” Vaithish Velazhahan*, Prezmyslaw Glaza, Saurav Misra, Michal Zoliewski, Nicholas A. Wallace, Brian V. Geisbrecht, and Kathrin Schrick (Award of Excellence)

16. K-INBRE Symposium (2018) “Translesion Synthesis Protein Abundance in Proliferating Cells.” Jazmine Snow*, Sebastian Wendel, Nicholas A. Wallace (Award of Excellence)

15. Emerging Researchers National Conference. (2018) “Evaluating the Ability of Merkel Cell Polyomavirus Large T Antigen to Change UV Sensitivity.” Adelina Parral*, Jazmine Snow*, Tristan McCalister*, Nicholas A. Wallace

14. American Head and Neck Society Meeting (2018) "Overexpression of homologous repair proteins in human papillomavirus positive head and neck squamous cell carcinoma by immunohistochemistry analysis. A potential target for molecular therapies" Andrew Holcomb, Laura Brown, Yelizaveta Shnayder, Rashna Madan, Ossama Tawfik, Sufi Mary Thomas, Nicholas A. Wallace

13. Sigma Xi Student Poster Session (2018) "Translesion Synthesis Protein Abundance in Proliferating Cells." Jazmine Snow*, Sebastian Wendel, Nicholas A. Wallace

12. KSU Division of Biology Undergraduate Research Scholar's Forum (2018) "Translesion Synthesis Protein Abundance in Proliferating Cells." Jazmine Snow*, Sebastian Wendel, Nicholas A. Wallace

11. Developing Scholars Program Award Ceremony. (2018) "Targeted Therapeutics to Treat Cancers Derived from Human Papillomavirus." Jazmine Snow*, Sebastian Wendel, Nicholas A. Wallace

10. ASM Missouri Valley Branch Regional Meeting. (2018) "Translesion Synthesis Protein Abundance in Proliferating Cells." Jazmine Snow*, Sebastian Wendel, Nicholas A. Wallace

9. Undergraduate Research Day at the State Capitol (2018) "Targeted Therapeutics to Treat Cancers Derived from Human Papillomavirus." Jazmine Snow*, Sebastian Wendel, Nicholas A. Wallace

8. Intercampus Virology Meeting (2018) "β-HPV E6 inhibits non-homologous end joining" Changkun Hu. Monica Gamez, Nicholas A. Wallace

7. Intercampus Virology Meeting (2018) "β-HPV E6's impact on Nucleotide Excision Repair" Vaibhav Murthy, Nicholas A. Wallace

6. KSU Division of Biology Undergraduate Research Scholars' Forum (2017) "Effects of Merkel Cell Polyomavirus Large T Antigen on UV Sensitivity." Jazmine Snow*, Tristan McCallister*, Adelina Parral*, Nicholas A. Wallace

5. ASM Missouri Valley Branch Regional Meeting (2018) "Effects of Merkel Cell Polyomavirus Large T Antigen on UV Sensitivity." Jazmine Snow*, Tristan McCallister*, Adelina Parral*, Nicholas A. Wallace

4. K-INBRE Symposium (2017) "Effects of Merkel Cell Polyomavirus Large T Antigen on UV Sensitivity." Jazmine Snow*, Tristan McCallister*, Adelina Parral*, Nicholas A. Wallace

3. KSU Division of Biology Undergraduate Research Scholars' Forum (2017) "Cisplatin Resistance in Cervical Cancer Cells" Andrew Kahn*, Sebastian Wendel, Nicholas A. Wallace

2. Intercampus Virology Meeting. (2017) "HPV Oncogenes E6 and E7 Increases Cells Sensitivity to DNA Crosslinking Agents" Monica Gamez, Sebastian Wendel, Nicholas A. Wallace.

1. KS-LSAMP Poster Session (2016) "Evaluating the Ability of Merkel Cell Polyomavirus Large T Antigen to Change UV Sensitivity." Adelina Parral*, Jazmine Snow*, Tristan McCalister*, Nicholas A. Wallace (Best Poster Presentation)8. 6th Workshop on Emerging Issues in Oncogenic Virus Research. Manduria, Italy. (2020) "β-HPV E6 Attenuates UV Repair" (Abstract Accepted, Conference Cancelled)

- **Website(s) or other Internet site(s)**

  - www.WallaceLabKSU.weebly.com
    - **This is our personal lab website. It broadcasts our twitter handle and announces major accomplishments.**
  - @wallaceHPVlab is our twitter handle.
    - This twitter account disseminates the daily activities and science news from our group. We use it to connect with our over 1100 followers. It is an effective outreach tool.

- **Technologies or techniques**

Nothing to report

- **Inventions, patent applications, and/or licenses**

Nothing to report

- **Other Products**

Nothing to report

7. PARTICIPANTS & OTHER COLLABORATING ORGANIZATIONS

What individuals have worked on the project?

Name:	*Dalton Dacus*
Project Role:	*Graduate Student*
Researcher Identifier (e.g. ORCID ID):	*Not Applicable*
Nearest person month worked:	*48*
Contribution to Project:	Mr. Dacus performed most of analysis of the hippo (Aim 2) and some of the work for AIM3
Funding Support:	*CDMRP and Wallace Startup funds*

Name:	*Changkun Hu*
Project Role:	*Graduate Student*
Researcher Identifier (e.g. ORCID ID):	*Not Applicable*
Nearest person month worked:	*48*
Contribution to Project:	*Mr. Hu has performed the analysis of the N pathway.*
Funding Support:	*CDMRP and Wallace Startup Funds*

Name:	*Jazmine Snow*
Project Role:	*Research Assistant*
Researcher Identifier (e.g. ORCID ID):	*Not Applicable*
Nearest person month worked:	*4*
Contribution to Project:	*Ms. Snow has performed the characterization of ATM signaling described above in Specific AIM 1.*
Funding Support:	*Wallace Startup funds*

Name:	*Nicholas Wallace*
Project Role:	*Primary Investigator*
Researcher Identifier (e.g. ORCID ID):	*0000-0002-3971-716X*
Nearest person month worked:	*12*
Contribution to Project:	*Dr. Wallace oversaw the work on each projects. He wrote an all manuscripts. He also submitted grants to fund future relev studies. He mentored the graduate students, post doc and res assistant in his lab. He also presented the lab's findings to ex and internal audiences.*
Funding Support:	*CDMRP Support and NIH Support*

Name:	*Laimonis Laimins*
Project Role:	*Designated Mentor*
Researcher Identifier (e.g. ORCID ID):	0000-0002-6314-623X
Nearest person month worked:	*1*
Contribution to Project:	*Dr. Laimins advised and mentored Dr. Wallace as necessary throughout the budget period.*
Funding Support:	*Dr. Laimins is supported by 2 RO1's from the NCI R21 from NIAID.*

Has there been a change in the active other support of the PD/PI(s) or senior/key personnel since the last reporting period?

Nothing to report.

What other organizations were involved as partners?

Nothing to report

8. SPECIAL REPORTING REQUIREMENTS

COLLABORATIVE AWARDS:

QUAD CHARTS:

Nothing to report

9. APPENDICES:

We have appended copies of all our published materials.

frontiers in Microbiology

REVIEW
published: 15 November 2017
doi: 10.3389/fmicb.2017.02250

Loss of Genome Fidelity: Beta HPVs and the DNA Damage Response

*Sebastian O. Wendel and Nicholas A. Wallace**

Division of Biology, Kansas State University, Manhattan, KS, United States

While the role of genus alpha human papillomaviruses in the tumorigenesis and tumor maintenance of anogenital and oropharyngeal cancers is well-established, the role of genus beta human papilloviruses (β-HPVs) in non-melanoma skin cancers (NMSCs) is less certain. Persistent β-HPV infections cause NMSCs in sun-exposed skin of people with a rare genetic disorder, epidermodysplasia verruciformis. However, β-HPV infections in people without epidermodysplasia verruciformis are typically transient. Further, β-HPV gene expression is not necessary for tumor maintenance in the general population as on average there is fewer than one copy of the β-HPV genome per cell in NMSC tumor biopsies. Cell culture, epidemiological, and mouse model experiments support a role for β-HPV infections in the initiation of NMSCs through a "hit and run" mechanism. The virus is hypothesized to act as a cofactor, augmenting the genome destabilizing effects of UV. Supporting this idea, two β-HPV proteins (β-HPV E6 and E7) disrupt the cellular response to UV exposure and other genome destabilizing events by abrogating DNA repair and deregulating cell cycle progression. The aberrant damage response increases the likelihood of oncogenic mutations capable of driving tumorigenesis independent of a sustained β-HPV infection or continued viral protein expression. This review summarizes what is currently known about the deleterious effects of β-HPV on genome maintenance in the context of the virus's putative role in NMSC initiation.

Keywords: beta HPV, DNA-damage response, skin cancer, genomic fidelity, tumorigenesis, epidermodysplasia verruciformis, viral oncogenesis, p300

OPEN ACCESS

Edited by:
Herbert Johannes Pfister, University of Cologne, Germany

Reviewed by:
Koenraad Van Doorslaer, University of Arizona, United States
Dohun Pyeon, University of Colorado Denver School of Medicine, United States

****Correspondence:***
Nicholas A. Wallace
nwallac@ksu.edu

Specialty section:
This article was submitted to Virology, a section of the journal Frontiers in Microbiology

Received: *28 September 2017*
Accepted: *31 October 2017*
Published: *15 November 2017*

Citation:
Wendel SO and Wallace NA (2017) Loss of Genome Fidelity: Beta HPVs and the DNA Damage Response. Front. Microbiol. 8:2250. doi: 10.3389/fmicb.2017.02250

INTRODUCTION

Human papillomavirus (HPV) is a family of small, non-enveloped double-stranded DNA viruses that infect mucosal and cutaneous epithelia. This family is comprised of five genera (alpha, beta, gamma, nu, and mu) spanning across over 396 different HPV types potentially inhabiting human skin (Bzhalava et al., 2014). Classification of the HPV family is based on the sequence of the L1 capsid protein (Bernard et al., 2010; de Villiers, 2013). The alpha and beta genera are most widely studied because of the pathogenesis associated with some members of these genera. α-HPV causes genital warts (low risk types, HPV 6, and 11 for example) and genital cancer (high risk types, HPV 16, 18, 31, and 45 for example) (Tommasino, 2014; Doorbar et al., 2015). While β-HPV is known to cause flat warts and non-melanoma skin cancer in individuals with compromised immune systems (Cubie, 2013), there is a growing interest in determining if these viruses can cause tumors in the general population. Further, while so called "high risk" α-HPVs have been identified, the relative oncogenic potential among the beta genus of HPV is still being discussed. Moreover, despite already consisting of ∼50 types of HPV that are sub-classified in five species (Van Doorslaer, 2013), it is likely that a large portion of β-HPV types have yet to be discovered (Ekström et al., 2013;

Bzhalava et al., 2014, 2015). Because the first β-HPV types isolated were HPV 5 and HPV 8 from cutaneous squamous cell carcinomas (cSCC) of patients with the rare disorder Epidermodysplasia Verruciformis (EV) (Pfister et al., 1981; Kremsdorf et al., 1982, 1983), these two β-HPVs have been the most extensively examined.

Because β-HPVs do not generally persist in tumors, they are hypothesized to act through a "hit and run" mechanism (Pfister, 2003; Hufbauer and Akgül, 2017). Specifically, β-HPVs are believed to hinder the repair of DNA damage caused by UV radiation making mutations more likely. For a virus that infects an area frequently exposed to UV radiation and yet requires proliferating cells to complete its lifecycle, it is reasonable that β-HPVs have developed mechanisms to prevent the cell cycle arrest that accompanies repair of UV damaged DNA. However, this could have severe consequences for the host cell as the UV-induced mutations will remain after the viral infection is cleared and could drive the development of non-melanoma skin cancers (NMSCs) without continued expression of β-HPV genes. In this review, we will begin by providing a brief synapsis of the evidence that β-HPV infections cause NMSCs as well as the cellular signaling pathways that respond to UV insults. We will provide a concise discussion of α-HPV associated tumorigenesis, as these more clearly defined mechanisms of transformation provide a useful and relevant comparison for β-HPV associated oncogenesis. Then, we will move on to the *in vitro* and *in vivo* data that demonstrate the ability of β-HPV genes to disrupt the repair of DNA, destabilizing the host genome in a manner consistent with a "hit and run" mechanism of tumorigenesis.

Transformation by Alpha Genus HPV Oncogenes

Extensive evidence has established α-HPV as the causative agent in cervical cancers and in many other malignancies in the oropharynx and throughout the anogenital tract (Hobbs et al., 2006; Moody and Laimins, 2010; Carter et al., 2011; D'Souza and Dempsey, 2011; Tommasino, 2014). Infections with high risk α-HPVs can begin a multi-decade process where cells are immortalized, accumulate destabilized genomes, and are ultimately transformed into deadly malignant tumors. Two oncogenes, α-HPV E6 and E7 proteins drive this progression by activating telomerase and degrading two tumor suppressor, p53 and pRB (Dyson et al., 1989; Münger et al., 1989; Scheffner et al., 1990; Werness et al., 1990; Huibregtse et al., 1991; Boyer et al., 1996; Klingelhutz et al., 1996; Kiyono et al., 1998; Oh et al., 2001). These oncogenes also induce aberrant activation of the DNA damage response (DDR) and in some case, impair the cells ability to repair DNA damage (Patel et al., 1999; Zimmermann et al., 1999; Moody and Laimins, 2009; Sakakibara et al., 2011; Gillespie et al., 2012; Reinson et al., 2013; Hong et al., 2015; Wallace et al., 2017). In notable contrast to β-HPV associated malignancies, tumors caused by α-HPV are dependent on the continued expression of α-HPV E6 and E7 (Hwang et al., 1993; Goodwin and DiMaio, 2000; Goodwin et al., 2000). Because the β-HPV homologs of these α-HPV oncogenes are believed to be the primary contributors to NMSC, β-HPV E6, and E7 are frequently compared to α-HPV E6 and E7. When informative, we will make similar comparisons.

Beta-HPV in Epidermodysplasia Verruciformis Patients and Organ Transplant Recipients

The oncogenic potential of β-HPV is most firmly established in people with compromised immune systems. β-HPV associated cSCCs occur in 30–60% of people with the rare genetic disorder epidermodysplasia verruciformis (EV) and presented the first link between β-HPV infections and skin carcinogenesis (Orth, 1986). β-HPV+ tumors found in people with EV generally contain a high copy number (∼300 copies/cell) of viral DNA (Dell'Oste et al., 2009). In contrast, β-HPV+ tumors of non-EV patients show a very low viral DNA copy number <1 per cell (Weissenborn et al., 2005; Arron et al., 2011). The most frequently β-HPV types associated with EV are β-HPV 5 and 8 (also less often β-HPV 14 and 20) (de Oliveira et al., 2004; Dell'Oste et al., 2009). Tumors in individuals with EV occur predominantly in parts of the body frequently exposed to the sun, suggesting a role for UV in β-HPV associated tumorigenesis (Pfister, 2003). Another group at risk for β-HPV associated cSCCs are people receiving immunosuppressive therapy following organ transplant. Organ transplant recipients (OTRs) (Bouwes Bavinck et al., 2001) show an increased susceptibility to β-HPV infections, a higher prevalence of viral DNA and a greater risk of developing non-melanoma skin cancer (Boyle et al., 1984; Kiviat, 1999). This increased risk is particularly notable if they are seropositive for β-HPV, with a hazard ratio of 2.8 (Genders et al., 2015). Both, EV-patients and OTRs display a significantly elevated viral load than the immunocompetent population (Dell'Oste et al., 2009; Weissenborn et al., 2012). Further, OTRs that have similar β-HPV viral loads to patients with EV show a 100-fold increase of cSCC incidence (Weissenborn et al., 2012). Investigations in to NMSCs in EV and OTR patient groups provide strong evidence that β-HPV infections have oncogenic potential. Additionally, the OTR patient group shows that β-HPV associated cSCCs are not limited to patients with the rare EV disorder (Howley and Pfister, 2015; Tommasino, 2017). These "special" scenarios provide the proof of context specific β-HPV induced oncogenesis, but defining the breath of β-HPV's contribution to NMSC development is a critical area of research as millions of people are diagnosed with these malignancies each year.

Beta-HPV in the General Population

β-HPVs inhabit the cutaneous epithelium and are found in abundance throughout the population (Casabonne et al., 2009; de Koning et al., 2009; Weissenborn et al., 2012; Farzan et al., 2013). A particularly frequent site of infection is the hair follicles of eyebrows (Weissenborn et al., 2012; Neale et al., 2013; Iannacone et al., 2014). Unlike α-HPV infections, which are usually sexually transmitted and occur later in life, β-HPV infections often occur during early childhood through skin to skin contact (Antonsson et al., 2003; Weissenborn et al., 2009). The persistence of α- and

β-HPVs is a further differentiating factor, although the exact mechanisms driving this difference are not fully appreciated. Median β-HPV infection duration is 8.6 months in eyebrow hairs, while infections of the skin are less common but have a median persistence of 11.3 months (Hampras et al., 2014). In contrast α-HPV infections persist longer (18.3 months on average), and upon accidental genome-integration are present for decades (Richardson et al., 2003). Suggesting reinfections, β-HPV infections can persist within a family for several years without manifestation of clinical symptoms (Hsu et al., 2009). While infections first occur in infants, advanced age is a risk-factor for a β-HPV infection (Hazard et al., 2007; Weissenborn et al., 2009). Sunburn is another risk factor, potentially due to local immune suppression (Hampras et al., 2014). The evidence of β-HPV's involvement in cSCCs of EV patients led to the classification of HPV 5 and HPV 8 as possibly carcinogenic by a WHO-IARC 2009 work group (Bouvard et al., 2009).

Epidemiology

Epidemiologically, β-HPV antibody positivity is associated with an increased risk for cSCCs, especially for infections by β-HPV 38 (Bzhalava et al., 2013; Chahoud et al., 2016). There is also a difference of β-HPV prevalence by anatomical site (Hampras et al., 2017). The most common site of infection was genital skin (81.6%), followed by forearm skin (64.4%), eyebrow hairs (60.9%), oral mucosa (35.6%), and anal mucosa (33.3%). The most common type on the sunlight exposed and therefore risk associated sites eyebrows and forearm are β-HPV 38 and β-HPV 12 respectively. High loads of β-HPV DNA are statistically associated with increased cutaneous SCC incidences at an odds ratio of ∼3 in immunocompetent Australians and immunosuppressed OTRs (Bouwes et al., 2010; Neale et al., 2013). People with cSCCs more frequently test positive for viral DNA in skin as well as anti β-HPV L1 antibodies than the general population (Forslund et al., 2007; Waterboer et al., 2008; Karagas et al., 2010; Iannacone et al., 2012; Farzan et al., 2013). The involvement of β-HPV in cSCC carcinogenesis is somewhat challenged by the low relative incidence rate of β-HPV+ cSCCs considering the high prevalence of 80% for β-HPV infections. Furthermore, unlike α-HPV+ cancers, the expression of β-HPV viral proteins is not required for tumor maintenance and the viral DNA copy-number is <1 per cell in β-HPV associated cSCCs (Meyer et al., 2001; Nindl et al., 2006). Since cSCC tumors typically occur in parts of the body exposed mutagenic UV radiation from the sun, the role of β-HPV is thought to be in the initiation and acceleration of genomic destabilization.

The phrase "hit and run" was coined to describe the hypothesize contribution of β-HPV infections to NMSCs, where the virus acts as a cofactor along with UV during tumor initiation (Bavinck et al., 2008). The destabilization of the host genome caused by sun exposure is augmented by β-HPV's ability to attenuate the cellular response to UV damage and thus increase the risk of oncogenic mutations capable of driving tumor development independent of continued β-HPV gene expression. Epidemiological studies support this hypothesis (Forslund et al., 2007; Iannacone et al., 2012) as there is increased prevalence and frequency of β-HPV in precancerous, actinic keratinosis lesions (AK). AK, otherwise known as solar keratinosis, is an abnormal growth of the skin, induced by UV exposure (Moy, 2000). Consistent with a role in tumor initiation, despite being found at very low copy numbers in cSCCs, the β-HPV viral load in AK is >50 copies/cell (Weissenborn et al., 2005). Together these data form the foundation that supports the "hit and run" model of β-HPV associated skin cancer, but this hypothesis is dependent on the ability of β-HPV infections to make UV more mutagenic.

DNA Damage Response-Pathways

The most likely way that β-HPV could amplify the destabilization of the host genome induced by UV is through the aberration of the cellular DDR. The primary type of DNA damage caused by UV are DNA intrastrand crosslinks, most often cyclobutane purimidine dimers or CPDs (Yang, 2011). Failure to properly repair these lesions can result in point mutations (Brash et al., 1991; Keohavong et al., 1991). Crosslinked DNA can also cause a replication fork collapse and subsequent double strand break in DNA (DSB) (Jeggo and Löbrich, 2007). If DSBs are not repaired, the damage becomes much more deleterious, including chromosome rearrangement or loss of entire chromosome arms (Pankotai and Soutoglou, 2013). In this section, we will introduce the biochemical pathways that coordinate the cellular response to UV-damage to preserve the integrity of the human genome. A graphical representation of the cellular response to UV induced DNA damage in S-phase can be found in **Figure 1**. During S-phase, translesion synthesis (TLS) prevents UV-induced DNA crosslinks from causing replication fork collapse by facilitating the bypass of the damaged bases (Lerner et al., 2017). Depending on the position in the cell cycle, nucleotide excision repair (NER), and the Fanconi Anemia (FA) pathways repair these crosslinks (Moldovan and D'Andrea, 2009; Marteijn et al., 2014). While FA requires sister chromosomes to complete repair and is thus limited to cells that have undergone replication, NER is not bound by cell cycle position. UV-induced DSBs are the result of replication fork collapse and therefore must occur during S-phase. Although DSB repair occurs through two major pathways, non-homologous end joining (NHEJ) and homologous recombination (HR), DSBs occurring during S-phase are repaired predominantly by HR (Mao et al., 2008). Repairing DNA lesions usually requires pausing the cell cycle to avoid escalating the damage during replication (Willis and Rhind, 2009). Finally, should the cell receive more damage than can be repaired, the intrinsic apoptosis pathway will initiate program cell death (Offer et al., 2002).

Although recognized as distinct pathways, the individual proteins that make up these repair mechanisms are often shared. This is particularly true for repair kinases (Yang et al., 2003; Yan et al., 2014). For instance, ATR controls the rate limiting step of NER (through phosphorylation mediated stabilization of XPA) and facilitates translesion synthesis by phosphorylating the TLS-specific polymerase, Polη (Chen et al., 2008; Göhler et al., 2011; Lee et al., 2014). ATR's kinase activity is similarly necessary for the repair of crosslinked DNA by the FA pathway and plays a role in DSB repair via the homologous recombination pathway (Jazayeri et al., 2006; Shiotani and Zou, 2009; Shigechi et al., 2012;

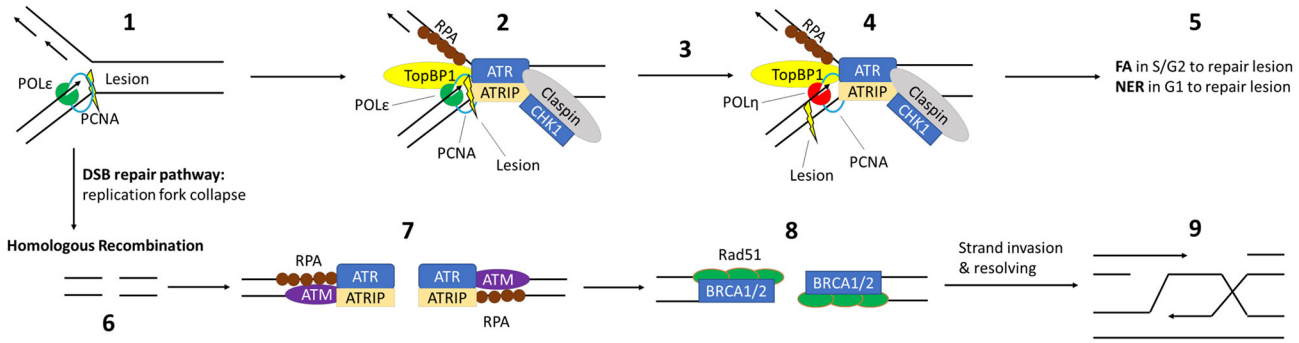

FIGURE 1 | Critical DDR Pathways for UV induced DNA Damage: (1) UV induces an intrastrand lesion, causing the replication fork to stall in S-pase. (2) Exposed ssDNA is coated with RPA, followed by recruitment of TopBP1 and ATR/ATRIP. TopBP1 accelerates autophosphorylation of ATR. Claspin and CHK1 are recruited and phosphorylated, promoting fork stabilization. (3) This leads to Rad6/Rad18 recruitment and mono-ubiquitination of PCNA (not shown), triggering the switch from high fidelity replication DNA-polymerases to y-family polymerase Polη. (4) Then, Polη replicates past the lesion and normal replication can continue after a repeated polymerase switch back to the high-fidelity replication polymerase. (5) The lesion itself is repaired by either the FA or NER pathway. (6) Prolonged stalling leads to replication fork collapse into a DSB. The MRE11, Rad50 and Nbs1 complex (not shown) is recruited to this DSB, initiating strand resection and recruitment/activation of ATM. (7) After strand resection, the exposed ssDNA is coated by RPA and ATR/ATRIP is recruited. (8) RPA is then replaced by RAD51, with the assistance of BRCA1 and BRCA2. (9) This facilitates homology-dependent single strand invasion and resolution of the lesion.

Maréchal and Zou, 2013). A similar situation exists for the related kinase, ATM. ATM phosphorylates proteins critical for the FA, NER, and HR repair pathways (Ray et al., 2013, 2016; Shiloh and Ziv, 2013). It may also play a role in translesion synthesis. Further, both ATM and ATR can stabilize p53 in response to DNA damage, causing p53-dependent DNA repair or apoptosis (Kruse and Gu, 2009; Cheng and Chen, 2010). ATM and ATR are both classically involved in DNA damage induced cell cycle arrest (Reinhardt and Yaffe, 2009). Both of these kinases also help pause the cell cycle progression by phosphorylating/activating cell cycle regulatory proteins (CHK1 and CHK2) (Branzei and Foiani, 2008). Finally, ATM and ATR also facilitate programed cell death or apoptosis should the cell's DNA be too extensively damaged. Specifically, their phosphorylation of p53 stabilizes the tumor suppressor and can result in p53-dependent apoptosis (Banin et al., 1998; Tibbetts et al., 1999; Shiloh and Ziv, 2013).

The RPA complex (RPA14, RPA32, and RPA70), BRCA1 and BRCA2 are similarly important for a myriad of DDRs (Yoshida and Miki, 2004; Maréchal and Zou, 2015). The RPA heterotrimer binds single stranded DNA (ssDNA) protecting it from degradation. Because ssDNA intermediates occur during both homologous recombination and translesion synthesis, RPA proteins are essential for these repair mechanisms. Both the FA and HR pathways require BRCA1 and BRCA2. FA pathway proteins contain the prefix "FANC" in their names indicating that many of these proteins were named after loss of the gene was shown to result in the clinical manifestation (Fanconi Anemia) from which the repair pathway derives its name, for example, FANCA, FANCB, FANC. Indicative of its requirement for FA repair an alternative name for BRCA2 is FANCD1. Moreover, BRCA1 was recently shown to be a critical component of the FA pathway (Domchek et al., 2013; Sawyer et al., 2015) and even described as the pathway's "missing link" (D'Andrea, 2013). The requirement of BRCA1 and BRCA2 in repair of DSBs by homologous recombination has been established for over a decade. Further indicative of how intertwined the cellular DNA response is, ATR and ATM both play regulatory roles in repair by phosphorylating the RPA complex, BRCA1 as well as BRCA2.

EFFECTS OF β-HPV E6 ON DNA DAMAGE RESPONSE

Inhibition of Apoptosis

The E6 protein of β-HPV can hinder both DNA repair machinery and apoptotic pathways in response to DNA damage. Unlike high risk α-HPVs, it does not commonly degrade the "guardian of the genome," p53, one of the most prominent high-risk E6 targets, directly (Scheffner et al., 1990; White et al., 2014). The tumor-suppressor, p53, is an important signaling protein that regulates two large subsets of target proteins: negative regulators of cell cycle progression (p21, 14-3-3, GADD45α) and pro-apoptotic proteins (PUMA, BAX, BAK). In normal cells, p53 has to balance on a fine line between sufficient activity to ensure genome fidelity and tumor suppression as well as avoiding hyperactivity that would induce abnormal aging by depleting stem-cell populations (Vogelstein et al., 2000; Reinhardt and Schumacher, 2012). Compared to high risk α-HPV E6s, β-HPV E6, apart from β-HPV 49, have a lower affinity for a cellular E3 ubiquitin ligase, known as E6AP or UBE3A, and are therefore not able to form the E6-E6AP complex required for proteasomal degradation of p53 (Huibregtse et al., 1991; Cornet et al., 2012). Instead, β-HPV types 17, 38, and 92 have been shown to bind to p53 directly and stabilize it (White et al., 2012), while β-HPV 23 has been shown to interfere with the phosphorylation-dependent activation of p53 by inhibiting HIPK2 (Muschik et al., 2011). β-HPV 5 and β-HPV 8 delay the stabilization and phosphorylation after UV irradiation (Wallace et al., 2014). HIPK2 is a protein kinase that can phosphorylate p53 at Ser 46, which subsequently leads to the acetylation of p53 at Lys 382 and a promotion of p53 target gene expression. More specifically, HIPK2's activity is UV-induced

and UV exposure leads to HIPK2 mediated growth arrest or apoptosis via p53. β-HPV 38 E6 induces the accumulation of ΔNp73, altering p53 functions (Accardi et al., 2006). These effects cause the alteration or loss of p53's activity as a transcriptional co-factor and impact both apoptosis- (Fas, BAX) and cell cycle checkpoint pathway (p21) gene expression (White et al., 2014). p53 is also a known transcription factor for the TLS polymerase Polη, implying the TLS DDR pathway as a suitable target for investigation (Lerner et al., 2017).

The selection between a p53-mediated checkpoint activation and p53-mediated apoptosis depends on a cell type specific threshold of p53 expression and activation (Kracikova et al., 2013). Mild DNA damage triggers p53-dependent checkpoint activation and subsequent DNA repair while moderate DNA damage causes p53-mediated senescence. Excessive DNA damage or failed cytokinesis induce apoptosis (Chen et al., 1996). β-HPV E6 can also inhibit apoptosis downstream of p53. The interaction of E6 with a pro-apoptotic protein, Bcl2 homologous antagonist killer (BAK), is a highly conserved function across HPV types and genera (Thomas and Banks, 1999; Simmonds and Storey, 2008; Underbrink et al., 2008; Jackson and Bartek, 2009; Holloway et al., 2015; Tomaić, 2016). Increases in BAK abundance are an essential step in the intrinsic apoptotic pathway (Chittenden et al., 1995). β-HPV E6 prevents the accumulation of Bak following UV-irradiation inducing DNA damage. An overview of the different pathways for β-HPV E6 mediated inhibition of apoptosis and the β-HPV types involved can be found in the upper right panel of **Figure 2**.

Interference with Checkpoint Signaling & DNA Damage Repair

Upstream of the inhibition of apoptosis, β-HPV E6 can attenuate G1 to S-phase cell cycle checkpoint induction in response to DNA damage (Wallace et al., 2012; Hufbauer et al., 2015) and continue cellular proliferation while DNA damage repair is attenuated (Giampieri and Storey, 2004). These effects arise from the interaction of β-HPV E6 with the acetyltransferase p300 (Muench et al., 2010; Howie et al., 2011). As an important coactivator of DDR gene transcription, the loss of p300 activity has far reaching consequences. β-HPV 5 and 8 have been shown to facilitate the destabilization of p300 (Howie et al., 2011; Wallace et al., 2012, 2013), while β-HPV 38 has been shown to inhibit p300 acetyltransferase activity (Muench et al., 2010). The steady state levels of the DDR kinases ATM and ATR as well as BRCA1 and BRCA2 are reduced because of the lack of p300 in β-HPV 5 and β-HPV 8 E6 expressing cells (Wallace et al., 2012, 2013, 2015). This attenuates the repair of UV induced cyclobutane pyrimidine dimer (CPD), increases the UV-induced frequency of DSBs and attenuates LINE-1 retrotransposition. Double strand breaks can be a secondary effect of UV-induced DNA damage, occurring when a replication fork collapses at an unrepaired CPD. Both the repair of CPDs (ATR dependent) as well as the repair of DSBs (ATM, BRCA1 and BRCA2 dependent) are significantly delayed by β-HPV 5 and β-HPV 8 E6 (Giampieri and Storey, 2004; Wallace et al., 2012, 2015). γH2AX is a known marker for DSBs and its foci kinetics can be utilized as indicators for DSB-repair. The (β-HPV 5 E6 and 8 E6) p300 degradation-dependent attenuation of BRCA1/BRCA2 expression and foci formation led

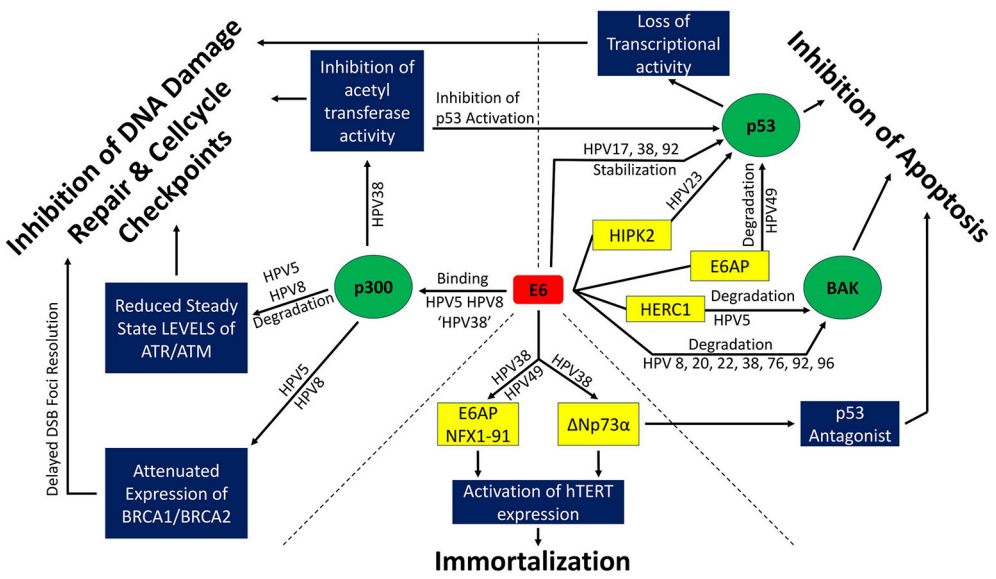

FIGURE 2 | β-HPV E6 and its effects on genome stability. Interactions among β-HPV E6s and proteins involved in DNA repair and cell cycle check points (upper left third), apoptotic signaling (upper right third), and immortalization (bottom third) are depicted. Green circles denote cellular proteins that are central to β-HPV E6's ability to alter the cellular response to DNA damage. Blue boxes depict the diversity of cellular processes altered through the manipulation of the green circular proteins. Yellow boxes represent proteins that cooperate in the manipulation of the green circular proteins or facilitate immortalization. 'HPV 38' refers to the fact that while β-HPV 38 E6 can bind p300, it does not bind it strong enough to destabilize the histone acetyltransferase.

to delayed γH2AX foci resolution after DSBs were induced by ionizing radiation (Wallace et al., 2015).

ATR and ATM activate cell cycle checkpoints by phosphorylating checkpoint kinases Chk1 and Chk2 respectively. Activation of Chk1/Chk2 induces cell cycle arrest and DDR (Reinhardt and Yaffe, 2009). β-HPV 5 and 8 E6 reduce steady state levels of ATM and ATR *in vitro* as well as reduced pATM and pATR levels *in vitro* and *in vivo* (Hufbauer et al., 2015). This leads to an attenuated Chk1 phosphorylation and impaired G1 to S-phase checkpoint activation, presenting a bypass to an important tumor-suppressing barrier. Furthermore, p300 is an important transcriptional cofactor for BRCA1, BRCA2 (Both essential proteins for HR) (Goodman and Smolik, 2000; Pao et al., 2000; Yoshida and Miki, 2004) and has been shown to be essential for proper cytokinesis and the faithful resolution of mitotic figures (Turnell et al., 2005; Xia et al., 2012). Attenuation of proper checkpoint signaling and the consequent possible unscheduled cell cycle progression leaves pre-existing DNA damage unaddressed. This allows less severe types of damage (for example, UV-induced intrastrand crosslinks) to evolve into more deleterious types of DNA damage like DSBs. β-HPV E6 expressing cells have been shown to contain a significantly larger portion of multinucleated cells *in vitro* (Wallace et al., 2014), pointing to a possible attenuation of the Hippo pathway. The Hippo pathway stabilizes p53, inactivates the oncogene YAP and induces apoptosis in the event of failed cytokinesis (Harvey et al., 2013; Ganem et al., 2014). The mechanisms through which β-HPV E6 disrupts the DDR are depicted in the upper left panel of **Figure 2**.

In addition to p300-dependent checkpoint inhibition, β-HPV 5E6 and 8E6 can bind the transcription factor SMAD3, thereby inhibiting the transforming growth factor-beta (TGF-β) pathway (Mendoza et al., 2006). TGF-β has a well-described dual role in carcinogenesis. In normal cells and early carcinomas, it acts as tumor suppressor through cytostatic effects. As the cancer progresses, the TGF-β aids proliferation, survival, invasion, and angiogenesis of tumor cells (Lebrun, 2012). Destabilization of the SMAD3 may attenuate these tumor suppressive effects by inhibiting the expression of CDK inhibitors p16, p17, p21, and p27 and possibly promoting unscheduled cell cycle progression from G1- into S-phase (Itoh et al., 2000; ten Dijke and Hill, 2004). Disruption of the TGF-β pathway has also been linked to an impaired function of DSB-repair following ionizing radiation (Kirshner et al., 2006; Bouquet et al., 2011; Kim et al., 2015).

Additional Functions of β-HPV E6

Additional notable functions of β-HPV E6 include hTERT stabilization (β-HPV 5, 20, 22, 38; Bedard et al., 2008; Gabet et al., 2008; Cornet et al., 2012), which may stabilize the genome by preventing unstably short telomers. Conversely, it could decrease genome fidelity by aborting the role of telomers as a "cellular clock" that prevent proliferation of older cells that are more likely to contain mutations (Sharma et al., 2003). Another target of β-HPV 5 and 8 E6 is the Notch signaling pathway. The Notch signaling pathway has been shown to have tumor suppressive functions in epithelial cells (Reichrath and Reichrath, 2012) and can decide cell fate (Lai, 2004). It can also act as a negative regulator of the ATM-dependent DDR (Vermezovic et al., 2015). β-HPV 5 and 8 interfere with the Notch signaling pathway through interaction with MAML1. The β-HPV E6-mediated repression of Notch signaling delays S-phase cell cycle exit and differentiation (Brimer et al., 2012; Meyers et al., 2013). Prolonged or perpetual existence in S-phase in combination with impaired DNA-damage signaling and attenuated DDR could lead to cross-amplification of these individual effects.

Summary

β-HPV E6 attenuates UV-induced apoptosis and DDR through interaction with multiple targets. BAK degradation and prevention of apoptosis is highly conserved throughout the β-HPV genus. Less common is the inhibition of apoptosis through direct interaction with and degradation of p53 (β-HPV 49, E6AP mediated) or the inhibition of p53 activation (β-HPV 23 through HIPK2 interaction). β-HPV 17, 38, and 92 E6 interact with p53 directly, leading to its stabilization but altering or restricting p53's transcriptional activity. β-HPV 5, 8, and 38 E6 interfere with DDR and checkpoint signaling through interaction with p300. A combination of inhibited apoptosis, impaired DNA damage signaling and attenuated DSB response bears a potential to destabilize the genome over time or cause carcinogenesis in combination with DNA-damaging agents that is consistent with β-HPV's proposed contribution to skin cancer. Notably, although through markedly different mechanisms, high risk α-HPV oncogenes similarly contribute to tumorigenesis by impairing the cellular response to genome destabilizing events.

E7 AND ITS INFLUENCE ON CELL CYCLE PROGRESSION AND DDR

Promotion of Cell Cycle Progression

A canonical function of the high risk α-HPV E7 oncogene is the degradation of the tumor suppressor pRb (Moody and Laimins, 2010). In normal cells, the function of pRb is the suppression of E2F transcription factor dependent genes through binding E2F and inhibiting its association with promoters (Dyson, 1998). E2F-family proteins facilitate cell cycle progression and proliferation by promoting the expression of a variety of genes encoding for proteins involved in G1/S-phase transition (Bertoli et al., 2013). High risk α-HPV E7 oncogenes bind directly to pRb via the highly conserved LXCXE binding motif (Münger et al., 1989). This leads to the disruption of the E2F—pRb complex, allows E2F to bind to its transcriptional targets (Chellappan et al., 1992). E2F target expression (for example cyclin A or cyclin E) then facilitate premature cell cycle progression and S-phase entry (Zerfass et al., 1995). Cell cycle checkpoints are meant to pause the cell cycle in case of DNA damage and allow time to repair the damage, or, if the damage surpasses a threshold, induce senescence or apoptosis. Cell cycle checkpoints are an integral part of a cells quest to maintain genome integrity. Consequently, attenuated checkpoint activation leads to a destabilization of the genome through accumulating DNA damage (Malumbres and Barbacid, 2009). α-HPV E7 allows keratinocytes with damaged DNA to progress through cell cycle check points, even when p53 is induced (Demers et al., 1994). Much like these α-HPV

E7s, several of the β-HPV E7s (β-HPV 5, 8, 38, 49) can interact with Rb (Yamashita et al., 1993; Caldeira et al., 2003; Cornet et al., 2012). However, the β-HPV E7 interactions tend to cause a hyperphosphorylation of Rb in Keratinocytes, rather than its destabilization (Caldeira et al., 2003; Cornet et al., 2012). Hyperphosphorylation of Rb inhibits its ability to bind and inactivate E2F, allowing E2F to promote transcription of its target genes (Bertoli et al., 2013). Additionally, β-HPV 24, 38, and 49 E7 severely attenuate pRb half-life in rodent fibroblasts, while β-HPV 14, 22, 23, and 36 do not affect pRb's half-life (Cornet et al., 2012). Cornet et al. also found that in the context of E6 and E7 expressing cells, β-HPV 14 and 22 can degrade pRb, but do not induce the expression of cyclin A or Cdk1. Cdk1 is essential for cell cycle progression(Santamaria et al., 2007).

Alteration of the p53-Transcriptional Network

The tumor suppressor p53 is an essential factor in the avoidance of inappropriate cell proliferation in the presence of genotoxic stress. It has transcriptional targets in several pathways, including DNA damage tolerance and apoptosis (Espinosa et al., 2003; Yu and Zhang, 2005; Beckerman and Prives, 2010). While the mechanisms of how high Risk α-HPV E7 disrupts p53 activity remain a poorly defined, significantly more is known about how some β-HPV E7 proteins disrupt this essential tumor suppressor. ΔNp73 is an important antagonist of the p53 gene family and participating in a negative feedback loop with p53 (Bailey et al., 2011). β-HPV-38 E7 promotes the accumulation and stability of ΔNp73α through both transcriptional and post-translational mechanisms (Accardi et al., 2006, p.73; Saidj et al., 2013). β-HPV 38 E7 promotes the accumulation of double monophosphorylated p53 (serine 15 and 392) in the nucleus. These dual p53 phosphorylation events increase ΔNp73α expression. β-HPV 38 E7 also mediates the nuclear translocation of the IκB kinase (IKKβ) that increases the stability of ΔNp73α by phosphorylating it at serine 422 (Accardi et al., 2011). Furthermore, IKKβ, ΔNp73α, DNMT1, and EZH2 form a transcription regulatory complex. This complex is able to bind to a subset of p53 regulated promoters and interferes with the expression of DDR pathway- and apoptosis-related genes, but not with pro-survival genes like Survivin. This implies a role of β-HPV-38 E7 in the inhibition of p53 dependent apoptosis and allows for speculation on the influence of β-HPV E7 over DDR-proteins that depend on p53 activity as a transcriptional factor (for example Polη of the TLS pathway and XPC of the NER pathway) (Fischer, 2017).

Other Functions Related to DDR

A systematic screening of E7 interacting protein has shown that E7 from β-HPVs 8, 25, and 92 can interact with the tyrosine phosphatase and tumor suppressor PTPN14. While several high- and low-risk α-HPV types have been shown to degrade PTPN14 (White et al., 2016; Szalmás et al., 2017), the role of the β-HPV E7—PTPN14 interaction is yet to be investigated. PTPN14 is a required regulator of the Hippo signaling pathway, as it is necessary for the translocation of the Hippo transcription factor, YAP1, from the nucleus to the cytoplasm (Wang et al., 2012). This indicates that β-HPV E7 may attenuate the Hippo pathway, if β-HPV E7 proves to also be capable of PTPN14 destabilization. The Hippo pathway plays a crucial role in the control of proliferation and induces apoptosis in the event of cytokinesis (Ganem et al., 2014). Phosphorylation of Yap1, a part of the hippo pathway, is a critical step in the induction of apoptosis in response to DNA damage (Levy et al., 2008). β-HPV infections occur in the skin and thus in an environment where UV-induced cell cycle arrest and apoptosis occur with some frequency. As a result, it would not be surprising if there yet undiscovered abilities of β-HPV E7 to disconnect the cellular response to UV in manners that promote the β-HPV lifecycle.

MOUSE MODELS: EVIDENCE FOR A ROLE OF β-HPV IN CARCINOGENESIS VIA A HIT AND RUN MECHANISM

Mouse models can be an effective tool for elucidating the oncogenic potential of β-HPVs. The most common of these is the transgenic (tg) mouse model that expresses can individual and groups of β-HPV genes (E2, E6, E7, E6/E7) or the entire early region of the virus under a keratin promoter. Placing the expression under a keratin promoter restricts expression to keratinocytes, the cell type infected by β-HPV. The result is that genes are only expressed at anatomical sites relevant in the context of β-HPV infections. Our review of the literature shows that β-HPV 8 is the most frequently investigated β-HPV type, followed by β-HPV 38, β-HPV 49, and β-HPV 20. Additionally, one study has investigated β-HPV 5 E7 in a nude mouse/artificial skin graft model (Buitrago-Pérez et al., 2012).

β-HPV 8 Transgenic-Mouse Models

Schaper et al. established the first β-HPV tg-model using the Keratin 14 (K14) promoter to express the entire early gene region of β-HPV 8. Transgene expression was the highest for E2, followed by E6 and E7 (Schaper et al., 2005). While the tg-negative littermates did not develop lesions on the skin or other organs, 91% of the β-HPV 8 tg-positive mice developed single- or multifocal benign tumors. Of this population, 25% showed varying degrees of dysplasia and finally 6% developed SCCs spontaneously. The SCCs developed without additional DNA-damaging events. This established an *in vivo* link between β-HPV 8 and carcinogenesis. A caveat, however, is the stable oncogene expression in tg-mice. β-HPV infections, and therefore expression of β-HPV genes in the immunocompetent population, are transient.

In a follow up study, a possible role of β-HPV 8 E2 in skin tumor induction was revealed when 60% of the E2 positive population, but none of the E2 negative population developed spontaneous ulcerous lesions of the skin (Pfefferle et al., 2008). Moreover, 3 weeks after UV irradiation, 87% of a tg-mouse line with high E2 expression levels and 36% of a tg-mouse line with lower E2 expression levels developed skin tumors. On the other hand, irradiation of tg-negative mice did not lead to tumor formation. This could point toward a potential synergy between β-HPV 8 E2, E6, and E7 for their role in carcinogenesis.

Later, by expressing E6 individually under the K14 promoter, it was shown that β-HPV 8 E6 is the major driving force behind both spontaneous tumor development in tg-mice and that tumor formation could be prevented via DNA vaccination (Marcuzzi et al., 2009, 2014). Rapid tumor development by induction, either through UV irradiation or wounding, was demonstrated. This observation that persistent β-HPV 8 infections combined with UV exposure and wound healing processes pose a significant risk factor for skin cancer is consistent with observations in individuals with persistent β-HPV 8 infections due to EV. A potential role of the signal transducer and activator of transcription 3 (Stat3) was demonstrated in tg mice expressing the early region of β-HPV 8 that additionally had an epidermis restricted ablation of Stat3 (Andrea et al., 2010, p.3). The Stat3 heterozygous line was significantly less prone to spontaneous tumor development and these tumors did not progress to malignancy. Hufbauer et al. showed that β-HPV 8 E6 expressing tg-mice dysregulate mi-RNA expression (Hufbauer et al., 2011). Following UV induced inflammation and wound healing, the levels of mi-RNA for regulatory targets including cell-cycle (Rb) and apoptosis (PTEN, PDCD4) remained dysregulated, while dysregulation in wt-mice was transient. Hufbauer et al. also demonstrated that β-HPV 8 E6 expression leads to an impaired DNA-damage response in tg-mice following UV irradiation (Hufbauer et al., 2015). β-HPV 8 E6 expressing mice were shown to be thymine-dimer positive for an extended period while wt-mice efficiently repaired the UV induced DNA damage within 48 h. More importantly, probing for the DSB marker, γH2AX, revealed that the persistence of UV induced lesions in β-HPV 8 E6 expressing cells ultimately led to the formation of highly mutagenic and more dangerous DSBs. Immunohistochemical analysis of tg-mouse skin biopsies showed an increased signal for γH2AX at both, early (3d, 5d) and later (13d, 24d) timepoints. This not only demonstrates β-HPV 8 E6's attenuation of DDR, but also its ability to enhance the cells tolerance of persistent and increasingly severe DNA-damage. UV radiation typically causes intrastrand lesions that are tolerated by TLS- and repaired by NER-pathway. If this type of damage persists it will lead to increased rates of DSBs. The emergence and persistence of DSBs could point toward a broad influence of β-HPV 8 E6 on the DNA-damage response machinery, stretching from pathways meant to handle minor DNA damage (TLS, NER) to pathways that control and repair highly mutagenic DSBs (NHEJ, HR).

The role of β-HPV 8 E7 has also been investigated in tg-mice (Sperling et al., 2012; Heuser et al., 2016). It was shown that β-HPV 8 E7, but not β-HPV 8 E6 enables an escape from the immune response of β-HPV 8^+ lesions. β-HPV 8 E7 achieved this by inhibiting chemotactic signaling. β-HPV 8 E7 binds to C/EBPβ and inhibits its interaction with the CCL20 promoter, leading to decreased levels of CCL20, a chemoattractant for Langerhans cells. β-HPV 8 E7 is also critical for the invasiveness of hyperproliferating keratinocytes by dysregulating cell-cell interactions.

β-HPV 38 Transgenic-Mouse Models

While β-HPV 8 tg-mice demonstrated spontaneous tumor formation, tg-models of other β-HPV types do not exhibit the same behavior. Dong et al. showed that a mouse model for β-HPV 38 E6/E7 expressing mice under the Keratin 10 promoter exhibit hyperproliferation of the skin, but require external stimuli for carcinogenesis (Dong et al., 2005). Furthermore, ΔNp73α has been identified as integral to the attenuation of cell cycle arrest after UV exposure (Dong et al., 2007). Loss of p53 attenuated ΔNp73α expression and partially restored cell cycle arrest while loss of p73 lead to loss of ΔNp73α and consequently to high levels of p21 expression and cell cycle arrest after UV exposure. Differential susceptibility to chemically induced (DMBA/TPA) carcinogenesis correlates with differential oncogene expression levels and indicates a dose-dependency for risk of carcinogenesis. Irradiation of wt-mice with a single UV-dose led to accumulation of p21 and cell cycle arrest in the epidermis, while β-HPV 38 E6/E7 expressing mice inhibited cell cycle arrest through attenuation of p21 accumulation. Chronic irradiation of tg-mice with UV led to the formation of AK-like lesions that are considered precursors to SCCs in humans, while wt-mice did not develop lesions. Some of the AK-like lesions progressed to SCCs after 22 weeks (Viarisio et al., 2011). This provides evidence for the carcinogenesis-risk amplifying potential of the β-HPV 38 oncogenes E6 and E7.

Other β-HPV Transgenic-Mouse Models

The K14 tg-model for β-HPV 49 E6/E7 does neither show spontaneous tumor development nor tumor development after UV-irradiation (Viarisio et al., 2016). However, the β-HPV 49 tg-mice lines where susceptible to chemically induced carcinogenesis of the upper digestive tract. When exposed to 4 nitroquinoline 1-oxide (4NQO), 87% of the β-HPV 49 tg-mice developed tumors in the upper digestive tract while 4NQO treatment had little effect on β-HPV 38 tg-mice, which are susceptible to UV-triggered skin carcinogenesis.

A model for β-HPV 20 E6/E7 showed enhanced proliferation and papilloma formation in the evaluated transgenic lines, when compared to non-transgenic controls (Michel et al., 2006). Chronic exposure to UV radiation led to the development of SCCs and proliferation was enhanced for several weeks after UV treatment. The tg-lines also showed a reduced expression of differentiation markers (involucrin & loricrin and irregular patterns of p53 expression post UV, while controls showed a continued expression of proliferation markers and even expression of p53.

Summary

Mouse models provide a valuable *in vivo* tool to dissect the relative ability of β-HPV genes to induce tumorigenesis. They also allow a distinction between different carcinogenic potentials exhibited by E2, E6, or E7 to be accessed. The mouse models make it evident that β-HPV E6 carries a particularly high potential due to its effects on both apoptotic pathways and the DDR. The tg-mouse models also support the "hit and run" hypothesis regarding β-HPV induced malignancies, since most models require external stimuli to induce malignant tumors. β-HPV 8 has the potential for spontaneous transformation in tg-models, but it remains unclear whether the potential persists when β-HPV 8 early gene expression is transient, as it is the

case in most humans. It also should be pointed out that the average daily UV dose of an American is ∼94 J/m^2 (Godar et al., 2001), while the dosages used in the β-HPV tg-model studies discussed here reach 45-fold great levels. Although constrains in experimental design may require doses of this magnitude, it is a necessary caveat to considered when evaluating tg models of β-HPV induced skin cancer.

CONCLUSIONS

The impact of genus β-HPV on the DNA damage as well as the ability of these viruses to induce carcinogenesis is diverse and manifest in both *in vitro* and *in vivo* investigations. Generally, β-HPV viruses effect on DDR may be explained by their interest of uninterrupted proliferation, despite the presence of DNA damage. While most β-HPV E6 inhibit apoptosis by degrading the pro-apoptotic protein BAK, only a subset (β-HPV 5 and 8 E6) bind p300 strongly enough to destabilize the histone acetyltransferase, causing delayed repair of thymine dimers and double strand breaks (Giampieri and Storey, 2004; Muench et al., 2010; Howie et al., 2011; Hufbauer et al., 2011; Wallace et al., 2012, 2013, 2015). A larger subset of β-HPV E6 proteins (β-HPV 5, 8, 17, 23, 38, 49, and 92) interfere with p53 activity, but they do so through different mechanisms. Continuing the theme of diversity among β-HPVs, β-HPV 38 E6 immortalizes cells through a ΔNp73α-dependent mechanism, while β-HPV 49 E6 acts more similarly to high risk α-HPV E6, immortalizing cells through interactions with E6AP and NFX1-91 (Caldeira et al., 2003; Gabet et al., 2008; Muench et al., 2010). **Figure 2** depicts these diverse effects of β-HPV E6.

There are notable differences between β-HPV E7 proteins as well. A large cohort of these viral proteins (β-HPV 5, 8, 24, 38, and 49 E7) impair pRB function. The sole mechanism of pRB interference by β-HPV 5 and 8 E7 is through binding and induction of hyperphosphorylation of pRB. In addition to promoting the phosphorylation of pRB, β-HPV 38 and 49 E7 also decrease the half-life of pRB. β-HPV 24 E7 is only known to reduce pRB's half-life. Further, β-HPV 38 E7 has the ability to interfere with p53 activity by stabilizing the p53 antagonist, ΔNp73α, and increase inhibitory post-translational modifications of p53.

Not surprisingly, *in vivo* transgenic mouse models of β-HPV associated tumorigenesis reflect the varied ability of β-HPV to degrade the fidelity of host cells (Dong et al., 2005; Michel et al., 2006; Viarisio et al., 2011). The tg-mouse models of β-HPV 8 show spontaneous tumor formation (Schaper et al., 2005; Pfefferle et al., 2008; Marcuzzi et al., 2009). While carcinogenesis is augmented by UV exposure in β-HPV 8 mouse models, similar models of other β-HPV induced cancers (β-HPV 20, 38, and 49) require external stimulants to develop tumors. The required stimulants vary as well. Expression of β-HPV 20 and 38 proteins cause cancer in mice exposed to UV, but only β-HPV 49 proteins cause upper digestive tract tumors after exposure to 4NQO. Notably, the transient nature of β-HPV infections in immunocompetent individuals is not reflected in the mouse models discussed above and the ability of persistent β-HPV infection to cause cancer is generally accepted. Further, the amount of UV exposure necessary to cause tumors in β-HPV tg mice is often well above what humans typically receive. Thus, new *in vivo* models will be quintessential to drive the field forward and may include mice infected with the murine papillomavirus (MmuPV1) that recapitulates some but not all of the characteristics of β-HPV (Meyers et al., 2017).

The bulk of evidence for β-HPV infections playing a role in NMSCs suggests that β-HPV 5, 8, and 38 are the most tumorigenic, with a particular and unsurprising emphasis on

TABLE 1 | Characteristics and differences of several β-HPV strands and high risk α-HPVs.

	HPV5	HPV8	HPV38	HPV49	high risk αHPVs
Impact on DDR	•Delay UV repair •Destabilize p300 •ATM, ATR, BRCA1/2 ↓	•Delay UV repair •Destabilize p300 •ATM, ATR, BRCA1/2 ↓	•Delayed UV repair •ΔNp73α ↑ •Inhibit p300	•Unknown	•Attenuate and repurpose several DDR proteins
Prevention of Apoptosis	•Degrade BAK	•Degrade BAK	•Stabilize p53 •Alter p53 activity •Degrade BAK	•Degrade p53	•Degrade p53
Proliferation	•Hyperphosphorylate pRb	•Hyperphosphorylate pRb	•Attenuate p21 accumulation •Phosphorylate pRB	•Hyperphosphorylate pRb	•Degrade pRb
Immortalization	•No	•No	•Yes	•Yes	•Yes
Tumor maintenance	•Not required	•Not required	•Not required	•Not required	•Required
E6 motif	•No PDZ domain	•No PDZ domain	•No PDZ domain	•No PDZ domain	•PDZ domain present
Animal Models	•Artificial skin graft model •UV-induced lesion formation	•Spontaneous tumor formation	•UV DNA damage induced tumor formation	•No cSCC formation •Chemically-induced carcinogenesis in digestive tract	•Spontaneous tumor formation

This table compares the impact of several β-HPVs and high risk α-HPVs on DDR and other pathways relevant to carcinogenesis. ↑ and ↓ indicate increased or decreased abundance, respectively.

the homologous of high risk α-HPV oncogenes (E6 and E7). These viruses are expected to promote carcinogenesis via the "hit and run" model that is dependent on their amplification of UV's genome destabilizing effects and otherwise decreasing genome fidelity. Since the mechanisms of abrogating genome stability vary among β-HPVs, it is reasonable to expect that the carcinogenic potential of individual β-HPVs depends on their cellular environment during infection. As a result, not only is the clear delineation of pathways and proteins impacted by β-HPV necessary to understand their oncogenic potential, but also the relative ability among β-HPVs to disrupt these pathways. A major knowledge gap regarding β-HPV induced oncogenesis is the extent that the reduced availability of ATM, ATR, BRCA1, and BRCA2 affects the activity of these proteins in each of the repair pathways that they participate in. This could expand the known ability of β-HPV proteins to disrupt DNA repair to include nearly every cellular response to damaged DNA. Alternatively, if the impairment of these repair proteins was context specific, it could highlight particularly deleterious situations for a β-HPV infection to occur. Further, there is a diversity of genome destabilizing events beyond DNA damage (failed cytokinesis, centrosome duplication errors, etc.) that if disrupted would fit the ascribed "hit and run" model of tumorigenesis. Defining the mutagenic potential of β-HPV infections is essential to take next steps in preventing disease associated with these viruses. **Table 1** compares β-HPV 5, 8, 38, and 49 as well as high-risk α-HPV oncogenes regarding their oncogenic potential. A possible intervention is the development of β-HPV specific vaccines. While β-HPV infection occurs in early childhood, a vaccine against specific "high-risk" types may prevent re-infection. Additionally, immunity acquired through vaccination may be more effective than immunity through infection. The FDA-approved technology to make the current vaccine could be readily adapted to prevent β-HPV infections or specific inhibitors of β-HPVs could be developed and added to sunscreens to precisely target the intersection of UV and viral infection. A commonly stated challenge to the development of a vaccine against β-HPV is the fact that these infections are initially acquired soon after birth and that β-HPV infections do not illicit a protective immune response. Although true, vaccination could mitigate disease by preventing reinfection and potential initial infection with particularly oncogenic β-HPVs not necessarily acquired at birth. Further, vaccination is effective against members of the alpha HPV genus despite poor natural adaptive immune responses to those infections. Ultimately, these ambitious goals are dependent on advancements in the dissection of β-HPV biology and its ability to hinder the cellular DDR.

AUTHOR CONTRIBUTIONS

Wrote the manuscript: SW and NW. Reviewed and edited the manuscript: SW and NW.

FUNDING

This work was supported by Department of Defense CMDRP PRCRP CA160224 (NW) and made possible through generous support from the Les Clow family and the Johnson Cancer Research Center at Kansas State University.

ACKNOWLEDGMENTS

The authors would like to thank Dr. Zhilong Yang for providing his valuable insight and feedback on the manuscript.

REFERENCES

Accardi, R., Dong, W., Smet, A., Cui, R., Hautefeuille, A., Gabet, A. S., et al. (2006). Skin human papillomavirus type 38 alters p53 functions by accumulation of deltaNp73. *EMBO Rep.* 7, 334–340. doi: 10.1038/sj.embor.7400615

Accardi, R., Scalise, M., Gheit, T., Hussain, I., Yue, J., Carreira, C., et al. (2011). IkappaB kinase beta promotes cell survival by antagonizing p53 functions through DeltaNp73alpha phosphorylation and stabilization. *Mol. Cell. Biol.* 31, 2210–2226. doi: 10.1128/MCB.00964-10

Andrea, M. D., Rittà, M., Landini, M. M., Borgogna, C., Mondini, M., Kern, F., et al. (2010). Keratinocyte-specific stat3 heterozygosity impairs development of skin tumors in human papillomavirus 8 transgenic mice. *Cancer Res.* 70, 7938–7948. doi: 10.1158/0008-5472.CAN-10-1128

Antonsson, A., Karanfilovska, S., Lindqvist, P. G., and Hansson, B. G. (2003). General acquisition of human papillomavirus infections of skin occurs in early infancy. *J. Clin. Microbiol.* 41, 2509–2514. doi: 10.1128/JCM.41.6.2509-2514.2003

Arron, S. T., Ruby, J. G., Dybbro, E., Ganem, D., and DeRisi, J. L. (2011). Transcriptome sequencing demonstrates that human papillomavirus is not active in cutaneous squamous cell carcinoma. *J. Invest. Dermatol.* 131, 1745–1753. doi: 10.1038/jid.2011.91

Bailey, S. G., Cragg, M. S., and Townsend, P. A. (2011). Family friction as ΔNp73 antagonises p73 and p53. *Int. J. Biochem. Cell Biol.* 43, 482–486. doi: 10.1016/j.biocel.2010.12.022

Banin, S., Moyal, L., Shieh, S., Taya, Y., Anderson, C. W., Chessa, L., et al. (1998). Enhanced phosphorylation of p53 by ATM in response to DNA damage. *Science* 281, 1674–1677. doi: 10.1126/science.281.5383.1674

Bavinck, J. N. B., Plasmeijer, E. I., and Feltkamp, M. C. W. (2008). β-Papillomavirus infection and skin cancer. *J. Invest. Dermatol.* 128, 1355–1358. doi: 10.1038/jid.2008.123

Beckerman, R., and Prives, C. (2010). Transcriptional Regulation by P53. *Cold Spring Harb. Perspect. Biol.* 2:a000935. doi: 10.1101/cshperspect.a000935

Bedard, K. M., Underbrink, M. P., Howie, H. L., and Galloway, D. A. (2008). The E6 oncoproteins from human betapapillomaviruses differentially activate telomerase through an E6AP-dependent mechanism and prolong the lifespan of primary keratinocytes. *J. Virol.* 82, 3894–3902. doi: 10.1128/JVI.01818-07

Bernard, H. U., Burk, R. D., Chen, Z., van Doorslaer, K., zur Hausen, H., and de Villiers, E. M. (2010). Classification of papillomaviruses (PVs) based on 189 PV types and proposal of taxonomic amendments. *Virology* 401, 70–79. doi: 10.1016/j.virol.2010.02.002

Bertoli, C., Skotheim, J. M., and de Bruin, R. A. M. (2013). Control of cell cycle transcription during G1 and S phases. *Nat. Rev. Mol. Cell Biol.* 14, 518–528. doi: 10.1038/nrm3629

Bouquet, F., Pal, A., Pilones, K. A., Demaria, S., Hann, B., Akhurst, R. J., et al. (2011). TGFβ1 inhibition increases the radiosensitivity of breast cancer cells *in vitro* and promotes tumor control by radiation *in vivo*. *Clin. Cancer Res. Off. J. Am. Assoc. Cancer Res.* 17, 6754–6765. doi: 10.1158/1078-0432.CCR-11-0544

Bouvard, V., Baan, R., Straif, K., Grosse, Y., Secretan, B., Ghissassi, F. E., et al. (2009). A review of human carcinogens—Part B: biological agents. *Lancet Oncol.* 10, 321–322. doi: 10.1016/S1470-2045(09)70096-8

Bouwes, B., Neale, R. E., Abeni, D., Euvrard, S., Green, A. C., Harwood, C. A., et al. (2010). Multicenter study of the association between betapapillomavirus infection and cutaneous squamous cell carcinoma. *Cancer Res.* 70, 9777–9786. doi: 10.1158/0008-5472.CAN-10-0352

Bouwes Bavinck, J. N., Feltkamp, M., Struijk, L., and ter Schegget, J. (2001). Human papillomavirus infection and skin cancer risk in organ transplant recipients. *J. Investig. Dermatol. Symp. Proc.* 6, 207–211. doi: 10.1046/j.0022-202x.2001.00048.x

Boyer, S. N., Wazer, D. E., and Band, V. (1996). E7 protein of human papilloma virus-16 induces degradation of retinoblastoma protein through the ubiquitin-proteasome pathway. *Cancer Res.* 56, 4620–4624.

Boyle, J., Briggs, J. D., Mackie, R., Junor, B. J. R., and Aitchison, T. C. (1984). Cancer, warts, and sunshine in renal transplant patients. *Lancet* 323, 702–705. doi: 10.1016/S0140-6736(84)92221-9

Branzei, D., and Foiani, M. (2008). Regulation of DNA repair throughout the cell cycle. *Nat. Rev. Mol. Cell Biol.* 9, 297–308. doi: 10.1038/nrm2351

Brash, D. E., Rudolph, J. A., Simon, J. A., Lin, A., McKenna, G. J., Baden, H. P., et al. (1991). A role for sunlight in skin cancer: UV-induced p53 mutations in squamous cell carcinoma. *Proc. Natl. Acad. Sci. U.S.A.* 88, 10124–10128. doi: 10.1073/pnas.88.22.10124

Brimer, N., Lyons, C., Wallberg, A. E., and Vande Pol, S. B. (2012). Cutaneous papillomavirus E6 oncoproteins associate with MAML1 to repress transactivation and NOTCH signaling. *Oncogene* 31, 4639–4646. doi: 10.1038/onc.2011.589

Buitrago-Pérez, Á., Hachimi, M., Dueñas, M., Lloveras, B., Santos, A., Holguín, A., et al. (2012). A humanized mouse model of HPV-associated pathology driven by E7 expression. *PLoS ONE* 7:e41743. doi: 10.1371/journal.pone.0041743

Bzhalava, D., Eklund, C., and Dillner, J. (2015). International standardization and classification of human papillomavirus types. *Virology* 476, 341–344. doi: 10.1016/j.virol.2014.12.028

Bzhalava, D., Guan, P., Franceschi, S., Dillner, J., and Clifford, G. (2013). A systematic review of the prevalence of mucosal and cutaneous human papillomavirus types. *Virology* 445, 224–231. doi: 10.1016/j.virol.2013.07.015

Bzhalava, D., Mühr, L. S. A., Lagheden, C., Ekström, J., Forslund, O., Dillner, J., et al. (2014). Deep sequencing extends the diversity of human papillomaviruses in human skin. *Sci. Rep.* 4:5807. doi: 10.1038/srep05807

Caldeira, S., Zehbe, I., Accardi, R., Malanchi, I., Dong, W., Giarrè, M., et al. (2003). The E6 and E7 proteins of the cutaneous human papillomavirus type 38 display transforming properties. *J. Virol.* 77, 2195–2206. doi: 10.1128/JVI.77.3.2195-2206.2003

Carter, J. R., Ding, Z., and Rose, B. R. (2011). HPV infection and cervical disease: a review. *Aust. N. Z. J. Obstet. Gynaecol.* 51, 103–108. doi: 10.1111/j.1479-828X.2010.01269.x

Casabonne, D., Waterboer, T., Michael, K. M., Pawlita, M., Mitchell, L., Newton, R., et al. (2009). The seroprevalence of human papillomavirus by immune status and by ethnicity in London. *Infect. Agent. Cancer* 4:14. doi: 10.1186/1750-9378-4-14

Chahoud, J., Semaan, A., Chen, Y., Cao, M., Rieber, A. G., Rady, P., et al. (2016). Association between β-genus human papillomavirus and cutaneous squamous cell carcinoma in immunocompetent individuals—a meta-analysis. *JAMA Dermatol.* 152, 1354–1364. doi: 10.1001/jamadermatol.2015.4530

Chellappan, S., Kraus, V. B., Kroger, B., Munger, K., Howley, P. M., Phelps, W. C., et al. (1992). Adenovirus E1A, simian virus 40 tumor antigen, and human papillomavirus E7 protein share the capacity to disrupt the interaction between transcription factor E2F and the retinoblastoma gene product. *Proc. Natl. Acad. Sci. U.S.A.* 89, 4549–4553. doi: 10.1073/pnas.89.10.4549

Chen, X., Ko, L. J., Jayaraman, L., and Prives, C. (1996). p53 levels, functional domains, and DNA damage determine the extent of the apoptotic response of tumor cells. *Genes Dev.* 10, 2438–2451. doi: 10.1101/gad.10.19.2438

Chen, Y.-W., Cleaver, J. E., Hatahet, Z., Honkanen, R. E., Chang, J.-Y., Yen, Y., et al. (2008). Human DNA polymerase eta activity and translocation is regulated by phosphorylation. *Proc. Natl. Acad. Sci. U.S.A.* 105, 16578–16583. doi: 10.1073/pnas.0808589105

Cheng, Q., and Chen, J. (2010). Mechanism of p53 stabilization by ATM after DNA damage. *Cell Cycle Georget. Tex* 9, 472–478. doi: 10.4161/cc.9.3.10556

Chittenden, T., Harrington, E. A. O., Connor, R., Flemington, C., Lutz, R. J., Evan, G. I., et al. (1995). Induction of apoptosis by the Bcl-2 homologue Bak. *Nature* 374, 733–736. doi: 10.1038/374733a0

Cornet, I., Bouvard, V., Campo, M. S., Thomas, M., Banks, L., Gissmann, L., et al. (2012). Comparative analysis of transforming properties of E6 and E7 from different beta human papillomavirus types. *J. Virol.* 86, 2366–2370. doi: 10.1128/JVI.06579-11

Cubie, H. A. (2013). Diseases associated with human papillomavirus infection. *Virology* 445, 21–34. doi: 10.1016/j.virol.2013.06.007

D'Andrea, A. D. (2013). BRCA1: a missing link in the Fanconi anemia/BRCA pathway. *Cancer Discov.* 3, 376–378. doi: 10.1158/2159-8290.CD-13-0044

D'Souza, G., and Dempsey, A. (2011). The role of HPV in head and neck cancer and review of the HPV vaccine. *Prev. Med.* 53, S5–S11. doi: 10.1016/j.ypmed.2011.08.001

de Koning, M. N. C., Weissenborn, S. J., Abeni, D., Bouwes Bavinck, J. N., Euvrard, S., Green, A. C., et al. (2009). Prevalence and associated factors of betapapillomavirus infections in individuals without cutaneous squamous cell carcinoma. *J. Gen. Virol.* 90, 1611–1621. doi: 10.1099/vir.0.010017-0

Dell'Oste, V., Azzimonti, B., De Andrea, M., Mondini, M., Zavattaro, E., Leigheb, G., et al. (2009). High β-HPV DNA loads and strong seroreactivity are present in epidermodysplasia verruciformis. *J. Invest. Dermatol.* 129, 1026–1034. doi: 10.1038/jid.2008.317

Demers, G. W., Foster, S. A., Halbert, C. L., and Galloway, D. A. (1994). Growth arrest by induction of p53 in DNA damaged keratinocytes is bypassed by human papillomavirus 16 E7. *Proc. Natl. Acad. Sci. U.S.A.* 91, 4382–4386. doi: 10.1073/pnas.91.10.4382

de Oliveira, W. R. P., He, Q., Rady, P. L., Hughes, T. K., Neto, C. F., Rivitti, E. A., et al. (2004). HPV typing in Brazilian patients with epidermodysplasia verruciformis: high prevalence of EV-HPV 25. *J. Cutan. Med. Surg.* 8, 110–115. doi: 10.1177/120347540400800206

de Villiers, E.-M. (2013). Cross-roads in the classification of papillomaviruses. *Virology* 445, 2–10. doi: 10.1016/j.virol.2013.04.023

Domchek, S. M., Tang, J., Stopfer, J., Lilli, D. R., Hamel, N., Tischkowitz, M., et al. (2013). Biallelic deleterious BRCA1 mutations in a woman with early-onset ovarian cancer. *Cancer Discov.* 3, 399–405. doi: 10.1158/2159-8290.CD-12-0421

Dong, W., Arpin, C., Accardi, R., Gissmann, L., Sylla, B. S., Marvel, J., et al. (2007). Loss of p53 or p73 in human papillomavirus type 38 E6 and E7 transgenic mice partially restores the UV-activated cell cycle checkpoints. *Oncogene* 27, 2923–2928. doi: 10.1038/sj.onc.1210944

Dong, W., Kloz, U., Accardi, R., Caldeira, S., Tong, W.-M., Wang, Z.-Q., et al. (2005). Skin hyperproliferation and susceptibility to chemical carcinogenesis in transgenic mice expressing e6 and e7 of human papillomavirus type 38. *J. Virol.* 79, 14899–14908. doi: 10.1128/JVI.79.23.14899-14908.2005

Doorbar, J., Egawa, N., Griffin, H., Kranjec, C., and Murakami, I. (2015). Human papillomavirus molecular biology and disease association. *Rev. Med. Virol.* 25, 2–23. doi: 10.1002/rmv.1822

Dyson, N. (1998). The regulation of E2F by pRB-family proteins. *Genes Dev.* 12, 2245–2262. doi: 10.1101/gad.12.15.2245

Dyson, N., Howley, P. M., Munger, K., and Harlow, E. (1989). The human papilloma virus-16 E7 oncoprotein is able to bind to the retinoblastoma gene product. *Science* 243, 934–937. doi: 10.1126/science.2537532

Ekström, J., Mühr, L. S. A., Bzhalava, D., Söderlund-Strand, A., Hultin, E., Nordin, P., et al. (2013). Diversity of human papillomaviruses in skin lesions. *Virology* 447, 300–311. doi: 10.1016/j.virol.2013.09.010

Espinosa, J. M., Verdun, R. E., and Emerson, B. M. (2003). p53 functions through stress- and promoter-specific recruitment of transcription initiation components before and after DNA damage. *Mol. Cell* 12, 1015–1027. doi: 10.1016/S1097-2765(03)00359-9

Farzan, S. F., Waterboer, T., Gui, J., Nelson, H. H., Li, Z., Michael, K. M., et al. (2013). Cutaneous alpha, beta and gamma human papillomaviruses in relation to squamous cell carcinoma of the skin: a population-based study. *J. Int. Cancer* 133, 1713–1720. doi: 10.1002/ijc.28176

Fischer, M. (2017). Census and evaluation of p53 target genes. *Oncogene* 36, 3943–3956. doi: 10.1038/onc.2016.502

Forslund, O., Iftner, T., Andersson, K., Lindelof, B., Hradil, E., Nordin, P., et al. (2007). Cutaneous human papillomaviruses found in sun-exposed skin: beta-papillomavirus species 2 predominates in squamous cell carcinoma. *J. Infect. Dis.* 196, 876–883. doi: 10.1086/521031

Gabet, A.-S., Accardi, R., Bellopede, A., Popp, S., Boukamp, P., Sylla, B. S., et al. (2008). Impairment of the telomere/telomerase system and genomic instability are associated with keratinocyte immortalization induced by the skin human papillomavirus type 38. *FASEB J.* 22, 622–632. doi: 10.1096/fj.07-8389com

Ganem, N. J., Cornils, H., Chiu, S. Y., O'Rourke, K. P., Arnaud, J., Yimlamai, D., et al. (2014). Cytokinesis failure triggers hippo tumor suppressor pathway activation. *Cell* 158, 833–848. doi: 10.1016/j.cell.2014.06.029

Genders, R. E., Mazlom, H., Michel, A., Plasmeijer, E. I., Quint, K. D., Pawlita, M., et al. (2015). The presence of betapapillomavirus antibodies around transplantation predicts the development of keratinocyte carcinoma in organ transplant recipients: a cohort study. *J. Invest. Dermatol.* 135, 1275–1282. doi: 10.1038/jid.2014.456

Giampieri, S., and Storey, A. (2004). Repair of UV-induced thymine dimers is compromised in cells expressing the E6 protein from human papillomaviruses types 5 and 18. *Br. J. Cancer* 90, 2203–2209. doi: 10.1038/sj.bjc.6601829

Gillespie, K. A., Mehta, K. P., Laimins, L. A., and Moody, C. A. (2012). Human papillomaviruses recruit cellular DNA repair and homologous recombination factors to viral replication centers. *J. Virol.* 86, 9520–9526. doi: 10.1128/JVI.00247-12

Godar, D. E., Wengraitis, S. P., Shreffler, J., and Sliney, D. H. (2001). UV doses of americans. *Photochem. Photobiol.* 73, 621–629. doi: 10.1562/0031-8655(2001)074<0787:udoaca>2.0.co;2

Göhler, T., Sabbioneda, S., Green, C. M., and Lehmann, A. R. (2011). ATR-mediated phosphorylation of DNA polymerase η is needed for efficient recovery from UV damage. *J. Cell Biol.* 192, 219–227. doi: 10.1083/jcb.201008076

Goodman, R. H., and Smolik, S. (2000). CBP/p300 in cell growth, transformation, and development. *Genes Dev.* 14, 1553–1577. doi: 10.1101/gad.14.13.1553

Goodwin, E. C., and DiMaio, D. (2000). Repression of human papillomavirus oncogenes in HeLa cervical carcinoma cells causes the orderly reactivation of dormant tumor suppressor pathways. *Proc. Natl. Acad. Sci. U.S.A.* 97, 12513–12518. doi: 10.1073/pnas.97.23.12513

Goodwin, E. C., Yang, E., Lee, C.-J., Lee, H.-W., DiMaio, D., and Hwang, E.-S. (2000). Rapid induction of senescence in human cervical carcinoma cells. *Proc. Natl. Acad. Sci. U.S.A.* 97, 10978–10983. doi: 10.1073/pnas.97.20.10978

Hampras, S. S., Giuliano, A. R., Lin, H.-Y., Fisher, K. J., Abrahamsen, M. E., Sirak, B. A., et al. (2014). Natural history of Cutaneous Human Papillomavirus (HPV) infection in men: the HIM study. *PLoS ONE* 9:e104843. doi: 10.1371/journal.pone.0104843

Hampras, S. S., Rollison, D. E., Giuliano, A. R., McKay-Chopin, S., Minoni, L., Sereday, K., et al. (2017). Prevalence and concordance of cutaneous beta human papillomavirus infection at mucosal and cutaneous sites. *J. Infect. Dis.* 216, 92–96. doi: 10.1093/infdis/jix245

Harvey, K. F., Zhang, X., and Thomas, D. M. (2013). The Hippo pathway and human cancer. *Nat. Rev. Cancer* 13, 246–257. doi: 10.1038/nrc3458

Hazard, K., Karlsson, A., Andersson, K., Ekberg, H., Dillner, J., and Forslund, O. (2007). Cutaneous human papillomaviruses persist on healthy skin. *J. Invest. Dermatol.* 127, 116–119. doi: 10.1038/sj.jid.5700570

Heuser, S., Hufbauer, M., Marx, B., Tok, A., Majewski, S., Pfister, H., et al. (2016). The levels of epithelial anchor proteins β-catenin and zona occludens-1 are altered by E7 of human papillomaviruses 5 and 8. *J. Gen. Virol.* 97, 463–472. doi: 10.1099/jgv.0.000363

Hobbs, C. G., Sterne, J. A. C., Bailey, M., Heyderman, R. S., Birchall, M. A., and Thomas, S. J. (2006). Human papillomavirus and head and neck cancer: a systematic review and meta-analysis. *Clin. Otolaryngol.* 31, 259–266. doi: 10.1111/j.1749-4486.2006.01246.x

Holloway, A., Simmonds, M., Azad, A., Fox, J. L., and Storey, A. (2015). Resistance to UV-induced apoptosis by β-HPV5 E6 involves targeting of activated BAK for proteolysis by recruitment of the HERC1 ubiquitin ligase. *Int. J. Cancer* 136, 2831–2843. doi: 10.1002/ijc.29350

Hong, S., Cheng, S., Iovane, A., and Laimins, L. A. (2015). STAT-5 regulates transcription of the topoisomerase IIβ-binding protein 1 (TopBP1) gene to activate the ATR pathway and promote human papillomavirus replication. *mBio* 6, e02006–e02015. doi: 10.1128/mBio.02006-15

Howie, H. L., Koop, J. I., Weese, J., Robinson, K., Wipf, G., Kim, L., et al. (2011). Beta-HPV 5 and 8 E6 promote p300 degradation by blocking AKT/p300 association. *PLOS Pathog.* 7:e1002211. doi: 10.1371/journal.ppat.1002211

Howley, P. M., and Pfister, H. J. (2015). Beta genus papillomaviruses and skin cancer. *Virology* 479, 290–296. doi: 10.1016/j.virol.2015.02.004

Hsu, J. Y.-C., Chen, A. C. H., Keleher, A., McMillan, N. A. J., and Antonsson, A. (2009). Shared and persistent asymptomatic cutaneous human papillomavirus infections in healthy skin. *J. Med. Virol.* 81, 1444–1449. doi: 10.1002/jmv.21529

Hufbauer, M., and Akgül, B. (2017). Molecular mechanisms of human papillomavirus induced skin carcinogenesis. *Viruses* 9:187. doi: 10.3390/v9070187

Hufbauer, M., Cooke, J., van der, H., Pfister, H., Storey, A., and Akgül, B. (2015). Human papillomavirus mediated inhibition of DNA damage sensing and repair drives skin carcinogenesis. *Mol. Cancer* 14:183. doi: 10.1186/s12943-015-0453-7

Hufbauer, M., Lazić, D., Reinartz, M., Akgül, B., Pfister, H., and Weissenborn, S. J. (2011). Skin tumor formation in human papillomavirus 8 transgenic mice is associated with a deregulation of oncogenic miRNAs and their tumor suppressive targets. *J. Dermatol. Sci.* 64, 7–15. doi: 10.1016/j.jdermsci.2011.06.008

Huibregtse, J. M., Scheffner, M., and Howley, P. M. (1991). A cellular protein mediates association of p53 with the E6 oncoprotein of human papillomavirus types 16 or 18. *EMBO J.* 10, 4129–4135.

Hwang, E. S., Riese, D. J., Settleman, J., Nilson, L. A., Honig, J., Flynn, S., et al. (1993). Inhibition of cervical carcinoma cell line proliferation by the introduction of a bovine papillomavirus regulatory gene. *J. Virol.* 67, 3720–3729.

Iannacone, M. R., Gheit, T., Pfister, H., Giuliano, A. R., Messina, J. L., Fenske, N. A., et al. (2014). Case–control study of genus-beta human papillomaviruses in plucked eyebrow hairs and cutaneous squamous cell carcinoma. *J. Int. Cancer* 134, 2231–2244. doi: 10.1002/ijc.28552

Iannacone, M. R., Gheit, T., Waterboer, T., Giuliano, A. R., Messina, J. L., Fenske, N. A., et al. (2012). Case-control study of cutaneous human papillomaviruses in squamous cell carcinoma of the skin. *Cancer Epidemiol. Biomark. Prev.* 21, 1303–1313. doi: 10.1158/1055-9965.EPI-12-0032

Itoh, S., Itoh, F., Goumans, M. J., and Ten Dijke, P. (2000). Signaling of transforming growth factor-beta family members through Smad proteins. *Eur. J. Biochem.* 267, 6954–6967. doi: 10.1046/j.1432-1327.2000.01828.x

Jackson, S. P., and Bartek, J. (2009). The DNA-damage response in human biology and disease. *Nature* 461, 1071–1078. doi: 10.1038/nature08467

Jazayeri, A., Falck, J., Lukas, C., Bartek, J., Smith, G. C. M., Lukas, J., et al. (2006). ATM- and cell cycle-dependent regulation of ATR in response to DNA double-strand breaks. *Nat. Cell Biol.* 8, 37–45. doi: 10.1038/ncb1337

Jeggo, P. A., and Löbrich, M. (2007). DNA double-strand breaks: their cellular and clinical impact? *Oncogene* 26, 7717–7719. doi: 10.1038/sj.onc.1210868

Karagas, M. R., Waterboer, T., Li, Z., Nelson, H. H., Michael, K. M., Bavinck, J. N. B., et al. (2010). Genus β human papillomaviruses and incidence of basal cell and squamous cell carcinomas of skin: population based case-control study. *BMJ* 341:c2986. doi: 10.1136/bmj.c2986

Keohavong, P., Liu, V. F., and Thilly, W. G. (1991). Analysis of point mutations induced by ultraviolet light in human cells. *Mutat. Res.* 249, 147–159. doi: 10.1016/0027-5107(91)90141-A

Kim, M.-R., Lee, J., An, Y. S., Jin, Y. B., Park, I.-C., Chung, E., et al. (2015). TGFβ1 protects cells from γ-IR by enhancing the activity of the NHEJ repair pathway. *Mol. Cancer Res.* 13, 319–329. doi: 10.1158/1541-7786.MCR-14-0098-T

Kirshner, J., Jobling, M. F., Pajares, M. J., Ravani, S. A., Glick, A. B., Lavin, M. J., et al. (2006). Inhibition of transforming growth factor-β1 signaling attenuates ataxia telangiectasia mutated activity in response to genotoxic stress. *Cancer Res.* 66, 10861–10869. doi: 10.1158/0008-5472.CAN-06-2565

Kiviat, N. B. (1999). Papillomaviruses in non-melanoma skin cancer: epidemiological aspects. *Semin. Cancer Biol.* 9, 397–403. doi: 10.1006/scbi.1999.0143

Kiyono, T., Foster, S. A., Koop, J. I., McDougall, J. K., Galloway, D. A., and Klingelhutz, A. J. (1998). Both Rb/p16INK4a inactivation and telomerase activity are required to immortalize human epithelial cells. *Nature* 396, 84–88. doi: 10.1038/23962

Klingelhutz, A. J., Foster, S. A., and McDougall, J. K. (1996). Telomerase activation by the E6 gene product of human papillomavirus type 16. *Nature* 380, 79–82. doi: 10.1038/380079a0

Kracikova, M., Akiri, G., George, A., Sachidanandam, R., and Aaronson, S. A. (2013). A threshold mechanism mediates p53 cell fate decision between growth arrest and apoptosis. *Cell Death Differ.* 20, 576–588. doi: 10.1038/cdd.2012.155

Kremsdorf, D., Jablonska, S., Favre, M., and Orth, G. (1982). Biochemical characterization of two types of human papillomaviruses associated with epidermodysplasia verruciformis. *J. Virol.* 43, 436–447.

Kremsdorf, D., Jablonska, S., Favre, M., and Orth, G. (1983). Human papillomaviruses associated with epidermodysplasia verruciformis. II. Molecular cloning and biochemical characterization of human papillomavirus 3a, 8, 10, and 12 genomes. *J. Virol.* 48, 340–351.

Kruse, J. P., and Gu, W. (2009). Modes of p53 Regulation. *Cell* 137, 609–622. doi: 10.1016/j.cell.2009.04.050

Lai, E. C. (2004). Notch signaling: control of cell communication and cell fate. *Development* 131, 965–973. doi: 10.1242/dev.01074

Lebrun, J.-J. (2012). The dual role of TGF in human cancer: from tumor suppression to cancer metastasis. *Int. Sch. Res. Not.* 2012:381428. doi: 10.5402/2012/381428

Lee, T. H., Park, J. M., Leem, S. H., and Kang, T. H. (2014). Coordinated regulation of XPA stability by ATR and HERC2 during nucleotide excision repair. *Oncogene* 33, 19–25. doi: 10.1038/onc.2012.539

Lerner, L. K., Francisco, G., Soltys, D. T., Rocha, C. R. R., Quinet, A., Vessoni, A. T., et al. (2017). Predominant role of DNA polymerase eta and p53-dependent translesion synthesis in the survival of ultraviolet-irradiated human cells. *Nucleic Acids Res.* 45, 1270–1280. doi: 10.1093/nar/gkw1196

Levy, D., Adamovich, Y., Reuven, N., and Shaul, Y. (2008). Yap1 phosphorylation by c-Abl Is a critical step in selective activation of proapoptotic genes in response to DNA damage. *Mol. Cell* 29, 350–361. doi: 10.1016/j.molcel.2007.12.022

Malumbres, M., and Barbacid, M. (2009). Cell cycle, CDKs and cancer: a changing paradigm. *Nat. Rev. Cancer* 9, 153–166. doi: 10.1038/nrc2602

Mao, Z., Bozzella, M., Seluanov, A., and Gorbunova, V. (2008). DNA repair by nonhomologous end joining and homologous recombination during cell cycle in human cells. *Cell Cycle Georget. Tex* 7, 2902–2906. doi: 10.4161/cc.7.18.6679

Marcuzzi, G. P., Awerkiew, S., Hufbauer, M., Schädlich, L., Gissmann, L., Eming, S., et al. (2014). Tumor prevention in HPV8 transgenic mice by HPV8-E6 DNA vaccination. *Med. Microbiol. Immunol.* 203, 155–163. doi: 10.1007/s00430-014-0327-4

Marcuzzi, G. P., Hufbauer, M., Kasper, H. U., Weißenborn, S. J., Smola, S., and Pfister, H. (2009). Spontaneous tumour development in human papillomavirus type 8 E6 transgenic mice and rapid induction by UV-light exposure and wounding. *J. Gen. Virol.* 90, 2855–2864. doi: 10.1099/vir.0.012872-0

Maréchal, A., and Zou, L. (2013). DNA damage Sensing by the ATM and ATR kinases. *Cold Spring Harb. Perspect. Biol.* 5:a012716. doi: 10.1101/cshperspect.a012716

Maréchal, A., and Zou, L. (2015). RPA-coated single-stranded DNA as a platform for post-translational modifications in the DNA damage response. *Cell Res.* 25, 9–23. doi: 10.1038/cr.2014.147

Marteijn, J. A., Lans, H., Vermeulen, W., and Hoeijmakers, J. H. J. (2014). Understanding nucleotide excision repair and its roles in cancer and ageing. *Nat. Rev. Mol. Cell Biol.* 15, 465–481. doi: 10.1038/nrm3822

Mendoza, J.-A., Jacob, Y., Cassonnet, P., and Favre, M. (2006). Human papillomavirus type 5 E6 oncoprotein represses the transforming growth factor β signaling pathway by binding to SMAD3. *J. Virol.* 80, 12420–12424. doi: 10.1128/JVI.02576-05

Meyer, T., Arndt, R., Christophers, E., Nindl, I., and Stockfleth, E. (2001). Importance of human papillomaviruses for the development of skin cancer. *Cancer Detect. Prev.* 25, 533–547.

Meyers, J. M., Spangle, J. M., and Munger, K. (2013). The human papillomavirus type 8 E6 protein interferes with NOTCH activation during keratinocyte differentiation. *J. Virol.* 87, 4762–4767. doi: 10.1128/JVI.02527-12

Meyers, J. M., Uberoi, A., Grace, M., Lambert, P. F., and Munger, K. (2017). Cutaneous HPV8 and MmuPV1 E6 proteins target the NOTCH and TGF-β tumor suppressors to inhibit differentiation and sustain keratinocyte proliferation. *PLOS Pathog.* 13:e1006171. doi: 10.1371/journal.ppat.1006171

Michel, A., Kopp-Schneider, A., Zentgraf, H., Gruber, A. D., and de Villiers, E.-M. (2006). E6/E7 expression of human papillomavirus type 20 (HPV-20) and HPV-27 influences proliferation and differentiation of the skin in UV-irradiated SKH-hr1 transgenic mice. *J. Virol.* 80, 11153–11164. doi: 10.1128/JVI.00954-06

Moldovan, G. L., and D'Andrea, A. D. (2009). How the Fanconi Anemia pathway guards the genome. *Annu. Rev. Genet.* 43, 223–249. doi: 10.1146/annurev-genet-102108-134222

Moody, C. A., and Laimins, L. A. (2009). Human papillomaviruses activate the ATM DNA damage pathway for viral genome amplification upon differentiation. *PLOS Pathog.* 5:e1000605. doi: 10.1371/journal.ppat.1000605

Moody, C. A., and Laimins, L. A. (2010). Human papillomavirus oncoproteins: pathways to transformation. *Nat. Rev. Cancer* 10, 550–560. doi: 10.1038/nrc2886

Moy, R. L. (2000). Clinical presentation of actinic keratoses and squamous cell carcinoma. *J. Am. Acad. Dermatol.* 42, S8–S10. doi: 10.1067/mjd.2000.103343

Muench, P., Probst, S., Schuetz, J., Leiprecht, N., Busch, M., Wesselborg, S., et al. (2010). Cutaneous papillomavirus E6 proteins must interact with p300 and block p53-mediated apoptosis for cellular immortalization and tumorigenesis. *Cancer Res.* 70, 6913–6924. doi: 10.1158/0008-5472.CAN-10-1307

Münger, K., Werness, B. A., Dyson, N., Phelps, W. C., Harlow, E., and Howley, P. M. (1989). Complex formation of human papillomavirus E7 proteins with the retinoblastoma tumor suppressor gene product. *EMBO J.* 8, 4099–4105.

Muschik, D., Braspenning-Wesch, I., Stockfleth, E., Rösl, F., Hofmann, T. G., and Nindl, I. (2011). Cutaneous HPV23 E6 prevents p53 phosphorylation through interaction with HIPK2. *PLoS ONE* 6:e27655. doi: 10.1371/journal.pone.0027655

Neale, R. E., Weissenborn, S., Abeni, D., Bavinck, J. N. B., Euvrard, S., Feltkamp, M. C. W., et al. (2013). Human papillomavirus load in eyebrow hair follicles and risk of cutaneous squamous cell carcinoma. *Cancer Epidemiol. Prev. Biomark.* 22, 719–727. doi: 10.1158/1055-9965.EPI-12-0917-T

Nindl, I., Koehler, A., Meyer, T., Forschner, T., Meijer, C. J. L. M., Snijders, P. J. F., et al. (2006). Detection of human papillomavirus DNA in primary squamous cell carcinoma and metastases. *Br. J. Dermatol.* 154, 797–799. doi: 10.1111/j.1365-2133.2006.07173.x

Offer, H., Erez, N., Zurer, I., Tang, X., Milyavsky, M., Goldfinger, N., et al. (2002). The onset of p53-dependent DNA repair or apoptosis is determined by the level of accumulated damaged DNA. *Carcinogenesis* 23, 1025–1032. doi: 10.1093/carcin/23.6.1025

Oh, S. T., Kyo, S., and Laimins, L. A. (2001). Telomerase activation by human papillomavirus type 16 E6 protein: induction of human telomerase reverse transcriptase expression through Myc and GC-Rich Sp1 binding sites. *J. Virol.* 75, 5559–5566. doi: 10.1128/JVI.75.12.5559-5566.2001

Orth, G. (1986). Epidermodysplasia verruciformis: a model for understanding the oncogenicity of human papillomaviruses. *Ciba Found. Symp.* 120, 157–174.

Pankotai, T., and Soutoglou, E. (2013). Double strand breaks. *Transcription* 4, 34–38. doi: 10.4161/trns.22879

Pao, G. M., Janknecht, R., Ruffner, H., Hunter, T., and Verma, I. M. (2000). CBP/p300 interact with and function as transcriptional coactivators of BRCA1. *Proc. Natl. Acad. Sci. U.S.A.* 97, 1020–1025. doi: 10.1073/pnas.97.3.1020

Patel, D., Huang, S. M., Baglia, L. A., and McCance, D. J. (1999). The E6 protein of human papillomavirus type 16 binds to and inhibits co-activation by CBP and p300. *EMBO J.* 18, 5061–5072. doi: 10.1093/emboj/18.18.5061

Pfefferle, R., Marcuzzi, G. P., Akgül, B., Kasper, H. U., Schulze, F., Haase, I., et al. (2008). The Human papillomavirus type 8 E2 protein induces skin tumors in transgenic mice. *J. Invest. Dermatol.* 128, 2310–2315. doi: 10.1038/jid.2008.73

Pfister, H. (2003). Chapter 8: human papillomavirus and skin cancer. *J. Natl. Cancer Inst. Monogr.* 52–56. doi: 10.1093/oxfordjournals.jncimonographs.a003483

Pfister, H., Nürnberger, F., Gissmann, L., and zur Hausen, H. (1981). Characterization of a human papillomavirus from epidermodysplasia verruciformis lesions of a patient from upper-volta. *Int. J. Cancer* 27, 645–650. doi: 10.1002/ijc.2910270511

Ray, A., Blevins, C., Wani, G., and Wani, A. A. (2016). ATR- and ATM-mediated DNA damage response is dependent on excision repair assembly during G1 but not in S phase of cell cycle. *PLoS ONE* 11:e0159344. doi: 10.1371/journal.pone.0159344

Ray, A., Milum, K., Battu, A., Wani, G., and Wani, A. A. (2013). NER initiation factors, DDB2 and XPC, regulate UV radiation response by recruiting ATR and ATM kinases to DNA damage sites. *DNA Repair* 12, 273–283. doi: 10.1016/j.dnarep.2013.01.003

Reichrath, J., and Reichrath, S. (2012). Notch-signaling and nonmelanoma skin cancer: an ancient friend, revisited. *Adv. Exp. Med. Biol.* 727, 265–271. doi: 10.1007/978-1-4614-0899-4_20

Reinhardt, H. C., and Schumacher, B. (2012). The p53 network: cellular and systemic DNA damage responses in aging and cancer. *Trends Genet.* 28, 128–136. doi: 10.1016/j.tig.2011.12.002

Reinhardt, H. C., and Yaffe, M. B. (2009). Kinases that control the cell cycle in response to DNA damage: Chk1, Chk2, and MK2. *Curr. Opin. Cell Biol.* 21, 245–255. doi: 10.1016/j.ceb.2009.01.018

Reinson, T., Toots, M., Kadaja, M., Pipitch, R., Allik, M., Ustav, E., et al. (2013). Engagement of the ATR-dependent DNA damage response at the human papillomavirus 18 replication centers during the initial amplification. *J. Virol.* 87, 951–964. doi: 10.1128/JVI.01943-12

Richardson, H., Kelsall, G., Tellier, P., Voyer, H., Abrahamowicz, M., Ferenczy, A., et al. (2003). The natural history of type-specific human papillomavirus infections in female university students. *Cancer Epidemiol. Prev. Biomark* 12, 485–490.

Saidj, D., Cros, M. P., Hernandez-Vargas, H., Guarino, F., Sylla, B. S., Tommasino, M., et al. (2013). Oncoprotein E7 from beta human papillomavirus 38 induces formation of an inhibitory complex for a subset of p53-regulated promoters. *J. Virol.* 87, 12139–12150. doi: 10.1128/JVI.01047-13

Sakakibara, N., Mitra, R., and McBride, A. A. (2011). The papillomavirus E1 helicase activates a cellular DNA damage response in viral replication foci?. *J. Virol.* 85, 8981–8995. doi: 10.1128/JVI.00541-11

Santamaria, D., Barrière, C., Cerqueira, A., Hunt, S., Tardy, C., Newton, K., et al. (2007). Cdk1 is sufficient to drive the mammalian cell cycle. *Nature* 448, 811–815. doi: 10.1038/nature06046

Sawyer, S. L., Tian, L., Kähkönen, M., Schwartzentruber, J., Kircher, M., and University of Washington Centre for Mendelian Gnomics (2015). Biallelic mutations in BRCA1 cause a new Fanconi anemia subtype. *Cancer Discov.* 5, 135–142. doi: 10.1158/2159-8290.CD-14-1156

Schaper, I. D., Marcuzzi, G. P., Weissenborn, S. J., Kasper, H. U., Dries, V., Smyth, N., et al. (2005). Development of skin tumors in mice transgenic for early genes of human papillomavirus type 8. *Cancer Res.* 65, 1394–1400. doi: 10.1158/0008-5472.CAN-04-3263

Scheffner, M., Werness, B. A., Huibregtse, J. M., Levine, A. J., and Howley, P. M. (1990). The E6 oncoprotein encoded by human papillomavirus types 16 and 18 promotes the degradation of p53. *Cell* 63, 1129–1136. doi: 10.1016/0092-8674(90)90409-8

Sharma, G. G., Gupta, A., Wang, H., Scherthan, H., Dhar, S., Gandhi, V., et al. (2003). hTERT associates with human telomeres and enhances genomic stability and DNA repair. *Oncogene* 22, 131–146. doi: 10.1038/sj.onc.1206063

Shigechi, T., Tomida, J., Sato, K., Kobayashi, M., Eykelenboom, J. K., Pessina, F., et al. (2012). ATR-ATRIP kinase complex triggers activation of the Fanconi anemia DNA repair pathway. *Cancer Res.* 72, 1149–1156. doi: 10.1158/0008-5472.CAN-11-2904

Shiloh, Y., and Ziv, Y. (2013). The ATM protein kinase: regulating the cellular response to genotoxic stress, and more. *Nat. Rev. Mol. Cell Biol.* 14, 197–210. doi: 10.1038/nrm3546

Shiotani, B., and Zou, L. (2009). Single-stranded DNA orchestrates an ATM-to-ATR switch at DNA breaks. *Mol. Cell* 33, 547–558. doi: 10.1016/j.molcel.2009.01.024

Simmonds, M., and Storey, A. (2008). Identification of the regions of the HPV 5 E6 protein involved in Bak degradation and inhibition of apoptosis. *Int. J. Cancer* 123, 2260–2266. doi: 10.1002/ijc.23815

Sperling, T., Ołdak, M., Walch-Ruckheim, B., Wickenhauser, C., Doorbar, J., Pfister, H., et al. (2012). Human papillomavirus type 8 interferes with a novel C/EBPβ-mediated mechanism of keratinocyte CCL20 chemokine expression and langerhans cell migration. *PLoS Pathog.* 8:e1002833. doi: 10.1371/journal.ppat.1002833

Szalmás, A., Tomaić, V., Basukala, O., Massimi, P., Mittal, S., Kónya, J., et al. (2017). The PTPN14 tumor suppressor is a degradation target of human papillomavirus E7. *J. Virol.* 91:e00057-17. doi: 10.1128/JVI.00057-17

ten Dijke , P., and Hill, C. S. (2004). New insights into TGF-β-Smad signalling. *Trends Biochem. Sci.* 29, 265–273. doi: 10.1016/j.tibs.2004.03.008

Thomas, M., and Banks, L. (1999). Human papillomavirus (HPV) E6 interactions with Bak are conserved amongst E6 proteins from high and low risk HPV types. *J. Gen. Virol.* 80(Pt 6), 1513–1517. doi: 10.1099/0022-1317-80-6-1513

Tibbetts, R. S., Brumbaugh, K. M., Williams, J. M., Sarkaria, J. N., Cliby, W. A., Shieh, S. Y., et al. (1999). A role for ATR in the DNA damage-induced phosphorylation of p53. *Genes Dev.* 13, 152–157. doi: 10.1101/gad.13.2.152

Tomaić, V. (2016). Functional roles of E6 and E7 oncoproteins in HPV-induced malignancies at diverse anatomical sites. *Cancers* 8:95. doi: 10.3390/cancers8100095

Tommasino, M. (2014). The human papillomavirus family and its role in carcinogenesis. *Semin. Cancer Biol.* 26, 13–21. doi: 10.1016/j.semcancer.2013.11.002

Tommasino, M. (2017). The biology of beta human papillomaviruses. *Virus Res.* 231, 128–138. doi: 10.1016/j.virusres.2016.11.013

Turnell, A. S., Stewart, G. S., Grand, R. J. A., Rookes, S. M., Martin, A., Yamano, H., et al. (2005). The APC/C and CBP/p300 cooperate to regulate transcription and cell-cycle progression. *Nature* 438, 690–695. doi: 10.1038/nature04151

Underbrink, M. P., Howie, H. L., Bedard, K. M., Koop, J. I., and Galloway, D. A. (2008). E6 Proteins from multiple human betapapillomavirus types degrade Bak and protect keratinocytes from apoptosis after UVB irradiation. *J. Virol.* 82, 10408–10417. doi: 10.1128/JVI.00902-08

Van Doorslaer, K. (2013). Evolution of the papillomaviridae. *Virology* 445, 11–20. doi: 10.1016/j.virol.2013.05.012

Vermezovic, J., Adamowicz, M., Santarpia, L., Rustighi, A., Forcato, M., Lucano, C., et al. (2015). Notch is a direct negative regulator of the DNA-damage response. *Nat. Struct. Mol. Biol.* 22, 417–424. doi: 10.1038/nsmb.3013

Viarisio, D., Mueller-Decker, K., Kloz, U., Aengeneyndt, B., Kopp-Schneider, A., Gröne, H. J., et al. (2011). E6 and E7 from Beta Hpv38 cooperate with ultraviolet light in the development of actinic keratosis-like lesions and squamous cell carcinoma in mice. *PLOS Pathog.* 7:e1002125. doi: 10.1371/journal.ppat.1002125

Viarisio, D., Müller-Decker, K., Zanna, P., Kloz, U., Aengeneyndt, B., Accardi, R., et al. (2016). Novel ß-HPV49 transgenic mouse model of upper digestive tract cancer. *Cancer Res.* 76, 4216–4225. doi: 10.1158/0008-5472.CAN-16-0370

Vogelstein, B., Lane, D., and Levine, A. J. (2000). Surfing the p53 network. *Nature* 408, 307–310. doi: 10.1038/35042675

Wallace, N. A., Gasior, S. L., Faber, Z. J., Howie, H. L., Deininger, P. L., and Galloway, D. A. (2013). HPV 5 and 8 E6 expression reduces ATM protein levels and attenuates LINE-1 retrotransposition. *Virology* 443, 69–79. doi: 10.1016/j.virol.2013.04.022

Wallace, N. A., Khanal, S., Robinson, K. L., Wendel, S. O., Messer, J. J., and Galloway, D. A. (2017). High-risk *alphapapillomavirus* oncogenes impair the homologous recombination pathway. *J. Virol.* 91:e01084-17. doi: 10.1128/JVI.01084-17

Wallace, N. A., Robinson, K., and Galloway, D. A. (2014). Beta human papillomavirus E6 expression inhibits stabilization of p53 and increases tolerance of genomic instability. *J. Virol.* 88, 6112–6127. doi: 10.1128/JVI.03808-13

Wallace, N. A., Robinson, K., Howie, H. L., and Galloway, D. A. (2012). HPV 5 and 8 E6 abrogate ATR activity resulting in increased persistence of UVB induced DNA damage. *PLoS Pathog.* 8:e1002807. doi: 10.1371/journal.ppat.1002807

Wallace, N. A., Robinson, K., Howie, H. L., and Galloway, D. A. (2015). β-HPV 5 and 8 E6 disrupt homology dependent double strand break repair by attenuating BRCA1 and BRCA2 expression and foci formation. *PLoS Pathog.* 11:e1004687. doi: 10.1371/journal.ppat.1004687

Wang, W., Huang, J., Wang, X., Yuan, J., Li, X., Feng, L., et al. (2012). PTPN14 is required for the density-dependent control of YAP1. *Genes Dev.* 26, 1959–1971. doi: 10.1101/gad.192955.112

Waterboer, T., Abeni, D., Sampogna, F., Rother, A., Masini, C., Sehr, P., et al. (2008). Serological association of beta and gamma human papillomaviruses with squamous cell carcinoma of the skin. *Br. J. Dermatol.* 159, 457–459. doi: 10.1111/j.1365-2133.2008.08621.x

Weissenborn, S. J., De Koning, M. N. C., Wieland, U., Quint, W. G. V., and Pfister, H. J. (2009). Intrafamilial transmission and family-specific spectra of cutaneous betapapillomaviruses. *J. Virol.* 83, 811–816. doi: 10.1128/JVI.01338-08

Weissenborn, S. J., Nindl, I., Purdie, K., Harwood, C., Proby, C., Breuer, J., et al. (2005). Human Papillomavirus-DNA loads in actinic keratoses exceed those in non-melanoma skin cancers. *J. Invest. Dermatol.* 125, 93–97. doi: 10.1111/j.0022-202X.2005.23733.x

Weissenborn, S., Neale, R. E., Waterboer, T., Abeni, D., Bavinck, J. N. B., Green, A. C., et al. (2012). Beta-papillomavirus DNA loads in hair follicles

of immunocompetent people and organ transplant recipients. *Med. Microbiol. Immunol.* 201, 117–125. doi: 10.1007/s00430-011-0212-3

Werness, B. A., Levine, A. J., and Howley, P. M. (1990). Association of human papillomavirus types 16 and 18 E6 proteins with p53. *Science* 248, 76–79. doi: 10.1126/science.2157286

White, E. A., Kramer, R. E., Tan, M. J. A., Hayes, S. D., Harper, J. W., and Howley, P. M. (2012). Comprehensive analysis of host cellular interactions with human papillomavirus E6 proteins identifies new E6 binding partners and reflects viral diversity. *J. Virol.* 86, 13174–13186. doi: 10.1128/JVI.02172-12

White, E. A., Münger, K., and Howley, P. M. (2016). high-risk human papillomavirus E7 proteins target PTPN14 for degradation. *mBio* 7:e01530-16. doi: 10.1128/mBio.01530-16

White, E. A., Walther, J., Javanbakht, H., and Howley, P. M. (2014). Genus beta human papillomavirus E6 proteins vary in their effects on the transactivation of p53 target genes. *J. Virol.* 88, 8201–8212. doi: 10.1128/JVI.01197-14

Willis, N., and Rhind, N. (2009). Regulation of DNA replication by the S-phase DNA damage checkpoint. *Cell Div.* 4:13. doi: 10.1186/1747-1028-4-13

Xia, P., Wang, Z., Liu, X., Wu, B., Wang, J., Ward, T., et al. (2012). EB1 acetylation by P300/CBP-associated factor (PCAF) ensures accurate kinetochore–microtubule interactions in mitosis. *Proc. Natl. Acad. Sci. U.S.A.*109, 16564–16569. doi: 10.1073/pnas.1202639109

Yamashita, T., Segawa, K., Fujinaga, Y., Nishikawa, T., and Fujinaga, K. (1993). Biological and biochemical activity of E7 genes of the cutaneous human papillomavirus type 5 and 8. *Oncogene* 8, 2433–2441.

Yan, S., Sorrell, M., and Berman, Z. (2014). Functional interplay between ATM/ATR-mediated DNA damage response and DNA repair pathways in oxidative stress. *Cell. Mol. Life Sci. CMLS* 71, 3951–3967. doi: 10.1007/s00018-014-1666-4

Yang, J., Yu, Y., Hamrick, H. E., and Duerksen-Hughes, P. J. (2003). ATM, ATR and DNA-PK: initiators of the cellular genotoxic stress responses. *Carcinogenesis* 24, 1571–1580. doi: 10.1093/carcin/bgg137

Yang, W. (2011). Surviving the sun: repair and bypass of DNA UV lesions. *Protein Sci. Publ. Protein Soc.* 20, 1781–1789. doi: 10.1002/pro.723

Yoshida, K., and Miki, Y. (2004). Role of BRCA1 and BRCA2 as regulators of DNA repair, transcription, and cell cycle in response to DNA damage. *Cancer Sci.* 95, 866–871. doi: 10.1111/j.1349-7006.2004.tb02195.x

Yu, J., and Zhang, L. (2005). The transcriptional targets of p53 in apoptosis control. *Biochem. Biophys. Res. Commun.* 331, 851–858. doi: 10.1016/j.bbrc.2005.03.189

Zerfass, K., Schulze, A., Spitkovsky, D., Friedman, V., Henglein, B., and Jansen-Dürr, P. (1995). Sequential activation of cyclin E and cyclin A gene expression by human papillomavirus type 16 E7 through sequences necessary for transformation. *J. Virol.* 69, 6389–6399.

Zimmermann, H., Degenkolbe, R., Bernard, H.-U., and O'Connor, M. J. (1999). The human papillomavirus type 16 E6 oncoprotein can down-regulate p53 activity by targeting the transcriptional coactivator CBP/p300. *J. Virol.* 73, 6209–6219.

Conflict of Interest Statement: The authors declare that the research was conducted in the absence of any commercial or financial relationships that could be construed as a potential conflict of interest.

PLOS | PATHOGENS

OPINION

The curious case of APOBEC3 activation by cancer-associated human papillomaviruses

Nicholas A. Wallace[1]*, **Karl Münger**[2]*

1 Division of Biology, Kansas State University, Manhattan, Kansas, United States of America, **2** Department of Developmental, Molecular and Chemical Biology, Tufts University School of Medicine, Boston, Massachusetts, United States of America

* nwallac@ksu.edu (NAW); karl.munger@tufts.edu (KM)

Citation: Wallace NA, Münger K (2018) The curious case of APOBEC3 activation by cancer-associated human papillomaviruses. PLoS Pathog 14(1): e1006717. https://doi.org/10.1371/journal.ppat.1006717

Editor: Carolyn B Coyne, University of Pittsburgh, UNITED STATES

Published: January 11, 2018

Funding: The authors' research on HPV is supported by PHS grant CA066980 (KM) and DoD CDMRP CA160224 (NAW) and P20 GM103418 (NAW). The funders had no role in study design, data collection and analysis, decision to publish, or preparation of the manuscript.

Competing interests: The authors have declared that no competing interests exist.

High-risk human papillomavirus (HR-HPV) infections cause approximately 5% of all human cancers worldwide. These include almost all cervical carcinomas, a leading global cause of cancer deaths, as well as a significant percentage of other anogenital tract cancers and a growing fraction of oropharyngeal carcinomas. To accommodate their life cycles, HR-HPVs need to extensively rewire infected cells. The HR-HPV E6 and E7 proteins are the main drivers of this process, and their expression elicits a barrage of cellular defense responses that restrict this unfriendly takeover of the host cell.

Not surprisingly, HR-HPVs have in turn evolved mechanisms to escape or curb antiviral and anti-oncogenic cellular responses. These mechanisms include degradation of the retinoblastoma (RB1) and the p53 (TP53) tumor suppressors by HR-HPV E7 and E6, respectively. If unopposed, RB1 and TP53 would cause cell cycle arrest, senescence, or cell death in response to HR-HPV infection (Fig 1). Other antiviral pathways, including DNA sensing and interferon signaling, are also blunted by HR-HPV E6 and E7 proteins [1].

Surprisingly, HR-HPVs have not evolved strategies to counteract restriction by apolipoprotein B mRNA editing enzyme, catalytic polypeptide-like 3 (APOBEC3, or simply A3). A3s are interferon-regulated DNA cytosine-to-uracil deaminases encoded as a cluster of seven genes (A3A–A3H; there is no A3E) on human chromosome 22, which are all expressed, albeit at vastly different levels, in epithelial cells [2], which are the natural hosts of HPV infection. While their cytidine deaminase activity causes deoxycytidine (C) to deoxythymidine (T) mutations during viral genome synthesis, A3s also restrict viral replication through cytidine deaminase-independent mechanisms [3].

In response, many viruses have evolved mechanisms to evade A3 restriction. The human immunodeficiency virus 1 (HIV1) Viral infectivity factor (Vif) protein targets A3 family members for degradation, and the HIV2 Viral protein X (Vpx) protein targets A3A for degradation [4, 5]. The Hepatitis B Virus X protein impairs this pathway by packaging A3G into exosomes [6]. Human polyomaviruses—including the Merkel Cell Polyomavirus (McPyV)—trigger A3 activity, yet McPyV-positive Merkel cell carcinomas do not show an A3 mutational signature [7, 8]. This strongly suggests that McPyV overrides A3 restriction [8].

While ectopically expressed HR-HPV E7 and E6 have each been reported to increase expression of A3 family members, and A3A can restrict infection with in vitro–generated HPV16 pseudovirions, A3 activity is not blocked by HR-HPVs [3, 9–11]. Despite the fact that HPV genomes contain fewer than predicted A3 recognition sites [12], the mutational drift caused by A3 mutagenesis is extensive; many of the thousands of HPV16 variants that were detected in a recent study exhibit nucleotide changes that are consistent with A3 action [13].

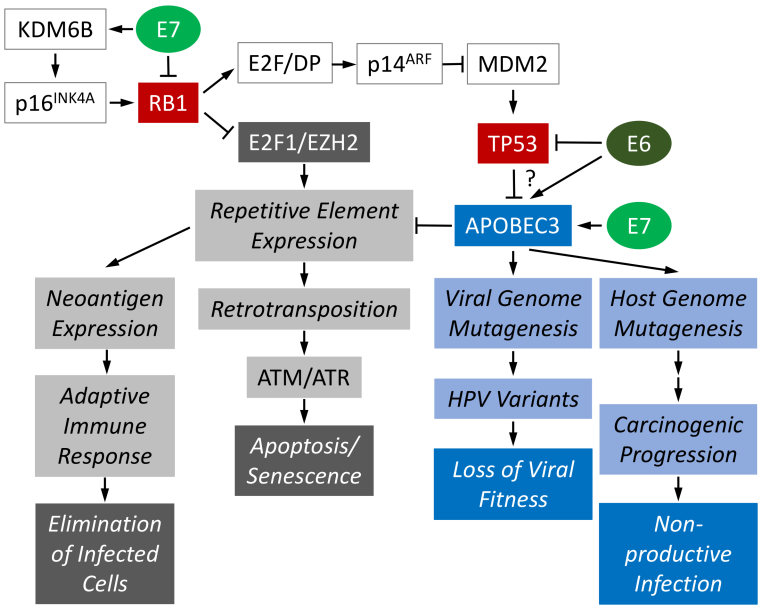

Fig 1. Molecular consequences of APOBEC3 induction in HR-HPV–infected cells. See text for detail. APOBEC3, apolipoprotein B mRNA editing enzyme, catalytic polypeptide-like 3; HR-HPV, high-risk human papillomavirus.

https://doi.org/10.1371/journal.ppat.1006717.g001

Furthermore, A3 expression causes nucleotide changes in the host cellular genome. Integration of HPV sequences during malignant progression is accompanied by increased A3A levels [14], and cervical carcinomas and other HPV-associated cancers exhibit A3 mutational signatures [15, 16]. Indeed, A3-mediated host genome destabilization may be one of the mechanisms that drive carcinogenic progression of HR-HPV–associated lesions as evidenced by Phosphatidylinositol-4,5-Bisphosphate 3-Kinase Catalytic Subunit Alpha (PIK3CA) mutations that are consistent with A3 mutagenesis that have been detected in HPV-associated cancers [17]. HPV-associated cancers are generally nonproductive lesions [1], therefore increased carcinogenicity is unlikely to provide an evolutionary benefit to the life cycles of HR-HPVs and does not explain why HR-HPVs have not evolved to block A3 mutagenesis.

Why, then, have HR-HPVs not evolved to subvert this highly active cellular defense response? It has been argued that A3 activation serves to generate viral diversity, and there is no doubt that HPVs are incredibly diverse; the current count stands at more than 300 HPV genotypes, as well as thousands of variants, many of which may have been generated as a result of A3 mutagenesis [13].

The recent discovery by Fred Dick's research group that RB1 plays a key role in the epigenetic silencing of repetitive elements may provide an alternative explanation as to why it may be beneficial for HR-HPVs not to counteract A3 restriction [18]. RB1 silences repetitive elements by associating with a unique E2F1 transcription factor complex that contains the Enhancer Of Zeste 2 Polycomb Repressive Complex 2 Subunit (EZH2) methyl transferase. The degradation of RB1 by HR-HPV E7 proteins is therefore predicted to cause transcription of repetitive elements [18]. Because translation of some of these—most notably the Long INterspersed Element-1 (LINE1 or L1)—results in neoantigen expression, transcription of repetitive elements would put HR-HPV–infected cells at risk of extinction through adaptive immune responses. Moreover, the LINE1 open reading frame 2 (ORF2) encodes an endonuclease that facilitates the mobilization of LINE1 elements through a "copy and paste" mechanism referred to as retrotransposition. Excessive double-strand DNA breaks caused by the ORF2

endonuclease can result in senescence or apoptosis, which would also lead to the elimination of HR-HPV–infected cells (Fig 1). While the majority of the LINE1 copies in the human genome are 5′ truncated and do not express functional endonucleases, it has been estimated that the remaining functional LINE1 elements may cause 0.3% of all human mutations [19, 20]. This staggering number likely underestimates the mutational impact of LINE1 element mobilization. LINE1 can also mobilize nonautonomous transposable elements, which only requires its second open reading (ORF2) that frequently remains intact even with 5′-truncated LINE1 copies. A3s are well known to restrict expression of repetitive elements, including LINEs, via deaminase-independent activity [21]. Therefore, HR-HPV–infected cells would gain significant advantages from this A3-dependent restriction of LINE elements. Because even unrestrained A3 activity will not completely prevent retrotransposition, the residual activation of double-strand DNA break sensing and repair machinery may be beneficial for efficient HR-HPV genome replication given its well-documented dependence on these factors, including the Ataxia Telangiectasia Mutated (ATM) and Ataxia Telangiectasia And Rad3-Related Protein (ATR) kinases [22].

In addition, HR-HPV–mediated RB1 degradation causes high-level expression of satellite RNAs that can lead to formation of R-loops, a DNA RNA three-stranded structure, which causes replication forks to stall [18]. A3 target the single-stranded DNA in R-loops and can thereby also activate the DNA damage response [23], which benefits HPV replication. Lastly, HR-HPVs may benefit from a deaminase-independent activity of A3, making the A3 mutational signature in HPV-associated tumors simply a by-product of the viruses' requirement for another function of A3.

Because nearly every unvaccinated, sexually active individual has been infected with an HR-HPV, such an incredibly successful virus should have evolved a defensive strategy against the potent restriction of viral replication and viral persistence by A3 unless it provides them with a selective advantage. HR-HPVs uniquely cause RB1 degradation and thus are predicted to de-repress retrotransposon expression. TP53 is known to restrict retrotransposition [24–26], and HR-HPV E6–mediated TP53 degradation may further increase LINE1 activity. While activation of double-strand DNA sensing and repair pathways induced by retrotransposition triggered by RB1 degradation and R-loop resolution by A3s may stimulate HR-HPV genome replication and progeny synthesis, A3 restriction of repetitive elements may protect HR-HPV–infected cells from undergoing excessive, lethal DNA damage and genomic instability. Moreover, A3 restriction will prevent elimination of HR-HPV–infected cells by adaptive immune responses to neoantigen expression due to expression of repetitive elements.

Acknowledgments

The authors thank Dr. Marta Gaglia and Dr. Alison McBride as well as the three anonymous reviewers for their thoughtful comments on this manuscript.

References

1. Moody CA, Laimins LA. Human papillomavirus oncoproteins: pathways to transformation. Nat Rev Cancer. 2010; 10(8):550–60. https://doi.org/10.1038/nrc2886 PMID: 20592731.
2. Harden ME, Prasad N, Griffiths A, Munger K. Modulation of microRNA-mRNA Target Pairs by Human Papillomavirus 16 Oncoproteins. MBio. 2017; 8(1). https://doi.org/10.1128/mBio.02170-16 PMID: 28049151.
3. Warren CJ, Westrich JA, Van Doorslaer K, Pyeon D. Roles of APOBEC3A and APOBEC3B in Human Papillomavirus Infection and Disease Progression. Viruses. 2017; 9:233. https://doi.org/10.3390/v9080233 PMID: 28825669

4. Simon V, Bloch N, Landau NR. Intrinsic host restrictions to HIV-1 and mechanisms of viral escape. Nat Immunol. 2015; 16(6):546–53. https://doi.org/10.1038/ni.3156 PMID: 25988886.
5. Berger G, Durand S, Fargier G, Nguyen XN, Cordeil S, Bouaziz S, et al. APOBEC3A is a specific inhibitor of the early phases of HIV-1 infection in myeloid cells. PLoS Pathog. 2011; 7(9):e1002221. https://doi.org/10.1371/journal.ppat.1002221 PMID: 21966267.
6. Chen R, Zhao X, Wang Y, Xie Y, Liu J. Hepatitis B virus X protein is capable of down-regulating protein level of host antiviral protein APOBEC3G. Sci Rep. 2017; 7:40783. https://doi.org/10.1038/srep40783 PMID: 28098260.
7. Verhalen B, Starrett GJ, Harris RS, Jiang M. Functional Upregulation of the DNA Cytosine Deaminase APOBEC3B by Polyomaviruses. J Virol. 2016; 90(14):6379–86. https://doi.org/10.1128/JVI.00771-16 PMID: 27147740.
8. Starrett GJ, Marcelus C, Cantalupo PG, Katz JP, Cheng J, Akagi K, et al. Merkel Cell Polyomavirus Exhibits Dominant Control of the Tumor Genome and Transcriptome in Virus-Associated Merkel Cell Carcinoma. MBio. 2017; 8(1). https://doi.org/10.1128/mBio.02079-16 PMID: 28049147.
9. Vieira VC, Leonard B, White EA, Starrett GJ, Temiz NA, Lorenz LD, et al. Human papillomavirus E6 triggers upregulation of the antiviral and cancer genomic DNA deaminase APOBEC3B. MBio. 2014; 5(6). https://doi.org/10.1128/mBio.02234-14 PMID: 25538195.
10. Wang Z, Wakae K, Kitamura K, Aoyama S, Liu G, Koura M, et al. APOBEC3 deaminases induce hypermutation in human papillomavirus 16 DNA upon beta interferon stimulation. J Virol. 2014; 88(2): 1308–17. https://doi.org/10.1128/JVI.03091-13 PMID: 24227842.
11. Warren CJ, Xu T, Guo K, Griffin LM, Westrich JA, Lee D, et al. APOBEC3A functions as a restriction factor of human papillomavirus. J Virol. 2015; 89(1):688–702. https://doi.org/10.1128/JVI.02383-14 PMID: 25355878.
12. Warren CJ, Van Doorslaer K, Pandey A, Espinosa JM, Pyeon D. Role of the host restriction factor APOBEC3 on papillomavirus evolution. Virus Evol. 2015; 1(1). https://doi.org/10.1093/ve/vev015 PMID: 27570633.
13. Mirabello L, Yeager M, Yu K, Clifford GM, Xiao Y, Zhu B, et al. HPV16 E7 Genetic Conservation Is Critical to Carcinogenesis. Cell. 2017; 170(6):1164–74 e6. https://doi.org/10.1016/j.cell.2017.08.001 PMID: 28886384.
14. Kondo S, Wakae K, Wakisaka N, Nakanishi Y, Ishikawa K, Komori T, et al. APOBEC3A associates with human papillomavirus genome integration in oropharyngeal cancers. Oncogene. 2017; 36(12): 1687–97. https://doi.org/10.1038/onc.2016.335 PMID: 27694899.
15. Burns MB, Temiz NA, Harris RS. Evidence for APOBEC3B mutagenesis in multiple human cancers. Nat Genet. 2013; 45(9):977–83. https://doi.org/10.1038/ng.2701 PMID: 23852168.
16. Roberts SA, Lawrence MS, Klimczak LJ, Grimm SA, Fargo D, Stojanov P, et al. An APOBEC cytidine deaminase mutagenesis pattern is widespread in human cancers. Nat Genet. 2013; 45(9):970–6. https://doi.org/10.1038/ng.2702 PMID: 23852170.
17. Henderson S, Chakravarthy A, Su X, Boshoff C, Fenton TR. APOBEC-mediated cytosine deamination links PIK3CA helical domain mutations to human papillomavirus-driven tumor development. Cell Rep. 2014; 7(6):1833–41. https://doi.org/10.1016/j.celrep.2014.05.012 PMID: 24910434.
18. Ishak CA, Marshall AE, Passos DT, White CR, Kim SJ, Cecchini MJ, et al. An RB-EZH2 Complex Mediates Silencing of Repetitive DNA Sequences. Mol Cell. 2016; 64(6):1074–87. https://doi.org/10.1016/j.molcel.2016.10.021 PMID: 27889452.
19. Kazazian HH, Jr. An estimated frequency of endogenous insertional mutations in humans. Nat Genet. 1999; 22(2):130. https://doi.org/10.1038/9638 PMID: 10369250.
20. Deininger PL, Batzer MA. Alu repeats and human disease. Mol Genet Metab. 1999; 67(3):183–93. https://doi.org/10.1006/mgme.1999.2864 PMID: 10381326.
21. Koito A, Ikeda T. Intrinsic immunity against retrotransposons by APOBEC cytidine deaminases. Front Microbiol. 2013; 4:28. https://doi.org/10.3389/fmicb.2013.00028 PMID: 23431045.
22. Moody CA, Laimins LA. Human papillomaviruses activate the ATM DNA damage pathway for viral genome amplification upon differentiation. PLoS Pathog. 2009; 5(10):e1000605. https://doi.org/10.1371/journal.ppat.1000605 PMID: 19798429.
23. Sollier J, Cimprich KA. Breaking bad: R-loops and genome integrity. Trends Cell Biol. 2015; 25(9): 514–22. https://doi.org/10.1016/j.tcb.2015.05.003 PMID: 26045257.
24. Haoudi A, Semmes OJ, Mason JM, Cannon RE. Retrotransposition-Competent Human LINE-1 Induces Apoptosis in Cancer Cells With Intact p53. J Biomed Biotechnol. 2004; 2004(4):185–94. https://doi.org/10.1155/S1110724304403131 PMID: 15467158.

25. Harris CR, Dewan A, Zupnick A, Normart R, Gabriel A, Prives C, et al. p53 responsive elements in human retrotransposons. Oncogene. 2009; 28(44):3857–65. https://doi.org/10.1038/onc.2009.246 PMID: 19718052.

26. Wylie A, Jones AE, D'Brot A, Lu WJ, Kurtz P, Moran JV, et al. p53 genes function to restrain mobile elements. Genes Dev. 2016; 30(1):64–77. https://doi.org/10.1101/gad.266098.115 PMID: 26701264.

COMMENTARY
Host-Microbe Biology

mSphere of Influence: the Value of Simplicity in Experiments and Solidarity among Lab Members

Nicholas A. Wallace[a]

[a]Division of Biology, Kansas State University, Manhattan, Kansas, USA

ABSTRACT Nicholas Wallace studies how human papillomaviruses cause cancer throughout the genital and oropharyngeal tracts as well as in the skin. These viruses inhibit host DNA repair to promote their life style and in doing increase the risk of oncogenic mutations. In this mSphere of Influence article, he reflects on how two papers influenced him. "Human Papillomaviruses Activate the ATM DNA Damage Pathway for Viral Genome Amplification upon Differentiation" by C. A. Moody and L. Laimins (PLoS Pathog 5:e10000605, 2009, https://doi.org/10.1371/journal.ppat.1000605) reminded him of the power of straightforward approaches, while "Forty-Five Years of Cell-Cycle Genetics" by B. Reid et al. (B. J. Reid, J. G. Culotti, R. S. Nash, and J. R. Pringle, Mol Biol Cell 26:4307–4312, 2015, https://doi.org/10.1091/mbc.E14-10-1484) gave him the inspiration for his lab management style.

KEYWORDS DNA repair, cervical cancer, human papillomavirus

Every scientist has their own unique approach, generated from a myriad of influences and personal experiences. Mentoring styles are even more individualized. Obviously, research mentors play an outsized role in shaping our approach to science. We are influenced by daily interactions with peers and lab mates, and every so often, there is a paper that changes the way we look at the world around us. The first time I read "Human Papillomaviruses Activate the ATM DNA Damage Pathway for Viral Genome Amplification upon Differentiation" by Cary Moody and Laimonis "Lou" Laimins is a vivid and influential memory (1). I had studied genomic instability induced by retrotransposons as a graduate student and had recently begun work as a postdoc in Denise Galloway's group at the Fred Hutchinson Cancer Research Center (affectionately known as "The Hutch"). The question of how much skin cancer resulted from cutaneous human papillomavirus (HPV) infections fascinated me, but I was struggling to find my footing in this new field. My first ambitious project had plenty of technological bells and whistles. It had also just completely bombed. I felt left behind in the race to develop the fanciest approach to match the experiments that everyone else seemed to be running.

In the midst of these doldrums, Denise casually dropped Cary and Lou's paper on my desk with a passing comment about it seeming like "something up your alley." It was. Not only did the paper help me connect my graduate work to my new interests in viral oncology, it relied on elegantly designed experiments, rather than fancy, but hard to replicate approaches. The results were clear and definitive, relying on Southern and Western blotting combined with immunofluorescence microscopy to dissect HPV's manipulation of DNA repair processes. Using familiar techniques, Cary and Lou had shown undeniable evidence that hyperactivation of a DNA repair signaling pathway facilitated HPV genome amplification. I felt hopeful again. Sure cutting edge techniques can drive a field forward, but there were clearly other paths to success. I poured my energy back into asking important questions and trying to answer them directly and precisely. The impact of Cary and Lou's dissection of altered ATM signaling is easy to

Citation Wallace NA. 2019. mSphere of Influence: the value of simplicity in experiments and solidarity among lab members. mSphere 4:e00172-19. https://doi.org/10.1128/mSphere.00172-19.

Address correspondence to nwallac@ksu.edu.

The views expressed in this article do not necessarily reflect the views of the journal or of ASM.

Getting to talk about two very influential papers was a pleasure. I hope this commentary draws interest to the authors' wonderful work. @wallaceHPVlab

Published 19 June 2019

find in every paper from my lab. Perhaps more generally important, it is a steady reminder that flashiness is not a requirement for good science.

Several years later and at another transition point in my life, I encountered a different kind of article that was similarly impactful. It was not a primary research article or even a review. "Forty-Five Years of Cell-Cycle Genetics" by Brian Reid et al. is a retrospective commentary about the early years in Leland Hartwell's lab that was published almost exactly 1 week after I started my first faculty job (2). I read it about 3 months later, when I was back visiting the Galloway lab over the winter holidays. Brian's lab and office are just down the hall from Denise's at the Hutch, so we had spoken each day for years. It must have surprised him to see me back to my morning routine when I greeted him. I remember being filled with excitement from my new position, but beginning to realize how much I was unprepared for. I peppered him with questions, "Who should I hire?" "What should I do first?" "How do I attract students?" "How can I help undergraduate students do 'good' science?" and on and on. When I paused to breathe, Brian matched my enthusiasm with stories of his time as a student in the Hartwell lab. It was wonderful to see that the memory of 40 years earlier still energized him.

Before I left, he sent me a copy of the article that he and his contemporaries in the Hartwell lab penned about their early days together. It should be required reading for any new principal investigator, especially if they plan to interact with undergraduates. I would love for my students to have half as positive of an experience as Brian and his colleagues had. The article describes the perfect atmosphere for science and is filled with motivational quotes like "although the group was not large, it never seemed small, in part because interaction among the lab members was so constant and intense". Who would not want to work in that environment?!? Life as a scientist has peaks of exhilaration, but it is also brutal. Surviving negative reviews, rejections, misbehaving experiments, and unexplained contaminations are a daunting task that we all face. Your lab environment can make all the difference. I model my lab atmosphere after the one described in "Forty-Five Years of Cell-Cycle Genetics". It is the first paper people read when they join our team. "An atmosphere of total openness and high collegiality, in which no one worried about who would get credit for a particular idea" sounds like science utopia. The camaraderie that Brian Reid, Joseph Culotti, Robert Nash, and John Pringle describe should be the goal of every leader.

REFERENCES

1. Moody CA, Laimins LA. 2009. Human papillomaviruses activate the ATM DNA damage pathway for viral genome amplification upon differentiation. PLoS Pathog 5:e1000605. https://doi.org/10.1371/journal.ppat.1000605.
2. Reid BJ, Culotti JG, Nash RS, Pringle JR. 2015. Forty-five years of cell-cycle genetics. Mol Biol Cell 26:4307–4312. https://doi.org/10.1091/mbc.E14-10-1484.

Gene 688 (2019) 44–53

Contents lists available at ScienceDirect

Gene

journal homepage: www.elsevier.com/locate/gene

Research paper

Cervical cancer cell lines are sensitive to sub-erythemal UV exposure

Wenyi Gu[a,1], Surong Sun[a,c], Andrew Kahn[b], Dalton Dacus[b], Sebastian O. Wendel[b], Nigel McMillan[a,*], Nicholas A. Wallace[b,*]

[a] School of Medical Sciences, Griffith University, Gold Coast Campus, Australia
[b] Division of Biology, Kansas State University, Manhattan, KS, United States of America
[c] Xinjiang Key Laboratory of Biological Resources and Genetic Engineering, College of Life Science and Technology, Xinjiang University, Urumqi 830046, China

ARTICLE INFO

Keywords:
Human papillomavirus
UV damage
Cervical cancer
Cisplatin
Drug resistance
HPV E6
HPV E7
DNA repair
Genomic instability

ABSTRACT

High risk human papillomavirus (HPV) infections are the causative agent in virtually every cervical cancer as well as a host of other anogenital and oropharyngeal malignancies. These viruses must activate DNA repair pathways to facilitate their replication, while avoiding the cell cycle arrest and apoptosis that can accompany DNA damage. HPV oncoproteins facilitate each of these goals, but also reduce genome stability. Our data dissect the cytotoxic and cytoprotective characteristics of HPV oncogenes in cervical cancer cells. These data show that while the transformation of keratinocytes by HPV oncogene leaves these cells more sensitive to UV, the oncogenes also protect against UV-induced apoptosis. Cisplatin and UV resistant cervical cancer cell lines were generated and probed for their sensitivity to genotoxic agents. Cervical cancer cells can acquire resistance to one DNA crosslinking agent (UV or cisplatin) without gaining broad tolerance of crosslinked DNA. Further, cisplatin resistance may or may not result in sensitivity to PARP1 inhibition.

1. Introduction

Cervical cancers are the third most common and second deadliest cancer in women worldwide. Over half a million new cases of cervical cancer are diagnosed annually killing nearly 300,000 people (Parkin and Bray, 2006). Access to healthcare is a major factor in the development of cervical cancer with as many as 80% of cases occurring in developing countries (Sherris et al., 2001; Siegel et al., 2012; Tota et al., 2011). In addition to differences in screening and care, environmental factors (smoking and UV exposure for instance) increase the risk of cervical cancer (Fonseca-Moutinho, 2011; Godar et al., 2014). Nearly every cervical cancer is the result of a human papillomavirus infection (zur Hausen, 2002). This very large family of double stranded circular DNA viruses is divided into 5 genera based on sequence differences in their L1 major capsid gene (Bernard et al., 2010). While members of both the genus alpha and beta of human papillomaviruses are associated with cancer (Godar et al., 2014; Howley and Pfister, 2015; Wendel and Wallace, 2017), members of the genus alpha human papillomaviruses are further divided into high risk and low risk papillomaviruses based on the relative ability to cause cancer. Among the high risk alpha papillomaviruses, human papillomaviruses 16 and 18 cause 70% of cervical cancers (Winer et al., 2006). In this manuscript, we will refer to these two viruses as simply as HPV.

Much is known about the molecular basis of how HPV manipulates the host cell both to promote its life cycle and to cause malignant transformation. Although the E5 protein from these viruses has oncogenic potential, the two canonical HPV oncogenes are HPV E6 and HPV E7 (Roman and Munger, 2013; Wallace and Galloway, 2015). HPV E6 binds a cellular ubiquitin ligase (E6AP) and uses it to promote p53 degradation (Huibregtse et al., 1991; Scheffner et al., 1993, p. 53). HPV E6 also activates the catalytic subunit of telomerase (Klingelhutz et al., 1996). HPV E7 disengages cell cycle checkpoints by degrading RB and RB family proteins (Dyson et al., 1989; Roman and Munger, 2013; Zhang et al., 2006). The lack of evolutionary pressure to mutate or otherwise inactivate these tumor suppressors results in tumors that are dependent on continued HPV E6 and E7 expression (Chang et al., 2010).

In addition to their well-characterized ability to inactivate p53 and RB, HPV oncogenes have a complicated relationship with cellular response to UV (Wallace and Galloway, 2014). HPV E7 prevents HPV-

Abbreviations list: HPV, human papillomavirus; UV, ultraviolet radiation; E6AP, E6 associated protein; RB, retinoblastoma protein; TLS, translesion synthesis; NER, nucleotide excision repair; MTT, 3-(4,5-dimethylthiazol-2-yl)-2,5-diphenyltetrazolium bromide

* Corresponding authors.
E-mail addresses: n.mcmillan@griffith.edu.au (N. McMillan), nwallac@ksu.edu (N.A. Wallace).
[1] Current address: Australian Institute for Bioengineering and Nanotechnology (Building 75), The University of Queensland, Cooper Rd., St Lucia, Brisbane QLD 4072, Australia.

https://doi.org/10.1016/j.gene.2018.11.079
Received 19 November 2018; Accepted 24 November 2018
Available online 02 December 2018

transformed cells from undergoing the G1 arrest after UV necessary to avoid replication fork collapse (Flynn and Zou, 2011; Gujuluva et al., 1994; Morandell et al., 2012; Wieringa et al., 2016). HPV E6's degradation of p53 prevents the induction of p53 target genes (Gu et al., 1994). HPV E6 blocks the induction of NER proteins (McKay et al., 2001) correlating with limited NER and more mutations after UV exposure (El-Mahdy et al., 2000; Havre et al., 1995; Rey et al., 1999). Both HPV oncogenes hinder the homologous recombination pathways that respond to double strand DNA breaks that can result from UV-induced replication fork collapse (Wallace et al., 2017). The repair mechanisms that respond to UV are also critical for repairing lesions caused a number by genotoxic drugs that cause DNA crosslinks (Alt et al., 2007; Furuta et al., 2002; Ho et al., 2006). It is not surprising then that HPV E6 and E7 sensitize cells to this class of chemotherapeutics (Koivusalo et al., 2002; Liu et al., 2000; Wallace et al., 2012). The dependence of cervical cancers on these viral oncogenes suggests that these drugs would be particularly lethal to cervical malignancies.

However, HPV oncogenes also activate a plethora of DNA repair proteins including those in the pathways that respond to UV damage; nucleotide excision repair (NER), Fanconi anemia repair (FA) and translesion synthesis (TLS) (Alan and D'Andrea, 2010; Knobel and Marti, 2011; Schärer, 2013). HPV depends on DNA repair pathways to replicate its genome (Anacker et al., 2014; Gillespie et al., 2012; Hong et al., 2015; Moody and Laimins, 2009; Spriggs and Laimins, 2017a). In addition to creating an environment that is seemingly primed to respond to crosslinked DNA, HPV oncogenes inhibit the apoptosis induced by these lesions (Garnett et al., 2006; Garnett and Duerksen-Hughes, 2006; Jackson et al., 2000; Leverrier et al., 2007). Thus in at least certain scenarios, HPV E6 can protect against DNA crosslinking agents (Koivusalo et al., 2002).

The balance between chemo-sensitization and chemo-resistance is critical in the management of any cancer. DNA repair and damage tolerance pathways are particularly important with regard to cervical cancer as a DNA crosslinking agent, cisplatin, is currently the standard of care (Lorusso et al., 2014). Resistance to cisplatin in advanced and recurrent cervical cancers results in only a 10–20% chance of living through the year (Diaz-Padilla et al., 2013). As a result, substantial effort has been made to identify potential mechanisms of cisplatin resistance as well as ways to re-sensitize cervical cancer cells (Kilic et al., 2015; Roy and Mukherjee, 2014; Zhu et al., 2016). The efficacy of cisplatin is at least partially determined by gene expression patterns in cervical cancer cells, with multiple DNA repair genes being identified as important predictors of cisplatin sensitivity (Garzetti et al., 1996; Hasegawa et al., 2011; Henríquez-Hernández et al., 2011; Kitahara et al., 2002; Saito et al., 2004; Zhu et al., 2016). Because cisplatin induces DNA damage, increased repair capability likely accounts for the resistance (Woods and Turchi, 2013).

Conversely, if HPV oncogenes block repair in a predictable manner, these defects could be leveraged therapeutically. The sensitivity of BRCA1 or BRCA2 deficient breast and ovarian cancers is the most publicized link between known repair deficiencies and improved cancer treatments (D'Amours et al., 1999; Jasin, 2002). A similar relationship exists for cisplatin sensitivity. Specifically, the response of TLS and NER to UV predicts the lethality of cisplatin exposure (Gueranger et al., 2008; Marteijn et al., 2014; Rosell et al., 2003; Srivastava et al., 2015). In this manuscript, we characterize the interplay between HPV oncogene-induced sensitivity to crosslinking agents and their protection from these genotoxins in the context of cervical cancer cell lines. We show that, compared to control cells, cervical cancer cells are more sensitive to sub-erythemal UV exposure and low doses of cisplatin. We demonstrate that these cells have a greater tendency to undergo apoptosis after UV. Interestingly, HPV E6 and E7 also block apoptosis after UV. We generate UV- and cisplatin-resistance cervical cancer cell lines and define their cross sensitivity. Finally, we determine the toxicity of a chemotherapeutic agent (olaparib) with a different mechanism of action (PARP1 inhibition) in cervical cancer cells that are resistant to cisplatin.

2. Methods and materials

2.1. MTT assays

LD50s were determined by MTT assay. HeLa cells were seeded in a 96 well plates and treated with UV, cisplatin, or olaparib at specified doses. 48 h after treatment, MTT solution was added to the cells and solubilized 24 h later. Plates were then read for optical density by spectrophotometer with a dual reading at frequencies 550 and 655 nm.

2.2. Cell culture

HeLa cells are HPV 18 positive *Homo sapiens* adenocarcinomas grown in Dulbecco's Modified Eagle Medium (ThermoFisher Scientific, catalog number: 12100046), supplemented with 10% fetal bovine serum (VWR, catalog number: 89510-194) and Pen-strep (Calsson Labs, catalog number: PSL02-6X100ML). Human foreskin keratinocytes or HFKs were derived from neonatal human foreskins and were grown in EpiLife medium supplemented with calcium chloride (60 μM), human keratinocyte growth supplement (Cascade Biologics, Portland, OR), and penicillin-streptomycin. Multiple cell lines were derived from several donors for this work. The cells were incubated at 37 °C in a 5% CO_2 environment. Cells were washed with 0.1% EDTA (Invitrogen catalog #15-576-028) and raised from plate with 0.05% Trypsin (Sigma-Aldrich catalog # T4049-500ML).

2.3. Immunoblotting

HeLa Cells transfected by different plasmids (PLL3.7, 18E6-1, 16E7-1) were cultured for different times (0 h, 3 h, 6 h, 24 h) in 6 cell-well plate after using UV light dose (8 mJ/cm^2) treatment, then both adherent and floating cells were collected and lysed in ice-cold RIPA buffer (50 mM Tris–HCl, 150 mM NaCl, 1 mM ethylene diamine tetraacetic acid (EDTA), 1 mM ethylene glycol tetraacetic acid (EGTA), 20 mM NaF, 1% Nonidet P-40 (NP-40), 1 mM phenylmethylsulfonyl fluoride (PMSF), 100 mM Na3VO4, 1% Triton X-100, 10 mg/mL Aprotinin and 10 mg/mL Leupeptin) for 30 min. The lysates were centrifuged at 12,000 rpm for 10 min and the supernatant was collected. Equal amount of protein lysates were electrophoresed on a 12% SDS polyacrylamide gel and transferred onto nitrocellulose filter (NC) membrane. The membrane was washed 3 times for 10 min in TBST (Tris-Buffered Saline and Tween-20), then after blocking with 2.5% skim milk suspended in TBST for 1 h, membranes were individually incubated respectively with the appropriate primary antibodies Tubulin, P53, Bax, HPV E7 (1:1000) overnight followed by secondary antibodies (1:1000) for 1 h at room temperature. Protein bands were detected using ECL assay kit (Invitrogen, Australia) and exposed using a Kodak medical X-ray processor (Kodak, USA). Anti-human p53 and β-tubulin monoclonal antibodies were purchased from Sigma (Sydney, Australia). Anti-HPV 18E7 polyclonal antibody was purchased from Santa Cruz Biotechnology. Anti-human Bax polyclonal antibody was from Cell Signaling Technology.

2.4. Resistant colony generation and isolation

Colony isolation was performed using sterile cloning disks (SP Scienceware catalog # F37847-0001). Cells were grown at low confluence in a 10 cm plate and treated 4 times every 2 weeks for a 2-month period. Cells were observed from single cells, with their growth monitored microscopically. They were washed with 0.1% EDTA, before colonies were isolated by placing a sterile cloning disks soaked in trypsin on them. Individual disks were then put in a well of a 24-well plate containing growth media, allowing cells to detach from the disk. Cells were then expanded, and acquisition of resistance was assessed.

2.5. Colony formation assays

Colony formation assays were performed by seeding low concentrations of cells on six well plates. They were then treated with UV 48 h after seeding and allowed to grow until colonies appeared. Twenty-four hours after the first colonies with 15 or more cells were seen, colonies were stained with a crystal violet solution (0.2% crystal violet, 5% ascetic acid, and 2.5% 2-proponol) and hand counted.

2.6. shRNA transfections

Cell transduction was basically according to the method described previously (Gu et al., 2006). Briefly, HeLa cells were maintained in complete DMEM medium (Gibco-Invitrogen) and were plated in T75 flasks (4×10^5/flask) overnight culture. LV-shRNAs was diluted in 2.0 mL cultural medium containing polybrene (8 μg/mL) and added to the cells for culture for 1 h at 37 °C. After this, 8 mL of fresh polybrene medium was added to the cells and incubation continued for 24 h. Polybrene medium was then replaced with fresh DMEM culture medium, and the cells were further cultured for assays.

2.7. UV irradiation

To prepare cells for UV irradiation the media was aspirated, and the cells were washed with 1× PBS (Bio Basic catalog # PD8117). A thin layer of PBS was added to the wells or plate and then cells were irradiated in a UV Stratalinker 2400 (Stratagene Catalog # 400075-03) at specified doses. Media was then added, and the cells were incubated at 37 °C.

2.8. Flow cytometry

Flow cytometry analysis was carried out with the FACSCalibur™ (Becton Dickinson). The acquisition and analysis of data was done with the program Cell Quest Pro.

2.9. Apoptosis assay

The Dead Cell Apoptosis Kit (ThermoFisher Scientific catalog #V13242) and the Countess™ II FL Automated Cell Counter (ThermoFisher Scientific catalog #AMQAF1000) were used to measure apoptosis. Cells were seeded at 50,000 cells/well in a 6-well plate and incubated at 37 °C overnight. Cells were then UV irradiated at specified intervals and incubated at 37 °C for 48 h. Cells were then washed with 0.1% EDTA and incubated with Trypsin for 3 min at 37 °C. DMEM was then added to cells and they were incubated at 37 °C for 30 min. Cells were then pelleted by centrifuging at 188 ×*g* for 5 min. After aspiration of DMEM, they were resuspended in ~1×10^6 cells/mL in 1× annexin binding buffer and incubated with propidium iodide for 15 min at RT. Cells then were loaded onto slides and imaged using appropriate fluorescent filters on Countess™ II FL Automated Cell Counter.

2.10. Reagents

Cisplatin: cisplatin (Sigma-Aldrich catalog # 479306-1G) is a platinum based antineoplastic agent that forms cytotoxic adducts with the DNA dinucleotide d(pGpG) that induces intrastrand cross-links.

Olaparib: olaparib (LC laboratories catalog # O-9201) is a selective inhibitor of PARP1/2 with IC50 of 5 nM/1 nM in cell-free assays.

3. Results

3.1. HPV+ cervical cancer cell lines are sensitive to sub-erythemal doses of UV

Cells mitigate the toxicity of low dose UV by pausing the cell cycle and inducing a highly coordinated signaling response. HPV oncogenes transform keratinocyte cells in part by disrupting both processes. HPV E7 degrades the master cell cycle regulator, RB. While both HPV E6 and E7 induce aberrant activation of DNA damage proteins. We hypothesize that the continued expression of HPV E6 and E7 in cervical cancer cell lines will make them less able to respond to UV and as a result more sensitive to UV exposure. This hypothesis was tested by defining the

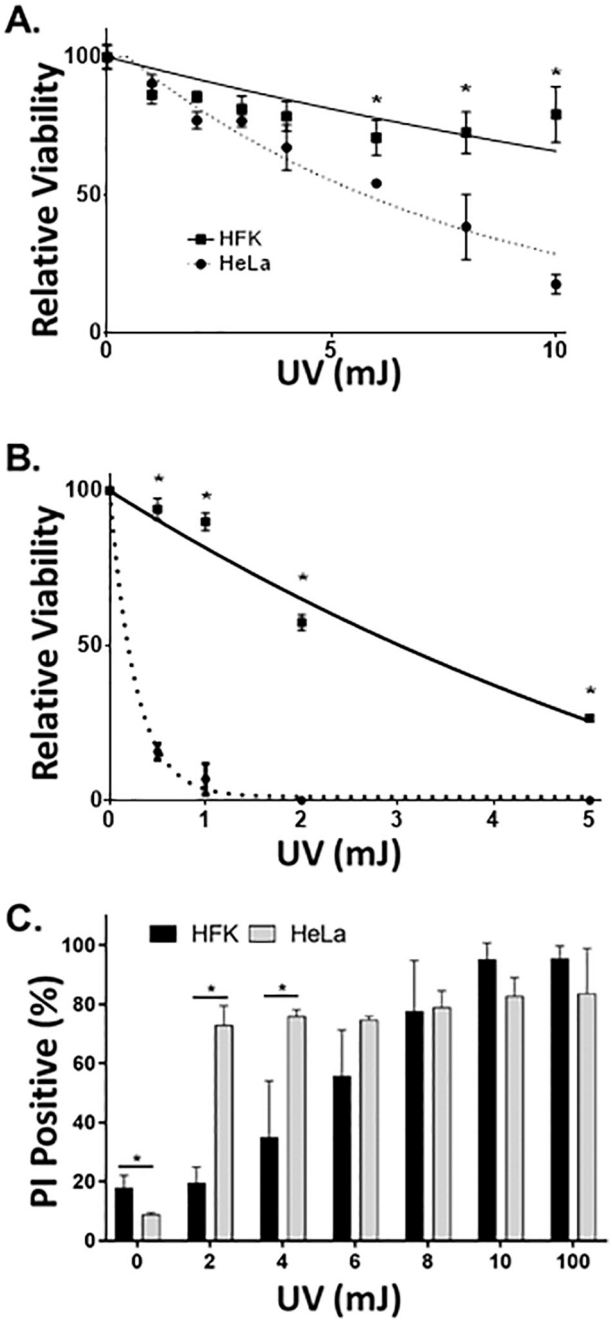

Fig. 1. Sensitivity of cervical cancer to UV. A. This graph depicts the sensitivity of cervical cancer cell lines to ultraviolet radiation when compared to primary human foreskin keratinocytes (HFK) as measured by MTT. The black square points and solid line represent HFKs. The black circle points and dotted line represent HeLa cells, a cervical cancer cell line. B. This graph depicts the combined results of the colony formation assays. The solid black line and solid black squares represent HeLa and the dotted line and dot points are non-cancer HFK. C. This graph depicts the percentage of apoptotic (propidium iodide positive) cells 48 h after increasing doses of UV. For all, $n = 3$, $^*p < 0.05$ by unpaired *t*-test and error bars represent mean ± SD.

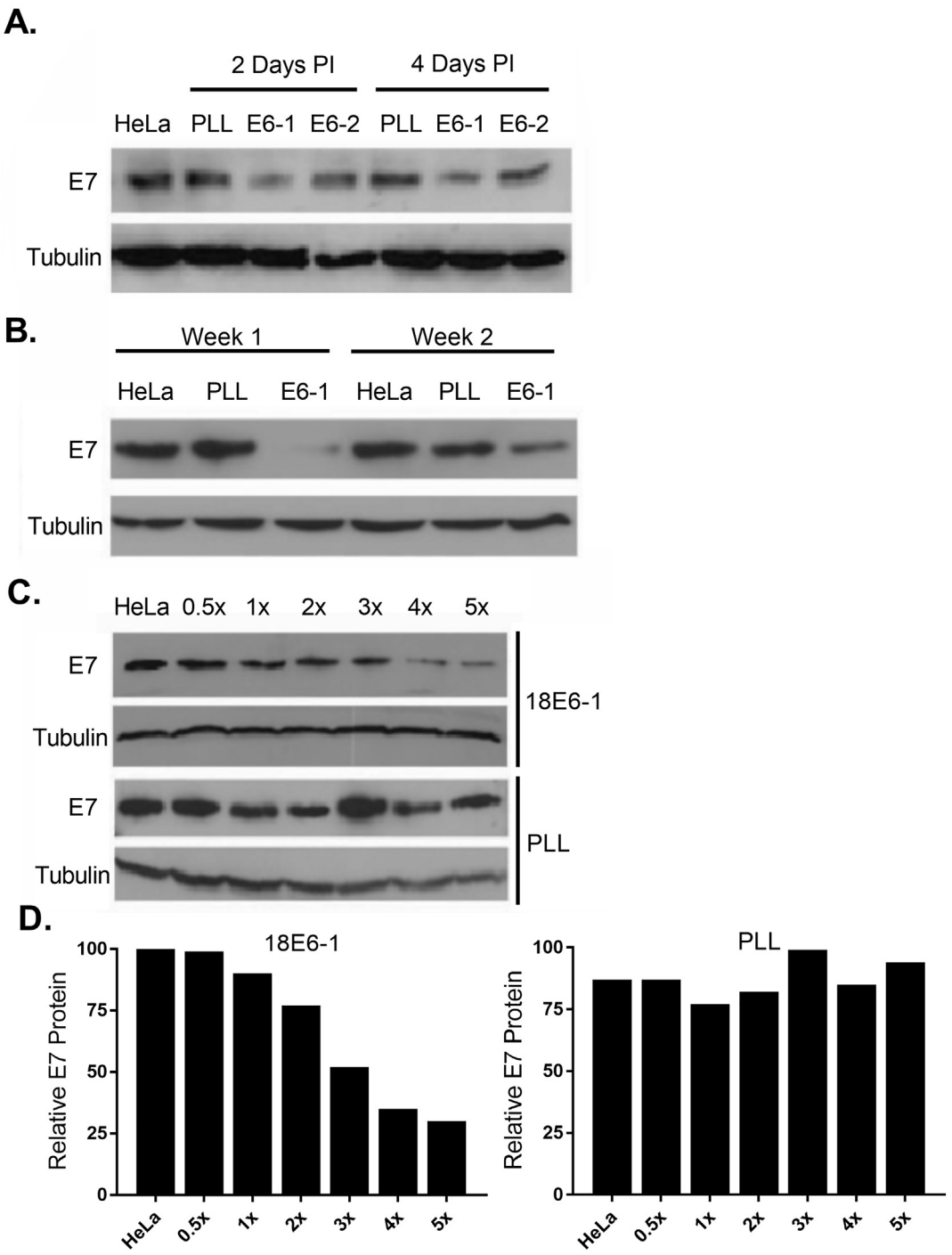

Fig. 2. Confirmation of lentiviral transduction. A. Representative immunoblot showing E7 levels in HeLa cells transduced with the empty vector PLL, shRNA E6-1, or shRNA E6-2. Lysates were collected 2 days post-lentiviral infection (PI) or 4 days PI. Tubulin is the loading control. B. Representative immunoblot showing E7 levels in HPV18 HeLa cells transduced with empty vector PLL or a gradient of shRNA 18E6-1. C. Representative immunoblot showing E7 levels in HeLa cells transduced with the empty vector PLL or shRNA E6-1. Lysates were collected 1 and 2 weeks PI. Tubulin is the loading control. D. Graphs showing relative E7 protein determined by densitometry.

sensitivity of a HPV+ cervical cancer cell line (HeLa) to UV. As a control, untransformed primary keratinocytes derived from neonatal foreskins (HFKs) were also observed because HPV infects and transforms keratinocytes. HeLa cells were significantly more sensitive to a gradient of low dose UV (0–10 mJ/cm^2) than HFKs when viability was measured by MTT assay (Fig. 1A).

As a complimentary measure of UV sensitivity, a colony formation assay was used to measure the toxicity of the same range of UV doses. These results confirm the data obtained by the MTT assay. Indeed, HeLa cells were significantly more sensitive to all exposures of UV in the colony formation assay, with virtually no colonies visible after 1 mJ/cm^2 of exposure (Fig. 1B and Supplemental Fig. 1). Conversely, HFKs formed readily detectable colonies at all observed doses of UV.

The sensitivity resulting from an inability to properly respond to UV

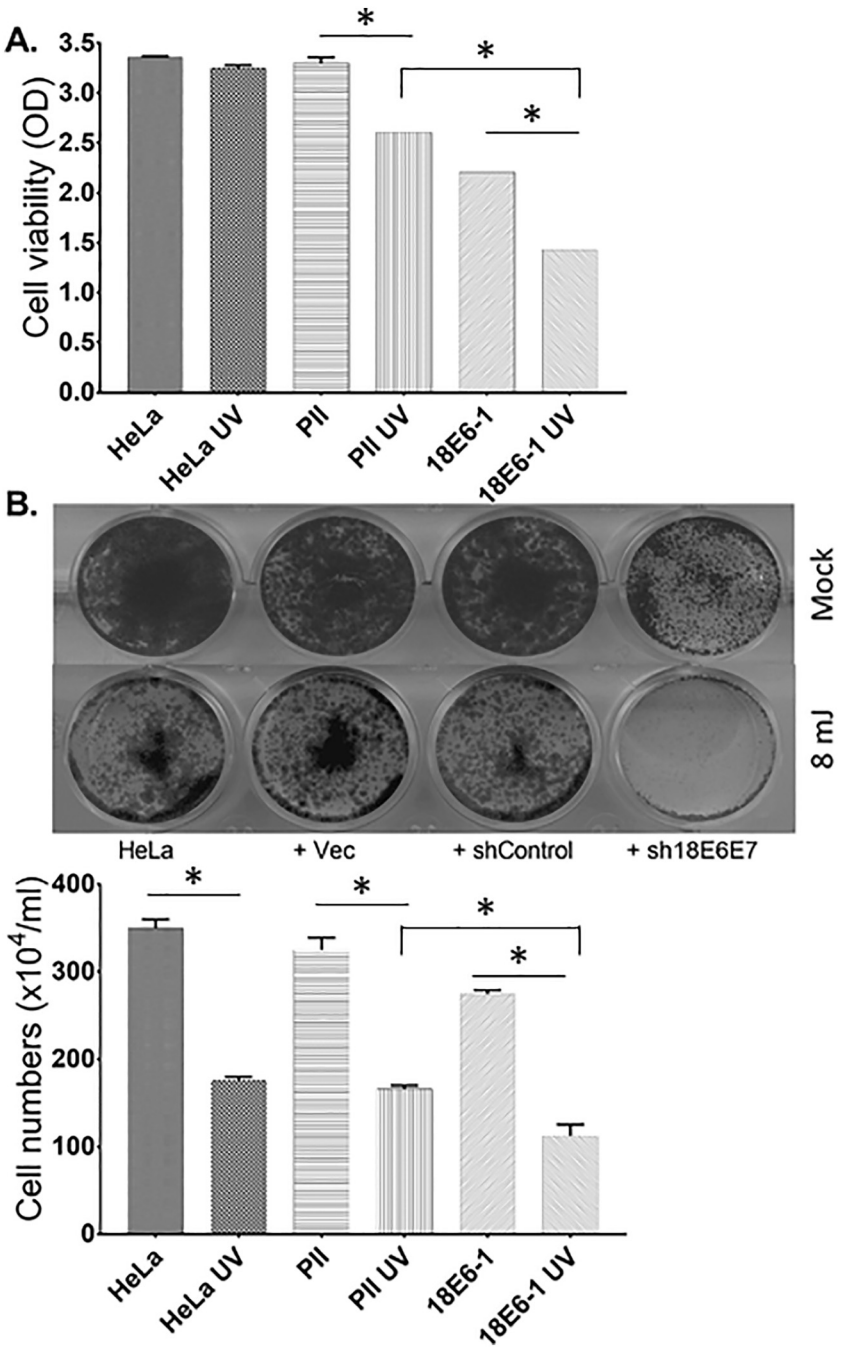

Fig. 3. Increased UV sensitivity in E6/E7 knockdown HeLa cells. A. This graph depicts UV sensitivity in HeLa cells transduced with the empty vector PLL or shRNA E6-1 as measured by MTT assay. B. This image depicts UV sensitivity in HeLa cells transduced with empty vector, a shRNA Control, or a shRNA 18E6E7 by colony formation assay (CFA). C. This graph depicts UV sensitivity in HeLa cells transduced with the empty vector PLL or shRNA 18e6-1 by cell counting. For all, $n = 3$, $^*p < 0.05$ by unpaired *t*-test and error bars represent mean ± SD.

damage is likely manifest in elevated apoptosis. Unfortunately, neither a colony formation assay nor a MTT detect apoptosis directly and thus they cannot distinguish apoptosis from other types of cell death. To determine if HPV+ cervical cancers have an increased propensity to undergo apoptosis after UV exposure, we measured propidium iodide (PI) staining as a standard indicator of apoptosis (Fig. 1C). PI is a membrane impermeable dye that intercalates between DNA base pairs. We used a fluorescence-based assay to detect PI. Cell membranes become permeable during apoptosis allowing PI uptake measurable at 617 nm. Taking the ratio of cells that are stained with PI to the total cell count allows us to determine the percentage of apoptotic cells after UV exposure. We found HeLa cells had significantly higher levels of PI staining compared to HFKs when both were exposed to either 2 or 4 mJ/cm^2 of UV (Fig. 1C).

3.2. HPV oncogenes decrease sub-erythemal UV-induced apoptosis

This increased sensitivity is likely due to HPV E6 and E7 disrupting cell cycle regulation and causing abnormal activation of DNA damage response genes. However, HPV oncogenes also mitigate the deleterious consequences of DNA damage by inhibiting apoptosis. To define the ability of HPV oncogenes to block the apoptosis in the context of a cervical cancer cell line exposed to UV, a shRNA system (PLL E61) was used to partially deplete HPV oncogenes in HeLa cells. HeLa cells with

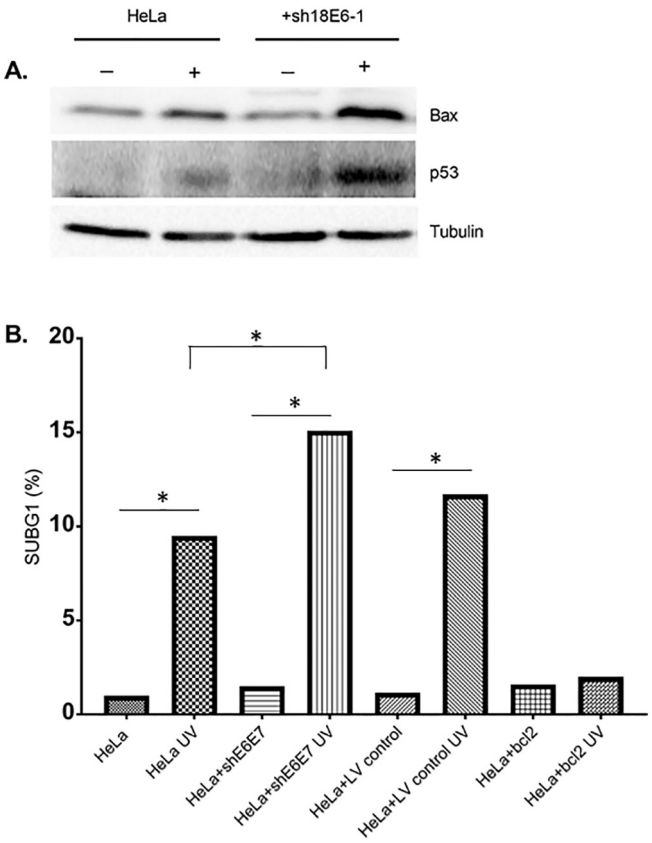

Fig. 4. Increased cell cycle arrest and apoptosis due to UV sensitivity in E6/E7 knockdown HeLa cells. A. Representative immunoblot showing BCL-2 related X protein (Bax) and p53 levels in shRNA 18E6-1 transduced HeLa cells with and without UV. Tubulin is the loading control. B. This graph depicts the percentage of HeLa cells in sub G1 after or without UV treatment. Cells were transduced with shRNA E6E7, lentiviral control, and BCL-2 exogenously expressed. For all, $n = 3$, $^*p < 0.05$ by unpaired *t*-test and error bars represent mean ± SD.

PLL E61 cells had decreased HPV E7 levels 2 and 4 days after treatment with shRNA (Fig. 2A). Because these genes share a promoter, their expression is known to be linked. Indeed, a recent study was unable to achieve knockdown of HPV E6 or HPV E7 individually (Wechsler et al., 2018). Thus, decreased HPV E7 abundance is a reliable marker of HPV E6 for which a dependable antibody does exist. To determine if this knockdown was persistent, oncogene levels were measured at 1 and 2 weeks after transfection with shRNA. Transfection with PLL E61 was able to detectably decrease the abundance of HPV E7 at these late time points (Fig. 2B). As a final measure of the PLL E61's ability to diminish HPV oncogene levels, the abundance of HPV oncogenes was determined after transfection with increasing amounts of PLL E61. Immunoblot analysis shows a dose dependent decrease in HPV E7 levels (Fig. 2C). Since there is no viable commercially available antibody to HPV E6, the degradation of its target protein, p53, is used as a surrogate for HPV E6 expression. P53 levels were determined by immunoblot after treatment with PLL E6. Notably, the reduction in oncogene abundance remains below the levels that result in apoptosis (data not shown).

Having characterized PLL E61's ability to decrease the amount of HPV oncogenes in HeLa cells, the approach was used to define the role of HPV oncogenes in the apoptosis induced by low doses of UV. Supporting a role for HPV oncogenes in repressing UV-induced apoptosis, both MTT and colony formation assays demonstrated that UV was more toxic to HeLa cells when HPV E6 and E7 were targeted by shRNA (Fig. 3A–B). Specifically, the knockdown of HPV oncogenes combined with exposure to a low dose of UV resulted in lower cellular viability and fewer colonies than either knockdown or UV exposure alone.

As noted, these assays do not directly measure apoptosis, so the abundance of BAX, a pro-apoptotic protein, was defined by immunoblot. After exposure to a sub-erythemal amount of UV, HeLa cells demonstrated a mild induction of both BAX and p53 (Fig. 4A). In contrast, UV-induce increases in BAX and p53 abundance were enhanced by HPV E6 and E7 knockdown. Notably, PLL E6.1 also increased the abundance of p53 in untreated HeLa cells further confirming the knockdown of HPV E6. To more directly detect the role of HPV oncogenes in protecting cervical cancer cells against apoptosis, flow cytometry was used to define the population of sub-G0/G1 cells after UV. The results from this assay are consistent with HPV oncogene-mediated inhibition of apoptosis as the percentage of sub-G0/G1 cells after UV was significantly increased by oncogene knockdown (Fig. 4B). As a control and to further confirm that the increase in the sub-G0/G1 population was due to BAX-induced apoptosis, BCL2, an anti-apoptotic BAX antagonist was transfected into HeLa cells. BCL2 expression prevented the accumulation of sub-G0/G1 cells after UV (Fig. 4B).

3.3. Generation of UV- and cisplatin-resistant HPV+ cervical cancer cells

The ability of HPV oncogenes to both sensitize cells to UV and protect them from UV-induced apoptosis portrays the complexity of their manipulation of the cellular damage response. To further probe this relationship, UV-resistant HeLa cell lines were generated by repeated exposure to UV followed by a recovery period (Fig. 5A). This process was repeated at least 4 times and until individual resistant colonies could be isolated using trypsin soaked cloning rings. These colonies were then expanded and their sensitivity to UV was compared to parental HeLa cells via MTT assay. The LD50 was calculated for each resistant cell line and used to select highly resistant cells for further analysis (Fig. 5B and Table 1).

Cisplatin is a genotoxic agent that is quite effective at killing HPV+ cervical cancers. Cisplatin works by inducing DNA crosslinking that activate many of the same cellular responses induced by UV exposure (McKay et al., 2001). For comparison with the UV-resistant HeLa cells, cisplatin-resistant HeLa cells were generated using the previously described treatment-recovery cycle (Fig. 5A). Resistance was again established using MTT assays to determine LD50 values (Fig. 5C and Table 1). This approach allowed resistant cells to be identified and selected for further analysis. UV resistant HeLa A and B as well as cisplatin resistant HeLa A were chosen because they had the most robust resistance.

3.4. Sensitivity of UV- and cisplatin-resistant HPV+ cervical cancer cells to other genotoxic agents

We postulated that resistance to one type of crosslinking agent may not necessary result in resistance to agents that similar damage DNA. To begin testing this hypothesis and to characterize the mechanisms of resistance in these cell lines, MTT assays were conducted to define the LD50 for UV for the most cisplatin-resistant HeLa lines (Fig. 6A and Table 1). Although individual matched data points were not significantly between resistant and parental cell lines, a statistical analysis comparing the full data sets to each other revealed that a significant increase in UV resistance accompanied acquired cisplatin resistance in HeLa cells (Wilcoxon Matched Pairs Test, $p < 0.05$). The average LD50 increased from 65.47 in parental HeLa to 108.6 in the cisplatin resistant colony demonstrating an almost 2-fold difference in sensitivity. Next, MTT assays defined the LD50 for cisplatin in the most UV-resistant HeLa lines (Fig. 6B and Table 1). This analysis demonstrated that cells that acquired UV resistance could become more sensitive to other crosslinking agents. Finally, a recent report indicated that acquired cisplatin resistance could sensitize cells to PARP inhibition (Michels et al., 2013). To determine if this was true for the cisplatin-resistant HeLa cells described in this report, MTT assays were used to measure sensitivity to olaparib, a commercially available inhibitor of PARP1

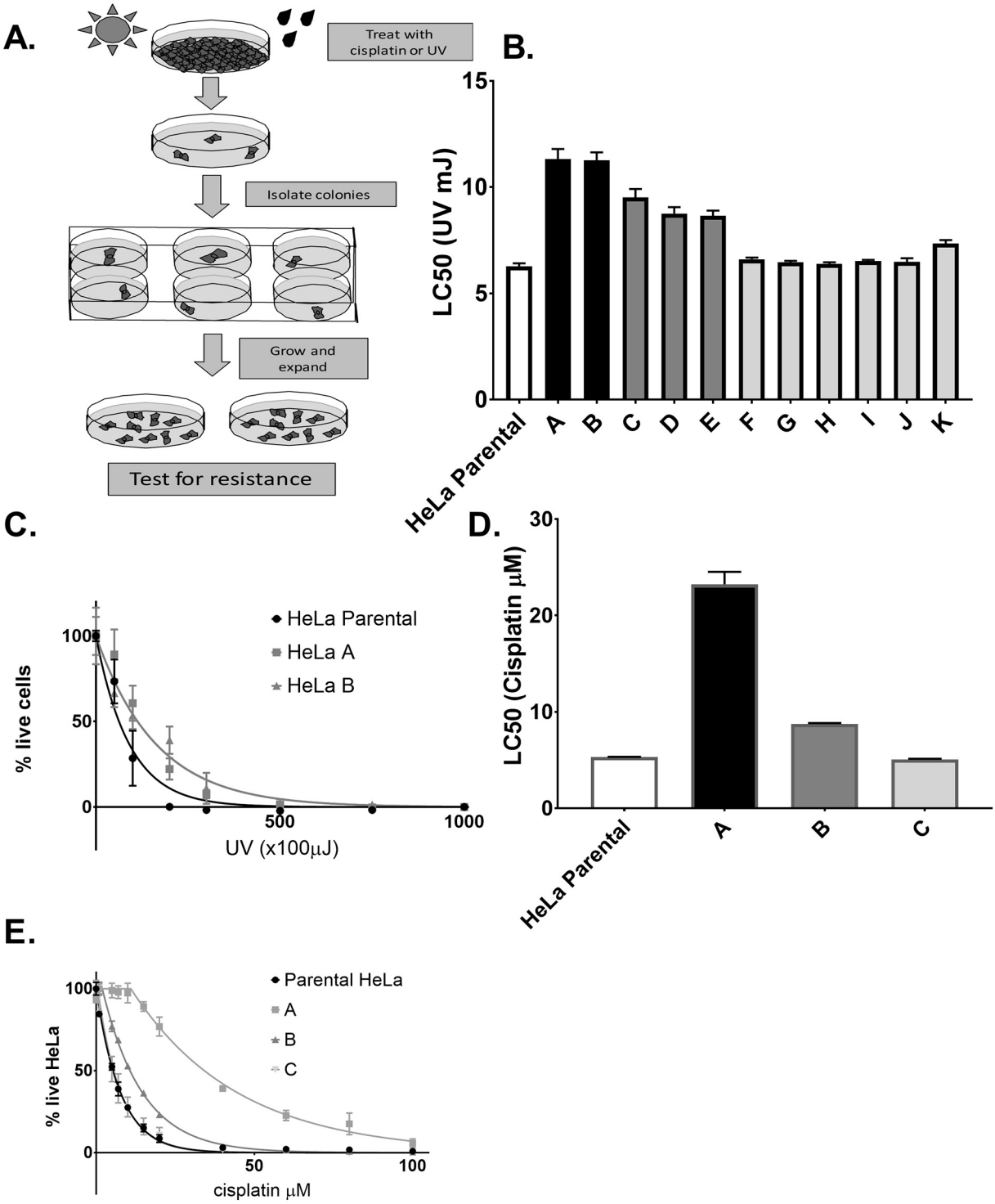

Fig. 5. Creating cross-linker resistant HeLa and SiHa cell lines. A. This image depicts the steps used to generate the cross linker resistant cell lines. Briefly, cells were treated 4 times with either 10 μM cisplatin or 5 mJ UV and given recovery periods between treatments. The resulting colonies were then isolated and transferred to individual wells of a 6-well plate for expansion. The resulting clonal populations were then tested for acquired resistance by MTT. B. This chart depicts the LC50s (amount required to kill 50% of cells) for each isolated cell line. The color gradient represents increasing resistance with black being the most resistant. C. This graph depicts UV sensitivity of the 2 most UV resistant HeLa cell lines as measured by MTT. The solid black line and circles represent the parental HeLa. The grey line, square, and triangle represent the 2 most resistance colonies. D. This chart depicts the LC50s for each isolated cell line with error bars representing the 95% confidence intervals. The color gradient represents increasing resistance with black being the most resistant. E. This graph depicts the cisplatin sensitivity of the isolated cell lines as measured by MTT. The solid black line and circle points represent Parental HeLa. The light grey line and square points represent the most resistant colony. For all, $n = 3$, $^{*}p < 0.05$ by unpaired *t*-test and error bars represent mean ± SD.

(Fig. 6C and Table 1). This analysis demonstrated that the sensitivity to PARP1 inhibition in HeLa cells that acquired cisplatin resistance depended on the concentration of inhibitor. At lower concentrations, cisplatin resistance was associated with increased resistance to PARP1 inhibition, while at very high concentrations of inhibitor the cells were notably more sensitive. Since this result differed from published

Table 1
Lethal Concentrations in UV and cisplatin-resistant HeLa and SiHa. This table depicts the toxicities in cell lines before and after acquisition of resistance to cisplatin and UV. LC50 denotes the concentration or dose required to kill 50% of the cells calculated from MTT data (Fig. 6). 95% CI denotes the 95% confidence intervals. * denotes significance difference compared to parental cell line determined by Student *t*-test (p value ≤ 0.05).

Cell type	LC_{50}	LC_{50} 95% CI
UV toxicity (mJ/cm^2)		
HeLa parental	6.547	5.46 to 7.8
HeLa cisplatin resistant A	10.8	8.49 to 13.73
Cisplatin toxicity (μM)		
HeLa parental	19.08	17.3 to 21.1
HeLa UV resistant A	19.89	16.7 to 23.6
HeLa UV resistant B	6.113*	5.9 to 6.3
Olaparib toxicity (μM)		
HeLa parental	845.3	674.8 to 1084
HeLa cisplatin resistant A	982	650 to 1656
SiHa parental	636	556 to 731.1
SiHa cisplatin resistant pooled	523.6	499.1 to 549.6

reports, we generated a pool cisplatin-resistant cervical cancer cell line using SiHa cells (Supplemental Fig. 2). Unlike clonal populations of resistant cells, this cell line is likely to have gained resistance through multiple mechanisms providing a broader representation of resistance mechanisms. SiHa cisplatin resistant pooled cells were more sensitive to PARP1 inhibition via olaparib (Supplemental Fig. 3 and Table 1), suggesting that the increased dependence on PARP1 activity varies depending on the individual tumor or more likely the mode of resistance.

4. Discussion

We investigated the response of cervical cancer cells to low dose UV exposure. Particularly, our efforts illuminate the increased likelihood of UV-induced apoptosis in these cells. HPV oncogenes seem to counter the inclination towards programed cell death as their shRNA mediated knockdown caused increased p53- and BAX-associated apoptosis, suggesting dying cervical cancer cells sustain a greater abundance of DNA damage. This is somewhat suspected given the ability of HPV oncogenes to impair cellular DNA repair. We also generated clonal populations of cervical cancer cells that were resistant to chemical- or radiation-induced DNA crosslinks and measured their sensitivity to other crosslinking agents and a PARP1-inhibitor.

4.1. HPV oncogenes have both protective and detrimental effects on a cell's response to UV

One realization from this study is that HPV oncogenes sensitize cells to UV while also protecting them from UV-induced apoptosis. HPV oncogenes cause constitutive activation of both ATM and ATR, two keystone repair kinases (Gillespie et al., 2012; Johnson et al., 2017; Moody and Laimins, 2009). While this indicates repair initiation, successful repair also requires resolution of these signaling events as well. HPV E6 also mislocalizes repair proteins from sites of damage allowing the existence of active repair complexes without resolution of the damage they were activated in response to (Mehta and Laimins, 2018; Wallace et al., 2017). Such a disruption of repair signaling is consistent with the increased sensitivity to crosslinked DNA. HPV oncogenes protect the cell from BAK-mediated apoptosis, consistent with the virus's extensive efforts to avoid immune detection by minimizing its cytotoxic effects (Jackson et al., 2000).

While the benefits of evading the immune system are obvious, the evolutionary pressures that drove HPV to sensitize cells to UV are more cryptic. Unlike cutaneous members of the papillomavirus family, infections in the genital tract would not encounter sunlight often, making it unlikely they evolved a mechanism to change the cellular response to UV. The increased toxicity is more likely an unintended consequence of the role repair factors play in replicating the HPV genome. Perhaps being recruited to sites of viral replication prevents ATM and ATR from coordinating the robust response required to avoid the deleterious effect of UV-damage.

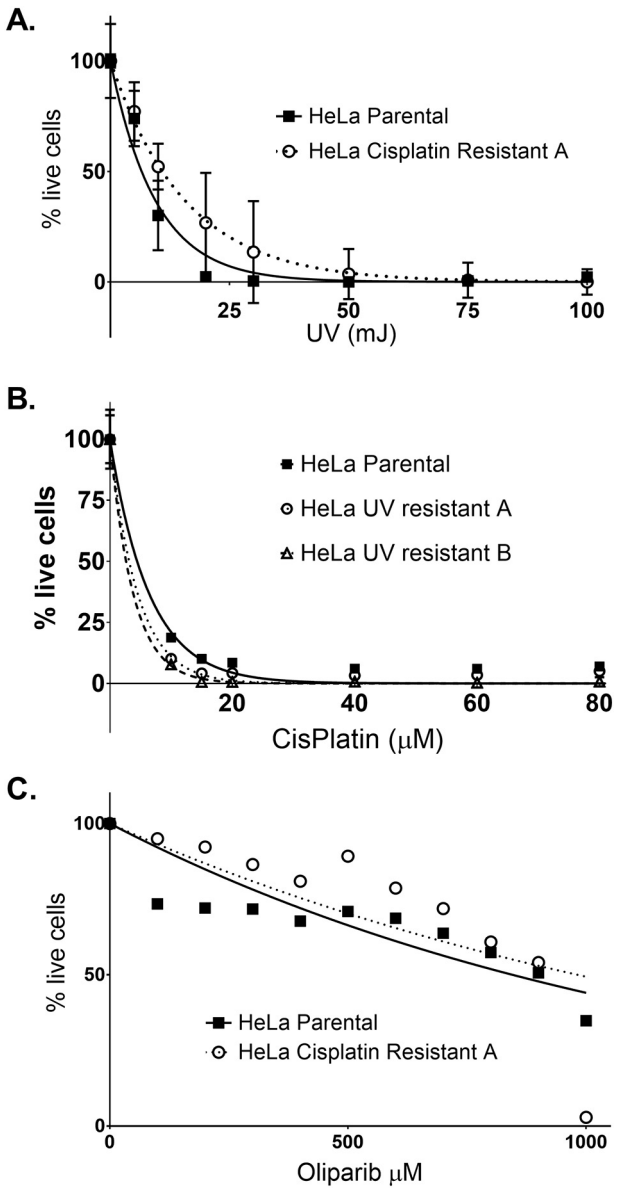

Fig. 6. Sensitivity to cross-linking agents in UV and cisplatin resistant cells. A. This graph depicts the sensitivity of HeLa cells as measured by MTT to ultraviolet radiation before and after acquiring resistance to cisplatin. The square points and solid line represent parental HeLa. The circle points and dotted line represent the Clone A of HeLa cells that acquired resistance to cisplatin. B. This graph depicts the sensitivity of HeLa cells to cisplatin measured by MTT before and after acquiring UV resistance. The square points and solid line represent the parental HeLa. The circle points and dotted line depict data from Clone A of UV resistant HeLa cells. The triangle points and the dashed line represent data from Clone B of UV resistant HeLa cells. C. This graph depicts the PARP1 inhibitor (Olaparib) sensitivity of HeLa cells measured by MTT before and after cisplatin resistance was acquired. Black squares represent the parental HeLa line while open circles depict data from Clone A of cisplatin resistant HeLa cells. The untreated controls are set at 100. For all, $n = 3$, $^*p < 0.05$ by unpaired *t*-test and error bars represent mean ± SD.

4.2. Resistance to crosslinking agents does not guarantee resistance to other genotoxic agents

We generated cervical cancer cell lines that were resistant to two different sources of DNA crosslinks. The clonal populations of resistant cells insured that the acquisition of resistance occurred separately in each cell line. Although we did not determine the mechanism of resistance in these cells, the clonality suggests that cells gained the ability to survived either UV or cisplatin through diverse means. A significant amount is known about the ways that cells become tolerant of genotoxic drugs. Potential resistance strategies include reducing the functional concentration of the drug in the cell by pumping it out of the cell or obtaining a mutation that restores expression of a repair factor (Michels et al., 2013; Rosell et al., 2003; Srivastava et al., 2015; Zhu et al., 2016). Less is known about the ways cells come to be more tolerant of UV, but our observations are in line with previous reports indicating UV-resistance does not confer resistance to other DNA crosslinking agents (Petersen et al., 1995). Instead, UV-resistance appears to have fitness costs as cells grow slower and can be more sensitive to cisplatin (Data not shown, Fig. 6 and (Petersen et al., 1995)). Similarly, sensitivity to small molecule PARP1 inhibitor may or may not accompany resistance to cisplatin (Fig. 6 and Table 1). Moreover, cisplatin resistance was not accompanied with proportionate resistance to UV (Fig. 6 and Table 1). Together, this adds to the evidence that understanding underlying mechanisms of resistance is critical for predicting the response of tumors to other genotoxic drugs.

4.3. Implications for therapeutic intervention

Virtually every cervical cancer is the result of a human papillomavirus infection. HPV transforms cells in part by blocking tumor suppressors (p53 and RB) and by activating the catalytic subunit of telomerase. HPV E6 and E7 also have a well-documented ability to disrupt DNA damage repair (Bristol et al., 2017; Moody, 2018; Spriggs and Laimins, 2017b). HPV transformed cells require continued expression of HPV oncogenes. Since HPV E6 and E7 hinder a cell's ability to protect itself from DNA crosslinks, every cell in HPV-associated tumors are predicted to share this defect. This could explain the efficacy of crosslinking agents like cisplatin in the treatment of malignancies caused by HPV. Therapeutics could be better designed to target HPV-associated cancers if a greater understanding of the mechanisms by which HPV oncogenes induce sensitivity to DNA crosslinks is gained. We show that it is possible to acquire resistance to one source of DNA crosslinks while remaining sensitive to crosslinks from other origins, suggesting that tumors that have acquired resistance to cisplatin could remain sensitive to other crosslinking drugs such as chlorambucil or mitomycin c.

Finally, the importance of measuring the effects of sub-erythemal doses of UV should be noted for studies addressing most clinically relevant questions, particularly those relevant to sensitivity or tumorigenicity. While exposure to high doses of UV or other crosslinking agents may provide interesting molecular insights, they likely induce different repair responses than the levels seen in common exposure to UV or after chemotherapy (Quinet et al., 2016). Further, excessive damage is more likely to induce an apoptotic response rather than a full-fledged effort to repair lesions.

Supplementary data to this article can be found online at https://doi.org/10.1016/j.gene.2018.11.079.

Declaration of interest statement

The authors declare they have no conflicts of interest relevant to this manuscript.

Acknowledgements

This work was supported by Department of Defense CMDRP PRCRP CA160224 (NAW) and made possible through generous support from the Les Clow family (NAW) and the Johnson Cancer Research Center at Kansas State University (NAW). Additional support came from the Kansas INBRE in the form of a fellowship to SOW (K-INBRE P20 GM103418).

References

Alan, D., D'Andrea, M.D., 2010. The Fanconi anemia and breast cancer susceptibility pathways. N. Engl. J. Med. 362, 1909–1919. https://doi.org/10.1056/NEJMra0809889.

Alt, A., Lammens, K., Chiocchini, C., Lammens, A., Pieck, J.C., Kuch, D., Hopfner, K.-P., Carell, T., 2007. Bypass of DNA lesions generated during anticancer treatment with cisplatin by DNA polymerase eta. Science 318, 967–970. https://doi.org/10.1126/science.1148242.

Anacker, D.C., Gautam, D., Gillespie, K.A., Chappell, W.H., Moody, C.A., 2014. Productive replication of human papillomavirus 31 requires DNA repair factor Nbs1. J. Virol. 88, 8528–8544. https://doi.org/10.1128/JVI.00517-14.

Bernard, H.-U., Burk, R.D., Chen, Z., van Doorslaer, K., Hausen, H. zur, de Villiers, E.-M., 2010. Classification of papillomaviruses (PVs) based on 189 PV types and proposal of taxonomic amendments. Virology 401, 70–79. https://doi.org/10.1016/j.virol.2010.02.002.

Bristol, M.L., Das, D., Morgan, I.M., 2017. Why human papillomaviruses activate the DNA damage response (DDR) and how cellular and viral replication persists in the presence of DDR signaling. Viruses 9. https://doi.org/10.3390/v9100268.

Chang, J.T.-C., Kuo, T.-F., Chen, Y.-J., Chiu, C.-C., Lu, Y.-C., Li, H.-F., Shen, C.-R., Cheng, A.-J., 2010. Highly potent and specific siRNAs against E6 or E7 genes of HPV16- or HPV18-infected cervical cancers. Cancer Gene Ther. 17, 827. https://doi.org/10.1038/cgt.2010.38.

D'Amours, D., Desnoyers, S., D'Silva, I., Poirier, G.G., 1999. Poly(ADP-ribosyl)ation reactions in the regulation of nuclear functions. Biochem. J. 342, 249–268.

Diaz-Padilla, I., Monk, B.J., MacKay, H.J., Oaknin, A., 2013. Treatment of metastatic cervical cancer: future directions involving targeted agents. Crit. Rev. Oncol. Hematol. 85, 303–314. https://doi.org/10.1016/j.critrevonc.2012.07.006.

Dyson, N., Howley, P.M., Munger, K., Harlow, E., 1989. The human papilloma virus-16 E7 oncoprotein is able to bind to the retinoblastoma gene product. Science 243, 934–937. https://doi.org/10.1126/science.2537532.

El-Mahdy, M.A., Hamada, F.M., Wani, M.A., Zhu, Q., Wani, A.A., 2000. p53-Degradation by HPV-16 E6 preferentially affects the removal of cyclobutane pyrimidine dimers from non-transcribed strand and sensitizes mammary epithelial cells to UV-irradiation. Mutat. Res. Repair 459, 135–145. https://doi.org/10.1016/S0921-8777(99)00066-X.

Flynn, R.L., Zou, L., 2011. ATR: a master conductor of cellular responses to DNA replication stress. Trends Biochem. Sci. 36, 133–140. https://doi.org/10.1016/j.tibs.2010.09.005.

Fonseca-Moutinho, J.A., 2011. Smoking and cervical cancer. ISRN Obstet. Gynecol. 2011. https://doi.org/10.5402/2011/847684.

Furuta, T., Ueda, T., Aune, G., Sarasin, A., Kraemer, K.H., Pommier, Y., 2002. Transcription-coupled nucleotide excision repair as a determinant of cisplatin sensitivity of human cells. Cancer Res. 62, 4899–4902.

Garnett, T., Duerksen-Hughes, P., 2006. Modulation of apoptosis by human papillomavirus (HPV) oncoproteins. Arch. Virol. 151, 2321–2335. https://doi.org/10.1007/s00705-006-0821-0.

Garnett, T., Filippova, M., Duerksen-Hughes, P., 2006. Accelerated degradation of FADD and procaspase 8 in cells expressing human papilloma virus 16 E6 impairs TRAIL-mediated apoptosis. Cell Death Differ. 13, 1915–1926. https://doi.org/10.1038/sj.cdd.4401886.

Garzetti, G.G., Ciavattini, A., Provinciali, M., Di Stefano, G., Lucarini, G., Goteri, G., Biagini, G., 1996. Expression of p53 and apoptosis of tumor cells in locally advanced cervical carcinoma after cisplatin based neoadjuvant chemotherapy. Anticancer Res. 16, 3229–3234.

Gillespie, K.A., Mehta, K.P., Laimins, L.A., Moody, C.A., 2012. Human papillomaviruses recruit cellular DNA repair and homologous recombination factors to viral replication centers. J. Virol. 86, 9520–9526. https://doi.org/10.1128/JVI.00247-12.

Godar, D.E., Tang, R., Merrill, S.J., 2014. Pharyngeal and cervical cancer incidences significantly correlate with personal UV doses among whites in the United States. Anticancer Res. 34, 4993–4999.

Gu, Z., Pim, D., Labrecque, S., Banks, L., Matlashewski, G., 1994. DNA damage induced p53 mediated transcription is inhibited by human papillomavirus type 18 E6. Oncogene 9, 629–633.

Gu, W., Putral, L., Hengst, K., Minto, K., Saunders, N.A., Leggatt, G., McMillan, N.a.J., 2006. Inhibition of cervical cancer cell growth in vitro and in vivo with lentiviral-vector delivered short hairpin RNA targeting human papillomavirus E6 and E7 oncogenes. Cancer Gene Ther. 13, 1023–1032. https://doi.org/10.1038/sj.cgt.7700971.

Gueranger, Q., Stary, A., Aoufouchi, S., Faili, A., Sarasin, A., Reynaud, C.-A., Weill, J.-C., 2008. Role of DNA polymerases eta, iota and zeta in UV resistance and UV-induced mutagenesis in a human cell line. DNA Repair 7, 1551–1562. https://doi.org/10.1016/j.dnarep.2008.05.012.

Gujuluva, C.N., Baek, J.H., Shin, K.H., Cherrick, H.M., Park, N.H., 1994. Effect of UV-irradiation on cell cycle, viability and the expression of p53, gadd153 and gadd45 genes in normal and HPV-immortalized human oral keratinocytes. Oncogene 9, 1819–1827.

Hasegawa, K., Kato, R., Torii, Y., Ichikawa, R., Oe, S., Udagawa, Y., 2011. The relationship between ERCC1 expression and clinical outcome in patients with FIGO stage I to stage II uterine cervical adenocarcinoma. Int. J. Gynecol. Cancer Off. J. Int. Gynecol. Cancer Soc. 21, 1479–1485. https://doi.org/10.1097/IGC.0b013e31822265e7.

Havre, P.A., Yuan, J., Hedrick, L., Cho, K.R., Glazer, P.M., 1995. p53 inactivation by HPV16 E6 results in increased mutagenesis in human cells. Cancer Res. 55, 4420–4424.

Henríquez-Hernández, L.A., Lloret, M., Pinar, B., Bordón, E., Rey, A., Lubrano, A., Lara, P.C., 2011. BCL-2, in combination with MVP and IGF-1R expression, improves prediction of clinical outcome in complete response cervical carcinoma patients treated by radiochemotherapy. Gynecol. Oncol. 122, 585–589. https://doi.org/10.1016/j.ygyno.2011.05.037.

Ho, G.P.H., Margossian, S., Taniguchi, T., D'Andrea, A.D., 2006. Phosphorylation of FANCD2 on two novel sites is required for mitomycin C resistance. Mol. Cell. Biol. 26, 7005–7015. https://doi.org/10.1128/MCB.02018-05.

Hong, S., Cheng, S., Iovane, A., Laimins, L.A., 2015. STAT-5 regulates transcription of the topoisomerase IIβ-binding protein 1 (TopBP1) gene to activate the ATR pathway and promote human papillomavirus replication. MBio 6, e02006–e02015. https://doi.org/10.1128/mBio.02006-15.

Howley, P.M., Pfister, H.J., 2015. Beta genus papillomaviruses and skin cancer. Virology 0, 290–296. https://doi.org/10.1016/j.virol.2015.02.004.

Huibregtse, J.M., Scheffner, M., Howley, P.M., 1991. A cellular protein mediates association of p53 with the E6 oncoprotein of human papillomavirus types 16 or 18. EMBO J. 10, 4129–4135.

Jackson, S., Harwood, C., Thomas, M., Banks, L., Storey, A., 2000. Role of Bak in UV-induced apoptosis in skin cancer and abrogation by HPV E6 proteins. Genes Dev. 14, 3065–3073.

Jasin, M., 2002. Homologous repair of DNA damage and tumorigenesis: the BRCA connection. Oncogene 21, 8981–8993. https://doi.org/10.1038/sj.onc.1206176.

Johnson, B.A., Aloor, H.L., Moody, C.A., 2017. The Rb binding domain of HPV31 E7 is required to maintain high levels of DNA repair factors in infected cells. Virology 500, 22–34. https://doi.org/10.1016/j.virol.2016.09.029.

Kilic, U., Sahin, K., Tuzcu, M., Basak, N., Orhan, C., Elibol-Can, B., Kilic, E., Sahin, F., Kucuk, O., 2015. Enhancement of cisplatin sensitivity in human cervical cancer: epigallocatechin-3-gallate. Front. Nutr. 1. https://doi.org/10.3389/fnut.2014.00028.

Kitahara, O., Katagiri, T., Tsunoda, T., Harima, Y., Nakamura, Y., 2002. Classification of sensitivity or resistance of cervical cancers to ionizing radiation according to expression profiles of 62 genes selected by cDNA microarray analysis. Neoplasia 4, 295–303. https://doi.org/10.1038/sj.neo.7900251.

Klingelhutz, A.J., Foster, S.A., McDougall, J.K., 1996. Telomerase activation by the E6 gene product of human papillomavirus type 16. Nature 380, 79–82. https://doi.org/10.1038/380079a0.

Knobel, P.A., Marti, T.M., 2011. Translesion DNA synthesis in the context of cancer research. Cancer Cell Int. 11, 39. https://doi.org/10.1186/1475-2867-11-39.

Koivusalo, R., Krausz, E., Ruotsalainen, P., Helenius, H., Hietanen, S., 2002. Chemoradiation of cervical cancer cells: targeting human papillomavirus E6 and p53 leads to either augmented or attenuated apoptosis depending on the platinum carrier ligand. Cancer Res. 62, 7364–7371.

Leverrier, S., Bergamaschi, D., Ghali, L., Ola, A., Warnes, G., Akgül, B., Blight, K., García-Escudero, R., Penna, A., Eddaoudi, A., Storey, A., 2007. Role of HPV E6 proteins in preventing UVB-induced release of pro-apoptotic factors from the mitochondria. Apoptosis 12, 549–560. https://doi.org/10.1007/s10495-006-0004-1.

Liu, Y., McKalip, A., Herman, B., 2000. Human papillomavirus type 16 E6 and HPV-16 E6/E7 sensitize human keratinocytes to apoptosis induced by chemotherapeutic agents: roles of p53 and caspase activation. J. Cell. Biochem. 78, 334–349.

Lorusso, D., Petrelli, F., Coinu, A., Raspagliesi, F., Barni, S., 2014. A systematic review comparing cisplatin and carboplatin plus paclitaxel-based chemotherapy for recurrent or metastatic cervical cancer. Gynecol. Oncol. 133, 117–123. https://doi.org/10.1016/j.ygyno.2014.01.042.

Marteijn, J.A., Lans, H., Vermeulen, W., Hoeijmakers, J.H.J., 2014. Understanding nucleotide excision repair and its roles in cancer and ageing. Nat. Rev. Mol. Cell Biol. 15, 465–481. https://doi.org/10.1038/nrm3822.

McKay, B.C., Becerril, C., Ljungman, M., 2001. P53 plays a protective role against UV- and cisplatin-induced apoptosis in transcription-coupled repair proficient fibroblasts. Oncogene 20, 6805. https://doi.org/10.1038/sj.onc.1204901.

Mehta, K., Laimins, L., 2018. Human papillomaviruses preferentially recruit DNA repair factors to viral genomes for rapid repair and amplification. MBio 9, e00064-18. https://doi.org/10.1128/mBio.00064-18.

Michels, J., Vitale, I., Galluzzi, L., Adam, J., Olaussen, K.A., Kepp, O., Senovilla, L., Talhaoui, I., Guegan, J., Enot, D.P., Talbot, M., Robin, A., Girard, P., Oréar, C., Lissa, D., Sukkurwala, A.Q., Garcia, P., Behnam-Motlagh, P., Kohno, K., Wu, G.S., Brenner, C., Dessen, P., Saparbaev, M., Soria, J.-C., Castedo, M., Kroemer, G., 2013. Cisplatin resistance associated with PARP hyperactivation. Cancer Res. 73, 2271–2280. https://doi.org/10.1158/0008-5472.CAN-12-3000.

Moody, C.A., 2018. The impact of replication stress in human papillomavirus pathogenesis. J. Virol. https://doi.org/10.1128/JVI.01012-17. JVI.01012-17.

Moody, C.A., Laimins, L.A., 2009. Human papillomaviruses activate the ATM DNA damage pathway for viral genome amplification upon differentiation. PLoS Pathog. 5, e1000605. https://doi.org/10.1371/journal.ppat.1000605.

Morandell, D., Kaiser, A., Herold, S., Rostek, U., Lechner, S., Mitterberger, M.C., Jansen-Dürr, P., Eilers, M., Zwerschke, W., 2012. The human papillomavirus type 16 E7 oncoprotein targets Myc-interacting zinc-finger protein-1. Virology 422, 242–253. https://doi.org/10.1016/j.virol.2011.10.027.

Parkin, D.M., Bray, F., 2006. Chapter 2: the burden of HPV-related cancers. Vaccine 24 (Suppl. 3), S3/11–25. https://doi.org/10.1016/j.vaccine.2006.05.111.

Petersen, L.N., Stevnsner, T., Bohr, V.A., 1995. DNA repair in a UV resistant Chinese hamster ovary cell line. Carcinogenesis 16, 3075–3081. https://doi.org/10.1093/carcin/16.12.3075.

Quinet, A., Martins, D.J., Vessoni, A.T., Biard, D., Sarasin, A., Stary, A., Menck, C.F.M., 2016. Translesion synthesis mechanisms depend on the nature of DNA damage in UV-irradiated human cells. Nucleic Acids Res. 44, 5717–5731. https://doi.org/10.1093/nar/gkw280.

Rey, O., Lee, S., Park, N.-H., 1999. Impaired nucleotide excision repair in UV-irradiated human oral keratinocytes immortalized with type 16 human papillomavirus genome. Oncogene 18, 6997. https://doi.org/10.1038/sj.onc.1203180.

Roman, A., Munger, K., 2013. The papillomavirus E7 proteins. Virology 445, 138–168. https://doi.org/10.1016/j.virol.2013.04.013.

Rosell, R., Taron, M., Barnadas, A., Scagliotti, G., Sarries, C., Roig, B., 2003. Nucleotide excision repair pathways involved in Cisplatin resistance in non-small-cell lung cancer. Cancer Control J. Moffitt Cancer Cent. 10, 297–305. https://doi.org/10.1177/107327480301000404.

Roy, M., Mukherjee, S., 2014. Reversal of resistance towards cisplatin by curcumin in cervical cancer cells. Asian Pac. J. Cancer Prev. APJCP 15, 1403–1410.

Saito, T., Takehara, M., Tanaka, R., Lee, R., Horie, M., Wataba, K., Ito, E., Kudo, R., 2004. Correlation between responsiveness of neoadjuvant chemotherapy and apoptosis-associated proteins for cervical adenocarcinoma. Gynecol. Oncol. 92, 284–292. https://doi.org/10.1016/j.ygyno.2003.09.027.

Schärer, O.D., 2013. Nucleotide excision repair in eukaryotes. Cold Spring Harb. Perspect. Biol. 5. https://doi.org/10.1101/cshperspect.a012609.

Scheffner, Martin, Huibregtse, J.M., Vierstra, R.D., Howley, P.M., 1993. The HPV-16 E6 and E6-AP complex functions as a ubiquitin-protein ligase in the ubiquitination of p53. Cell 75, 495–505. https://doi.org/10.1016/0092-8674(93)90384-3.

Sherris, J., Herdman, C., Elias, C., 2001. Cervical cancer in the developing world. West. J. Med. 175, 231–233.

Siegel, R., Naishadham, D., Jemal, A., 2012. Cancer statistics, 2012. CA Cancer J. Clin. 62, 10–29. https://doi.org/10.3322/caac.20138.

Spriggs, C.C., Laimins, L.A., 2017a. FANCD2 binds human papillomavirus genomes and associates with a distinct set of DNA repair proteins to regulate viral replication. MBio 8. https://doi.org/10.1128/mBio.02340-16.

Spriggs, C.C., Laimins, L.A., 2017b. Human papillomavirus and the DNA damage response: exploiting host repair pathways for viral replication. Viruses 9. https://doi.org/10.3390/v9080232.

Srivastava, A.K., Han, C., Zhao, R., Cui, T., Dai, Y., Mao, C., Zhao, W., Zhang, X., Yu, J., Wang, Q.-E., 2015. Enhanced expression of DNA polymerase eta contributes to cisplatin resistance of ovarian cancer stem cells. Proc. Natl. Acad. Sci. U. S. A. 112, 4411–4416. https://doi.org/10.1073/pnas.1421365112.

Tota, J.E., Chevarie-Davis, M., Richardson, L.A., Devries, M., Franco, E.L., 2011. Epidemiology and burden of HPV infection and related diseases: implications for prevention strategies. Prev. Med. 53 (Suppl. 1), S12–S21. https://doi.org/10.1016/j.ypmed.2011.08.017.

Wallace, N.A., Galloway, D.A., 2014. Manipulation of cellular DNA damage repair machinery facilitates propagation of human papillomaviruses. Semin. Cancer Biol. 26, 30–42. https://doi.org/10.1016/j.semcancer.2013.12.003.

Wallace, N.A., Galloway, D.A., 2015. Novel functions of the human papillomavirus E6 oncoproteins. Annu. Rev. Virol. 2, 403–423. https://doi.org/10.1146/annurev-virology-100114-055021.

Wallace, N.A., Robinson, K., Howie, H.L., Galloway, D.A., 2012. HPV 5 and 8 E6 abrogate ATR activity resulting in increased persistence of UVB induced DNA damage. PLoS Pathog. 8. https://doi.org/10.1371/journal.ppat.1002807.

Wallace, N.A., Khanal, S., Robinson, K.L., Wendel, S.O., Messer, J.J., Galloway, D.A., 2017. High risk alpha papillomavirus oncogenes impair the homologous recombination pathway. J. Virol. https://doi.org/10.1128/JVI.01084-17. JVI.01084-17.

Wechsler, E.I., Tugizov, S., Herrera, R., Da Costa, M., Palefsky, J.M., 2018. E5 can be expressed in anal cancer and leads to epidermal growth factor receptor-induced invasion in a human papillomavirus 16-transformed anal epithelial cell line. J. Gen. Virol. https://doi.org/10.1099/jgv.0.001061.

Wendel, S.O., Wallace, N.A., 2017. Loss of genome fidelity: beta HPVs and the DNA damage response. Front. Microbiol. 8. https://doi.org/10.3389/fmicb.2017.02250.

Wieringa, H.W., van der Zee, A.G.J., de Vries, E.G.E., van Vugt, M.A.T.M., 2016. Breaking the DNA damage response to improve cervical cancer treatment. Cancer Treat. Rev. 42, 30–40. https://doi.org/10.1016/j.ctrv.2015.11.008.

Winer, R.L., Hughes, J.P., Feng, Q., O'Reilly, S., Kiviat, N.B., Holmes, K.K., Koutsky, L.A., 2006. Condom use and the risk of genital human papillomavirus infection in young women. N. Engl. J. Med. 354, 2645–2654. https://doi.org/10.1056/NEJMoa053284.

Woods, D., Turchi, J.J., 2013. Chemotherapy induced DNA damage response: convergence of drugs and pathways. Cancer Biol. Ther. 14, 379–389. https://doi.org/10.4161/cbt.23761.

Zhang, B., Chen, W., Roman, A., 2006. The E7 proteins of low- and high-risk human papillomaviruses share the ability to target the pRB family member p130 for degradation. Proc. Natl. Acad. Sci. U. S. A. 103, 437–442. https://doi.org/10.1073/pnas.0510012103.

Zhu, H., Luo, H., Zhang, W., Shen, Z., Hu, X., Zhu, X., 2016. Molecular mechanisms of cisplatin resistance in cervical cancer. Drug Des. Devel. Ther. 10, 1885–1895. https://doi.org/10.2147/DDDT.S106412.

zur Hausen, H., 2002. Papillomaviruses and cancer: from basic studies to clinical application. Nat. Rev. Cancer 2, 342–350. https://doi.org/10.1038/nrc798.

CellPress
REVIEWS

Review

Catching HPV in the Homologous Recombination Cookie Jar

Nicholas A. Wallace[1,*]

To replicate, the human papillomaviruses (HPVs) that cause anogenital and oropharyngeal malignancies must simultaneously activate DNA repair pathways and avoid the cell cycle arrest that normally accompanies DNA repair. For years it seemed that HPV oncogenes activated the homologous recombination pathway to facilitate the HPV lifecycle. However, recent developments show that, although homologous recombination gene expression and markers of pathway activation are increased, homologous recombination itself is attenuated. This review provides an overview of the diverse ways that HPV oncogenes manipulate homologous recombination and ideas on how the resulting dysregulation and inhibition offer opportunities for improved therapies and biomarkers.

Highlights

HPV exploits the homologous recombination pathway to promote faithful replication of their genome.

Failure to address HPV E7 induced replication stress makes homologous recombination proteins available for HPV replication, but jeopardizes host genome integrity.

Despite notably mechanistic differences, homologous recombination attenuation is shared among HPV genera.

Manipulation of homologous recombination by HPV oncogenes is apparent in tumors associated with the virus.

Increased homologous recombination gene expression and attenuation of the pathway offer opportunities for biomarker development and improved therapeutic approaches, respectively.

Understanding Human Papillomaviruses and Host DNA Machinery to Combat Disease

According to the World Health Organization, human papillomavirus (HPV) infections cause cancers that kill someone about every 90 s. HPV transforms tissues throughout the anogenital tract and oral cavity [1]. There are several formulations of prophylactic vaccines against these infections, each with an admirable safety profile, that provide immunity against the deadliest HPV infections [2]. In the developed world, their primary limitation is under-utilization resulting from vaccine hesitancy and misconceptions about increased promiscuity associated with their protection. Despite nascent attempts to determine if HPV vaccination can benefit infected individuals, there is no evidence of therapeutic benefit [3–5]. Thus, the millions of HPV infections that occur each year remain a tremendous health hazard [6]. Because HPV-associated tumors often take decades to develop, universal vaccination would not immediately reduce HPV-associated malignancies [7,8]. Rather, the frequency of HPV-positive head and neck cancers grows at a staggering rate [9] and the United States' National Cancer Institute reports that 5-year survival rates for cervical cancer prognosis have not improved in decades. In low- and middle-income countries, where HPV is most deadly, additional barriers prevent full utilization of these vaccines. In these regions, vaccine-based intervention efforts also face financial and logistic limitations.

This has motivated researchers to interrogate HPV biology in the hope of improving these grim statistics. The relationship between HPV replication and the host DNA repair has gained significant interest because repair defects result in acute sensitivity to genotoxic chemotherapeutics. Each cell in our bodies repairs an estimated 10 000 lesions every day [10]. This bombardment is quite diverse and addressed by a complex and interwoven series of signaling cascades, collectively known as the **DNA damage response** (**DDR**; see Glossary). Whether DDR promotes or restricts viral propagation differs among viruses, but interplay between viral replication and host DDR is common [11,12]. For HPV, DDR activation is critical. However, HPV must also avoid the cell cycle arrest that accompanies DDR. While decoupling arrest and repair is advantageous for the virus, host genome integrity suffers, leading to an accumulation of tumorigenic mutations.

DDR is subdivided into pathways that fix specific types of lesion during particular portions of the cell cycle [13]. **Double-strand breaks** (**DSBs**) in DNA are arguably the most important type of lesion, both for HPV and the cell. DSBs are by far the worst type of damage faced by cells [10]. Improperly repaired DSBs result in large-scale deletions and rearrangements [10], such that a single unrepaired DSB can cause cell death [14]. As a result, there are overlapping pathways to fix these lesions. **Homologous recombination** (Figure 1A) is the best pathway for avoiding mutations and maintaining genome stability, but its use of the sister chromatid as a repair template restricts it to the S and G2 phases of the

[1]Division of Biology, Kansas State University, Manhattan, KS, USA

*Correspondence: nwallac@ksu.edu

cell cycle [15]. HPV replication is reliant on upregulating homologous recombination genes and recruiting these proteins to viral replication centers (Figure 1B).

This review offers a summary of recent revelations about the relationship between homologous recombination and HPV, with apologies for omission of the seminal earlier discoveries that made these breakthroughs possible. We focus mostly on the 'high risk' human papillomaviruses that are the most oncogenic and are referred to simply as HPV (see Box 1 for a discussion of diversity among genus α human papillomaviruses, or reference [16] for a more complete discussion of HPV diversity). There is also a brief discussion of homologous recombination and cutaneous genus β HPV infections.

HPV's Reliance on Host Homologous Recombination Proteins

HPV replication is not uniformly dependent on homologous recombination proteins. The HPV life cycle has two distinct phases (Figure 2A). The first begins with the virus infecting epithelial cells, gaining access to basal keratinocytes through microabrasions. When these cells divide laterally, the viral genome replicates along with the cell, keeping a steady number of genomes. This is the virus's maintenance phase [17]. Homologous recombination proteins are not necessary for maintenance. As basal cells divide and differentiate towards the skin's surface, HPV enters the second phase of its life cycle, known as amplification [17]. As the name suggests, HPV intensifies its replication efforts during amplification, reaching several hundred copies per cell (Figure 2B). A map of the major HPV gene products and genome features can be found in Figure 2C.

Amplification requires activation of **ataxia-telangiectasia mutated** (**ATM**) signaling [18]. ATM is a pinnacle DDR kinase that initiates DSB repair [19]. While its targets include cell cycle checkpoints and proteins in other repair pathways, ATM's role in amplification appears to be linked to its induction of homologous recombination. ATM phosphorylates SMC1, a known facilitator of homologous recombination [20,21]. During this period of the viral lifecycle, ATM also phosphorylates at least two homologous recombination proteins, **BRCA1** and **NBS1** [22]. Both of these proteins, and another homologous recombination factor, **RAD51**, are essential for amplification [22,23]. While a complete understanding of how ATM is activated by HPV is lacking, a cellular histone acetyltransferase, TIP60, is involved [24]. Signal transducer and activator of transcription 5 (**STAT5**), a member of the JAK/STAT signaling cascade, is necessary for HPV to activate ATM [25]. **HPV E7** is also the primary viral factor for inducing ATM during replication.

Activation of the DDR is not limited to the **HPV E6** and E7 oncogenes. HPV E1 and HPV E2 proteins directly facilitate HPV replication by activating DSB repair signaling. HPV E2 induces an ATM response [26], while HPV E1's helicase activity results in DDR machinery localizing to viral replication foci [27]. HPV E1 and E2 remain active in the face of exogenous DNA damage synthesizing DNA, albeit with loss of fidelity, suggesting that homologous recombination protects viral genome integrity [28]. Homologous recombination machinery's role in HPV replication is pervasive. Although the details of the advantage gained by this activation have not been fully delineated, homologous recombination may help to resolve replication errors as HPV rapidly and exponentially expands its copy number [11]. Inhibiting individual members of this pathway restricts HPV amplification *in vitro*, making HPV's interaction with these proteins attractive targets for antiviral drug development.

Taking Full Advantage of Host Homologous Recombination Factors

Because HPV is so dependent on the pathway, the virus has an array of tools for increasing its access to homologous recombination machinery. By binding and destabilizing the retinoblastoma protein (RB), HPV E7 increases homologous recombination protein abundance [29]. This is accomplished in part by raising RAD51 and BRCA1 stability. HPV E6 can cooperate with HPV E7 to further induce homologous recombination gene expression, increase the amount of RAD51, **RPA70**, BRCA1 and **BRCA2** in cells [30]. Some of the expression changes are the result of chromatin modifications. **SIRT1**, a deacetylase, remodels the host and viral DNA facilitating the recruitment of NBS1 and RAD51 to the HPV genome [31]. SIRT1 is also localized to the HPV origin of replication, where it regulates HPV E1- and E2-dependent replication via acetylation and stabilization of HPV E2 [32].

Glossary

ATM: an apical DNA repair kinase that typically responds to double-strand DNA breaks. It is activated during amplification and is necessary for the HPV lifecycle.
ATR: major DNA repair kinase. ATR most often responds to replication stress. HPV must activate ATR during amplification.
BRCA1/2: these two repair proteins are critical for homologous recombination and DNA crosslink repair. Both are induced by HPV oncogene expression, and BRCA1 is necessary for viral replication.
DDR: DNA damage repair; catch-all phrase encompassing any cell signaling process that responds to the ~10 000 DNA lesions per cell each day. HPV oncogenes activate and impair DDR.
DSB: double-strand break in DNA; a single DSB can result in cell death. HPV causes and delays their repair.
Homologous recombination: the least mutagenic means a cell has of repairing DSBs. This pathway is activated and subverted by HPV oncogenes to promote viral replication.
HPV E6: staves off apoptosis by degrading p53, impairing host genome fidelity in the process.
HPV E7: causes replication stress by promoting unregulated growth; it is responsible for most of the elevated DDR gene expression associated with HPV.
MCM helicase: cellular replicative polymerase responsible for unwinding DNA. It will continuing unwinding DNA when replicative polymerase stalls, exposing unstable single-stranded DNA.
NBS1: MRN complex member, with RAD50 and MRE11. It helps to resect DNA near DSBs, providing single-stranded DNA for homologous recombination. NBS1 is recruited to HPV replication sites.
Polymerase η or POLη: error-prone translesion synthesis polymerase. POLη's flexible active site allows it to bypass replication fork impediments. HPV low mutation rate suggests that POLη is not used during viral replication.
RAD51: required for HPV replication. During homologous recombination, RAD51 facilitates the search for homology and strand invasion that helps to use sister

During amplification, there is extensive colocalization of homologous recombination factors with the HPV genome that can be detected by immunofluorescence microscopy [33]. HPV oncogenes are active participants in recruiting these repair factors. When expressed without other viral factors or DNA, HPV E6 and E7 cause FANCD2 to be moved away from sites of DNA damage limiting the ability of RAD51 to localize to DSBs [30,34]. When expressed as part of the whole viral genome, RAD51 and BRCA1 are preferentially recruited away from cellular damage to the viral genome [35]. Notably, RAD51 and BRCA1 are required for HPV replication [36].

HPV E6 and E7 also inhibit homologous recombination indirectly by deregulating cell cycle checkpoints. Because homologous recombination relies on a homologous template to complete repair, it typically cannot be finished without a sister chromatid. As a result, cells avoid beginning homologous recombination during G1. Instead they use an alternative repair pathway (nonhomologous end joining) to fix breaks with minimal loss of sequence [36]. HPV E6 and E7 make it significantly more likely that nuclear RPA foci (an indirect indicator of resected single-stranded DNA) appear during G1 [30]. DDR proteins form increasingly large complexes around this type of hard-to-resolve lesion [37]. This would provide a noteworthy opportunity for HPV to 'steal' homologous recombination proteins. The fact that most HPV replication occurs during G2 is contrary to this idea, though. Perhaps it is an unintended consequence resulting from widespread deregulation of cell signaling, or maybe it creates a 'G2-like' environment where HPV can replicate [38].

Stressing the Cell to Gain Access

HPV amplification requires replication of typically quiescent cells. To satisfy this need, HPV E7 degrades Rb and RB-family proteins leading to increased E2F transcription and effectively preventing G1/S checkpoints [39]. By removing this constraint on cell proliferation, HPV E7 allows dysregulated growth that depletes nucleoside pools causing **replication stress** [40]. In response, the host cell undergoes multiple efforts to mitigate the replication stress. It becomes addicted to two demethylases (KDM6A and KDM6B), resulting in widespread methylation and gene expression changes [41–44]. A ribonucleotide reductase, RRM2, is also overexpressed, providing an alternative source of nucleosides [45].

In this environment, replication forks are presumably stalling as they wait for necessary building blocks. This should decouple replication fork progression from the **MCM helicase** activity and result in long stretches of single-stranded DNA (ssDNA). ssDNA is rapidly bound by the RPA complex (RPA14, RPA32, and RPA70) to help prevent fork collapse and activate **ATR** signaling [46]. ATR activation stabilizes the error prone **polymerase η** or **POLη**, beginning a process known as **translesion synthesis** (**TLS**) [47]. The stalled fork also promotes PCNA ubiquitination, allowing POLη to displace the replicative polymerase, easing replication restraints and preventing fork collapse into DSBs. Since the pathway responds to other replication stressors, TLS is presumably activated by HPV E7-induced replication stress. However, TLS likely falters before completion as HPV E7 induces double-strand breaks consistent with fork collapse [48]. Further, HPV's constitutive activation of ATR occurs via a TOPBP1-dependent mechanism, which would be expected if TLS begins, but is not completed [24]. This is clearly important for HPV replication as ATR activation promotes HPV replication.

On the surface, this seems disadvantageous for the virus as failed TLS results in DSBs that promote viral episome integration, after which HPV can no longer produce infectious virions [30]. However, there would be advantages for HPV that could outweigh the detriments. First, failed TLS leads to the ATR activation that is at least partially required for recruitment of DSB repair factors to viral replication centers [49]. Further, the DSBs that result from replication fork collapse are overwhelmingly repaired by homologous recombination increasing the availability of these factors. Finally, because the need for TLS reaches its maxima during amplification as HPV E7 levels rise, if the pathway failed then homologous recombination proteins would also peak during amplification when HPV has the greatest need for them.

chromatin as template for error-free repair.
Replication stress: general term encompassing the strain resulting from any impediment to replication. Common source of genome instability in cancers. HPV E7 induces replication stress by depleting nucleoside pools.
RPA70: a member of the RPA trimer that protects single-stranded DNA from degradation. HPV oncogenes increase RPA70 abundance and phosphorylation of fellow RPA trimer partner, RPA32.
SIRT1: host NAD-dependent deacetylase that controls HPV replication through histone modifications and recruitment of RAD51 and NBS1 to replication centers.
STAT5: a member of the JAK/STAT signaling family. STAT5 is required for ATM activation during HPV amplification.
Synthetic lethality: occurs when the combination of two conditions is exponentially more deleterious together than separately. Often the result of blocking two interconnected signaling pathways.
Translesion synthesis (TLS): translesion synthesis mitigates replication stress via polymerase barrier bypass. It is a recently identified mediator of chemotherapy resistance. Inhibition of the pathway could explain some of the DNA repair activation seen in cells expressing HPV oncogenes.

(A)

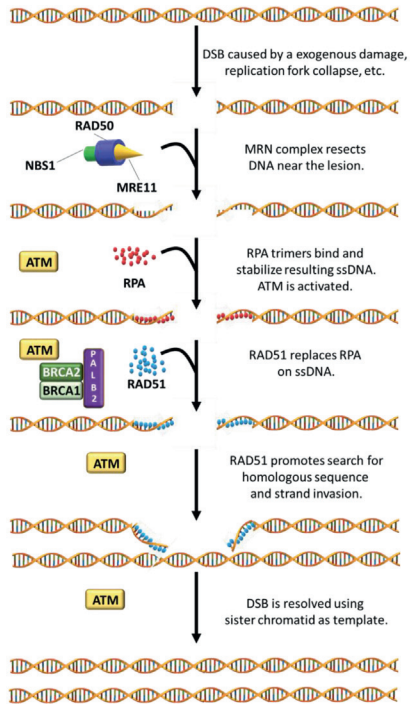

(B)

Protein(s)	Change in abundance	Localized to HPV replication foci
MRE11 [22]	UP	YES
RAD50 [22]	UP	YES
NBS1[22]	UP	YES
ATM [18]	UP	YES
RPA Complex [22, 34]	UP	YES
BRCA1 [23, 34]	UP	YES
BRCA2 [34]	UP	???
PALB2 [30]	DOWN	???
RAD51 [23, 34]	UP	YES
CHK2 [18]	UP	YES
SIRT1 [31, 32]	UP	YES

Trends in Microbiology

Figure 1. The Homologous Recombination Pathway Is Altered by Human Papillomavirus (HPV) Replication.
(A) Schematic of canonical homologous recombination pathway. (B) Table showing how HPV replication/gene expression alters the homologous recombination proteins. The column lists (left) genes involved in homologous recombination, (middle) changes in protein abundance during HPV replication or oncogene expression, and (right) whether the indicated protein localizes to HPV replication sites. CHK2 is phosphorylated by the DNA repair kinase ATM in response to a double-strand break (DSB) which induces a cell cycle checkpoint. SIRT1 promotes homologous recombination via deacetylation of target proteins. References [18,22,23,30,34] are provided in the first column.

Box 1. How Conserved Is the Abrogation of Homologous Recombination among Human Papillomaviruses?

This review focuses on cancer-associated HPVs from the alpha genus, but there is considerably more diversity in the genus. There are only 12 recognized 'high risk' αHPVs (HPV 16, HPV 18, HPV 31, HPV 33, HPV 35, HPV 45, HPV 51, HPV 52, HPV 56, HPV 58, HPV 59, and HPV 68). The other viruses in this genus are collectively referred to as 'low risk' HPVs and lack the ability to abolish p53- and RB-mediated cell signaling. Because they do not cause deadly cancers, these viruses are often neglected by researchers. When 'low risk' HPVs are studied, HPV 6 or HPV 11 are used as surrogates for the rest of the genus. These are chosen because they cause genital warts and reoccurring respiratory papillomas, more than for their ability to reflect the biology of the rest of the genus [83]. Even among the 'high risk' HPVs there is considerable bias towards studying the more clinically relevant viruses, with most studies investigating HPV 16, HPV18, and HPV31 biology. While there is good reason to believe that all 'high risk' HPVs share the ability to hinder homologous recombination, subtle differences in their manipulation of the pathway could explain why 70% of cervical cancers are caused by HPV 16 and HPV 18. There are more knowledge gaps with regard to the attenuation of repair by 'low risk' HPVs. The wart-causing 'low risk' HPVs (HPV 6 and HPV 11) have a significantly muted ability to alter DNA repair, compared to 'high risk' HPVs. However, less is known about how representative HPV 6 and HPV 11 are of less pathogenic 'low risk' HPVs. A more complete understanding of how other alpha genus HPVs thrive is an area ripe for investigation.

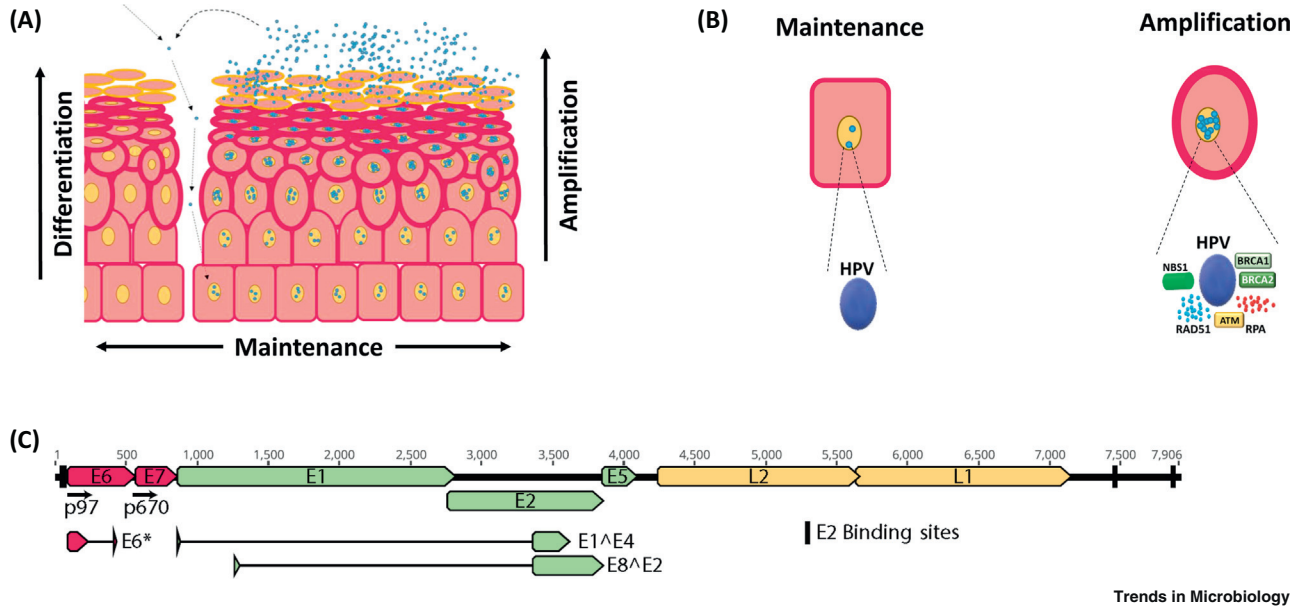

Figure 2. Homologous Recombination Proteins Localize to Viral Replication Sites during Amplification.

(A) Image depicts high-risk α-HPV life cycle in stratified epithelia. Differentiation in these cells is represented by changes in their shape. More differentiated cells are flatter ovals, while less differentiated cells are rectangular. Arrow and blue circle represent infectious viral particles infecting the basal layer and gaining access via microabrasions in the skin. Yellow circles depict nuclei. During horizontal replication of the host cells, high-risk α-HPV enters the maintenance phase of its life cycle where it maintains a relatively low genome copy number. As cells differentiate towards the surface, the number of viral genomes increase to remarkable levels, shown as a rising number of blue circles within cells. Human Papillomavirus (HPV) does not induce lysis; instead, it leaves as cells slough off naturally. Lighter pink cells with yellow borders represent this portion of the viral life cycle. (B) Enlarged image of cells [matching the morphology from (A)] highlighting the recruitment of homologous recombination proteins to sites of HPV replication, shown as blue spheres. (C) Linearized HPV genome with major transcripts. HPV genes are grouped by function and designated by color: HPV oncogenes (HPV E6, HPV E7, and splice variant HPV E6*) are pink, other early genes (HPV E1, HPV E2, HPV E5, HPV E1^E4, and HPV E8^E2) are green, and capsid genes (HPV L1 and L2) are yellow. The two primary promoters are noted with black arrows and numbers, indicating their location in the genome (p97 and p670). The HPV E2 bindings sites crucial for segregating HPV genomes during division are also noted.

Hurting without Killing: HPV's Repurposing of Homologous Recombination Factors Has Severe Consequences for Host Cells

Of course, HPV is not the only entity with an interest in how the cell responds to DSBs. Protecting genome fidelity is essential to the host cell's survival. HPV infections further complicate the host's mandate to protect its own DNA. The replication stress caused by the virus represents a notable challenge to cellular genome integrity [50]. As discussed in a preceding section, these responses are evidently unable to keep up as HPV oncogenes cause DSBs consistent with a failed or overwhelmed replication stress response. Unsurprisingly, HPV oncogenes make cells significantly more sensitive to replication stress from DNA crosslinking drugs, hydroxyurea, and UV [51,52].

HPV E6 and E7 also make DSBs more persistent, particularly in the host genome [30,35]. They lower homologous recombination efficiency by 50–60%, by causing a defect in the resolution of RAD51 foci [30]. The decreased homologous recombination efficiency suggests that the inhibitory effects of HPV oncogenes outpace any benefit to host that might come from the increased homologous recombination protein abundance. As expected from attenuated DSB repair, HPV oncogene-expressing cell lines are sensitive to endogenous and exogenous sources of DSBs [53–55].

It should be noted that the toxicity of replication stress and DSBs would likely be worse if HPV oncogenes were not simultaneously blocking repair and apoptosis. Apoptosis inhibition is often linked to HPV E6's promotion of p53 degradation, but the viral oncogenes have several other antiapoptotic activities [56]. This effectively amounts to a triple blockade of the cellular response to HPV E7-induced

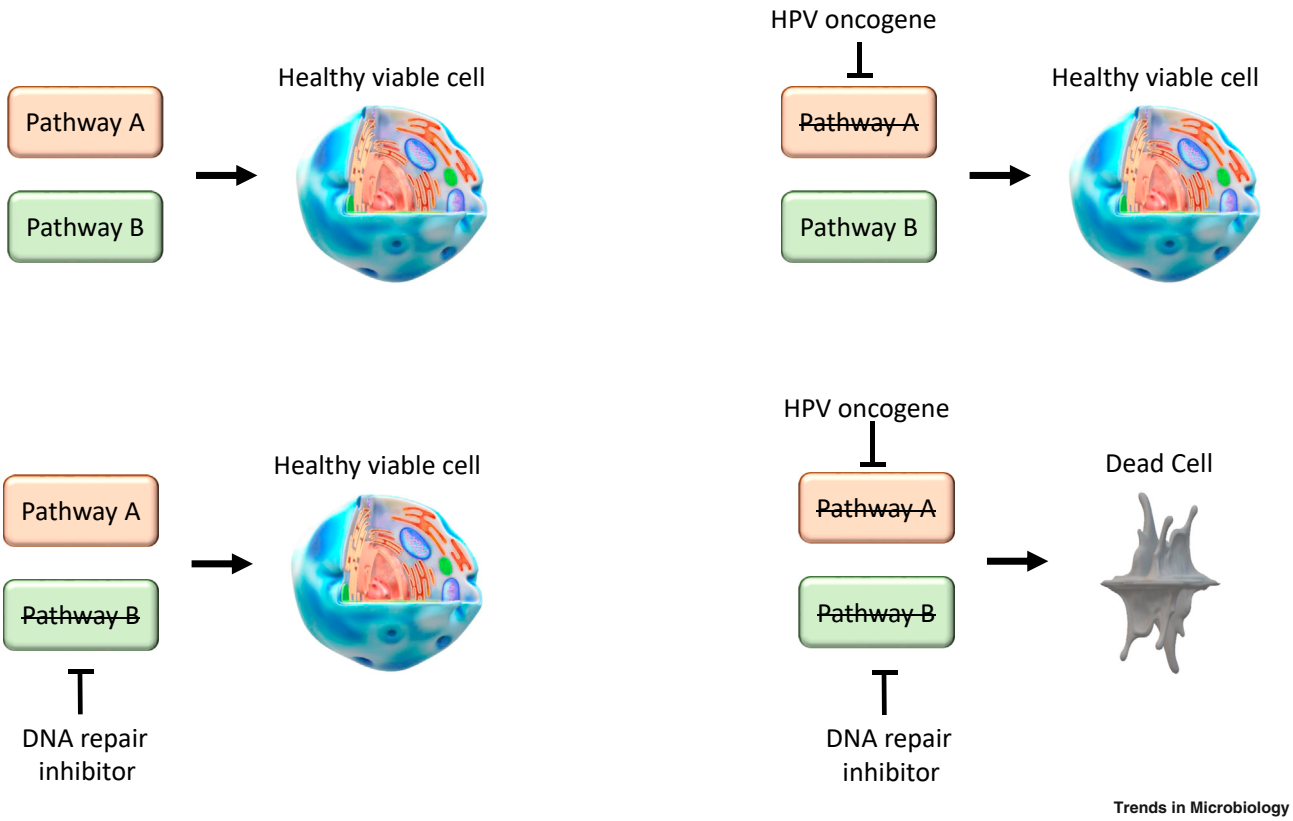

Figure 3. Potential Synthetic Lethal Relationship Where Human Papillomavirus (HPV) Oncogene Expression Is Combined with DNA Repair Inhibition.

On their own, the inhibition of Pathway A by HPV oncogene(s) or Pathway B by a DNA repair inhibitor are not deleterious to cells. However, when combined, they cause significant cytotoxicity. This would provide very targeted killing of HPV-associated cancer cells and requires continued characterization of DNA damage repair (DDR) pathways inhibited by HPV oncogenes. For example, HPV E6 and E7 inhibit the homologous recombination pathway (Pathway A), which is expected to create the potential for a synthetic lethal relationship with PARP1 inhibition (Pathway B).

replication stress. First, HPV oncogenes increase the likelihood of replication forks collapse. The repair of the resulting DSBs is attenuated and the last-ditch effort of programmed cell death is inhibited. Despite greater sensitivity, far more cells survive than would be prudent, and the host genome acquires tumorigenic mutations.

Targeting HPV Oncogene Biology for Direct Translational Implications

HPV-associated tumors are addicted to HPV oncogene expression. Even though HeLa cells have been grown in laboratories around the world for decades, they remain sensitive to reduction of HPV E6 or E7 [57]. This is notable given that HPV oncogenes promote acquisition of the additional mutations required for transformation. If cells with a notably impaired DDR do not acquire the necessary mutations to become independent of HPV oncogene expression after nearly 70 years in culture, it is unlikely that HPV-associated cancers would gain said mutations over the markedly shorter period that tumors exist *in vivo*. This results in a degree of tumor homogeneity that may be therapeutically targetable.

Synthetic lethality refers to gene mutations/chemical inhibitions that are very toxic together, but not particularly deleterious individually [58]. This concept has been the rationale for some chemotherapeutic regiments, where small-molecule inhibitors are more effective in certain genetic backgrounds. However, either extensive individual tumor profiling or biomarker development is required for this

approach. This may not be necessary in cervical cancers, where nearly all of the tumors are caused by constitutive HPV oncogene expression [59]. HPV-associated malignancies likely have an unusually high replication stress burden and a limited ability to complete homologous recombination. Figure 3 illustrates the concept of HPV oncogene-induced synthetic lethality. The efficacy of cisplatin and carboplatin at treating cervical cancers is consistent with this idea, as these drugs are more effective when replication stress is high or homologous recombination is impaired [60]. Using synthetic lethality approaches to target tumors with altered DNA repair is an area of considerable promise [61]. Breast cancers harboring BRCA1 or BRCA2 mutations can be effectively treated with PARP1 inhibitors [62]. PARP1 inhibition increases the number of DSBs during replication that would typically be repaired by homologous recombination, but BRCA1/BRCA2 mutations prevent the pathway from responding. HPV oncogenes also inhibit homologous recombination, and several ongoing clinical trials are using PARP1 inhibitors to treat cervical cancer [63–65].

The homogeneity resulting from HPV oncogene expression provides opportunities for improving biomarkers against HPV-associated tumors. DNA repair protein abundance increases in parallel with cervical premalignant lesion progression and was predicted based on HPV oncogene-driven changes first observed in tissue culture [66]. This approach is particularly helpful for tumors that may or may not be caused by HPV. Management of the ongoing HPV-positive head and neck squamous cell carcinoma (HPV^+ HNSCCs) epidemic would especially benefit, because response to therapy varies significantly between HPV-positive and -negative cancers [67]. In fact, individuals with HPV^+ HNSCCs are candidates for de-escalated therapies [68]. HPV status is currently determined using p16 status as a surrogate marker, but there are mutations that can change p16 abundance independently of HPV [69]. Since homologous recombination and other repair proteins are increased by HPV oncogenes, these proteins may be able to act as biomarkers, improving the specificity of p16 for predicting HPV status.

Cutaneous HPV Infections Repress Homologous Recombination

Although we have focused exclusively on high-risk members of the α-Papillomavirus genus to this point, other human papillomaviruses have clinically relevant interactions with the homologous recombination pathway. Members of the β-Papillomavirus genus (β-HPVs) have a tropism for cutaneous rather than anogenital and oropharyngeal keratinocytes. β-HPVs augment nonmelanoma skin cancer development, especially in people with immunosuppression [70]. The World Health Organization and the International Agency for Research on Cancer (IARC) recognize the oncogenic potential of two β-HPVs among the genus, designating β-HPV 5 and β-HPV 8 as possibly carcinogenic [71]. Although other members of the β-HPV genus may also be oncogenic [70,72,73], we follow the IARC's lead focusing only on β-HPV 5 and 8 and referring to them collectively as β-HPV (see Box 2

Box 2. Which β-HPVs Should We Worry about?

In this review, we focus on HPV 5 and HPV 8 as representative of β-HPVs, primarily because of their IARC designation. However, there is epidemiological evidence that more β-HPVs increase the risk of skin cancer. Along with HPV 5 and HPV 8, at least six other members of the genus (HPV 15, HPV 17, HPV 20, HPV 24, HPV 36, and HPV 38) are associated with a mild, yet significant, risk factor in cutaneous squamous-cell carcinoma [73]. There is also a variety of molecular evidence supporting broad, but mild, oncogenic potential within this genus. Many β-HPV E6s limit cells from undergoing UV-induced apoptosis [84]. Also, HPV 38 and HPV 49 oncogenes transform primary skin cells *in vitro* [85,86]. Among β-HPVs not designated 'possibly carcinogenic' by the IARC, HPV 38 is the best characterized. Transient expression of HPV 38 E6 and E7 promotes tumorigenesis in mice exposed to UV [72]. HPV 38E6 also reduces homologous recombination efficiency and activates telomerase [77,87]. Finally, HPV 38E6 binds p300, although more weakly than HPV 8E6 or 5E6, but does not cause its destabilization [88]. These data seem to justify reconsideration of IARC's characterization of β-HPVs. Further, given the diversity among β-HPVs, they may each have a specific genetic/immune environment where they are most transforming. Ultimately, continued interrogation of these viruses is necessary to understand the relative cancer risk associated with them and to identify appropriate antiviral treatments for any that are dangerous.

Key Figure

When a Double-Strand Break (DSB) Occurs in an S- or G2/M-Phase Cell's DNA, Homologous Recombination Proteins Assemble at the Lesion to Repair the Lesion (Repair Factor Color and Shape Match Those from Figures 1 and 2).

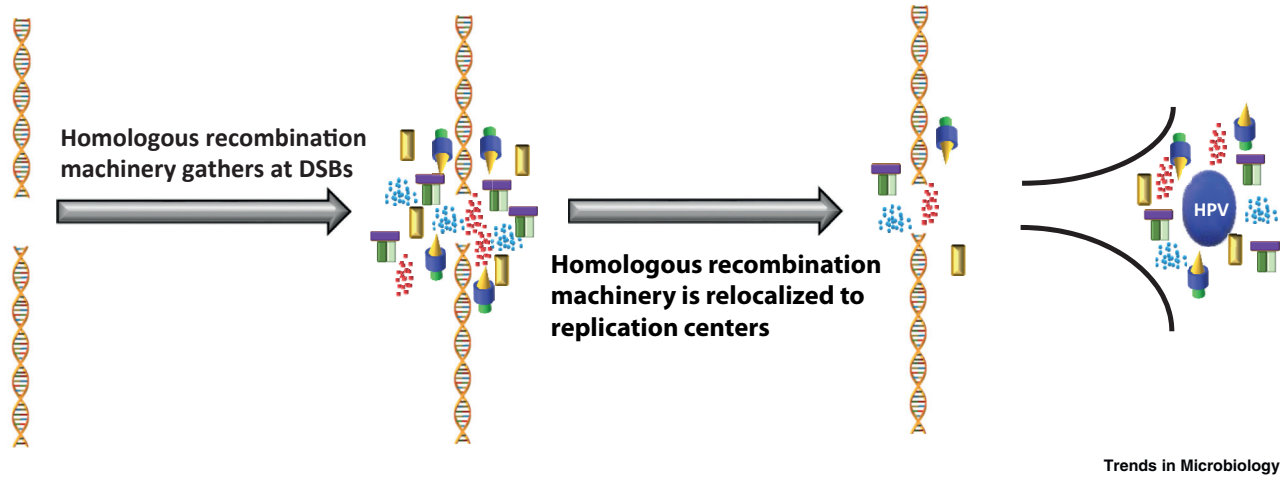

Figure 4. During an infection by human Papillomavirus (HPV), this repair machinery is leached away from cellular damage to viral replication centers (shown as a blue sphere).

for an expanded discussion of other β-HPVs). β-HPV infections appear to act by augmenting UV's mutagenic potential, making it more oncogenic. Unlike high-risk HPVs, β-HPV infections are transient. Indeed, their gene expression peaks in precancerous lesions and appears to be dispensable in tumors [74]. Similar to other HPVs, β-HPV have E6 and E7 genes (β-HPV E6 and β-HPV E7) that contain most of the virus's transforming potential. β-HPV E7 binds and destabilizes RB, but less completely than HPV E7 proteins from high-risk HPVs [71]. This likely removes cell cycle constraints, allowing cells to spend more time in parts of the cell cycle (S and G2/M phases), where DSBs are preferentially repaired via homologous recombination. β-HPV E6 attenuates multiple repair pathways, including homologous recombination, by binding and destabilizing the cellular histone acetyltransferase, p300 [75–77]. This makes UV more likely to result in a DSB and increases the risk that chromosome abnormalities (large deletions, fusions, etc.) result from crosslinked DNA [77]. Decreased p300 availability likely reaches further as p300 is a master transcription regulator [78]. We have already shown that, by destabilizing p300, β-HPV reduces the expression of four repair genes (ATM, ATR, BRCA1, BRCA2) that play critical roles in multiple repair pathways [75–77]. Presumably, by hindering repair, these viruses escape the cell cycle arrest associated with UV damage. Recently described infection models and established animal models are driving a renewed interest in this field [72,74,79,80]; however, some question the importance of p300 degradation in carcinogenesis. There are considerable basic and epidemiological gaps left to determine the extent that transient cutaneous HPV infections contribute to skin cancers, but they undoubtedly contribute to the tremendous tumor burden caused by HPV.

Concluding Remarks

Nearly all of the death and disease caused by HPV infections can be avoided through vaccinations. Unfortunately, the antivaccine movement is a persistent scourge. In the developing world, fiscal and logistic restrictions represent additional barriers. Together, this has undermined the full benefits of HPV vaccination in most countries other than Australia [81]. For unvaccinated individuals, and

people who are already infected with HPV, alternative therapies and improved biomarkers are still needed. HPV's utilization of homologous recombination provides an opportunity to meet both of these needs (Figure 4, Key Figure). We are already beginning to see this potential explored. Impaired homologous recombination synthesizes cells to PARP inhibitors and these drugs are being tested in cervical cancers [64]. Chemotherapeutic drugs that inhibit specific cell signaling pathways are becoming increasingly available in clinical settings. This is improving the opportunities to leverage an intimate understanding of HPV oncogene biology toward better patient outcomes [82]. HPV oncogene-induced changes in homologous recombination protein abundance also lead to targeted preclinical biomarker development. While there is undoubtedly a litany of remaining questions important to the field, we suggest five knowledge gaps that we find particularly compelling in the Outstanding Questions box. Using the knowledge of viral oncogene biology to improve treatment of the associated malignancies is not limited to homologous recombination and HPV-associated disease. Rather, these principles can be applied to the 15–20% of tumors with infectious origins. The lessons learned from HPV biology and therapeutic applications could thus have even larger public health consequences.

Outstanding Questions

What prevents translesion synthesis from mitigating HPV E7-induced replication stress?

Can changes in host DNA repair provide targets that improve care of HPV-associated cancers?

Why do cutaneous HPV infections take such a markedly different approach to homologous recombination?

To what extent is inhibition of homologous recombination shared among the Papillomavirus family?

Can HPV oncogenes serve as tools for dissecting homologous recombination and other DNA repair pathways?

Acknowledgments

I would like to thank Kansas State University's Johnson Cancer Research Center, and particularly the Les Clow family, for their support. Further, Dr Koenrad VanDoerslaer was instrumental in creating the stylized image of the HPV genome. Thanks Vanni.

References

1. Berman, T.A. and Schiller, J.T. (2017) Human papillomavirus in cervical cancer and oropharyngeal cancer: One cause, two diseases. *Cancer* 123, 2219–2229
2. Baldur-Felskov, B. *et al.* (2014) Early impact of human papillomavirus vaccination on cervical neoplasia – nationwide follow-up of young Danish women. *J. Natl. Cancer Inst.* 106, djt460
3. Kang, W.D. *et al.* (2013) Is vaccination with quadrivalent HPV vaccine after loop electrosurgical excision procedure effective in preventing recurrence in patients with high-grade cervical intraepithelial neoplasia (CIN2-3)? *Gynecol. Oncol.* 130, 264–268
4. Madeleine, M.M. *et al.* (2016) Natural antibodies to human papillomavirus 16 and recurrence of vulvar high-grade intraepithelial neoplasia (VIN3). *J. Low Genit. Tract. Dis.* 20, 257–260
5. Swedish, K.A. *et al.* (2012) Prevention of recurrent high-grade anal neoplasia with quadrivalent human papillomavirus vaccination of men who have sex with men: a nonconcurrent cohort study. *Clin. Infect. Dis.* 54, 891–898
6. de Martel, C. *et al.* (2017) Worldwide burden of cancer attributable to HPV by site, country and HPV type. *Int. J. Cancer* 141, 664–670
7. Sudenga, S.L. *et al.* (2016) Cervical HPV natural history among young Western Cape, South African women: the randomized control EVRI trial. *J. Infect.* 72, 60–69
8. Vink, M.A. *et al.* (2013) Clinical progression of high-grade cervical intraepithelial neoplasia: estimating the time to preclinical cervical cancer from doubly censored national registry data. *Am. J. Epidemiol.* 178, 1161–1169
9. Marur, S. *et al.* (2010) HPV-associated head and neck cancer: a virus-related cancer epidemic. *Lancet Oncol.* 11, 781–789
10. Jackson, S.P. and Bartek, J. (2009) The DNA-damage response in human biology and disease. *Nature* 461, 1071–1078
11. Bristol, M.L. *et al.* (2017) Why human papillomaviruses activate the DNA damage response (DDR) and how cellular and viral replication persists in the presence of DDR signaling. *Viruses* 9, E268
12. Hollingworth, R. and Grand, R.J. (2015) Modulation of DNA damage and repair pathways by human tumour viruses. *Viruses* 7, 2542–2591
13. Hustedt, N. and Durocher, D. (2016) The control of DNA repair by the cell cycle. *Nat. Cell Biol.* 19, 1–9
14. Nowsheen, S. and Yang, E.S. (2012) The intersection between DNA damage response and cell death pathways. *Exp. Oncol.* 34, 243–254
15. Jasin, M. and Rothstein, R. (2013) Repair of strand breaks by homologous recombination. *Cold Spring Harb. Perspect. Biol.* 5, a012740
16. Van Doorslaer, K. *et al.* (2017) The papillomavirus episteme: a major update to the papillomavirus sequence database. *Nucleic. Acids Res.* 45, D499–D506
17. Doorbar, J. *et al.* (2012) The biology and life-cycle of human papillomaviruses. *Vaccine* 30 (*Suppl.* 5), F55–F70
18. Moody, C.A. and Laimins, L.A. (2009) Human papillomaviruses activate the ATM DNA damage pathway for viral genome amplification upon differentiation. *PLoS Pathog.* 5, e1000605
19. Blackford, A.N. and Jackson, S.P. (2017) ATM, ATR, and DNA-PK: the trinity at the heart of the DNA damage response. *Mol. Cell* 66, 801–817
20. Mehta, K. *et al.* (2015) Human papillomaviruses activate and recruit SMC1 cohesin proteins for the differentiation-dependent life cycle through association with CTCF insulators. *PLoS Pathog.* 11, e1004763
21. Potts, P.R. *et al.* (2006) Human SMC5/6 complex promotes sister chromatid homologous recombination by recruiting the SMC1/3 cohesin complex to double-strand breaks. *EMBO J.* 25, 3377–3388
22. Anacker, D.C. *et al.* (2014) Productive replication of human papillomavirus 31 requires DNA repair factor Nbs1. *J. Virol.* 88, 8528–8544
23. Chappell, W.H. *et al.* (2015) Homologous recombination repair factors Rad51 and BRCA1 are

necessary for productive replication of human papillomavirus 31. *J. Virol.* 90, 2639–2652
24. Hong, S. *et al.* (2015) STAT-5 regulates transcription of the topoisomerase IIβ-binding protein 1 (TopBP1) gene to activate the ATR pathway and promote human papillomavirus replication. *mBio* 6, e02006–e02015
25. Hong, S. and Laimins, L.A. (2013) The JAK-STAT transcriptional regulator, STAT-5, activates the ATM DNA damage pathway to induce HPV 31 genome amplification upon epithelial differentiation. *PLoS Pathog.* 9, e1003295
26. Fradet-Turcotte, A. *et al.* (2011) Nuclear accumulation of the papillomavirus E1 helicase blocks S-phase progression and triggers an ATM-dependent DNA damage response. *J. Virol.* 85, 8996–9012
27. Sakakibara, N. *et al.* (2011) The papillomavirus E1 helicase activates a cellular DNA damage response in viral replication foci. *J. Virol.* 85, 8981–8995
28. Bristol, M.L. *et al.* (2016) DNA damage reduces the quality, but not the quantity of human papillomavirus 16 E1 and E2 DNA replication. *Viruses* 8, 175
29. Johnson, B.A. *et al.* (2017) The Rb binding domain of HPV31 E7 is required to maintain high levels of DNA repair factors in infected cells. *Virology* 500, 22–34
30. Wallace, N.A. *et al.* (2017) High risk alpha papillomavirus oncogenes impair the homologous recombination pathway. *J. Virol.* 91, e01084-17.
31. Langsfeld, E.S. *et al.* (2015) The deacetylase sirtuin 1 regulates human papillomavirus replication by modulating histone acetylation and recruitment of DNA damage factors NBS1 and Rad51 to viral genomes. *PLOS Pathog* 11, e1005181
32. Das, D. *et al.* (2017) The deacetylase SIRT1 regulates the replication properties of human papillomavirus 16 E1 and E2. *J. Virol.* 91, e00102–e00117
33. Gillespie, K.A. *et al.* (2012) Human papillomaviruses recruit cellular DNA repair and homologous recombination factors to viral replication centers. *J. Virol.* 86, 9520–9526
34. Khanal, S. and Galloway, D.A. (2019) High-risk human papillomavirus oncogenes disrupt the Fanconi anemia DNA repair pathway by impairing localization and de-ubiquitination of FancD2. *PLoS Pathog* 15, e1007442
35. Mehta, K. and Laimins, L. (2018) Human papillomaviruses preferentially recruit DNA repair factors to viral genomes for rapid repair and amplification. *mBio* 9, e00064–18.
36. Chang, H.H.Y. *et al.* (2017) Non-homologous DNA end joining and alternative pathways to double-strand break repair. *Nat. Rev. Mol. Cell Biol.* 18, 495–506
37. Lee, C.-S. *et al.* (2014) Dynamics of yeast histone H2A and H2B phosphorylation in response to a double-strand break. *Nat. Struct. Mol. Biol.* 21, 103–109
38. Reinson, T. *et al.* (2015) The cell cycle timing of human papillomavirus DNA replication. *PLoS One* 10, e0131675
39. McLaughlin-Drubin, M.E. and Münger, K. (2009) The human papillomavirus E7 oncoprotein. *Virology* 384, 335–344
40. Moody, C.A. (2019) The impact of replication stress in human papillomavirus pathogenesis. *J. Virol.* 93, e01003–e01018
41. Gameiro, S.F. *et al.* (2017) Human papillomavirus dysregulates the cellular apparatus controlling the methylation status of H3K27 in different human cancers to consistently alter gene expression regardless of tissue of origin. *Oncotarget* 8, 72564–72576
42. McLaughlin-Drubin, M.E. *et al.* (2011) Human papillomavirus E7 oncoprotein induces KDM6A and KDM6B histone demethylase expression and causes epigenetic reprogramming. *Proc. Natl. Acad. Sci. U. S. A.* 108, 2130–2135
43. McLaughlin-Drubin, M.E. *et al.* (2013) Tumor suppressor p16INK4A is necessary for survival of cervical carcinoma cell lines. *Proc. Natl. Acad. Sci. U. S. A.* 110, 16175–16180
44. Soto, D.R. *et al.* (2017) KDM6A addiction of cervical carcinoma cell lines is triggered by E7 and mediated by p21CIP1 suppression of replication stress. *PLOS Pathog.* 13, e1006661
45. Anacker, D.C. *et al.* (2016) HPV31 utilizes the ATR-Chk1 pathway to maintain elevated RRM2 levels and a replication-competent environment in differentiating keratinocytes. *Virology* 499, 383–396
46. Zou, L. (2007) Single- and double-stranded DNA: building a trigger of ATR-mediated DNA damage response. *Genes Dev.* 21, 879–885
47. Göhler, T. *et al.* (2011) ATR-mediated phosphorylation of DNA polymerase η is needed for efficient recovery from UV damage. *J. Cell Biol.* 192, 219–227
48. Leung, W. *et al.* (2019) Mechanisms of DNA damage tolerance: post-translational regulation of PCNA. *Genes (Basel)* 10, 10
49. Reinson, T. *et al.* (2013) Engagement of the ATR-dependent DNA damage response at the human papillomavirus 18 replication centers during the initial amplification. *J. Virol.* 87, 951–964
50. Singh, B. and Wu, P.-Y.J. (2019) Linking the organization of DNA replication with genome maintenance. *Curr. Genet.* 65, 677–683
51. Chen, B. *et al.* (2009) Human papilloma virus type16 E6 deregulates CHK1 and sensitizes human fibroblasts to environmental carcinogens independently of its effect on p53. *Cell Cycle* 8, 1775–1787
52. Gu, W. *et al.* (2019) Cervical cancer cell lines are sensitive to sub-erythemal UV exposure. *Gene* 688, 44–53
53. Mirghani, H. *et al.* (2015) Increased radiosensitivity of HPV-positive head and neck cancers: molecular basis and therapeutic perspectives. *Cancer Treat. Rev.* 41, 844–852
54. Nickson, C.M. *et al.* (2017) Misregulation of DNA damage repair pathways in HPV-positive head and neck squamous cell carcinoma contributes to cellular radiosensitivity. *Oncotarget* 8, 29963–29975
55. Park, J.W. *et al.* (2014) Human papillomavirus type 16 E7 oncoprotein causes a delay in repair of DNA damage. *Radiother. Oncol.* 113, 337–344
56. Yuan, C.-H. *et al.* (2012) Modulation of apoptotic pathways by human papillomaviruses (HPV): mechanisms and implications for therapy. *Viruses* 4, 3831–3850
57. Hall, A.H.S. and Alexander, K.A. (2003) RNA interference of human papillomavirus type 18 E6 and E7 induces senescence in HeLa cells. *J. Virol.* 77, 6066–6069
58. O'Neil, N.J. *et al.* (2017) Synthetic lethality and cancer. *Nat. Rev. Genet.* 18, 613–623
59. Cohen, P.A. *et al.* (2019) Cervical cancer. *Lancet* 393, 169–182
60. Puigvert, J.C. *et al.* (2016) Targeting DNA repair, DNA metabolism and replication stress as anti-cancer strategies. *FEBS J.* 283, 232–245
61. Shaheen, M. *et al.* (2011) Synthetic lethality: exploiting the addiction of cancer to DNA repair. *Blood* 117, 6074–6082
62. Zimmer, A.S. *et al.* (2018) Update on PARP inhibitors in breast cancer. *Curr. Treat. Options Oncol.* 19, 21
63. Kunos, C. *et al.* (2015) A phase I–II evaluation of veliparib (NSC#737664), topotecan, and filgrastim or pegfilgrastim in the treatment of persistent or recurrent carcinoma of the uterine cervix: an NRG

Oncology/Gynecologic Oncology Group study. *Int. J. Gynecol. Cancer* 25, 484–492
64. Matulonis, U.A. and Monk, B.J. (2017) PARP inhibitor and chemotherapy combination trials for the treatment of advanced malignancies: does a development pathway forward exist? *Ann. Oncol.* 28, 443–447
65. Thaker, P.H. *et al.* (2017) A phase I trial of paclitaxel, cisplatin, and veliparib in the treatment of persistent or recurrent carcinoma of the cervix: an NRG Oncology Study (NCT#01281852). *Ann. Oncol.* 28, 505–511
66. Spriggs, C.C. *et al.* (2019) Expression of HPV-induced DNA damage repair factors correlates with CIN progression. *Int. J. Gynecol. Pathol.* 38, 1–10
67. Dok, R. and Nuyts, S. (2016) HPV positive head and neck cancers: molecular pathogenesis and evolving treatment strategies. *Cancers (Basel)* 8, 41
68. Mirghani, H. and Blanchard, P. (2018) Treatment de-escalation for HPV-driven oropharyngeal cancer: where do we stand? *Clin. Transl. Radiat. Oncol.* 8, 4–11
69. Vokes, E.E. *et al.* (2015) HPV-associated head and neck cancer. *J. Natl. Cancer Inst.* 107, djv344
70. Tommasino, M. (2017) The biology of beta human papillomaviruses. *Virus Res.* 231, 128–138
71. Wendel, S.O. and Wallace, N.A. (2017) Loss of genome fidelity: beta HPVs and the DNA damage response. *Front. Microbiol.* 8
72. Viarisio, D. *et al.* (2018) Beta HPV38 oncoproteins act with a hit-and-run mechanism in ultraviolet radiation-induced skin carcinogenesis in mice. *PLoS Pathog.* 14, e1006783
73. Rollison, D.E. *et al.* (2019) An emerging issue in oncogenic virology: the role of beta human papillomavirus types in the development of cutaneous squamous cell carcinoma. *J. Virol.* 93, e01003–e01018
74. Hufbauer, M. and Akgül, B. (2017) Molecular mechanisms of human papillomavirus induced skin carcinogenesis. *Viruses* 9, 187
75. Wallace, N.A. *et al.* (2012) HPV 5 and 8 E6 abrogate ATR activity resulting in increased persistence of UVB induced DNA damage. *PLoS Pathog.* 8, e1002807
76. Wallace, N.A. *et al.* (2013) HPV 5 and 8 E6 expression reduces ATM protein levels and attenuates LINE-1 retrotransposition. *Virology* 443, 69–79
77. Wallace, N.A. *et al.* (2015) β-HPV 5 and 8 E6 disrupt homology dependent double strand break repair by attenuating BRCA1 and BRCA2 expression and foci formation. *PLoS Pathog.* 11, e1004687
78. Bedford, D.C. and Brindle, P.K. (2012) Is histone acetylation the most important physiological function for CBP and p300? *Aging (Albany NY)* 4, 247–255
79. Meyers, J.M. *et al.* (2017) Cutaneous HPV8 and MmuPV1 E6 proteins target the NOTCH and TGF-β tumor suppressors to inhibit differentiation and sustain keratinocyte proliferation. *PLOS Pathog.* 13, e1006171
80. Xue, X.-Y. *et al.* (2017) The full transcription map of mouse papillomavirus type 1 (MmuPV1) in mouse wart tissues. *PLoS Pathog.* 13, e1006715
81. Lee, L. and Garland, S.M. (2017) Human papillomavirus vaccination: the population impact. *F1000Res* 6, 866
82. Kelley, M.R. *et al.* (2014) Targeting DNA repair pathways for cancer treatment: what's new? *Future Oncol.* 10, 1215–1237
83. Egawa, N. and Doorbar, J. (2017) The low-risk papillomaviruses. *Virus Res.* 231, 119–127
84. Underbrink, M.P. *et al.* (2008) E6 proteins from multiple human betapapillomavirus types degrade Bak and protect keratinocytes from apoptosis after UVB irradiation. *J. Virol.* 82, 10408–10417
85. Cornet, I. *et al.* (2012) Comparative analysis of transforming properties of E6 and E7 from different beta human papillomavirus types. *J. Virol.* 86, 2366–2370
86. Muench, P. *et al.* (2010) Cutaneous Papillomavirus E6 proteins must interact with p300 and block p53-mediated apoptosis for cellular immortalization and tumorigenesis. *Cancer Res.* 70, 6913–6924
87. Bedard, K.M. *et al.* (2008) The E6 oncoproteins from human betapapillomaviruses differentially activate telomerase through an E6AP-dependent mechanism and prolong the lifespan of primary keratinocytes. *J. Virol.* 82, 3894–3902
88. Howie, H.L. *et al.* (2011) Beta-HPV 5 and 8 E6 promote p300 degradation by blocking AKT/p300 association. *PLoS Pathog.* 7, e1002211

Video Article

Characterizing DNA Repair Processes at Transient and Long-lasting Double-strand DNA Breaks by Immunofluorescence Microscopy

Vaibhav Murthy*[1], Dalton Dacus*[1], Monica Gamez[2], Changkun Hu[1], Sebastian O. Wendel[1], Jazmine Snow[1], Andrew Kahn[1], Stephen H. Walterhouse[1], Nicholas A. Wallace[1]

[1]Division of Biology, Kansas State University

[2]Bristol Medical School, Translational Health Sciences, University of Bristol

*These authors contributed equally

Correspondence to: Nicholas A. Wallace at nwallac@ksu.edu

URL: https://www.jove.com/video/57653
DOI: doi:10.3791/57653

Keywords: Cancer Research, Issue 136, Immunofluorescence microscopy, DNA repair, double-strand breaks, repair kinetics, homologous recombination, non-homologous end joining, H2AX

Date Published: 6/8/2018

Citation: Murthy, V., Dacus, D., Gamez, M., Hu, C., Wendel, S.O., Snow, J., Kahn, A., Walterhouse, S.H., Wallace, N.A. Characterizing DNA Repair Processes at Transient and Long-lasting Double-strand DNA Breaks by Immunofluorescence Microscopy. *J. Vis. Exp.* (136), e57653, doi:10.3791/57653 (2018).

Abstract

The repair of double-stranded breaks (DSBs) in DNA is a highly coordinated process, necessitating the formation and resolution of multi-protein repair complexes. This process is regulated by a myriad of proteins that promote the association and disassociation of proteins to these lesions. Thanks in large part to the ability to perform functional screens of a vast library of proteins, there is a greater appreciation of the genes necessary for the double-strand DNA break repair. Often knockout or chemical inhibitor screens identify proteins involved in repair processes by using increased toxicity as a marker for a protein that is required for DSB repair. Although useful for identifying novel cellular proteins involved in maintaining genome fidelity, functional analysis requires the determination of whether the protein of interest promotes localization, formation, or resolution of repair complexes.

The accumulation of repair proteins can be readily detected as distinct nuclear foci by immunofluorescence microscopy. Thus, association and disassociation of these proteins at sites of DNA damage can be accessed by observing these nuclear foci at representative intervals after the induction of double-strand DNA breaks. This approach can also identify mis-localized repair factor proteins, if repair defects do not simultaneously occur with incomplete delays in repair. In this scenario, long-lasting double-strand DNA breaks can be engineered by expressing a rare cutting endonuclease (*e.g.*, I-SceI) in cells where the recognition site for the said enzyme has been integrated into the cellular genome. The resulting lesion is particularly hard to resolve as faithful repair will reintroduce the enzyme's recognition site, prompting another round of cleavage. As a result, differences in the kinetics of repair are eliminated. If repair complexes are not formed, localization has been impeded. This protocol describes the methodology necessary to identify changes in repair kinetics as well as repair protein localization.

Video Link

The video component of this article can be found at https://www.jove.com/video/57653/

Introduction

Each day, every cell in the human body is bombarded with an estimated 10,000 DNA lesions[1]. This existential threat puts us at risk for mutations, oncogenesis as well as cell death. To protect genome fidelity, mammalian cells have evolved to respond to DNA damage with a complex series of protein associations and modifications. This response is organized into multiple pathways, collectively known as the DNA damage response (DDR)[2,3]. The DDR consists of the accumulation of DNA repair proteins at DNA lesions, coordinated both temporally and spatially. DDR frequently induces cell cycle arrest to avoid the propagation or intensification of damage that can occur during the replication of damaged DNA[2,4,5]. In turn, it is also necessary for the cellular viability to turn off cell cycle arrest by disassociating repair complexes after repair has been completed.

Among the various types of DNA damage, DSBs are the most deleterious. Failure to repair DSBs can result in chromosome rearrangements or large-scale deletions such as the loss of entire chromosome arms. The repair of DSBs is divided into two pathways[6,7,8]. Homologous recombination (HR) requires a sister chromosome to use as a DNA template and thus is limited to late S and G2/M phases of the cell cycle[9,10]. Non-homologous end joining (NHEJ) does not have these restrictions but can cause small deletions when repairing DSBs[11,12].

DSB repair specifically and the DDR in general are active areas of investigation. Despite being organized into conveniently separated pathways, there is a great deal of redundancy. Indeed, many proteins (BRCA1, BRCA2, and the RPA complex for example) are involved in multiple pathways[13,14,15,16]. The repair of a lesion by one pathway, can lead to a damage intermediate that must be repaired by another pathway[14]. The

intertwining of these pathways, combined with their complex task of recruiting the right proteins to the correct place for the precise amount of time necessary, requires a multi-tiered regulatory process.

A recent report highlights the intricacies of DDR by demonstrating that repair complex formation, resolution, and localization can each separately be impaired[17]. The overall goal of the following protocol is to definitively dissect the ability of cells to repair DSB. Using immunofluorescence microscopy, accumulation of repair proteins at the sites of damage can be visualized at the representative time points following the induction of DSBs.

This technique has several advantages to commonly used approaches. Frequently, repair is investigated at single time points and incapable of representing the dynamic process of assembly and dissociation of repair complexes. Observing the full range of repair from the initial activation to the full resolution ensures that a delay in repair is not misidentified as complete inhibition. Conversely, it assures that the induction of a repair response that is unable to inactivate said response is not misidentified as the normal or the excessive activation.

Delayed protein complex formation and the mis-localization of repair proteins, however, may not be unambiguously distinguished with this approach. To determine if repair proteins are mis-localized versus delayed in their localization, a "long-lasting" DSB can be introduced through enzymatic cleavage of cellular DNA. The resulting lesion is recut each time it is repaired, resulting in a distinct large nuclear repair focus and removing the temporal restriction from recruitment. This can be achieved by modifying the existing approach with the use of a rare cutting endonuclease (*e.g.*, I-SceI) to induce a long-lasting DSB. The longevity of DSBs enables the visualization of elusive repair proteins by immunofluorescence microscopy. The enhanced abundance could also improve the visualization when detection is hindered by limitation in the antibody quality, a feature that could be useful when lesser studied proteins are identified as having an impact on DNA repair.

Notably, we provide explicit instructions for a free image processing and analysis software (*e.g.*, ImageJ). This removes a major financial barrier in image analysis, opening the interrogation of DNA damage repair to a wider audience.

Protocol

Please note, this protocol is written for U2OS cells containing an I-SceI recognition site[18]. The cells need not be U2OS but must contain the I-SceI site. The protocol may need to be adjusted (*e.g.*, number of cells seeded and incubation times) depending on the type of cells used.

1. Defining the Kinetics of DSB Repair Complex Formation

1. Grow U20S-DRGFP cells on a 10 cm tissue culture plate until 85–90% confluent.
2. Remove the media and incubate at room temperature (RT) in 3 mL of EDTA for 2 min.
3. Replace EDTA with 1 mL of trypsin and incubate at 37 °C for 5 min. Ensure that the cells are detached from the surface of the plate by viewing under a microscope. Neutralize trypsin with 5 mL of Dulbecco's Modified Eagle Medium (DMEM) supplemented with 10% fetal bovine serum (FBS) and 1% penicillin/streptomycin.
4. Determine the concentration of cells in this suspension using a hemocytometer and the trypan blue exclusion method.
5. Seed 6 x 10^3 cells/well in 200 µL of a glass-bottom 96-well plate. Alternatively, seed 4 x 10^6 cells in 8 mL on 12 mm coverslips placed in a 10 cm plate.
   NOTE: Each well or coverslip represents a single time point, including the control.
6. Grow the cells overnight at 37 °C and 5% CO_2.
7. **Inducing DSBs**
   1. Replace the media from the 96-well plate/10 cm dish with H_2O_2 diluted to a concentration of 25 µM with DMEM + 10% FBS and incubate at 37 °C for 1 h.
   2. Wash the cells 3x with 1x PBS and replace with fresh DMEM supplemented with 10% FBS and 1% penicillin/streptomycin. Incubate the cells at 37 °C for 0, 1, 4, 8, 24, and 48 h. Ensure that fresh dilutions of H_2O_2 are used for each experiment.
      NOTE: To avoid killing cells at the H_2O_2 concentration used here, ensure that the dose of damage is low enough such that the bulk of cells will avoid apoptosis and senescence. It is critical to observe the recovery process. This is best achieved by measuring sensitivity to a range of doses. Perform an MTT assay or other cell viability assay to determine the minimal concentration of hydrogen peroxide that can be used.
8. **Fixing and permeabilizing cells**
   1. Wash the cells 3 times with 1x PBS. Remove a coverslip from the 10 cm plate for each time point and place it in a single well of a 24-well plate for fixing. Use the needle and forceps to carefully remove the coverslip and avoiding scratching cells off the coverslip surface.
   2. Fix the cells by incubating for 15 min with 4% paraformaldehyde (PFA) at designated times after 1 h of H_2O_2 exposure and fresh DMEM replacement (0, 1, 4, 8, 24, and 48 h).
   3. Wash the fixed coverslips 3 times with PBS. Permeabilize the cells with 0.5% non-ionic detergent diluted in 1x PBS. Incubate for 15 min at RT, before washing 3x with PBS.
      NOTE: After permeabilization, storage of coverslips is possible in PBS at 4 °C for at least a week.
9. **Repair complex visualization**
   1. Block the 96-well plate/coverslips in a solution of 3% bovine serum albumin (BSA) and 0.1% non-ionic detergent diluted in 1x PBS (3% BSA solution) for 1 h at RT.
   2. Incubate with primary antibodies that target the repair protein of interest, diluted according to the manufacturer's specifications in 3% BSA solution for 1 h at RT, before washing 3 times with 1x PBS.
   3. Incubate the 96-well plate/coverslips with secondary antibody diluted according to the manufacturer’s protocol in 3% BSA solution. Confirm that the secondary fluorophores do not have overlapping excitation or emission spectra.
   4. After washing the cells with PBS 3 times add DAPI, diluted according to the manufacturer’s specifications in 1x PBS and incubate at RT for 5 min.

5. Mount the coverslips onto slides with a drop of mounting agent, making sure the cell-side faces down. Press the coverslips carefully and soak up any excess mounting agent with a wipe.
6. Seal the coverslips with fast-drying transparent nail polish and ensure a complete seal of the coverslip with the slide.
7. Take the confocal microscope images by focusing on the DAPI channel, before other channels (with signals from DNA repair gene of interest) to avoid introducing bias into the experiment.
8. Alternatively, images can be acquired by taking Z-sections of the desired region and condensing the image into a single plane to visualize all detectable foci.
   NOTE: If DSB resolution or protein of interest is not observed at time points chosen, determine when DSBs resolve by selecting a wide range of time points initially (0–48 h post DSB induction). The time points of interest will vary by the method of DSB induction and the repair protein of interest.

10. **Use free ImageJ software to define the nuclei in the immunofluorescence microscopy images.**
    NOTE: To open microscope images, the Bio-Formats plugin must be installed in ImageJ.
    1. Open the confocal images (.czi or .tif) by dragging the image file into the ImageJ window, or by selecting "Bio-Formats Importer" from the "Plugin" toolbar in ImageJ.
       NOTE: The "Bio-Formats Import Option" window will appear.
    2. Select "Split Channels" to split the image into constitutive DAPI and fluorescent images within the "Bio-Formats Import Option" window.
    3. Select "Colorized" in "Color options" from the drop-down menu. Select "OK" to open the DAPI and Histone H2AX (H2AX) images as separate windows and choose the DAPI image.
    4. Select the "Image" toolbar and "Adjust Threshold" option to select nuclei.
       NOTE: A "Threshold" window will appear.
    5. Adjust the image threshold by sliding the bottom bar of the "Threshold" window completely to the right. Adjust the top bar until the nuclei appear completely red with distinct outlines, and the background black. DO NOT select apply. Close the "Adjust Threshold" window.
    6. Select the "Analyze" toolbar and "Analyze Particles" option. See an "Analyze Particles" window appearing on the screen.
    7. Input the minimum size of a nucleus.
       NOTE: Particles below the size inputted will not be counted as nuclei.
    8. From the "Show" dropdown menu, select "Outlines". Select the "Add to Manager" option. Click "OK" to open an "ROI Manager" window.
       NOTE: Outlines of nuclei will appear in a separate window.
    9. Assign numbers to the nuclei that can be selected from the "ROI Manager" window.

11. **Use ImageJ to quantify H2AX foci in immunofluorescence microscopy images.**
    1. Select the "H2AX" foci window (stained with fluorescently conjugated secondary antibody). Then, select the "Process" toolbar and choose "Find Maxima" to find the foci within the nuclei.
       NOTE: A "Find Maxima" window will open.
    2. Choose the "Single Points" option from the "Output Type" dropdown menu and select "Preview point selection" to visualize the maxima/foci. Input a "Noise Tolerance" value depending on the fluorescence intensity of the image (**Figure 1**). Check for the appearance of a white window with small black dots.
       NOTE: These dots represent the H2AX foci/maxima that have been detected. The noise tolerance value must be maintained constant for all images being analyzed. A low/high noise tolerance will depict too many/few maxima (foci) within the nucleus and will not be an accurate representation of the foci within the nucleus.
    3. Select the nuclei for which H2AX foci must be quantified for from the "ROI Manager" window. Select all the nuclei by checking the "show all" option.
    4. Select "Measure" to measure the number of maxima/foci within the selected nuclei.
       NOTE: The number of maxima/foci appear as multiples of 255, *i.e.*, one maximum has a "RawIntDen" (Integrated density) reading of 255.
    5. Copy the "RawIntDen" values and paste them into software for data analysis.

2. Analyzing Localization to a Long-lasting Double-strand DNA Break

1. Seed cells on 96-well plates/coverslips as described in sections 1.1 and 1.2.
2. **Induction of double-strand DNA breaks**
   1. Transfect cells with the I-SceI expression vector using a lipid-based transfection reagent according to the manufacturer's specifications. Wait 24–72 h after transfection to maximize the endonuclease expression. Determine if the transfection was successful by locating cells with a singular large nuclear γ-H2AX focus.

3. **Acquisition of images**
   1. Fix, permeabilize, block, and wash the 96-well plate/coverslips as described in section 1.8.
   2. Co-incubate cells with an antibody against γ-H2AX and the repair protein of interest (here, a primary antibody against RAD51 was used) diluted according to the manufacturer's specifications in 3% BSA solution.
   3. Wash the 96-well plate/coverslips 3 times with 1x PBS. Incubate the 96-well plate/coverslips with secondary antibody diluted according to the manufacturer's protocol in 3% BSA solution. Confirm that the secondary fluorophores do not have overlapping excitation or emission spectra.
   4. Identify cells that have a large nuclear γ-H2AX focus. Only take pictures of these cells to avoid bias.

4. **Analysis of long-lasting I-SceI induced foci**

1. Analyze the long-lasting foci manually, by counting both the number of cells that have the large γ-H2AX foci and co-localized foci of the repair protein of interest.

Representative Results

Figure 1 depicts the selection of the correct noise discrimination for maxima/foci quantification using ImageJ. The merged images of DAPI and the repair protein of interest are on the left panel. **Figure 1A** shows a noise discrimination of 90 and marks the correct number of foci. Nuclei on the edge (depicted with a pink arrow) and foci outside the nuclei (depicted with a yellow arrow) are not counted during the quantification. **Figure 1B** depicts a low noise tolerance of 50. Numerous maxima are identified outside the nucleus and within the nucleus. **Figure 1C** shows a high noise tolerance of 220. Only a single focus (a white arrow) was detected. To offer the reader a sense of "positive" and "negative" results, we have also compiled representative results in **Figure 2**. Specifically, **Figure 2A** depicts co-localization between a γ-H2AX focus (green) and a repair protein of interest (red). Similarly, an untransfected cell is shown in the upper left of this panel and a cell with a non-nuclear (false) γ-H2AX focus is shown in the upper right. Please note the micronuclei associate with DNA damage machinery are a likely source of these non-nuclear foci[19]. **Figure 2B** provides a higher magnification of the two right-most cells from **Figure 2A** to provide clarity in how they were determined to be interior and exterior to the nucleus, respectively. An example of a nuclear γ-H2AX focus without co-localization of a repair protein is shown in **Figure 2C**. A schematic of this protocol is provided in **Figure 3** that summarizes this approach to characterizing DNA repair.

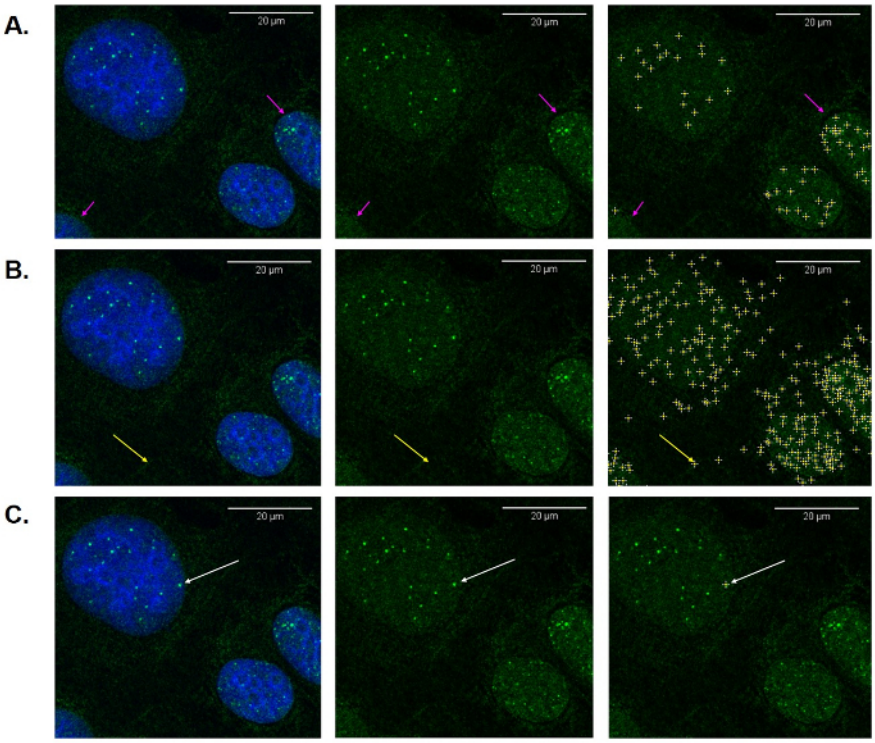

Figure 1: Representative analysis of double-strand DNA break repair kinetics. Representative images of γ-H2AX foci quantification using ImageJ (with Bio-Formats plugin) software. The left panels are composite images of nuclei (40X magnification), stained blue for DAPI and green for γ-H2AX. Center panels show reference un-analyzed nuclei with γ-H2AX foci/maxima. (**A**) The right panel shows maxima/foci detection with a noise tolerance of 90 and is representative of the actual estimation of the number of foci within the nucleus. (**B**) The right panel shows maxima quantification with a low noise tolerance (50). Maxima/foci can be detected outside the nucleus (yellow arrow), while majority of the maxima located within the nucleus are non-specific background signals. (**C**) The right panel shows maxima quantification with high noise tolerance (220). Only a single maximum/focus (white arrow) is detected within the nucleus and is not representative of the foci within the nucleus. Please click here to view a larger version of this figure.

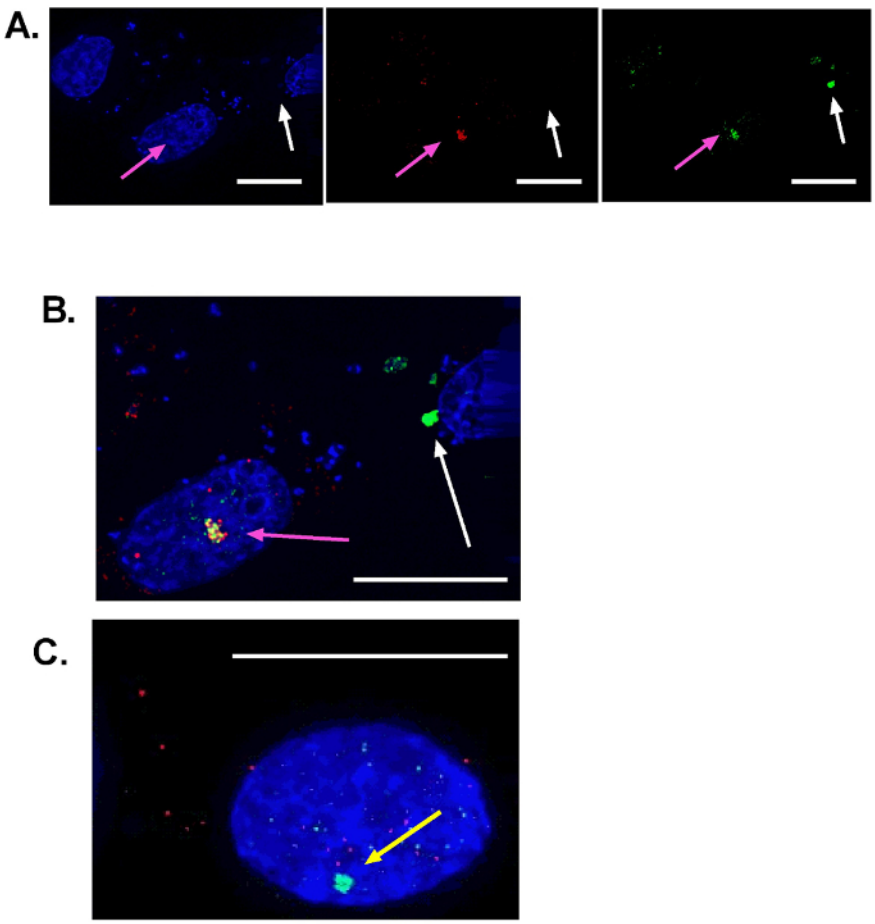

Figure 2: Representative I-SceI induced double-strand DNA breaks. Representative images of nuclei from cells grown on coverslips (40X magnification). Nuclei are stained blue. A repair protein (RAD51) is stained red and γ-H2AX is stained green. (**A**) The three panels show the same three cells. In the left most panel, nuclei are visible. In the middle panel, staining for RAD51 is shown. On the right panel, γ-H2AX staining is shown. The nucleus in the upper right corner does not show any sign of I-SceI induced DSBs. The nucleus in the center (pink arrow) represents a true positive event as it has both a large γ-H2AX nuclear focus and a co-localized RAD51 nuclear focus. The nucleus on the right side has a false large γ-H2AX focus as it is extranuclear. Foci outside of the nucleus should not be used for co-localization analysis. (**B**) This is a higher magnification of the merged image in part A (center and right most cells). The large nuclear yellow focus indicating overlap of RAD51 and H2AX signal is denoted by the pink arrow. (**C**) A representative image of a nuclear γ-H2AX focus without co-staining of the DNA repair protein of interest. Unlike the focus denoted with a white arrow in (A) and (B), the yellow arrow illustrates typical results when repair proteins are prevented from localizing to sites of damage. Scale bar = 15 μm. Please click here to view a larger version of this figure.

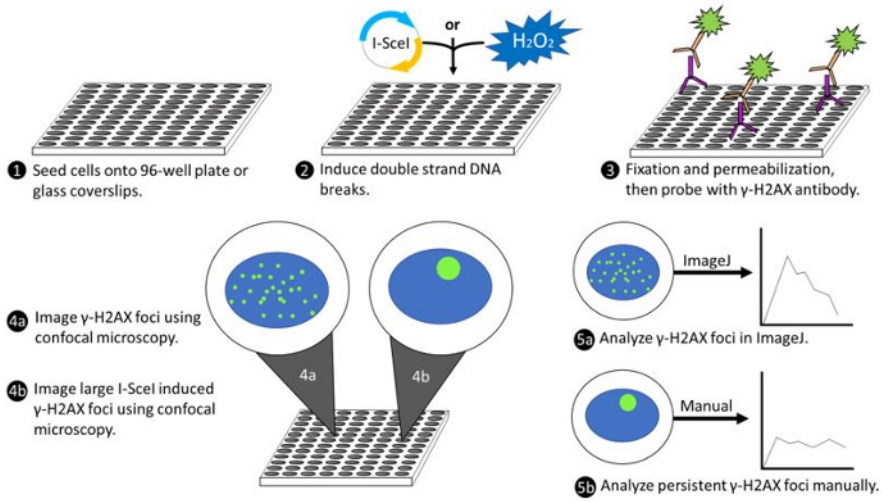

Figure 3: Visual depiction of protocol for analyzing double-strand DNA break repair. (**1**) Representation of protocol steps 1.1 for seeding cells onto coverslips/glass bottom plates. (**2**) Illustration of the induction of double-strand breaks by treating with hydrogen peroxide (right) or inducing long-lasting double-strand breaks by transfecting 3 µg of I-SceI. (**3**) Representation of protocol steps 1.4 to 1.5.3 for visualization of double-strand breaks. (**4a**) Image representing confocal microscopy of cell stained with DAPI (blue) and γ-H2AX foci (green). (**4b**) Image of singular large γ-H2AX foci (green) again nuclei stain DAPI (blue). (**5a**) Depiction of the analysis of γ-H2AX foci using ImageJ (protocol steps 1.10.1–1.11.5). (**5b**) Depiction of manual count of large long-lasting γ-H2AX foci (protocol step 2.4). Please click here to view a larger version of this figure.

Discussion

The analysis of DNA damage repair in general and the repair of double-stranded DNA breaks specifically is an active area of research because its consequences span tumorigenesis to basic biology[6,20]. This manuscript details an approach that accurately dissects the contribution of RAD51 and γ-H2AX proteins to the resolution of DSBs through HR. Looking forward, this method can be used to elucidate additional functions of repair proteins at DSBs[14]. The comparison of repair kinetics and the recruitment of repair machinery to I-SceI induced DSBs between control cells and cells with the protein of interest knocked out, would define the contribution of that protein to the recruitment, localization, and resolution of repair factors to DSBs.

Visualizing repair kinetics has several advantages over commonly used approaches. Frequently, repair is investigated at single time points, which is incapable of representing the dynamic process of assembly and dissociation of repair complexes. Observing the full range of repair from initial activation to full resolution ensures that a delay in repair is not misidentified as complete inhibition. Conversely, it assures that induction of a repair response without the ability to inactivate that response is not misidentified as normal or excessive activation. These are largely changes in the application of an established approach, but the use of a rare cutting endonuclease to induce a long-lasting DSB is a novel tool. It allows the investigator to unambiguously determine if the localization of a repair protein is inhibited instead of its recruitment being delayed a short period of time beyond the conclusion of the experiment. I-SceI induced DSB can last for days and theoretically as long as the enzyme is expressed (should the cell remain viable). The kinetics of DSB repair can also be observed via live cell imaging. However, although live cell imaging allows detection of repair events in real time, its application is hindered by the requirement that proteins be tagged with a fluorophore such as GFP. Such genetic manipulation has the potential to alter protein function and represents an additional technical barrier.

Image analysis via ImageJ software can be cumbersome to master. The step-by-step instruction for repair focus recognition and quantification using this software is provided in hopes of removing this obstacle for other groups. This could lead to increased utilization of the powerful software and eliminate the cost of more expensive programs at a time of shrinking pools of federal grant support.

In principle, the duration of these DSBs should enable the visualization of elusive repair proteins by immunofluorescence microscopy. This could be the case for proteins that are difficult to view because they do not accumulate in a high enough concentration to be detected, *e.g.*, the persistence of the I-SceI induced DSB results in a greater than typical accumulation of repair proteins at the lesion. The enhanced abundance could also improve the visualization when detection is hindered by a limitation in antibody quality; a feature that could be particularly useful when less studied proteins are identified as having an impact on DNA repair. To date, this approach has been verified for 4 DNA repair proteins, namely RAD51, RPA70, BRCA1, and BRCA2 (data not shown, **Figure 2**, and reference[17])

Finally, there are modifications that could be made to this protocol to expand the types of DNA damage that can be interrogated as well as the cellular environments. The most obvious modification would be changing the source or type of induced DNA damage. The proof of principle for using UVB, ionizing radiation, or radiomimetics (phleomycin, bleomycin, and etoposide) to study the kinetics of DNA repair has already been published[18,19,23,24,25]. With slight modification, this approach can also elucidate repair protein response by NHEJ to DSBs. Alternatively, Britton *et al.* describe a pre-extraction technique that could be used[26]. Further, there are homing nicking endonucleases (I-HmuI or I-BasI) that have extensive recognition sites, similar to I-SceI[27]. Distinguishing them from I-SceI, these enzymes cause single-strand DNA breaks (SSBs). Introducing the recognition site for these enzymes into a cell line would allow the analysis of SSB repair that parallels the protocol described in this manuscript for interrogating long-lasting DSBs. Notably, the process of integrating the I-SceI recognition site and verifying the introduction of the site can be laborious. Fortunately advances in genome editing technology (such as CRISPER/Cas9 systems) have eased this burden[28].

There is also a field of active research that has succeeded in engineering homing endonucleases to cut at a desired genomic location, which suggests that in the future, these engineering advancements and the use of CRISPR/Cas9 may lead this cloning step to be dispensable[28,29].

Disclosures

The authors have nothing to disclose.

Acknowledgements

We thank Joel Sanneman and Dr. Philine Wangemann of the Confocal Microscopy Core, funded by the Kansas State University College of Veterinary Medicine, for their support of efforts to develop this technique. pCBASceI was a gift from Maria Jasin (Addgene plasmid # 26477)30. U2OS DR-GFP cells were a kind gift from Maria Jasin[18].

References

1. Lindahl, T. Instability and decay of the primary structure of DNA. *Nature.* **362** (6422), 709-715 (1993).
2. Branzei, D., Foiani, M. Regulation of DNA repair throughout the cell cycle. *Nat Rev Mol Cell Biol.* **9** (4), 297-308 (2008).
3. Ciccia, A., Elledge, S.J. The DNA damage response: making it safe to play with knives. *Mol Cell.* **40** (2), 179-204 (2010).
4. Auclair, Y., Rouget, R., Drobetsky, E.A. ATR kinase as master regulator of nucleotide excision repair during S phase of the cell cycle. *Cell Cycle.* **8** (12), 1865-1871 (2009).
5. Awasthi, P., Foiani, M., Kumar, A. ATM and ATR signaling at a glance. *J Cell Sci.* **128** (23), 4255-4262 (2015).
6. Ceccaldi, R., Rondinelli, B., D'Andrea, A.D. Repair Pathway Choices and Consequences at the Double-Strand Break. *Trends Cell Biol.* **26** (1), 52-64 (2016).
7. Chapman, J.R., Taylor, M.R.G., Boulton, S.J. Playing the End Game: DNA Double-Strand Break Repair Pathway Choice. *Mol Cell.* **47** (4), 497-510 (2012).
8. Daley, J.M., Sung, P. 53BP1, BRCA1, and the Choice between Recombination and End Joining at DNA Double-Strand Breaks. *Mol Cell Biol.* **34** (8), 1380-1388 (2014).
9. Hartlerode, A., Odate, S., Shim, I., Brown, J., Scully, R. Cell Cycle-Dependent Induction of Homologous Recombination by a Tightly Regulated I-SceI Fusion Protein. *PLOS ONE.* **6** (3), e16501 (2011).
10. Brandsma, I., Gent, D.C. Pathway choice in DNA double strand break repair: observations of a balancing act. *Genome Integr.* **3**, 9 (2012).
11. Davis, A.J., Chen, D.J. DNA double strand break repair via non-homologous end-joining. *Transl Cancer Res.* **2** (3), 130-143 (2013).
12. Reid, D.A. et al. Organization and dynamics of the nonhomologous end-joining machinery during DNA double-strand break repair. *Proc Natl Acad Sci.* **112** (20), E2575-E2584 (2015).
13. Chen, J.-J., Silver, D., Cantor, S., Livingston, D.M., Scully, R. BRCA1, BRCA2, and Rad51 Operate in a Common DNA Damage Response Pathway. *Cancer Res.* **59** (7 Supplement), 1752s-1756s (1999).
14. D'Andrea, A.D. BRCA1: A Missing Link in the Fanconi Anemia/BRCA Pathway. *Cancer Discov.* **3** (4), 376-378 (2013).
15. Gudmundsdottir, K., Ashworth, A. The roles of BRCA1 and BRCA2 and associated proteins in the maintenance of genomic stability. *Oncogene.* **25** (43), 5864-5874 (2006).
16. Liu, S. et al. Distinct roles for DNA-PK, ATM and ATR in RPA phosphorylation and checkpoint activation in response to replication stress. *Nucleic Acids Res.* **40** (21), 10780-10794 (2012).
17. Wallace, N.A., Khanal, S., Robinson, K.L., Wendel, S.O., Messer, J.J., Galloway, D.A. High Risk Alpha Papillomavirus Oncogenes Impair the Homologous Recombination Pathway. *J Virol.* JVI.01084-17 (2017).
18. Pierce, A.J., Johnson, R.D., Thompson, L.H., Jasin, M. XRCC3 promotes homology-directed repair of DNA damage in mammalian cells. *Genes Dev.* **13** (20), 2633-2638 (1999).
19. Luzhna, L., Kathiria, P., Kovalchuk, O. Micronuclei in genotoxicity assessment: from genetics to epigenetics and beyond. *Front Genet.* **4** (2013).
20. Jasin, M. Homologous repair of DNA damage and tumorigenesis: the BRCA connection. *Oncogene.* **21** (58), 8981-8993 (2002).
21. Wallace, N.A., Robinson, K., Howie, H.L., Galloway, D.A. β-HPV 5 and 8 E6 Disrupt Homology Dependent Double Strand Break Repair by Attenuating BRCA1 and BRCA2 Expression and Foci Formation. *PLOS Pathog.* **11** (3), e1004687 (2015).
22. Wallace, N.A., Robinson, K., Howie, H.L., Galloway, D.A. HPV 5 and 8 E6 Abrogate ATR Activity Resulting in Increased Persistence of UVB Induced DNA Damage. *PLoS Pathog.* **8** (7) (2012).
23. Mah, L.-J., Vasireddy, R.S., Tang, M.M., Georgiadis, G.T., El-Osta, A., Karagiannis, T.C. Quantification of γH2AX Foci in Response to Ionising Radiation. *J Vis Exp.* (38), e1957 (2010).
24. Popp, H.D., Brendel, S., Hofmann, W.-K., Fabarius, A. Immunofluorescence Microscopy of γH2AX and 53BP1 for Analyzing the Formation and Repair of DNA Double-strand Breaks. *J Vis Exp.* (129), e56617 (2017).
25. Burma, S., Chen, B.P., Murphy, M., Kurimasa, A., Chen, D.J. ATM Phosphorylates Histone H2AX in Response to DNA Double-strand Breaks. *J Biol Chem.* **276** (45), 42462-42467 (2001).
26. Britton, S., Coates, J., Jackson, S.P. A new method for high-resolution imaging of Ku foci to decipher mechanisms of DNA double-strand break repair. *J Cell Biol.* **202** (3), 579-595 (2013).
27. Landthaler, M., Shen, B.W., Stoddard, B.L., Shub, D.A. I-BasI and I-HmuI: two phage intron-encoded endonucleases with homologous DNA recognition sequences but distinct DNA specificities. *J Mol Biol.* **358** (4), 1137-1151 (2006).
28. Lackner, D.H. et al. A generic strategy for CRISPR-Cas9-mediated gene tagging. *Nat Commun.* **6**, 10237 (2015).
29. Chan, S.-H., Stoddard, B.L., Xu, S.-Y. Natural and engineered nicking endonucleases--from cleavage mechanism to engineering of strand-specificity. *Nucleic Acids Res.* **39** (1), 1-18 (2011).

Virology 548 (2020) 174–181

Contents lists available at ScienceDirect

Virology

journal homepage: www.elsevier.com/locate/virology

DNA repair gene expression is increased in HPV positive head and neck squamous cell carcinomas

Andrew J. Holcomb[a], Laura Brown[b], Ossama Tawfik[b], Rashna Madan[b], Yelizaveta Shnayder[a], Sufi Mary Thomas[a], Nicholas A. Wallace[c,*]

[a] The University of Kansas Medical Center, Department of Otolaryngology, Head and Neck Surgery, 3901 Rainbow Boulevard, Kansas City, KS, 66160, USA
[b] The University of Kansas Medical Center, Department of Pathology and Lab Medicine, 3901 Rainbow Boulevard, Kansas City, KS 66160, USA
[c] Kansas State University, Department of Biology, 116 Ackert Hall, Manhattan, KS, 66506, USA

A B S T R A C T

The incidence of head and neck squamous cell carcinomas (HNSCCs) is rising in developed countries. This is driven by an increase in HNSCCs caused by high-risk human papillomavirus (HPV) infections or HPV + HNSCCs. Compared to HNSCCs not caused by HPV (HPV– HNSCCs), HPV + HNSCCs are more responsive to therapy and associated with better oncologic outcomes. As a result, the HPV status of an HNSCC is an important determinant in medical management. One method to determine the HPV status of an HNSCC is increased expression of p16 caused by the HPV E7 oncogene. We identified novel expression changes in HPV + HNSCCs. A comparison of gene expression among HPV+ and HPV- HNSCCs in The Cancer Genome Atlas demonstrated increased DNA repair gene expression in HPV + HNSCCs. Further, DNA repair gene expression correlated with HNSCC survival. Immunohistochemical analysis of a novel HNSCC microarray confirmed that DNA repair protein abundance is elevated in HPV + HNSCCs.

1. Introduction

Human papillomaviruses (HPVs) are a family of over 200 different viruses that are grouped into five genera (alpha-, beta-, gamma-, mu-, and nu-papillomaviruses) (Bernard et al., 2010). This large family of viruses causes a wide array of maladies by infecting human mucosal and epithelial tissue (Doorbar et al., 2012). The diseases associated with HPV infections range from relatively benign warts to deadly carcinomas (Doorbar et al., 2015). Oncogenicity has been most clearly demonstrated for a subset of the alpha-papillomavirus genus, termed high-risk alpha-papillomaviruses. For simplicity, we refer to high-risk alpha-papillomaviruses as HPVs in this report. HPVs cause nearly all cervical cancers through the expression of two viral oncogenes (HPV E6 and E7) that disrupt tumor suppressor pathways (Bosch et al., 2002). HPV E6 promotes p53 degradation and activates telomerase, while HPV E7 destabilizes Rb (Boyer et al., 1996, p. 53; Dyson et al., 1989; Huibregtse et al., 1991; Münger et al., 1989a, 1989b, p. 6). Both HPV E6 and E7 also manipulate the host DNA repair responses such that viral replication is promoted at the expense of host genome fidelity (Anacker et al., 2016, 2014; Chappell et al., 2015; Gillespie et al., 2012; Hong and Laimins, 2013; Mehta and Laimins, 2018; Wallace, 2020; Wallace and Galloway, 2014).

In addition to their role in cervical cancers, HPVs cause a growing subset of head and neck squamous cell carcinomas (HNSCCs) (Kobayashi et al., 2018). These HPV positive HNSCCs (HPV + HNSCCs) are an increasing proportion of malignancies in developed countries (Chaturvedi and Zumsteg, 2018; Marur et al., 2010). This increase is occurring as efforts to combat the abuse of tobacco and alcohol have decreased the number of HNSCCs that are not related to HPV infections (HPV– HNSCCs). There are notable differences in HPV+ and HPV- HNSCCs. Clinically, HPV + HNSCCs are typically less aggressive and more responsive to care (Ang et al., 2010; Ang and Sturgis, 2012). At the molecular level, HPV- HNSCC tend to have p53 mutations, while HPV + HNSCCs more often have wild type p53 and notably higher p16 abundance (Blons and Laurent-Puig, 2003; Maruyama et al., 2014; Westra et al., 2008).

We hypothesize that HPV oncogenes cause other gene expression differences in HNSCCs. To test this hypothesis and identify host gene changes associated with HPV, we used a combination of computational and standard pathology analyses. This mixed-method approach identified increased expression of DNA repair genes in HPV + HNSCCs compared to HPV- HNSCCs. More specifically, this examination of a publicly available dataset from The Cancer Genome Atlas (TCGA) shows genes from two repair pathways (homologous recombination (HR) and translesion synthesis (TLS)) are more robustly expressed in HPV + HNSCCs (Cancer Genome Atlas Network, 2015). Differential expression of three of these genes were associated with changes in HNSCC survival. We generated a novel tissue microarray (TMA) of HPV

* Corresponding author.
E-mail address: nwallac@ksu.edu (N.A. Wallace).

https://doi.org/10.1016/j.virol.2020.07.004
Received 24 April 2020; Received in revised form 1 July 2020; Accepted 3 July 2020
Available online 22 July 2020
0042-6822/

+ and HPV- HNSCCs to further probe this relationship. TMA immunohistochemical staining confirmed our *in silico* data, showing increased DNA repair protein abundance in HPV + HNSCCs. The most specific increase was seen for the homologous recombination protein, RAD51.

2. Results

2.1. DNA repair gene expression was increased in HPV positive HNSCCs compared to HPV negative HNSCCs

To understand how gene expression differed between HPV+ and HPV- HNSCCs, we segregated the TCGA dataset on HNSCCs by the clinical designation of HPV status as originally reported (Cancer Genome Atlas Network, 2015). There were data from 21 HPV + HNSCCs and 65 HPV- HNSCCs. We ranked genes that were differentially expressed in HPV + versus HPV- HNSCCs based on the statistical significance of the differences. We then used the Gene Ontology enRIchment anaLysis and visuaLizAtion tool (GOrilla) to determine if these differentially expressed genes were involved in any shared cellular processes (Eden et al., 2009) GOrilla analysis demonstrated that the genes that were differentially expressed in HPV + versus HPV- HNSCCs were frequently involved in the cellular stress response (Fig. 1 and Supplemental Data 1). More specifically, there was a striking enrichment for changes in DNA damage repair (DDR) gene expression ($p < 10^{-7}$).

These data demonstrate clear differences in DDR gene expression in HNSCCs based on HPV status, but they do not indicate whether repair gene expression is more often higher or lower in HPV + HNSCCs compared to HPV- HNSCCs. Therefore, we quantified the expression of 137 DDR genes in HPV+ and HPV- HNSCCs. DNA repair genes were chosen using unbiased definitions of six established repair pathways (nucleotide excision repair (NER), Fanconi Anemia repair (FA), base excision repair (BER), TLS, HR and non-homologous end joining (NHEJ)) (Alan and D'Andrea, 2010; Bult et al., 2019; Cooper, 2000; Davis and Chen, 2013; Kanehisa and Goto, 2000; Laat and Hoeijmakers, 1999; Prakash et al., 2005; Whitaker et al., 2017). The ratio of the expression difference and the significance of these changes was determined for each gene (Fig. 2A). This analysis demonstrated that DDR gene expression was commonly increased in HPV + HNSCCs relative to HPV- HNSCCs. We dissected this data further by defining the frequency of increased gene expression among the DDR pathways. Increased DDR gene expression in HPV + HNSCCs was evident across all DDR pathways, ranging from 81.8% of NER genes to 100% of the significant changes in TLS and FA genes (Fig. 2B).

Based on these findings and our laboratory's *in* vitro studies demonstrating HPV oncogenes manipulation of HR and TLS, we focused our analysis on genes from these two pathways [Wendel et al. submitted, 40]. Specifically, we chose four representative TLS genes (PCNA, RAD18, UBE2A and UBE2B) and four representative HR genes (BRCA1, BRCA2, RPA1, RAD51). These analyses included few genes and thus were more amenable to manipulation, so we moved from the clinical definition of HPV status to one defined by molecular signatures and also used in the original report from TCGA (Cancer Genome Atlas Network, 2015). When comparing the expression of these genes, all eight had increased expression in HPV + HNSCCs (Fig. 3A–H). Because the prognosis for HPV + HNSCCs is significantly better than HPV- HNSCCs, we evaluated whether expression of these eight genes was associated with differences in median survival. For this analysis, we included the complete TCGA dataset (Fig. 4). When analyzed together, increased expression of the eight representative TLS and HR genes was not associated with a significant difference in survival (Data Not Shown). However, when analyzed individually, the expression of three of these eight genes was associated changes in survival. Increased expression of two HR genes (BRCA1 and RPA1) was associated with increased HNSCC survival, while increased UBE2A expression correlated with decreased survival (Fig. 4).

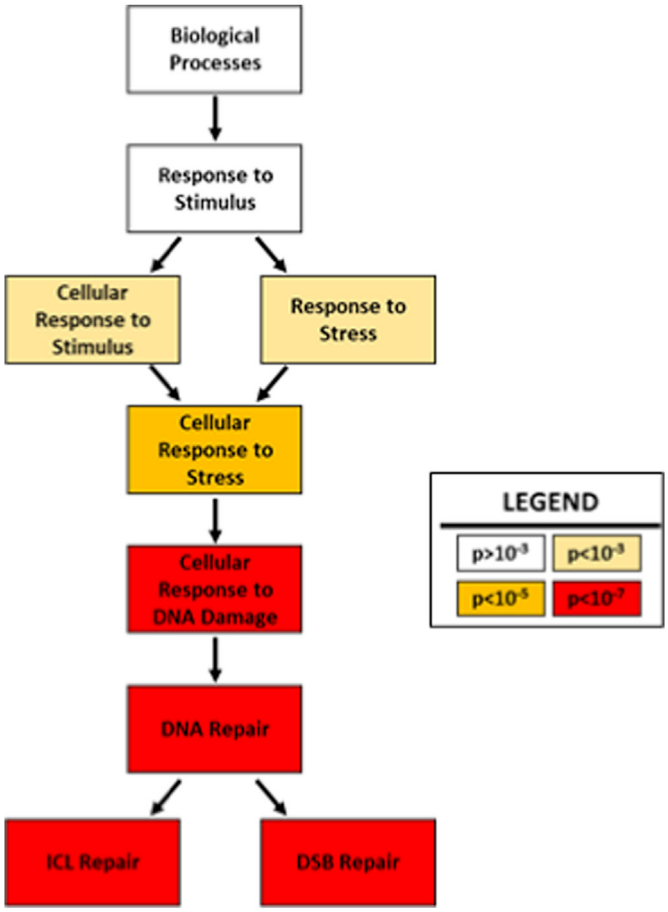

Fig. 1. Gene Ontology Analysis of Differential Gene Expression in HPV + versus HPV- HNSCCs. Results for gene ontology (GO) analysis of gene expression differences in HPV + compared to HPV- HNSCCs. Boxes show cellular functions in hierarchical order, descending from general to specific functions. Darker colors indicate greater statistical significance of enrichment.

2.2. Differences in homologous recombination and translesion synthesis protein abundance were detected in HNSCCs

Our data suggested that increased HR and TLS gene expression has the potential to serve as a biomarker for HPV status in HNSCCs. Unfortunately, detecting differences in gene transcripts is not practical clinically. However, immunohistochemical staining (IHC) is frequently used to distinguish tumors from margins and among different types of tumors. This includes the detections of increased p16 levels as a marker of HPV status in HNSCCs. An obvious and preliminary step in developing biomarkers for detection by IHC is confirming that there are detectable differences from control tissue. Based on our computational data, we hypothesized that elevated HR and TLS protein abundance would be detectable by IHC in a subset of HNSCCs. Specifically, we hypothesized that these increases would be seen more often in HPV + HNSCC. We began testing the first part of our hypothesis by comparing TLS and HR protein abundance in HNSCC and untransformed oral mucosa using the Human Protein Atlas (HPA) (Uhlén et al., 2015, 2005). This resource provided histology data for these tissue that had been scored by independent pathologists. As a positive control, we observed p16 staining (Fig. 5). There were detectable differences in p16 between control and transformed oral epithelial cells. P16 abundance was at times higher in HNSCCs than control tissue. However, to our surprise, p16 levels were most often reduced compared to control tissue. Because the HPV status of these samples was

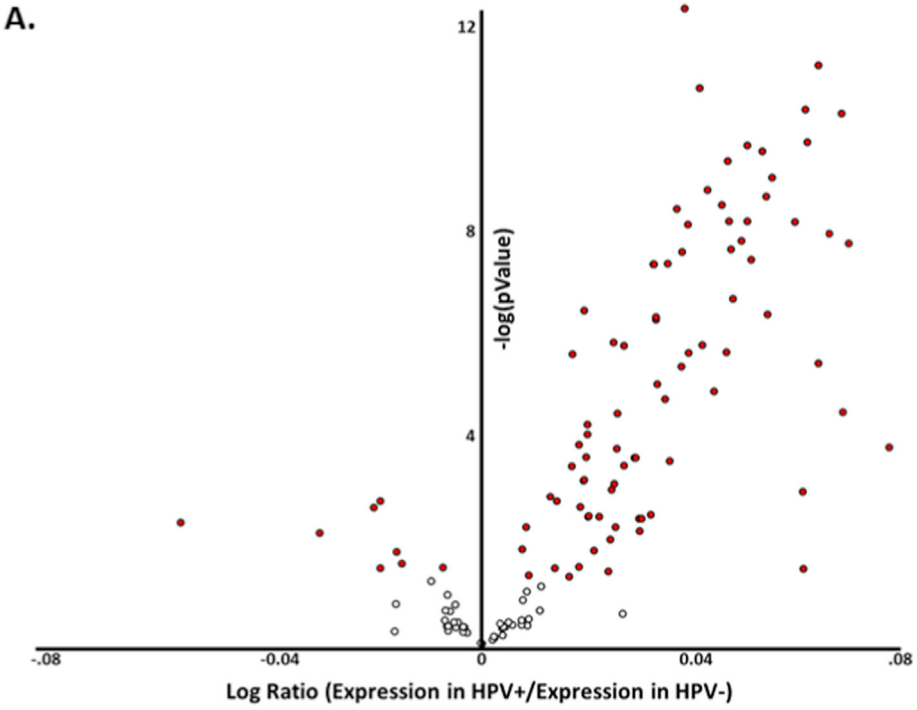

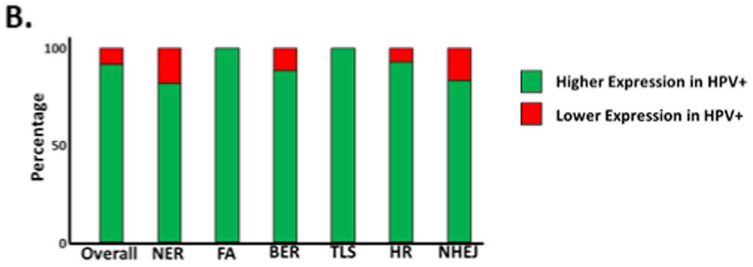

Fig. 2. Differences in DNA Repair Gene Expression Between HPV- and HPV + HNSCCs. A. Volcano plot of DNA repair gene expression compared between HPV+ and HPV- HNSCCs. Statistical significance is shown on the Y-axis, plotted as the negative log of the p-value. The log ratio of gene expression in HPV + HNSCCs compared to HPV- HNSCCs are shown on the X-axis. Red circles denote significant changes in expression ($p < 0.05$), while clear dots indicate points below this statistical cutoff. Data points to the left of the Y-axis have decreased expression in HPV + HNSCCs. Data points to the right of the Y-axis have increased expression in HPV + HNSCCs. B. Bar graph showing the ratio of differnces in DNA repair gene expression in HNSCCs based on HPV status. Red indicates the percentage of genes with lower expression in HPV + HNSCCs. Green indicates the percentage of genes with higher expression in HPV + HNSCCs. Data is shown for genes "overall" and grouped into six pathways (NER = nucleotide excision repair, FA = Fanconi anemia repair, BER = base excision repair, TLS = translesion synthesis, HR = homologous recombination, NHEJ = non-homologous end joining).

undetermined, this could indicate that most HNSCCs in the HPA are HPV negative. We used a housekeeping gene (nucleolin) as a negative control. There was no differential nucleolin staining between transformed or control tissue.

Having confirmed the utility of this resource, our next step was to use data contained in the HPA to conduct a preliminary analysis of TLS and HR proteins as biomarkers for HPV status in HNSCCs. Specifically, our goal was to determine if any of the gene products of BRCA1, RAD18, PCNA, UBE2A/B (RAD6), RAD51 and RPA1 (RPA70) could be detected at higher levels in HNSCCs compared to normal oral mucosa. These data were promising as a proportion of HNSCCs had BRCA1, RAD51, RAD18, and PCNA levels higher than control tissue. Notably, the frequency of their increase was at least as high as the frequency of increased p16 (Fig. 5).

While these data were encouraging, the inability to compare repair protein staining levels among HPV+ and HPV- HNSCC represented a significant shortcoming. To address this gap in our analysis, we generated a novel tissue microarray (TMA) to determine if the abundance of these seven representative DDR proteins differed between HPV+ and HPV- HNSCCs. The TMA consisted of 27 HPV+ and 9 HPV- HNSCCs. Patient demographic and tumor variables were compared between HPV positive and negative groups (Table 1). Significant differences in mean age existed between groups (58.7 in HPV+, 69.7 in HPV-, $p < 0.01$), consistent with the younger demographic of people with HPV + HNSCCs (Chaturvedi and Zumsteg, 2018). In addition, HPV + tumors were more likely to be poorly differentiated, though not statistically significant ($p = 0.11$). This reflects an established tendency for HPV + tumors to present with de-differentiated histopathology (Dahlstrom et al., 2003). Individuals with HPV- tumors were more likely to be recurrent or previously treated, though again not statistically significant ($p = 0.06$). This was consistent with the recognized tendency for HPV- HNSCCs to recur more frequently (Faraji et al., 2017). No other clinical or tumor characteristics were notably different between groups, including gender, tumor stage, perineural invasion and lymphovascular invasion status.

We used a composite scoring approach for the analysis of the TMA. This took into account percentage of the tumor stained and the intensity of the staining. Inter-rater reliability between pathologists was excellent with an intra-class correlation coefficient of 0.90. Computer assisted analysis was compared to pathologist analysis and demonstrated similar results (Pearson correlation coefficient = 0.68). While no differences were seen in four of queried proteins (RPA70, BRCA2, PCNA and RAD18), there was greater IHC staining for two HR proteins, RAD51 and BRCA1 (Fig. 6 and Supplemental Fig. 1). Mean composite scores in BRCA1 analysis for HPV+ and HPV- HNSCCs were 1.04 and 0.63 respectively, which approached significance ($p = 0.07$). Mean composite scores for RAD51 significantly differed between HPV+ and HPV- HNSCCs (2.06 and 0.76, respectively, $p < 0.01$, Fig. 6).

3. Conclusions

The incidence of HPV + HNSCC is rising rapidly (Chaturvedi and Zumsteg, 2018; Marur et al., 2010). Given the known differences between HPV+ and HPV- HNSCCs with respect to their epidemiology, clinical behavior, response to treatment, and prognosis, biomarkers capable of distinguishing between the two types of HNSCCs are useful

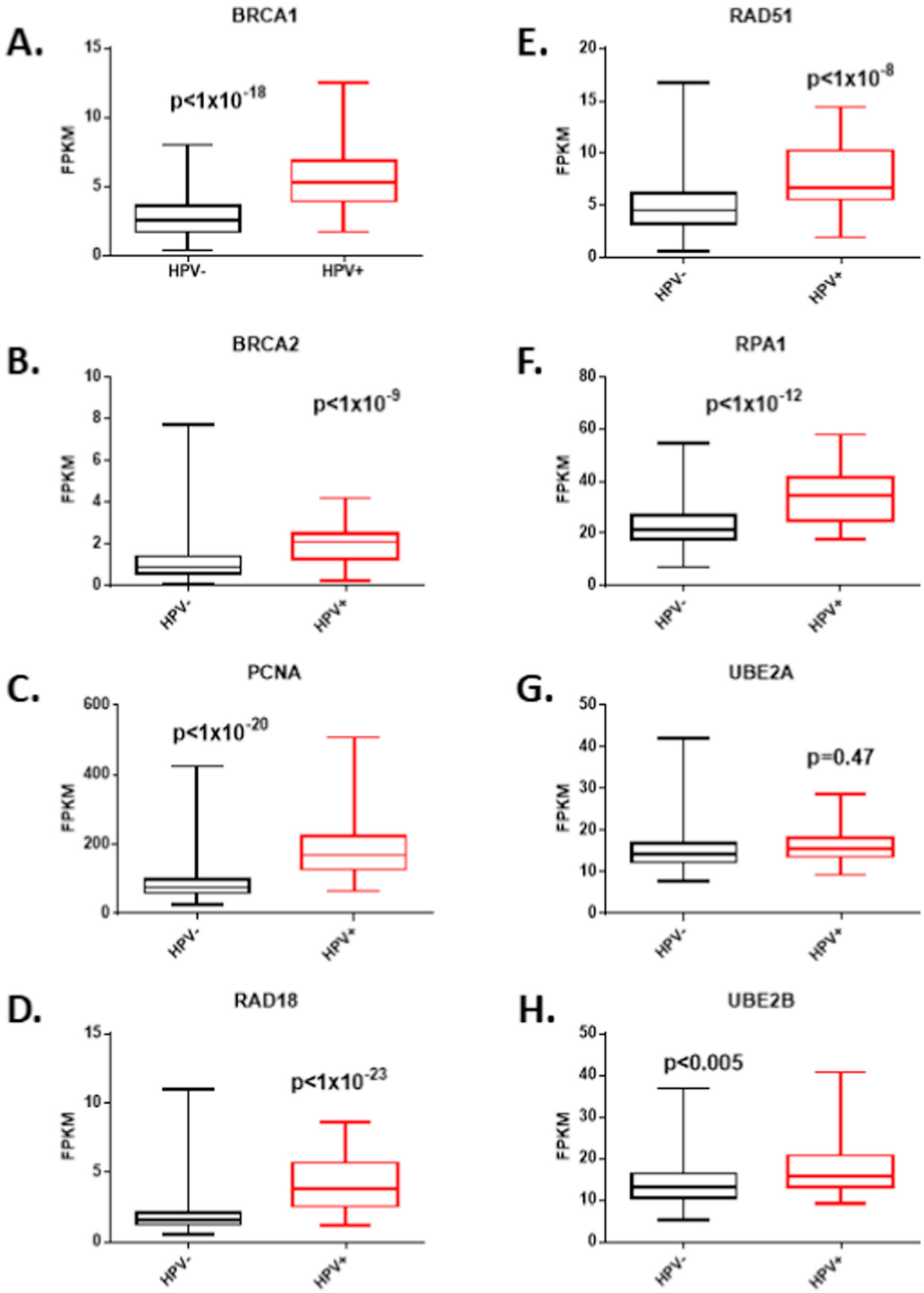

Fig. 3. Expression of Representative Translesion Synthesis and Homologous Recombination Genes is Higher in HPV + HNSCCs. Box plots depict the expression of A. BRCA1, B. BRCA2, C. PCNA, D. RAD18, E. RAD51, F. RPA1, G. UBE2A, and H. UBE2B gene expression in HPV + (red) and HPV- (black) HNSCCs. Expression is plotted as FPKM (fragments per kilobase of exon model per million reads mapped), a standard normalization of gene expression based on RNA-seq data found in the TCGA database.

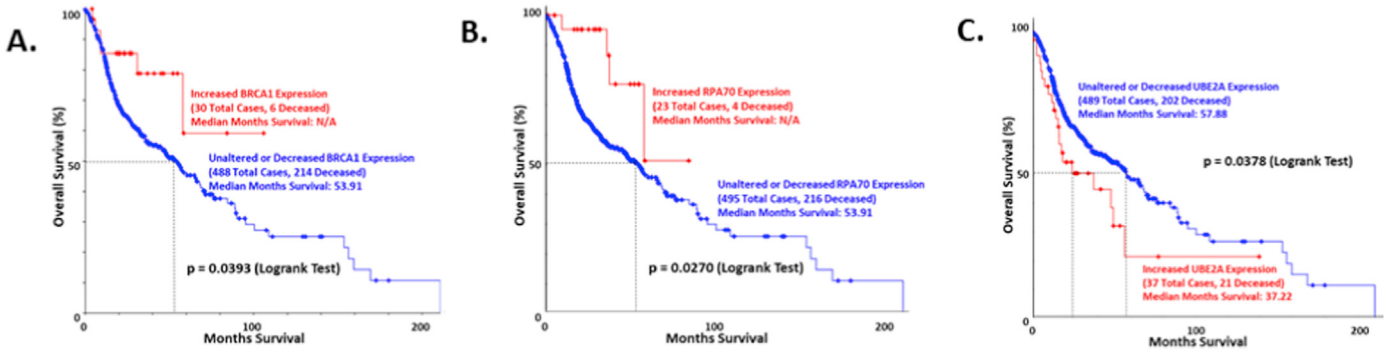

Fig. 4. Prognostic Value of DNA Repair Gene Expression in HNSCCs. Kaplan Meier curves for HNSCCs differentiated by expression of A. BRCA1, B. RPA70, and C. UBE2A. These plots were generated using data from the Cancer Genome Atlas. Patients who had cancers with significantly high expression (z score ≥ 2) are shown in red. All other patients are shown in blue. The dotted black line provides visualization of the median survival calculation. P-values denoting significant difference (log-rank test) in the two populations are indicated along with the population sizes.

(Ang et al., 2010; Ang and Sturgis, 2012; Gillison et al., 2008). While direct detection of HPV is an attractive option, it is more expensive than tradition pathologic approaches. This gap in clinical diagnostic tests merits new investigations of expression changes associated with HPV + HNSCCs. We took a multipronged approach to objectively identify genes that were differentially expressed in HPV + compared to HPV- HNSCCS. Our computational analysis of the TCGA database demonstrated that the expression of genes involved in DNA repair was higher in HPV + HNSCCs (Figs. 1–3). We also found that expression of three of these genes (UBE2A, BRCA1, and RPA1) significantly correlated with survival (Fig. 4). Importantly, increased UBE2A expression was a negative prognostic factor. This indicates that the relationship between DDR gene expression is nuanced and that all repair genes cannot be treated as indirect indicators of HPV status. Our transcriptomic analysis support this assertion as we found UBE2A expression did not significantly differ between HPV+ and HPV- HNSCCs. Our analysis of HNSCC tissues from the HPA demonstrated that it was possible to detect differences in DDR protein abundance in HNSCCs compared to control tissue. Moreover, these differences were similar to the differences detected when the same comparison was made using an established biomarker of HPV status, p16 (Fig. 5). Generating a TMA with HPV+ and HPV- HNSCCs allowed us to show that increased repair gene transcripts translated to increased protein that was detectable by IHC (Fig. 6). In summary, we found that DDR gene expression in HPV + HNSCC was similar to the alterations observed with tissue culture systems (Wallace, 2020; Wallace and Galloway, 2014). Further, these results are similar with another recent effort to understand if DNA repair protein abundance mirrored HPV status in HNSCCs (Kono et al., 2020). This supports the value and validity of *in vitro* characterization of HPV oncogene biology.

Currently, p16 is used as a surrogate marker of HPV in HNSCCs (Liang et al., 2012). p16 levels are higher in HPV + HNSCCs and much of the biology driving this change is understood. HPV E7 deregulates the cell cycle by disrupting Rb-E2F complexes (Dyson et al., 1989, p. 7).

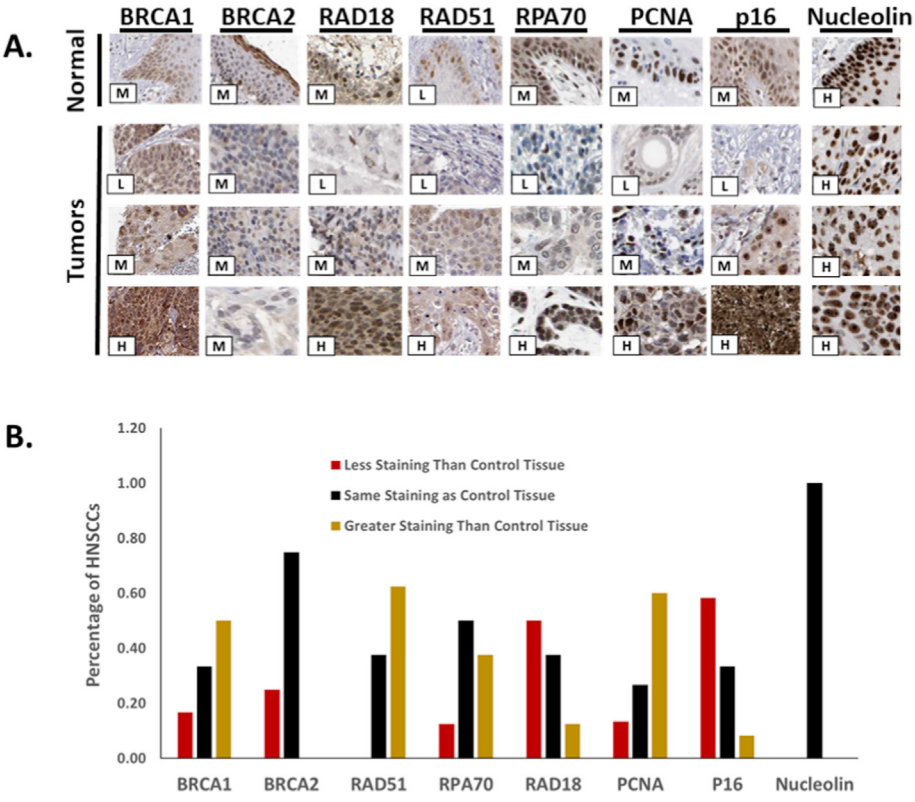

Fig. 5. DNA Repair Protein Abundance Varies Among HNSCCs and Compared to Normal Oral Epithelia. A. Representative IHC staining of DNA repair proteins in untransformed oral epithelia (normal) and HNSCCs (tumors) from the Human Protein Atlas (top). Letters in the lower left of each image indicate the composite score of the tissue shown. (H = High, M = Medium, L = Low) For normal tissue, the representative image corresponds to the knowledge-based annotation provided by Human Protein Atlas. B. The distribution of composite scores compared to control tissue. Red bars denote the percentage of tumors with a composite score lower than control tissue. Black bars denote the percentage of tumors with the same composite score as control tissue. Brown bars denote the percentage of tumors with a composite score higher than control tissue. P16 is included as an established biomarker of HPV status with more than half of its composite scores higher or lower than control tissue. Nucleolin is included as a negative control with composite scores that match control tissue.

Table 1
Tumor Microarray Demographic Data. Patient and tumor characteristics are compared between HPV+ and HPV- HNSCC groups.

		HPV Positive n = 26	HPV Negative n = 9	p =
Age (mean (SD))		58.7 (10.1)	69.7 (9.4)	0.0069
Sex (n (%))	Male	19 (73.1)	6 (66.7)	0.6936
	Female	7 (26.9)	3 (33.3)	
Tumor Site (n (%))	Tonsil	17 (65.4)	3 (33.3)	0.3241
	Base of tongue	9 (34.6)	5 (55.6)	
	Soft palate	0 (0)	1 (11.1)	
Perineural Invasion (n (%))		5 (19.2)	1 (11.1)	1
Lymphovascular Invasion (n (%))		4 (15.4)	2 (22.2)	0.6353
Recurrence/Prior Treatment (n (%))		0 (0)	2 (22.2)	0.0605
Histologic Grade (n (%))	1–2	12 (46.2)	1 (11.1)	0.1094
	3–4	14 (53.8)	8 (88.9%)	
T Stage (n (%))	1–2	22 (84.6)	7 (77.8)	0.6353
	3–4	4 (15.4)	2 (22.2)	

This causes replication stress and increased p16 expression. As a surrogate marker of HPV, p16 is notably sensitive. However, p16 is also influenced by stimuli other than HPV E7 (e.g., B-RAF activation) (Mackiewicz-Wysocka et al., 2017). Because differences in RAD51 abundance between HPV+ and HPV- are detectable by IHC, changes in RAD51 (and potentially other DDR protein levels) may be able to complement existing biomarkers. For instance, combining p16 with RAD51 could decrease the risk of false positives and more accurately triage HNSCCs by HPV status.

Expression of UBE2A, BRCA1 and RPA1 each significantly correlated with HNSCC survival. HPV oncogenes cause increased expression of both BRCA1 and RPA1 in cell culture systems (Wallace et al., 2017). This observation combined with the positive prognostic value of their expression suggests that they may also be acting as surrogate markers of HPV status. Our TMA data support this position. It is more difficult to explain the correlation of increased UBE2A expression with decreased survival. UBE2A expression did not significantly vary between HPV- and HPV + HNSCCs. An attractive explanation is that high UBE2A expression promotes Cisplatin resistance. Both HPV+ and HPV- HNSCCs are frequently treated with the drug and UBE2A is an essential component of TLS, a pathway that promotes Cisplatin resistance when over-activated (Albertella et al., 2005; Srivastava et al., 2015).

In summary, our data support the development of TLS and HR proteins as biomarkers of HPV status in HNSCCs. However, they also require further investigation and substantiation. Our future studies will focus on the expansion of our TMA. While the data presented here is interesting, expanding our TMA to include additional HPV+ and HPV- HNSCC samples as well as non-tumor control tissues would be an improvement. Further, determining HPV status by more definitive methods than p16 would also improve our analysis.

4. Materials and methods

Human Protein Atlas: Representative IHC and staining information was obtained from the HPA (Uhlén et al., 2005). Composite gene marker IHC scores were determined by evaluating staining intensity and frequency. These were then converted to categories corresponding to the knowledge-based annotation used by the HPA for control tissue.

The Cancer Genome Atlas (TCGA) Analysis: HNSCC TCGA data were analyzed to define mRNA expression (Uhlén et al., 2015, 2005). Expression levels were normalized to control tissues. For the analysis found in Figs. 1 and 2, HPV status was based on clinical criteria as reported to TCGA. To be considered "clinically positive" for HPV, the tumor had to be located in an oropharyngeal subsite and be accompanied by a positive assay for HPV that was reported in the electronic case report. Tumors where HPV status were not determined excluded from this analysis.

For the analysis of gene expression found in Fig. 3, the HPV status was based on molecular signatures that include microRNA, DNA methylation, gene expression (cellular and viral) as reported in TCGA manuscript (Cancer Genome Atlas Network, 2015). These approaches are similar, but identical to more recent efforts to analyze HPV status in HNSCCs (Johnson et al., 2018; Pérez Sayáns et al., 2019)

The web-based analysis tools at www.cbioportal.com were used to examine RNAseq data from these tumors (Cerami et al., 2012; Gao et al., 2013).

Protein and Gene Designations: When the gene and protein names differ, we show both in this format: GENE (PROTEIN).

Tissue Microarray Creation: De-identified archival formalin fixed, paraffin embedded patient tissue was obtained from the University of Kansas Medical Center, Biospecimen Repository Core Facility using an Institutional Review Board approved protocol. p16 IHC served as a marker of HPV positive samples. Tumors were considered p16 positive when there was strong and diffuse staining in at least 75% of tumor cells. Surgical specimens from HPV+ and HPV- HNSCCs were selected. Thirty-six total specimens were included in the TMA (27 HPV+ and nine HPV- specimens). Representative areas were marked on hematoxylin and eosin stained slides by a board certified pathologist for use. Using the marked slide as a map, 2-mm thick core punches were taken from the corresponding donor paraffin block and transferred to a recipient paraffin block using the TMArrayer instrument (Pathology Devices). The block containing unique donor cores were sectioned at 4um, mounted on adhesive slides, and dried prior to staining procedures.

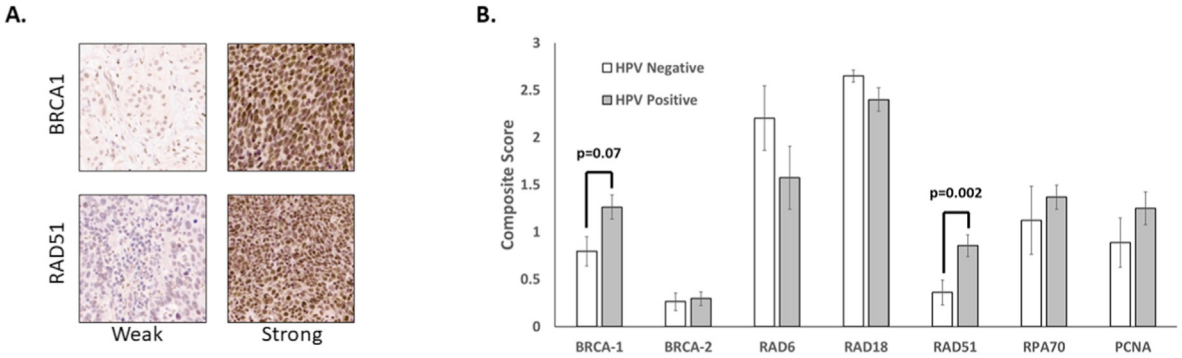

Fig. 6. Immunohistochemical analysis of DNA repair proteins in HPV positive and negative HNSCC. A. Representative images of tumor sections considered to have weak or strong staining for RAD51 or BRCA1 as indicated. B. Immunohistochemical analysis was performed for seven DNA repair proteins using a tissue microarray derived from 27 HPV positive and nine HPV negative HNSCC specimens. Staining intensity and percentage of nuclear staining were measured to derive composite scores that were compared between groups using Mann-Whitney U-test. P values are indicated for comparisons that approached or exceeded cutoffs for statistically significance. All other comparisons did not approach significance.

Immunohistochemistry: Slides were baked at 60 °C for 1 h. After deparaffinization and rehydration, tissue sections were treated with either citrate buffer or Borg Decloaker for 5 min in a pressure cooker for antigen retrieval. Hydrogen peroxide (3%) was applied to the sections for 10 min. Sections were incubated with primary antibodies against BRCA1 (Biocare Medical), BRCA2 (Proteintech), PCNA, RAD51 (Abcam), RAD6, RAD18 or RPA1/RPA70 (Abcam) for 30 min. After buffer rinsing, sections were incubated with anti-mouse HRP-labeled polymer (EnVision) or anti-HRP-labeled polymer (Mach2) for 30 min and buffer rinsed twice. Finally, the staining was visualized by DAB+ (Dako). IHC staining was performed using the IntelliPATH FLX Automated Stainer at room temperature. A light hematoxylin counterstain was performed, then slides were dehydrated, cleared, and mounted using permanent mounting media.

Immunohistochemical Analysis: TMA slides were analyzed independently by two board-certified pathologists who were blinded to the sample's HPV status. Tumors were scored for intensity of staining on a scale of zero to four and on the percentage of tumor cells that were positive. A composite score between zero and four was derived by multiplying the intensity by percent staining. Aperio ImageScope (Version 12.3.0) was used for a secondary computer-based analysis to validate pathologist's assessments. An algorithm was created within the program to capture staining intensity and percentage. This was optimized for accuracy on a series of sample slides.

Clinical Data Analysis: De-identified clinical data were received from the University of Kansas Medical Center's Biospecimen Repository Core Facility. Age was provided in five-year ranges and the median range was used for data analysis.

Statistical Analysis: SPSS software was used for statistical analyses of the TMA (version 22; IBM Corp). Fishers Exact and Analysis of Variance tests were applied to categorical variables and Mann-Whitney U tests were applied to continuous variables. Significance was only reported for p-values < 0.05. Kaplan-Meier curves display survival data, and the logrank test assessed survival differences. TCGA data were analyzed using the analysis tools at www.cbioportal.org (Cerami et al., 2012; Gao et al., 2013).

Pathway and Gene Ontology Analysis: The Kyoto Encyclopedia of Genes and Genomes and The Mouse Genome Informatics (MGI) were used to identify gene subsets specific to the following pathways: TLS, HR, NER, FA, BER, NHEJ (Bult et al., 2019; Kanehisa and Goto, 2000). MGI was used to define genes in the translesion synthesis pathway because this pathway was not included in the Kyoto Encyclopedia of Genes and Genomes. We compared differences in gene expression between HPV+ and HPV- HNSCC tumors and used p-value data to rank genes. Gene ontology analysis of this ranked list was conducted using the Gene Ontology enrichment anaLysisand visualizAtion (GOrilla) online tool. A threshold of $p < 10^{-5}$ was chosen.

CRediT authorship contribution statement

Andrew J. Holcomb: Conceptualization, Methodology, Validation, Writing - original draft, Writing - review & editing, Investigation. **Laura Brown:** Conceptualization, Methodology, Validation, Writing - original draft, Writing - review & editing, Investigation. **Ossama Tawfik:** Conceptualization, Methodology, Validation, Writing - original draft, Writing - review & editing, Investigation, Supervision, Funding acquisition. **Rashna Madan:** Conceptualization, Methodology, Validation, Writing - original draft, Writing - review & editing, Investigation, Supervision. **Yelizaveta Shnayder:** Conceptualization, Writing - original draft, Writing - review & editing, Resources, Supervision, Funding acquisition. **Sufi Mary Thomas:** Conceptualization, Writing - original draft, Writing - review & editing, Supervision, Funding acquisition. **Nicholas A. Wallace:** Conceptualization, Software, Methodology, Validation, Writing - original draft, Writing - review & editing, Investigation, Supervision, Funding acquisition.

Declaration of competing interest

The authors declare that they have no conflicts of interests related to the work described in our manuscript.

Acknowledgements

We acknowledge the University of Kansas Cancer Center's Biospecimen Repository Core Facility for helping obtain human specimens. This work was supported by the National Institutes of Health (P20-GM103418; YS and NAW and R01 CA227838; SMT), and the University of Kansas Cancer Center (CCSG P30CA168524; SMT).

Appendix A. Supplementary data

Supplementary data to this article can be found online at https://doi.org/10.1016/j.virol.2020.07.004.

References

Alan, D., D'Andrea, M.D., 2010. The Fanconi anemia and breast cancer susceptibility pathways. N. Engl. J. Med. 362, 1909–1919. https://doi.org/10.1056/NEJMra0809889.

Albertella, M.R., Green, C.M., Lehmann, A.R., O'Connor, M.J., 2005. A role for polymerase η in the cellular tolerance to cisplatin-induced damage. Canc. Res. 65, 9799–9806. https://doi.org/10.1158/0008-5472.CAN-05-1095.

Anacker, D.C., Aloor, H.L., Shepard, C.N., Lenzi, G.M., Johnson, B.A., Kim, B., Moody, C.A., 2016. HPV31 utilizes the ATR-chk1 pathway to maintain elevated RRM2 levels and a replication-competent environment in differentiating keratinocytes. Virology 499, 383–396. https://doi.org/10.1016/j.virol.2016.09.028.

Anacker, D.C., Gautam, D., Gillespie, K.A., Chappell, W.H., Moody, C.A., 2014. Productive replication of human papillomavirus 31 requires DNA repair factor Nbs1. J. Virol. 88, 8528–8544. https://doi.org/10.1128/JVI.00517-14.

Ang, K.K., Harris, J., Wheeler, R., Weber, R., Rosenthal, D.I., Nguyen-Tân, P.F., Westra, W.H., Chung, C.H., Jordan, R.C., Lu, C., Kim, H., Axelrod, R., Silverman, C.C., Redmond, K.P., Gillison, M.L., 2010. Human papillomavirus and survival of patients with oropharyngeal cancer. N. Engl. J. Med. 363, 24–35. https://doi.org/10.1056/NEJMoa0912217.

Ang, K.K., Sturgis, E.M., 2012. Human papillomavirus as a marker of the natural history and response to therapy of head and neck squamous cell carcinoma. Semin. Radiat. Oncol. 22, 128–142. https://doi.org/10.1016/j.semradonc.2011.12.004.

Bernard, H.-U., Burk, R.D., Chen, Z., van Doorslaer, K., Hausen, H. zur, de Villiers, E.-M., 2010. Classification of papillomaviruses (PVs) based on 189 PV types and proposal of taxonomic amendments. Virology 401, 70–79. https://doi.org/10.1016/j.virol.2010.02.002.

Blons, H., Laurent-Puig, P., 2003. TP53 and head and neck neoplasms. Hum. Mutat. 21, 252–257. https://doi.org/10.1002/humu.10171.

Bosch, F.X., Lorincz, A., Muñoz, N., Meijer, C.J.L.M., Shah, K.V., 2002. The causal relation between human papillomavirus and cervical cancer. J. Clin. Pathol. 55, 244–265.

Boyer, S.N., Wazer, D.E., Band, V., 1996. E7 protein of human papilloma virus-16 induces degradation of retinoblastoma protein through the ubiquitin-proteasome pathway. Canc. Res. 56, 4620–4624.

Bult, C.J., Blake, J.A., Smith, C.L., Kadin, J.A., Richardson, J.E., Mouse Genome Database Group, 2019. Mouse genome database (MGD) 2019. Nucleic Acids Res. 47, D801–D806. https://doi.org/10.1093/nar/gky1056.

Cancer Genome Atlas Network, 2015. Comprehensive genomic characterization of head and neck squamous cell carcinomas. Nature 517, 576–582. https://doi.org/10.1038/nature14129.

Cerami, E., Gao, J., Dogrusoz, U., Gross, B.E., Sumer, S.O., Aksoy, B.A., Jacobsen, A., Byrne, C.J., Heuer, M.L., Larsson, E., Antipin, Y., Reva, B., Goldberg, A.P., Sander, C., Schultz, N., 2012. The cBio cancer genomics portal: an open platform for exploring multidimensional cancer genomics data. Canc. Discov. 2, 401–404. https://doi.org/10.1158/2159-8290.CD-12-0095.

Chappell, W.H., Gautam, D., Ok, S.T., Johnson, B.A., Anacker, D.C., Moody, C.A., 2015. Homologous recombination repair factors Rad51 and BRCA1 are necessary for productive replication of human papillomavirus 31. J. Virol. 90, 2639–2652. https://doi.org/10.1128/JVI.02495-15.

Chaturvedi, A.K., Zumsteg, Z.S., 2018. A snapshot of the evolving epidemiology of oropharynx cancers. Cancer 124, 2893–2896. https://doi.org/10.1002/cncr.31383.

Cooper, G.M., 2000. Recombination between Homologous DNA Sequences.

Dahlstrom, K.R., Adler-Storthz, K., Etzel, C.J., Liu, Z., Dillon, L., El-Naggar, A.K., Spitz, M.R., Schiller, J.T., Wei, Q., Sturgis, E.M., 2003. Human papillomavirus type 16 infection and squamous cell carcinoma of the head and neck in never-smokers: a matched pair analysis. Clin. Canc. Res. 9, 2620–2626.

Davis, A.J., Chen, D.J., 2013. DNA double strand break repair via non-homologous end-joining. Transl. Cancer Res. 2, 130–143. https://doi.org/10.3978/j.issn.2218-676X.2013.04.02.

Doorbar, J., Egawa, N., Griffin, H., Kranjec, C., Murakami, I., 2015. Human papillomavirus molecular biology and disease association. Rev. Med. Virol. 25, 2–23. https://

doi.org/10.1002/rmv.1822.
Doorbar, J., Quint, W., Banks, L., Bravo, I.G., Stoler, M., Broker, T.R., Stanley, M.A., 2012. The biology and life-cycle of human papillomaviruses. Vaccine 30 (5), F55–F70. https://doi.org/10.1016/j.vaccine.2012.06.083.
Dyson, N., Howley, P.M., Münger, K., Harlow, E., 1989. The human papilloma virus-16 E7 oncoprotein is able to bind to the retinoblastoma gene product. Science 243, 934–937.
Eden, E., Navon, R., Steinfeld, I., Lipson, D., Yakhini, Z., 2009. GOrilla: a tool for discovery and visualization of enriched GO terms in ranked gene lists. BMC Bioinf. 10, 48. https://doi.org/10.1186/1471-2105-10-48.
Faraji, F., Eisele, D.W., Fakhry, C., 2017. Emerging insights into recurrent and metastatic human papillomavirus-related oropharyngeal squamous cell carcinoma. Laryngoscope Investig. Otolaryngol. 2, 10–18. https://doi.org/10.1002/lio2.37.
Gao, J., Aksoy, B.A., Dogrusoz, U., Dresdner, G., Gross, B., Sumer, S.O., Sun, Y., Jacobsen, A., Sinha, R., Larsson, E., Cerami, E., Sander, C., Schultz, N., 2013. Integrative analysis of complex cancer genomics and clinical profiles using the cBioPortal. Sci. Signal. 6, pl1. https://doi.org/10.1126/scisignal.2004088.
Gillespie, K.A., Mehta, K.P., Laimins, L.A., Moody, C.A., 2012. Human papillomaviruses recruit cellular DNA repair and homologous recombination factors to viral replication centers. J. Virol. 86, 9520–9526. https://doi.org/10.1128/JVI.00247-12.
Gillison, M.L., D'Souza, G., Westra, W., Sugar, E., Xiao, W., Begum, S., Viscidi, R., 2008. Distinct risk factor profiles for human papillomavirus type 16-positive and human papillomavirus type 16-negative head and neck cancers. J. Natl. Cancer Inst. 100, 407–420. https://doi.org/10.1093/jnci/djn025.
Hong, S., Laimins, L.A., 2013. The JAK-STAT transcriptional regulator, STAT-5, activates the ATM DNA damage pathway to induce HPV 31 genome amplification upon epithelial differentiation. PLoS Pathog. 9, e1003295. https://doi.org/10.1371/journal.ppat.1003295.
Huibregtse, J.M., Scheffner, M., Howley, P.M., 1991. A cellular protein mediates association of p53 with the E6 oncoprotein of human papillomavirus types 16 or 18. EMBO J. 10, 4129–4135.
Johnson, M.E., Cantalupo, P.G., Pipas, J.M., 2018. Identification of head and neck cancer subtypes based on human papillomavirus presence and E2F-regulated gene expression. mSphere 3. https://doi.org/10.1128/mSphere.00580-17.
Kanehisa, M., Goto, S., 2000. KEGG: Kyoto Encyclopedia of genes and genomes. Nucleic Acids Res. 28, 27.
Kobayashi, K., Hisamatsu, K., Suzui, N., Hara, A., Tomita, H., Miyazaki, T., 2018. A review of HPV-related head and neck cancer. J. Clin. Med. 7, 241. https://doi.org/10.3390/jcm7090241.
Kono, T., Hoover, P., Poropatich, K., Paunesku, T., Mittal, B.B., Samant, S., Laimins, L.A., 2020. Activation of DNA damage repair factors in HPV positive oropharyngeal cancers. Virology 547, 27–34. https://doi.org/10.1016/j.virol.2020.05.003.
Laat, W.L.de, Jaspers, N.G.J., Hoeijmakers, J.H.J., 1999. Molecular mechanism of nucleotide excision repair. Genes Dev. 13, 768–785.
Liang, C., Marsit, C.J., McClean, M.D., Nelson, H.H., Christensen, B.C., Haddad, R.I., Clark, J.R., Wein, R.O., Grillone, G.A., Houseman, E.A., Halec, G., Waterboer, T., Pawlita, M., Krane, J.F., Kelsey, K.T., 2012. Biomarkers of HPV in head and neck squamous cell carcinoma. Canc. Res. 72, 5004–5013. https://doi.org/10.1158/0008-5472.CAN-11-3277.
Mackiewicz-Wysocka, M., Czerwińska, P., Filas, V., Bogajewska, E., Kubicka, A., Przybyła, A., Dondajewska, E., Kolenda, T., Marszałek, A., Mackiewicz, A., 2017. Oncogenic BRAF mutations and p16 expression in melanocytic nevi and melanoma in the Polish population. Postepy Dermatol. Alergol. 34, 490–498. https://doi.org/10.5114/ada.2017.71119.
Marur, S., D'Souza, G., Westra, W.H., Forastiere, A.A., 2010. HPV-associated head and neck cancer: a virus-related cancer epidemic. Lancet Oncol. 11, 781–789. https://doi.org/10.1016/S1470-2045(10)70017-6.
Maruyama, H., Yasui, T., Ishikawa-Fujiwara, T., Morii, E., Yamamoto, Y., Yoshii, T., Takenaka, Y., Nakahara, S., Todo, T., Hongyo, T., Inohara, H., 2014. Human papillomavirus and p53 mutations in head and neck squamous cell carcinoma among Japanese population. Canc. Sci. 105, 409–417. https://doi.org/10.1111/cas.12369.
Mehta, K., Laimins, L., 2018. Human papillomaviruses preferentially recruit DNA repair factors to viral genomes for rapid repair and amplification. mBio 9https://doi.org/10.1128/mBio.00064-18. e00064-18.
Münger, K., Werness, B.A., Dyson, N., Phelps, W.C., Harlow, E., Howley, P.M., 1989a. Complex formation of human papillomavirus E7 proteins with the retinoblastoma tumor suppressor gene product. EMBO J. 8, 4099–4105.
Münger, K., Werness, B.A., Dyson, N., Phelps, W.C., Harlow, E., Howley, P.M., 1989b. Complex formation of human papillomavirus E7 proteins with the retinoblastoma tumor suppressor gene product. EMBO J. 8, 4099–4105.
Pérez Sayáns, M., Chamorro Petronacci, C.M., Lorenzo Pouso, A.I., Padín Iruegas, E., Blanco Carrión, A., Suárez Peñaranda, J.M., García García, A., 2019. Comprehensive genomic review of TCGA head and neck squamous cell carcinomas (HNSCC). J. Clin. Med. 8. https://doi.org/10.3390/jcm8111896.
Prakash, S., Johnson, R.E., Prakash, L., 2005. Eukaryotic translesion synthesis DNA polymerases: specificity of structure and function. Annu. Rev. Biochem. 74, 317–353. https://doi.org/10.1146/annurev.biochem.74.082803.133250.
Srivastava, A.K., Han, C., Zhao, R., Cui, T., Dai, Y., Mao, C., Zhao, W., Zhang, X., Yu, J., Wang, Q.-E., 2015. Enhanced expression of DNA polymerase eta contributes to cisplatin resistance of ovarian cancer stem cells. Proc. Natl. Acad. Sci. U.S.A. 112, 4411–4416. https://doi.org/10.1073/pnas.1421365112.
Uhlén, M., Björling, E., Agaton, C., Szigyarto, C.A.-K., Amini, B., Andersen, E., Andersson, A.-C., Angelidou, P., Asplund, A., Asplund, C., Berglund, L., Bergström, K., Brumer, H., Cerjan, D., Ekström, M., Elobeid, A., Eriksson, C., Fagerberg, L., Falk, R., Fall, J., Forsberg, M., Björklund, M.G., Gumbel, K., Halimi, A., Hallin, I., Hamsten, C., Hansson, M., Hedhammar, M., Hercules, G., Kampf, C., Larsson, K., Lindskog, M., Lodewyckx, W., Lund, J., Lundeberg, J., Magnusson, K., Malm, E., Nilsson, P., Odling, J., Oksvold, P., Olsson, I., Oster, E., Ottosson, J., Paavilainen, L., Persson, A., Rimini, R., Rockberg, J., Runeson, M., Sivertsson, A., Sköllermo, A., Steen, J., Stenvall, M., Sterky, F., Strömberg, S., Sundberg, M., Tegel, H., Tourle, S., Wahlund, E., Waldén, A., Wan, J., Wernérus, H., Westberg, J., Wester, K., Wrethagen, U., Xu, L.L., Hober, S., Pontén, F., 2005. A human protein atlas for normal and cancer tissues based on antibody proteomics. Mol. Cell. Proteomics 4, 1920–1932. https://doi.org/10.1074/mcp.M500279-MCP200.
Uhlén, M., Fagerberg, L., Hallström, B.M., Lindskog, C., Oksvold, P., Mardinoglu, A., Sivertsson, Å., Kampf, C., Sjöstedt, E., Asplund, A., Olsson, I., Edlund, K., Lundberg, E., Navani, S., Szigyarto, C.A.-K., Odeberg, J., Djureinovic, D., Takanen, J.O., Hober, S., Alm, T., Edqvist, P.-H., Berling, H., Tegel, H., Mulder, J., Rockberg, J., Nilsson, P., Schwenk, J.M., Hamsten, M., von Feilitzen, K., Forsberg, M., Persson, L., Johansson, F., Zwahlen, M., von Heijne, G., Nielsen, J., Pontén, F., 2015. Proteomics. Tissue-based map of the human proteome. Science 347, 1260419. https://doi.org/10.1126/science.1260419.
Wallace, N.A., 2020. Catching HPV in the homologous recombination cookie jar. Trends Microbiol. 28, 191–201. https://doi.org/10.1016/j.tim.2019.10.008.
Wallace, N.A., Galloway, D.A., 2014. Manipulation of cellular DNA damage repair machinery facilitates propagation of human papillomaviruses. Semin. Canc. Biol. 26, 30–42. https://doi.org/10.1016/j.semcancer.2013.12.003.
Wallace, N.A., Khanal, S., Robinson, K.L., Wendel, S.O., Messer, J.J., Galloway, D.A., 2017. High risk alpha papillomavirus oncogenes impair the homologous recombination pathway. J. Virol. JVI. https://doi.org/10.1128/JVI.01084-17. 01084-17.
Westra, W.H., Taube, J.M., Poeta, M.L., Begum, S., Sidransky, D., Koch, W.M., 2008. Inverse relationship between human papillomavirus-16 infection and disruptive p53 gene mutations in squamous cell carcinoma of the head and neck. Clin. Canc. Res. 14, 366–369. https://doi.org/10.1158/1078-0432.CCR-07-1402.
Whitaker, A.M., Schaich, M.A., Smith, M.S., Flynn, T.S., Freudenthal, BretD., 2017. Base excision repair of oxidative DNA damage: from mechanism to disease. Front. Biosci. (Landmark Ed) 22, 1493–1522.

Journal of Virology®

TRANSFORMATION AND ONCOGENESIS

Beta Human Papillomavirus 8E6 Attenuates LATS Phosphorylation after Failed Cytokinesis

Dalton Dacus,[a] Celeste Cotton,[a,b] Tristan X. McCallister,[a] Nicholas A. Wallace[a]

[a]Division of Biology, Kansas State University, Manhattan, Kansas, USA
[b]Langston University, Langston, Oklahoma, USA

ABSTRACT Beta genus human papillomaviruses (β-HPVs) cause cutaneous squamous cell carcinomas (cSCCs) in a subset of immunocompromised patients. However, β-HPVs are not necessary for tumor maintenance in the general population. Instead, they may destabilize the genome in the early stages of cancer development. Supporting this idea, β-HPV's 8E6 protein attenuates p53 accumulation after failed cytokinesis. This paper offers mechanistic insight into how β-HPV E6 causes this change in cell signaling. An *in silico* screen and characterization of HCT 116 cells lacking p300 suggested that the histone acetyltransferase is a negative regulator of Hippo pathway (HP) gene expression. HP activation restricts growth in response to stimuli, including failed cytokinesis. Loss of p300 resulted in increased HP gene expression, including proproliferative genes associated with HP inactivation. β-HPV 8E6 expression recapitulates some of these phenotypes. We used a chemical inhibitor of cytokinesis (dihydrocytochalasin B [H2CB]) to induce failed cytokinesis. This system allowed us to show that β-HPV 8E6 reduced activation of large tumor suppressor kinase (LATS), an HP kinase. LATS is required for p53 accumulation following failed cytokinesis. These phenotypes were dependent on β-HPV 8E6 destabilizing p300 and did not completely attenuate the HP. It did not alter H2CB-induced nuclear exclusion of the transcription factor YAP. β-HPV 8E6 also did not decrease HP activation in cells grown to a high density. Although our group and others have previously described inhibition of DNA repair, to the best of our knowledge, this marks the first time that a β-HPV E6 protein has been shown to hinder HP signaling.

IMPORTANCE β-HPVs contribute to cSCC development in immunocompromised populations. However, it is unclear if these common cutaneous viruses are tumorigenic in the general population. Thus, a more thorough investigation of β-HPV biology is warranted. If β-HPV infections do promote cSCCs, they are hypothesized to destabilize the cellular genome. *In vitro* data support this idea by demonstrating the ability of the β-HPV E6 protein to disrupt DNA repair signaling events following UV exposure. We show that β-HPV E6 more broadly impairs cellular signaling, indicating that the viral protein dysregulates the HP. The HP protects genome fidelity by regulating cell growth and apoptosis in response to a myriad of deleterious stimuli, including failed cytokinesis. After failed cytokinesis, β-HPV 8E6 attenuates phosphorylation of the HP kinase (LATS). This decreases some, but not all, HP signaling events. Notably, β-HPV 8E6 does not limit senescence associated with failed cytokinesis.

KEYWORDS cancer, cytokinesis, Hippo signaling pathway, human papillomavirus, skin cancer, apoptosis, senescence

The human papillomavirus (HPV) family includes over 200 double-stranded DNA viruses that are divided into five genera, all of which infect human epithelia (1). Upon infecting mucosal or cutaneous tissue, members of each genus can cause a broad array of pathologies. Of these, the most prominent diseases are the anogenital and

Citation Dacus D, Cotton C, McCallister TX, Wallace NA. 2020. Beta human papillomavirus 8E6 attenuates LATS phosphorylation after failed cytokinesis. J Virol 94:e02184-19. https://doi.org/10.1128/JVI.02184-19.

Editor Lawrence Banks, International Centre for Genetic Engineering and Biotechnology

Address correspondence to Nicholas A. Wallace, nwallac@ksu.edu.

Received 2 January 2020
Accepted 19 March 2020
Accepted manuscript posted online 1 April 2020
Published 1 June 2020

oropharyngeal carcinomas caused by alpha genus HPVs (2, 3). Cutaneous beta genus HPVs (β-HPVs) have also been linked to tumorigenesis via high viral DNA loads in cutaneous squamous cell carcinomas (cSCCs) of immunocompromised patients, primarily in sun-exposed skin (4–6).

While β-HPV infections are common in immunocompetent individuals, their contribution to cSCCs is less clear. The main etiological factor in skin cancer pathogenesis is UV. Further, the characterizations of cSCCs in the general population do not include continued β-HPV expression (7–9). Viral loads decrease as lesions progress from precancerous actinic keratosis (AK) to cSCC (10–12). These data have led to the hypothesized "hit-and-run" mechanism of oncogenesis, where β-HPVs cooperate with UV to enhance genomic instability in the early stages of carcinogenesis (10, 13, 14). This elevated mutational load then increases the chances of tumor progression independent of continued viral gene expression.

While it is hard to prove the role of a transient viral infection in persistent cancer, β-HPVs are also a common resident of our skin and are frequently found in AKs. Despite the billions of dollars spent on sun care products annually, 58 million Americans still have one or more AKs. Moreover, over $1 billion is spent during 5.2 million outpatient visits each year for AK treatment (15, 16). The cost of these AKs for the patient, both financial and emotional, increases if these lesions develop into malignancies. Within 1 year of diagnosis, an estimated 0.6% of AKs progress to cSCCs. This progression expands to 2.6% of AKs 5 years after diagnosis (17). Because β-HPV infections are quite common, even a mild increase in cancer risk would be notable. Thus, it is important to understand their potential contribution to the genome instability that drives cSCC progression.

A great deal is known about the tumorigenic potential of β-HPV proteins, particularly the E6 protein. The presence of the putative oncogene E6 from β-HPV 8 (β-HPV 8E6) is enough to cause cancers in mice without UV exposure (18, 19). β-HPV 8E6 inhibits differentiation and promotes proliferation by targeting the NOTCH and TGF-β signaling pathways (20). Another central theme of β-HPV E6 proteins is their ability to bind the cellular histone acetyltransferase p300 (21–24). β-HPV 8E6 and the E6 from β-HPV 5 bind p300 strongly, leading to its destabilization and decreasing DNA damage repair (DDR) gene expression (22, 25, 26). β-HPV type 38's E6 protein has a lower p300-binding affinity and cannot destabilize the cellular protein (27). Nevertheless, binding p300 is essential for HPV38-induced immortalization of human foreskin keratinocytes (HFKs) (28). This suggests that p300 binding may be a shared factor in β-HPV-promoted oncogenesis. Because p300 is a master regulator of gene expression (29, 30), other signaling pathways are likely to be altered by β-HPV 8E6's destabilization of the histone acetyltransferase.

Approximately 10% of skin cells do not divide after entering mitosis (25, 31). β-HPV 8E6 allows these cells to divide by preventing p53 stabilization in a p300-dependent manner (25). p53 accumulation requires the activation of large tumor suppressor kinase (LATS), a kinase in the Hippo signaling pathway (HP) (32). This suggests that β-HPV 8E6 may attenuate LATS activity. The HP also prevents growth by inhibiting the proproliferative activity of YAP/TAZ (32–34). Our analysis of transcriptomic data from cell lines segregated by their relative p300 expression was consistent with p300 acting as a negative regulator of HP and HP-responsive gene expression. We confirm that p300 modulates HP gene expression using HCT 116 cells with and without the p300 gene locus. Expressing β-HPV 8E6 in HFKs recapitulated some, but not all, of these effects. p300 is also important for responding to dihydrocytochalasin B (H2CB)-induced failed cytokinesis. HCT 116 cells without p300 had reduced LATS activation and p53 accumulation. β-HPV 8E6's destabilization of p300 similarly hindered LATS phosphorylation and p53 accumulation. Despite p53's role in apoptosis, elevated p53 levels did not correlate with increased apoptosis until the drug was washed off and the cells were allowed to recover. During this recovery period, β-HPV 8E6 displayed some ability to reduce markers of apoptosis. β-HPV 8E6 did not completely abrogate the HP's response

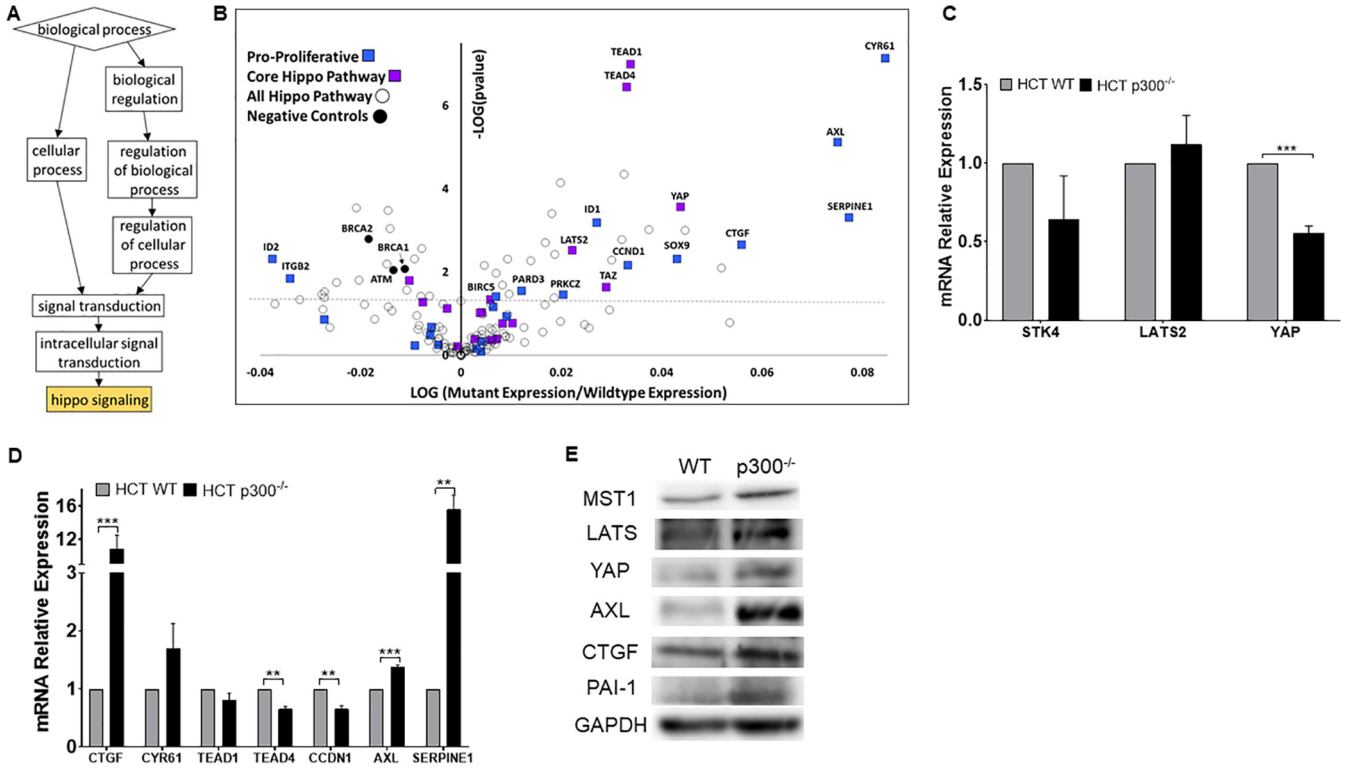

FIG 1 Loss of p300 leads to changes in Hippo pathway gene expression. (A) Gene ontology of 1,020 cancer cell lines via GOrilla. Boxes show GO biological process terms. Boxes descend from general to specific functions. Gold color indicates $P \leq 0.001$. (B) Volcano plot of 154 HP genes in 1,020 cancer cell lines with decreased EP300 expression. The colors blue, purple, and black represent proproliferative TEAD targets, core HP genes, and p300-negative controls, respectively. The horizontal line denotes $P = 0.05$. (C and D) Canonical HP genes (C) and TEAD-regulated mRNA expression (D) in HCT 116 WT and -p300$^{-/-}$ measured by RT-qPCR and normalized to β-actin mRNA. (E) Representative immunoblots of HP and TEAD-regulated proteins in HCT 116 WT and -p300$^{-/-}$. Figures depict the mean ± the standard error of the mean; $n \geq 3$. *, significant difference between indicated samples; *, $P \leq 0.05$; **, $P \leq 0.01$; ***, $P \leq 0.001$ (Student's *t* test).

to failed cytokinesis, as YAP was still excluded from the nucleus. β-HPV 8E6 also did not impede the HP induction in cells grown to a high density.

RESULTS

Loss of p300 alters Hippo pathway gene expression. Animal models show that certain β-HPV E6 genes can contribute to UV-associated carcinogenesis (18, 19, 23). *In vitro* studies from our group and others have added molecular details by describing β-HPV E6's ability to impair the DDR by destabilizing p300 (18, 22, 27, 28, 35, 36). Despite this focus on repair, there are DDR-independent pathways that protect genome fidelity (37–39). To identify p300-regulated pathways that could contribute to β-HPV E6-associated genome destabilization, we performed an *in silico* screen comparing RNA sequencing data among 1,020 cancer cell lines grouped by their relative p300 expression levels (Data Set S1 in the supplemental material) (40–42). The rationale for this approach is based on our prior observations that reducing p300 expression via RNA interference (RNAi) phenocopies β-HPV 8E6's p300-dependent reduction of gene expression (22, 26). We compared expression in cell lines with and without low p300 expression (Z scores of less than −1.64 and greater than −1.64, respectively). Of the cell lines screened, 71 had low p300 expression. The remaining 949 cell lines were considered as not having low p300 expression. This identified 4,211 genes that had altered expression in cells with lower p300 expression. Next, gene ontology (GO) analysis was performed using Gene Ontology enRIchment anaLysis and visuaLizAtion tool (GOrilla) to identify pathways that were significantly altered when p300 expression was reduced (43, 44). Notably, HP was the only pathway identified by GOrilla as significantly changed (Fig. 1A). We then performed a more detailed analysis of HP, using the Kyoto Encyclopedia of Genes and Genomes (KEGG) to provide an unbiased definition of the path-

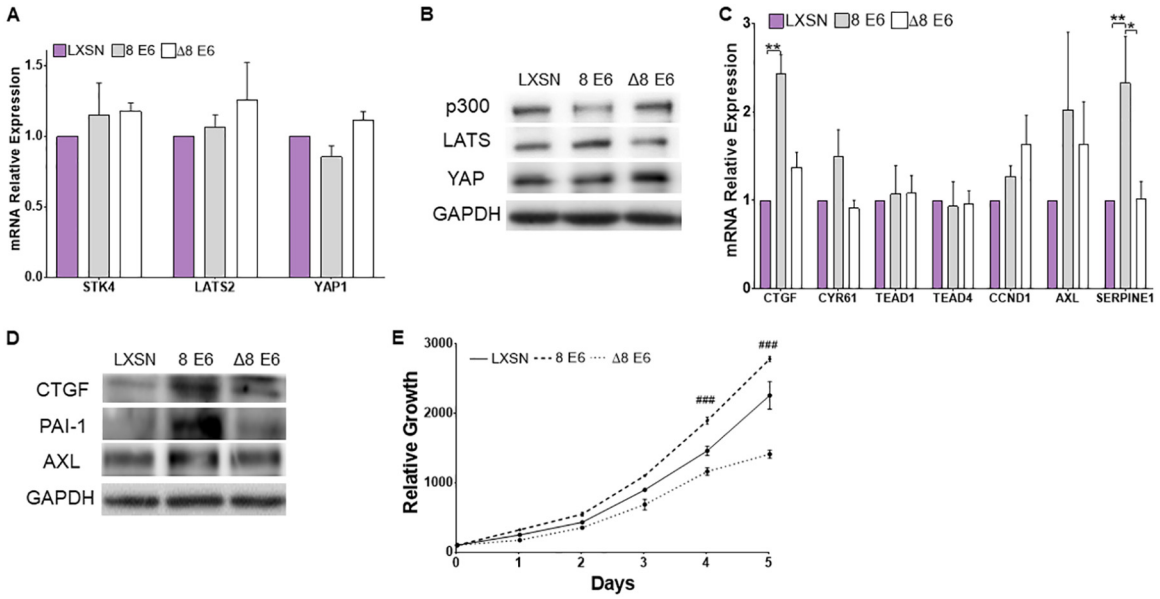

FIG 2 β-HPV 8E6 alters Hippo pathway gene expression. Canonical HP genes (A) and TEAD-regulated mRNA expression (C) in HFKs LXSN, β-HPV 8E6, and β-HPV Δ8E6 measured by RT-qPCR and normalized to β-actin mRNA. Representative immunoblots of HP (B) and TEAD-regulated proteins (D) in HFKs LXSN, β-HPV 8E6, and β-HPV Δ8E6. (E) Relative growth recorded over a 5-day period. Figures depict mean ± standard error of the mean; $n \geq 3$. *, significant difference between indicated samples; #, significant difference from LXSN; one symbol (* or #), $P \leq 0.05$; two symbols (** or ##), $P \leq 0.01$; three symbols (*** or ###), $P \leq 0.001$ (Student's *t* test). In β-HPV Δ8E6, residues 132 to 136 were deleted.

way's members. When p300 expression was reduced, many canonical HP genes were upregulated. However, the most striking changes occurred in proproliferative TEAD-responsive genes (e.g., CYR61, CTGF, AXL, and SERPINE1) (Fig. 1B). As expected, there was a significant reduction in the expression of genes (ATM, BRCA1, and BRCA2) that are dependent on p300 for robust transcription (26, 45, 46).

We used isogenic HCT 116 cells with (WT) or without the p300 gene ($p300^{-/-}$) deleted to confirm our *in silico* analysis (47). The p300 status of these cells was verified by immunoblot (data not shown) before the expression of canonical HP genes (LATS2, STK4, and YAP1) was measured by quantitative real-time PCR (RT-qPCR). Note, STK4 is the gene that encodes the HP kinase, MST1. Of the three HP genes analyzed, the expression of YAP was significantly decreased by p300 loss (Fig. 1C). Next, we defined the abundance of TEAD and TEAD-responsive gene transcripts by RT-qPCR. Seven genes (CTGF, CYR61, TEAD1, TEAD4, CCND1, AXL, and SERPINE1) were chosen based on indications that they were negatively regulated by p300 in our computational screen. Some of these transcripts were more abundant in HCT 116 cells that lacked p300, with increased expression of CTGF, AXL, and SERPINE1 reaching statistical significance (Fig. 1D). Next, we turned to immunoblots to determine if p300 loss leads to changes at the protein level. These data show that increased canonical HP proteins are increased in the absence of p300 (Fig. 1E). The elevated levels extended to AXL, CTGF, and PAI-1 (the protein encoded by the SERPINE1 gene).

***β*-HPV E6 expression alters Hippo pathway gene expression.** β-HPV 8E6 destabilizes p300, but this does not result in complete loss of the histone acetyltransferase. We questioned if this decrease in p300 was enough to dysregulate the HP. To determine the extent that the reduction of p300 by β-HPV 8E6 increased HP gene expression, we defined the expression of canonical HP genes using RT-qPCR. β-HPV 8E6 did not increase expression of the canonical HP genes in human foreskin keratinocytes or HFKs (Fig. 2A). Immunoblots of these cells were consistent with these results except for LATS, which was more abundant when β-HPV 8E6 was expressed (Fig. 2B). We continued this analysis by defining the amount of TEAD and TEAD-responsive genes in HFKs expressing β-HPV 8E6. RT-qPCR comparing expression between vector control

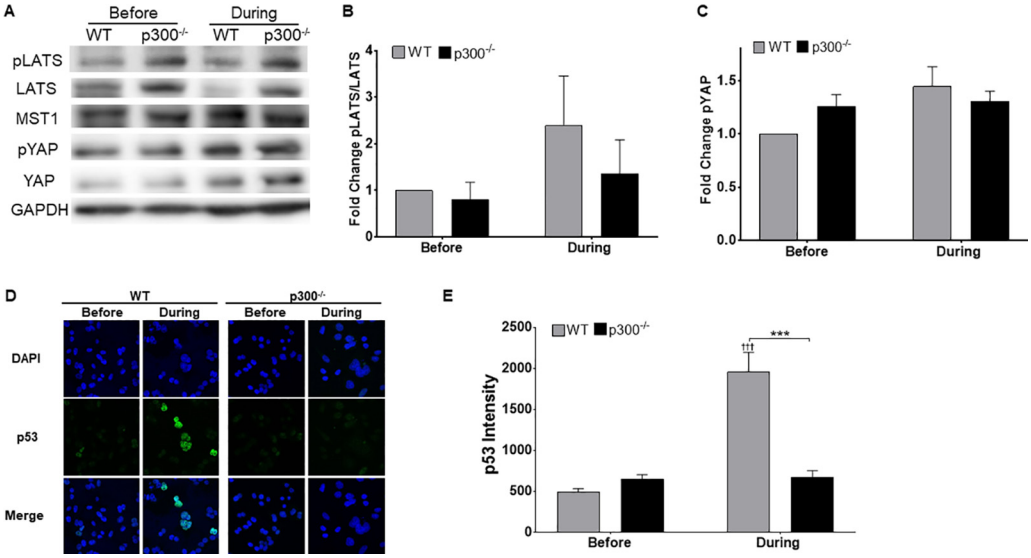

FIG 3 Loss of p300 impedes the Hippo pathway's response to failed cytokinesis. (A) Representative immunoblot of HP proteins before and during H2CB treatment. (B and C) Densitometry of immunoblots described in panel A. GAPDH was used as a loading control. (D) Representative images of p53 (green)- and DAPI (blue)-stained HCT 116 cells before and during H2CB exposure. (E) Relative p53 intensity in HCT 116 cells. At least 150 cells/line were image across three independent experiments. Figures depict mean ± standard error of the mean; $n \geq 3$. *, significant difference between indicated samples; †, significant difference relative to before H2CB; one symbol (* or †), $P \leq 0.05$; two symbols (** or ††), $P \leq 0.01$; three symbols (*** or †††), $P \leq 0.001$ (Student's *t* test). In β-HPV Δ8E6, residues 132 to 136 were deleted.

(LXSN) and β-HPV E6-expressing HFKs found β-HPV E6 increased expression of some TEAD-responsive genes (CTGF, CYR61, CCND1, AXL, and SERPINE1) (Fig. 2C). This was similar to our results in HCT 116 cells except for CCND1. Immunoblots were used to compare protein levels for TEAD-responsive genes, with elevated expression in HFKs expression in β-HPV 8E6. This demonstrated that β-HPV 8E6 increases CTGF, PAI-1, and AXL protein (Fig. 2D). A luciferase reporter assay showed a small but reproducible increase in luciferase expression driven from a TEAD-responsive promoter (data not shown). The increased expression of proproliferative TEAD-responsive genes correlated with increased proliferation (Fig. 2E). Consistent with a p300-dependent mechanism, β-HPV 8E6-driven changes in the HP were abrogated by the deletion of the p300-binding domain in a previously characterized mutant, β-HPV Δ8E6 (Fig. 2).

p300 is necessary for a robust Hippo pathway response to failed cytokinesis. The HP typically restricts growth in response to adverse conditions. This includes failed cytokinesis, induced by dihydrocytochalasin B (H2CB), an inhibitor of actin polymerization (48). Because the loss of p300 promoted proliferation gene expression and dysregulated the HP, we hypothesized that p300 was required for the cellular response to H2CB exposure. Confirming previous data, LATS phosphorylation increased in HCT 116 cells with exposure to 4 μM H2CB (Fig. 3A and B). YAP phosphorylation was similarly elevated by H2CB treatment (Fig. 3A and C). Loss of p300 in HCT 116 cells reduced LATS in response to H2CB (Fig. 3A and B). When cells are treated with H2CB, LATS activation leads to p53 accumulation (32). To determine if p300 was necessary for this response, we used immunofluorescence microscopy to detect p53 in wild-type (WT) and p300 knockout ($p300^{-/-}$) HCT 116 cells grown in H2CB-containing media. We were able to confirm previous reports of p53 buildup in response to the drug in WT HCT 116 cells (Fig. 3D and E). However, p53 did not accumulate in HCT 116 cells lacking p300.

***β*-HPV 8E6 attenuates LATS2 phosphorylation but does not impede nuclear exclusion of YAP.** These data suggest that β-HPV 8E6 alters H2CB induction of the HP. Before evaluating this possibility, we needed to confirm that β-HPV 8E6 did not impede H2CB-induced failed cytokinesis. The visualization of cells with more than one nucleus provides a straightforward measure of failed cytokinesis. We used bright-field and immunofluorescence microscopy to detect the presence of two or more nuclei in cells

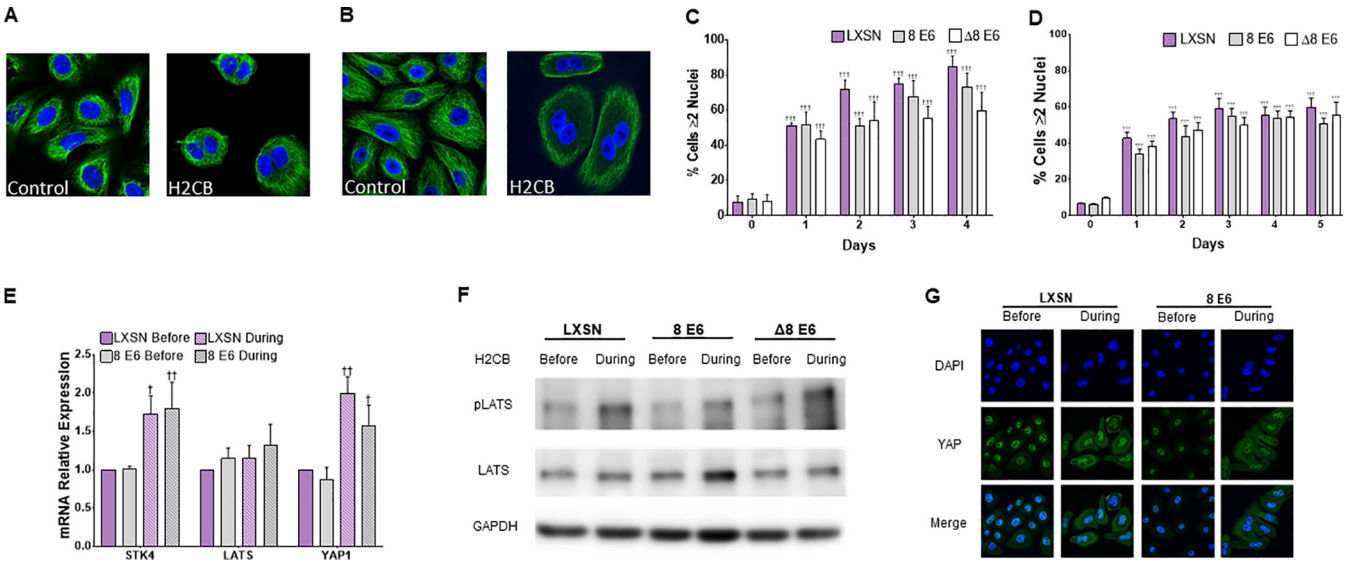

FIG 4 β-HPV 8E6 diminishes LATS phosphorylation during failed cytokinesis. Representative images of U2OS (A) and HFK (B) cells before and during H2CB exposure. Green and blue represent α-tubulin and DAPI, respectively. Quantification of U2OS (C) and HFK (D) cells with 2 or more nuclei as a function of time in H2CB. (E) STK4, LATS, and YAP1 expression before and after H2CB exposure measured by RT-qPCR; $n = 2$. (F) Representative immunoblot of pLATS and totals LATS protein levels in HFK cells before and during H2CB exposure. (G) Representative images of YAP (green)- and DAPI (blue)-stained HFK cells before and during H2CB treatment. At least 200 cells/line were imaged from three independent experiments. Figures depict mean ± standard error of the mean; $n \geq 3$. †, significant difference relative to before H2CB; †, $P \leq 0.05$; ††, $P \leq 0.01$; †††, $P \leq 0.001$ (Student's *t* test). In β-HPV Δ8E6, residues 132 to 136 were deleted.

grown in media containing H2CB (Fig. 4A to D). The percentage of cells with supernumerary nuclei increased as a function of time in H2CB. This was true in both HFK and U2OS cells. The frequency of these abnormal cells was also not notably altered by β-HPV 8E6 or β-HPV Δ8E6. H2CB increased STK4 and YAP1 gene expression. Neither β-HPV 8E6 nor β-HPV Δ8E6 changed this (Fig. 4E). Consistent with our observations in HCT 116 cells, β-HPV 8E6 reduced LATS phosphorylation in cells exposed to H2CB (Fig. 4F). β-HPV Δ8E6 did not attenuate LATS phosphorylation. β-HPV 8E6's restriction of HP signaling may be limited to reducing LATS phosphorylation. β-HPV 8E6 did not change YAP phosphorylation or the abundance of other HP proteins (data not shown). Moreover, immunofluorescence microscopy of YAP shows that β-HPV 8E6 did not hinder the nuclear exclusion of YAP associated with the protein's phosphorylation (Fig. 4G) (49). As expected from these results, H2CB reduced TEAD-responsive promoter activity. β-HPV 8E6 did not prevent this decrease (data not shown).

***β*-HPV 8E6 attenuates p53 accumulation after failed cytokinesis.** Seeing β-HPV 8E6 reduce LATS phosphorylation led us to hypothesize that β-HPV 8E6 would also reduce p53 accumulation in response to H2CB. To test this, we used immunofluorescence microscopy to detect p53 in U2OS grown in media containing H2CB. Consistent with our previous observations, H2CB increased the frequency of cells with more than one nucleus. H2CB increased p53 levels in vector control cells but not in cells expressing β-HPV E6 (Fig. 5A and B). This abrogation of p53 accumulation is likely dependent on p300 degradation, as β-HPV Δ8E6 expressing U2OS and vector control had a similar frequency of p53-stained cells. To validate these results, we used immunoblotting to detect p53 levels in cells grown in H2CB. These experiments also demonstrated that β-HPV 8E6 can repress p53 buildup in response to H2CB. Again, vector control U2OS and β-HPV Δ8E6-expressing U2OS behaved similarly in this assay (Fig. 5C and D). We speculated that the additional p53 found in cells grown with H2CB would result in apoptosis. Fluorescence-based detection of two apoptosis markers (propidium iodide and annexin V) were used to test this idea (50, 51). Surprisingly, we did not see exposure to H2CB associated with an increase in either of these apoptosis markers (Fig. 5E and F). There were also no differences in staining among vector control HFKs and HFKs expressing β-HPV 8E6 or β-HPV Δ8E6.

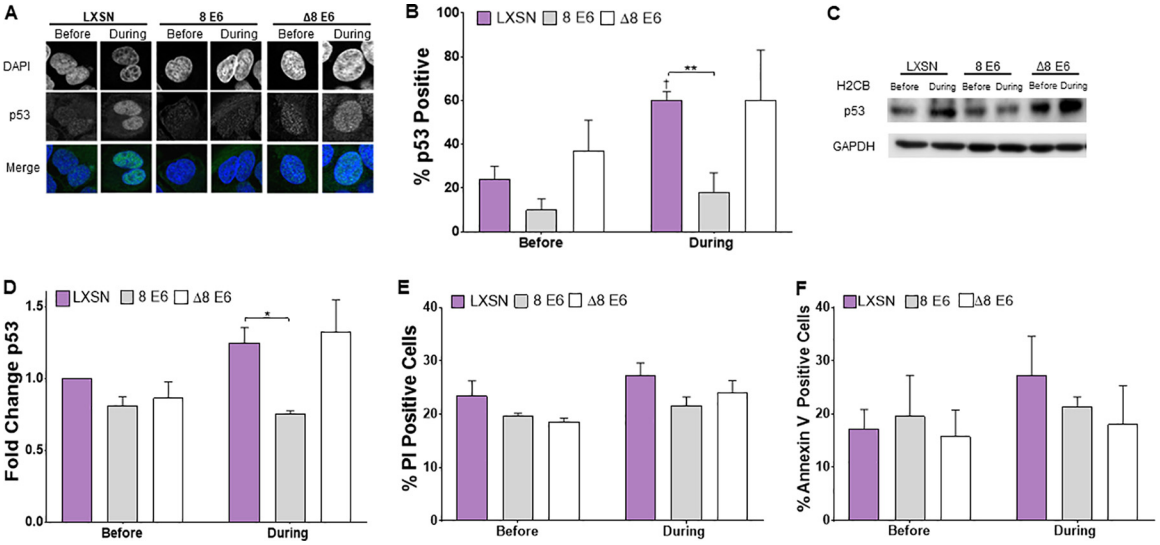

FIG 5 β-HPV 8E6 attenuates p53 accumulation upon H2CB-induced failed cytokinesis. (A) Representative images of p53 and DAPI staining in cells before and during H2CB treatment. (B) Percent of p53-positive U2OS cells. (C) Representative immunoblot of p53 before and during H2CB exposure. (D) Densitometry of immunoblots described in panel C. GAPDH was used as a loading control. Data were normalized to p53 levels in untreated LXSN cells (set to 1). (E) Percent of propidium iodide-stained HFK cells before and during H2CB exposure. (F) Percent of annexin V-stained HFK cells before and during H2CB treatment. At least 200 cells/line were imaged from three independent experiments. Figures depict mean ± standard error of the mean; $n \geq 3$. *, significant difference between indicated samples; †, significant difference relative to before H2CB; one symbol (* or †), $P \leq 0.05$; two symbols (** or ††), $P \leq 0.01$; three symbols (*** or †††), $P \leq 0.001$ (Student's *t* test). In β-HPV Δ8E6, residues 132 to 136 were deleted.

H2CB stalls cytokinesis. It was important to understand if/how those cells recover once the drug is removed and cytokinesis is again possible. To this end, we compared HFKs grown in three conditions: without H2CB (before), grown with 4 days of continual H2CB (during), and grown in H2CB for 4 days followed by 3 additional days without H2CB (after). Figure 6A depicts our experimental setup. We used microscopy to determine the frequency of HFKs with supernumerary nuclei (two or more) in each of these conditions. β-HPV 8E6 did not make supernumerary nuclei less prevalent before or during H2CB exposure (Fig. 6B). However, β-HPV 8E6 decrease supernumerary nuclei after H2CB. This appears to be dependent on p300 destabilization, as supernumerary nuclei were similarly prevalent in HFKs with β-HPV Δ8E6 or vector control. We next used immunoblots to determine if β-HPV 8E6 maintained its ability to attenuate LATS phosphorylation after H2CB. While LATS phosphorylation was elevated in vector control HFKs after H2CB, they remained low in HFKs expressing β-HPV 8E6. This phenotype was not seen in HFKs expressing β-HPV Δ8E6. We used immunofluorescence microscopy as an additional way of detecting p53. These experiments complement the results from immunoblotting, as p53-positive cells were more frequent after H2CB in the vector control but not β-HPV 8E6-expressing HFKs (Fig. 6D and E). We repeated the detection of propidium iodide (PI) and annexin described in Fig. 5 after H2CB. β-HPV 8E6 reduced the percentage of PI-positive HFKs after H2CB compared to vector control and β-HPV Δ8E6-expressing HFKs (Fig. 6F). Annexin V staining was also reduced, but this change did not reach statistical significance (Fig. 6G).

***β*-HPV 8E6 does not completely abrogate the Hippo pathway.** Having seen diminished LATS activation, we queried whether β-HPV 8E6 prevented the HP from restricting growth after H2CB was removed. We used immunofluorescence microscopy to detect Ki67, an established marker of proliferation. While we readily detected Ki67 in both vector control and β-HPV 8E6-expressing HFKs before H2CB, Ki67 was notably less abundant during and after H2CB (Fig. 7A). Ki67 staining intensity was also lower in HFKs expressing β-HPV 8E6 (Fig. 7B). Consistent with these results, HFKs were not capable of long-term proliferation with or without β-HPV 8E6 (data not shown). To understand what was happening to HFKs after H2CB, we stained for senescence-associated beta-

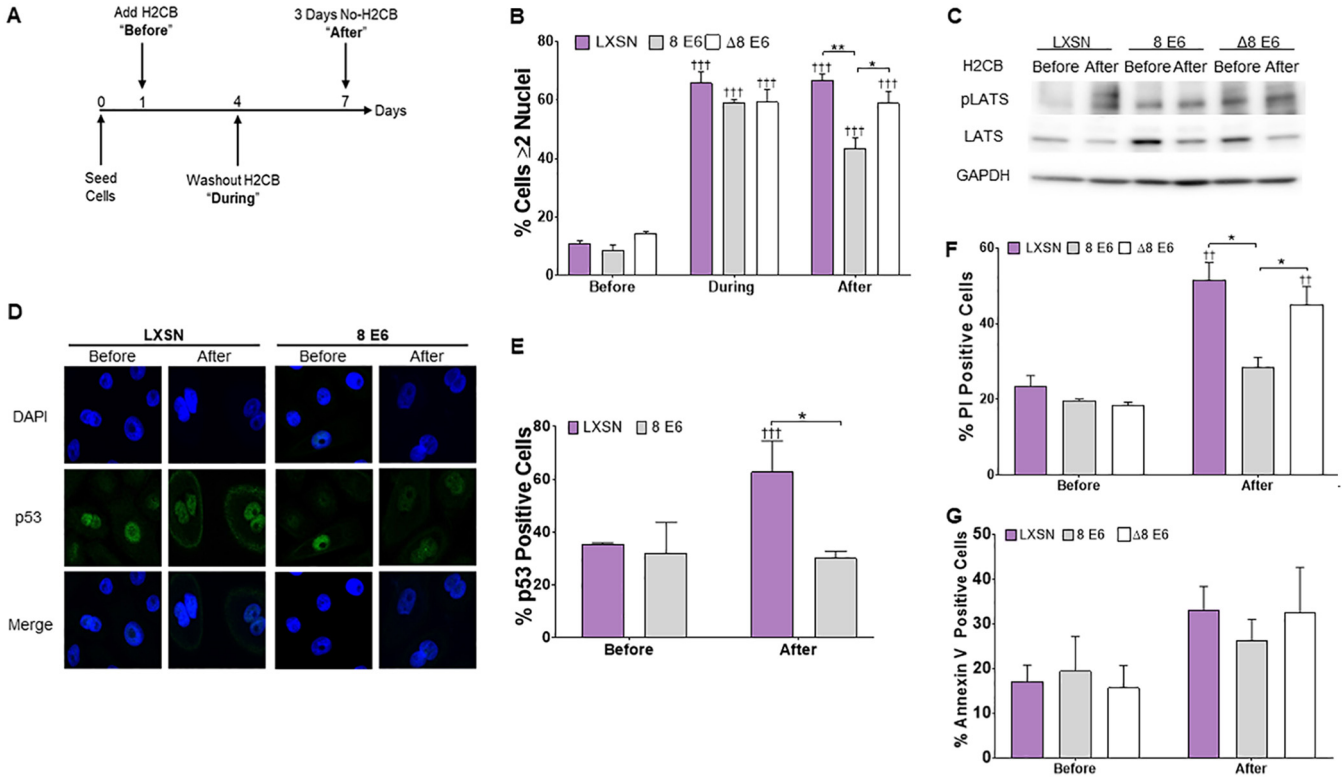

FIG 6 β-HPV 8E6 hinders LATS phosphorylation and p53 accumulation after failed cytokinesis. (A) Timeline for administration and removal of H2CB. (B) Percent of HFK cells with ≥ 2 nuclei per cell before, during, and after H2CB treatment. (C) Representative immunoblots of pLATS and totals LATS in HFKs before and after H2CB exposure. (D) Representative images of p53 and DAPI staining in cells before and after H2CB exposure. (E) Percent of p53-stained HFK cells before and after H2CB exposure. At least 200 cells/line were imaged across three independent experiments. (F) Percent of propidium iodide-stained HFK cells before and after H2CB exposure. (G) Percent of annexin V-stained HFK cells before and after H2CB treatment. Figures depict mean ± standard error of the mean; $n \geq 3$. *, significant difference between indicated samples; †, significant difference relative to before H2CB; one symbol (* or †), $P \leq 0.05$; two symbols (** or ††), $P \leq 0.01$; three symbols (*** or †††), $P \leq 0.001$ (Student's *t* test). In β-HPV Δ8E6, residues 132 to 136 were deleted.

galactosidase (SA β-Gal) activity as an indicator of cellular senescence. These data were consistent with our Ki67 staining experiments (Fig. 7C and D). HFKs were more likely to have SA β-Gal activity after H2CB, and β-HPV 8E6 expression amplified this phenotype.

The HP restricts growth by relocating YAP from the nucleus to the cytoplasm. We used immunofluorescence microscopy to define the subcellular localization of YAP in HFKs before, during, and after H2CB (Fig. 7E and F). Cytoplasmic YAP increased in HFKs during and after H2CB as expected. β-HPV 8E6 attenuated this only after H2CB exposure (Fig. 7F). Additionally, we saw a nominal decrease in nuclear-located YAP in HFKs expressing β-HPV 8E6 alone after H2CB treatment. To more precisely define YAP localization, we performed subcellular fractionation on HFKs before and after H2CB (Fig. 7G). Immunoblotting demonstrated that phosphorylated YAP was more abundant in the cytoplasm, particularly after H2CB. This was also true for phosphorylated LATS. After H2CB, β-HPV 8E6 decreased the amount of total YAP in the nuclear fraction, despite reducing total and cytoplasmic phospho-LATS1/2 (pLATS).

We wanted to determine the extent that β-HPV 8E6 could attenuate LATS phosphorylation in response to other stimuli. Because cell density is a commonly used activator of the HP, we compared LATS and YAP phosphorylation in confluent and subconfluent HFKs (Fig. 8A and B). Immunoblots of these cells demonstrate increased YAP phosphorylation in confluent HFKs compared to subconfluent HFKs. The phosphorylation of LATS did not increase under these conditions. Next, we used immunofluorescence microscopy to determine if HFKs increased p53 levels when grown to high confluence (Fig. 8C and D). As expected, p53 staining was more intense in confluent compared to subconfluent HFKs. In general, neither β-HPV 8E6 nor β-HPV Δ8E6 changed these responses. However, β-HPV Δ8E6 decreased p53 staining. We have no

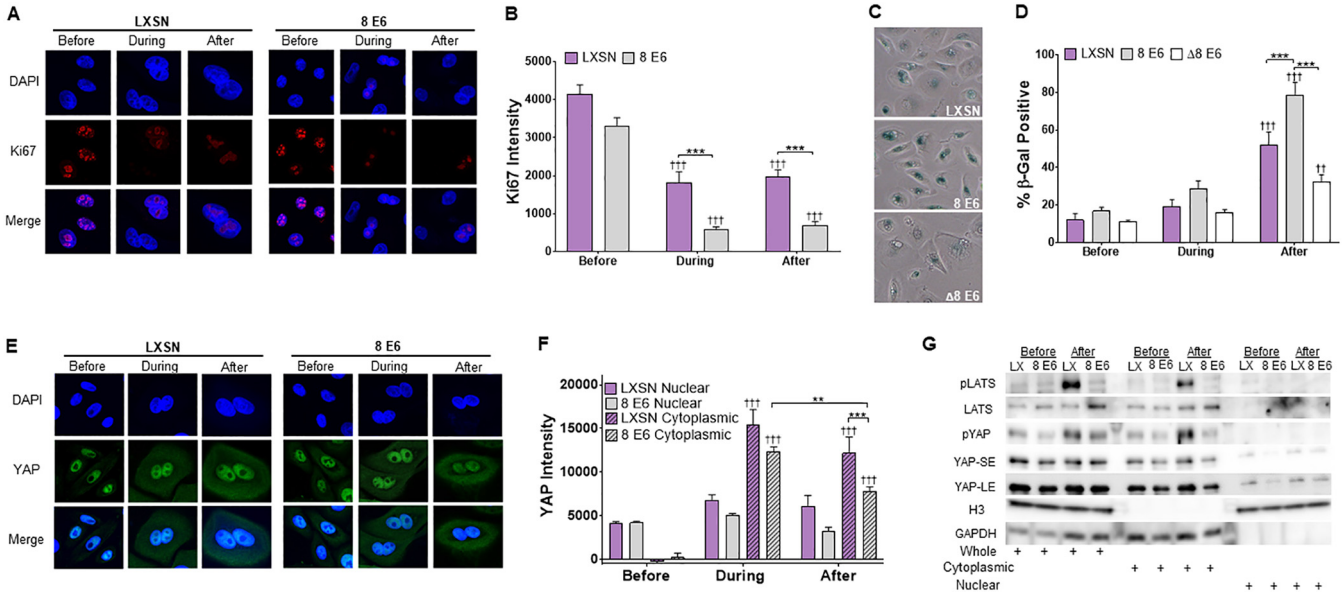

FIG 7 β-HPV 8E6 increases SA β-Gal staining and reduces YAP abundance after failed cytokinesis. (A) Representative images of Ki67 (red) and DAPI (blue) staining in HFK cells before, during, and after H2CB treatment. (B) Relative KI67 intensity in HFK cells before, during, and after H2CB treatment. At least 150 cells/line were imaged across three independent experiments. (C) Representative images of HFK cells stained for SA β-Gal activity (blue). (D) Percent of SA β-Gal-positive HFK cells before, during, and after H2CB exposure. (E) Representative images of HFK cells stained for YAP (green) and DAPI (blue). (F) Cytoplasmic and nuclear YAP intensity in HFK cells before, during, and after H2CB treatment. At least 205 images were imaged across three independent experiments. (G) Subcellular fractionation of HFKs harvested before and after H2CB treatment. Hippo pathway proteins were probed via immunoblotting. GAPDH and histone H3 serve as cytoplasmic and nuclear loading controls, respectively. YAP-SE and YAP-LE indicate short- and long-term exposure of YAP, respectively. Figures depict mean ± standard error of the mean; $n \geq 3$. *, significant difference between indicated samples; †, significant difference relative to before H2CB; one symbol (* or †), $P \leq 0.05$, two symbols (** or ††), $P \leq 0.01$; three symbols (*** or †††), $P \leq 0.001$ (Student's *t* test). In β-HPV Δ8E6, residues 132 to 136 were deleted.

explanation of this observation, but it does demonstrate that β-HPV Δ8E6 is not universally inactive.

DISCUSSION

Tumorigenesis is among the grave consequences associated with changes in ploidy. HP activation is one of the cellular mechanisms that prevents polyploidy by halting the proliferation of cells that do not divide after replication (32, 52). Despite the high stakes, cytokinesis fails in approximately 10% of skin cells that enter mitosis (25, 31). As a result, the HP may play an important role in preventing cSCCs. The growth arrest associated with HP activation is likely refractory to β-HPV replication, as HPV replicates in actively proliferating cells (53). Our work suggests that β-HPV 8E6 helps binucleated cells survive by mitigating HP activation. Presumably limiting HP signaling is beneficial to papillomaviruses in general, as genus α HPV oncogenes also dysregulate the Hippo pathway (54, 55).

The "evolutionary motivation" behind this could stem from the modest growth advantage that we report. However, this weak phenotype seems unlikely to drive convergent evolution toward HP dysregulation. Given the HP's role in immunity, it is more enticing to speculate that targeting the HP helps HPVs avoid an immune response (56, 57). Indeed, an MST1 deficiency increased β-HPV infections (58). Since the HP was only discovered 14 years ago (59), there could also be other currently unknown advantages to be gained by disrupting the pathway.

Less speculatively, we extend the understanding of β-HPV 8E6 biology. β-HPV E6 disrupts multiple cell signaling pathways necessary for DNA repair and regulating differentiation. Much of β-HPV E6's ability to disrupt DNA repair is linked to p300 destabilization. We demonstrate that changes in signaling associated with reduced p300 extend to the HP, as LATS phosphorylation is attenuated following failed cytokinesis. β-HPV 8E6 also displays some antiapoptotic properties in response to H2CB-

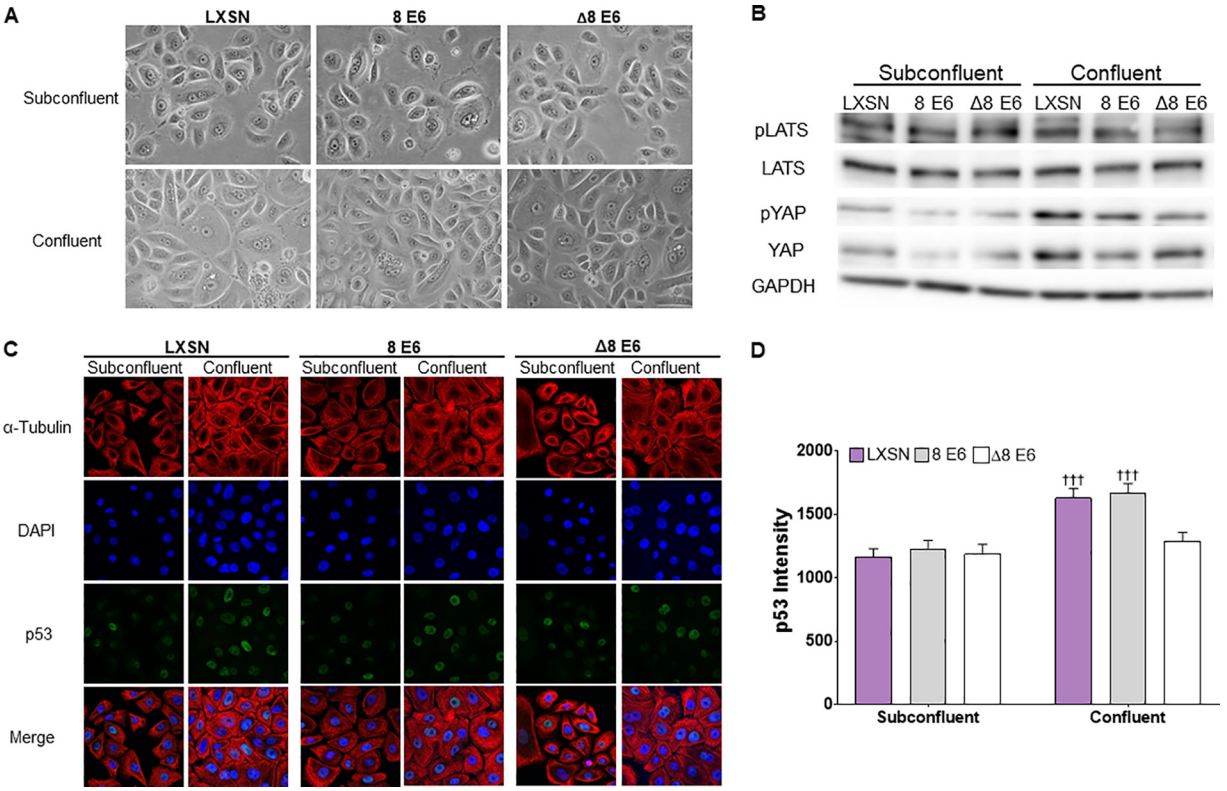

FIG 8 β-HPV 8E6 does not inhibit the Hippo pathway's response to cellular density. (A) Representative images of subconfluent and confluent HFKs. (B) Representative immunoblot of HP proteins in confluent and subconfluent HFKs. (C) Representative images of α-tubulin (red)-, p53 (green)-, and DAPI (blue)-stained subconfluent and confluent HFK cells. (D) Mean p53 intensity in HFK cells before and after confluence. At least 200 cells/line were imaged across 3 independent experiments; $n = 2$ for β-HPV Δ8E6. Figures depict mean ± standard error of the mean; $n \geq 3$. †, significant difference relative to before H2CB; †, $P \leq 0.05$; ††, $P \leq 0.01$; †††, $P \leq 0.001$ (Student's *t* test). In β-HPV Δ8E6, residues 132 to 136 were deleted.

induced failed cytokinesis. Together, these data demonstrate that β-HPV 8E6 is a versatile protein capable of a striking reprogramming of cellular signaling. We also extend the long history of using viral oncogenes to learn about cell biology by linking p300 to the HP- and TEAD-responsive gene expression.

The fact that most people get infected with β-HPV but a significantly lower number of those infections become cSCCs causes many to doubt that the virus is tumorigenic. β-HPV 8E6 may be more mutagenic in certain genetic backgrounds. For instance, β-HPV 8E6 reduces LATS phosphorylation after failed cytokinesis, but the cells still senesce. This suggests that mutations that help cells avoid senescence would augment β-HPVs tumorigenic potential. One could imagine any number of additional mutations that might synergize with β-HPV 8E6 to promote mutagenesis. Genetic landscapes where the opposite is true seem equally likely. Moreover, β-HPV E6 could also be more or less harmful when coexpressed with other β-HPV genes. Future studies are needed to evaluate these complexities.

MATERIALS AND METHODS

Cell cultures. U2OS and HCT 116 cells were maintained in Dulbecco modified Eagle medium (DMEM) supplemented with 10% fetal bovine serum (FBS) and penicillin-streptomycin. Primary HFKs were derived from neonatal human foreskins. HFKs were grown in EpiLife medium supplemented with calcium chloride (60 μM), human keratinocyte growth supplement (Thermo Fisher Scientific), and penicillin-streptomycin. HPV genes were cloned, transfected, and confirmed as previously described (25). We carefully monitored cell density in all experiments. To avoid confounding our experiments by activating the Hippo pathway via contact inhibition, experiments were aborted if unintended differences in seeding resulted in cell densities that were more than 10% different among cell lines at the beginning of an experiment.

Proliferation assays and H2CB cell viability assays. Cells were counted, and 4.0×10^4 cells were plated into 6 wells per cell line of 6-well tissue culture dishes. One well was trypsinized, resuspended, and

counted 3 times via hemocytometer with trypan blue. For dihydrocytochalasin B (H2CB) cell viability assays, cells were grown for 24 h and then treated with 2/4 μM H2CB, and fresh H2CB was readministered every 2 days while cells were trypsinized and counted 3 times via hemocytometer with trypan blue.

RT-qPCR. Cell were lysed using TRIzol (Invitrogen) and RNA isolated with the RNeasy kit (Qiagen). Two micrograms of RNA were reverse transcribed using the iScript cDNA synthesis kit (Bio-Rad). Quantitative real-time PCR (RT-qPCR) was performed in triplicate with the TaqMan FAM-MGB gene expression assay (Applied Biosystems) and C1000 touch thermal cycler (Bio-Rad). The following probes (Thermo Scientific) were used: ACTB (Hs01060665_g1), STK4 (Hs00178979_m1), LATS2 (referred to as LATS in the text) (Hs01059009_m1), YAP1 (Hs00902712_g1), CTGF (Hs00170014_m1), CYR61 (Hs00155479_m1), TEAD4 (Hs01125032_m1), TEAD1 (Hs00173359_m1), CCND1 (Hs00765553_m1), AXL (Hs01064444_m1), and SERPINE1 (Hs00167155_m1).

Immunoblotting. After being washed with ice-cold phosphate-buffered saline (PBS), cells were lysed with radioimmunoprecipitation assay (RIPA) lysis buffer (VWR Life Science) supplemented with Phosphatase inhibitor cocktail 2 (Sigma) and protease inhibitor cocktail (Bimake). The Pierce bicinchoninic acid (BCA) protein assay kit (Thermo Scientific) was used to determine protein concentration. Equal protein lysates were run on Novex 4-12% Tris-Glycine WedgeWell mini gels (Invitrogen) and transferred to Immobilon-P membranes (Millipore). Membranes were then probed with the following primary antibodies: glyceraldehyde-3-phosphate dehydrogenase (GAPDH) (Santa Cruz Biotechnologies; catalog no. sc-47724), LATS2 (Cell Signaling Technologies; clone D83D6), phospho-LATS1/2 (Ser909) (referred to as pLATS in the text) (Cell Signaling Technologies; product no. 9157), YAP (Cell Signaling Technologies; product no. 4912S), phospho-YAP (Ser127) (Referred to pYAP in the text) (Cell Signaling Technologies; product no. 4911S), MST1 (Cell Signaling Technologies; product no. 3682S), AXL (Cell Signaling Technologies; product no. 8661S), CTGF (Abcam; catalog no. ab6692), PAI-1 (Cell Signaling Technologies; product no. 11907S), p53 (Calbiochem; catalog no. OP43; 100 μg), p300 (Santa Cruz Biotechnologies; catalog no. sc-584), and histone H3 (Abcam; catalog no. ab1791). After exposure to the matching horseradish peroxidase (HRP)-conjugated secondary antibody, cells were visualized using SuperSignal West Femto maximum sensitivity substrate (Thermo Scientific).

cBioPortal and gene ontology analysis. Software from www.cbioportal.org was used to recognize, analyze, and categorize mutations and transcriptomic data from over 1,000 cancer cell lines (40–42) and cutaneous squamous cell carcinomas (60, 61). Gene Ontology enRIchment anaLysis and visuaLizAtion tool (GOrilla) identified and visualized enriched GO terms from these data (43, 44). The Kyoto Encyclopedia of Genes and Genomes (KEGG) was used to identify genes specific to the Hippo signaling pathway (hsa04390).

Senescence-associated β-galactosidase staining. Cells were seeded onto three 6-well plates and were grown for 24 h. Then, they were treated with 4 μM H2CB for stated times, after which cells were fixed and stained for senescence-associated β-galactosidase (β-Gal) expression according to the manufacturer's protocol (Cell Signaling Technologies).

Immunofluorescence microscopy. Cells were seeded onto either 96-well glass-bottom plates (Cellvis) or coverslips and grown overnight. Cells treated with H2CB for a specified time and concentration were fixed with 4% formaldehyde. Then, 0.1% Triton-X solution in PBS was used to permeabilize the cells, followed by blocking with 3% bovine serum albumin in PBS for 30 min. Cells were then incubated with the following: p53 (Cell Signaling Technologies; clone 1C12), YAP (Cell Signaling Technologies; product no. 4912S), Ki67 (Abcam; catalog no. ab15580), alpha-tubulin (Abcam; catalog no. ab18251), and α-tubulin (Cell Signaling Technologies; product no. 3873S). The cells were washed and stained with the appropriate secondary antibodies: Alexa Fluor 594 goat anti-rabbit (Thermo Scientific; catalog no. A11012) and Alexa Fluor 488 goat anti-mouse (Thermo Scientific A11001). After washing, the cells were stained with 28 μM 4′,6-diamidino-2-phenylindole (DAPI) in PBS and visualized with the Zeiss LSM 770 microscope. Images were analyzed using ImageJ techniques previously described in reference 62.

Apoptosis assay. After H2CB treatment, HFKs were harvested via trypsinization and then counted while incubating at 37°C for 30 min. After incubation, cells were resuspended to 1×10^6 cells/ml. Next, cells were stained with 100 μg/ml of propidium iodide (PI) and 1× annexin-binding buffer following the protocol from Dead Cell apoptosis kit (Invitrogen; catalog no. V13242). Stained cells were imaged with the Countess II FL automated cell counter (Invitrogen). Images were processed using ImageJ software.

Subcellular fractionation. Cells were seeded at 5.0×10^5 cells/10 cm^2 plate and grown for 24 h. Cells were then treated with 4 μM H2CB for 3 days, washed with PBS, and recovered in fresh EpiLife for 3 days (after H2CB treatment). Before and after H2CB exposure, cells were washed with ice-cold PBS and divided into cytosolic and nuclear fractions via Abcam's subcellular fractionation protocol. Afterward, lysates were treated the same as in the Immunoblotting section.

Statistical analysis. Unless otherwise noted, statistical significance was determined by an unpaired Student's *t* test and was confirmed when appropriate by two-way analysis of variance (ANOVA) with Turkey's correction. Only *P* values of less than 0.05 were reported as significant.

SUPPLEMENTAL MATERIAL

Supplemental material is available online only.

SUPPLEMENTAL FILE 1, XLSX file, 0.9 MB.

ACKNOWLEDGMENTS

We thank and acknowledge the Kansas State University College of Veterinary Medicine (KSU-CVM) Confocal Core, especially Joel Sanneman, for assisting with our

immunofluorescence imaging, Michael Underbrink for providing the telomerase reverse transcriptase (TERT)-immortalized HFKs, Stefano Piccolo for gifting the 8×GTIIC plasmid, along with Emily Burghardt and Jazmine Snow for their constructive criticism of the manuscript. Also, we thank members of the Zhilong Yang lab for their support.

This work was supported by Department of Defense grant CMDRP PRCRP CA160224 (to N.A.W.) and was made possible by generous support from the Les Clow family and the Johnson Cancer Research Center at Kansas State University.

REFERENCES

1. Van Doorslaer K, Li Z, Xirasagar S, Maes P, Kaminsky D, Liou D, Sun Q, Kaur R, Huyen Y, McBride AA. 2017. The Papillomavirus Episteme: a major update to the papillomavirus sequence database. Nucleic Acids Res 45:D499–D506. https://doi.org/10.1093/nar/gkw879.
2. Zur Hausen H. 2002. Papillomaviruses and cancer: from basic studies to clinical application. Nat Rev Cancer 2:342–350. https://doi.org/10.1038/nrc798.
3. Cogliano V, Baan R, Straif K, Grosse Y, Secretan B, El Ghissassi F, WHO International Agency for Research on Cancer. 2005. Carcinogenicity of human papillomaviruses. Lancet Oncol 6:204. https://doi.org/10.1016/S1470-2045(05)70086-3.
4. Orth G, Jablonska S, Favre M, Croissant O, Jarzabek-Chorzelska M, Rzesa G. 1978. Characterization of two types of human papillomaviruses in lesions of Epidermodysplasia verruciformis. Proc Natl Acad Sci U S A 75:1537–1541. https://doi.org/10.1073/pnas.75.3.1537.
5. Purdie KJ, Surentheran T, Sterling JC, Bell L, McGregor JM, Proby CM, Harwood CA, Breuer J. 2005. Human papillomavirus gene expression in cutaneous squamous cell carcinomas from immunosuppressed and immunocompetent individuals. J Invest Dermatol 125:98–107. https://doi.org/10.1111/j.0022-202X.2005.23635.x.
6. Harwood CA, McGregor JM, Proby CM, Breuer J. 1999. Human papillomavirus and the development of non-melanoma skin cancer. J Clin Pathol 52:249–253. https://doi.org/10.1136/jcp.52.4.249.
7. Chahoud J, Semaan A, Chen Y, Cao M, Rieber AG, Rady P, Tyring SK. 2016. Association between β-genus human papillomavirus and cutaneous squamous cell carcinoma in immunocompetent individuals—a meta-analysis. JAMA Dermatol 152:1354–1364. https://doi.org/10.1001/jamadermatol.2015.4530.
8. Masini C, Fuchs PG, Gabrielli F, Stark S, Sera F, Ploner M, Melchi CF, Primavera G, Pirchio G, Picconi O, Petasecca P, Cattaruzza MS, Pfister HJ, Abeni D. 2003. Evidence for the association of human papillomavirus infection and cutaneous squamous cell carcinoma in immunocompetent individuals. Arch Dermatol 139:890–894. https://doi.org/10.1001/archderm.139.7.890.
9. Chitsazzadeh V, Coarfa C, Drummond JA, Nguyen T, Joseph A, Chilukuri S, Charpiot E, Adelmann CH, Ching G, Nguyen TN, Nicholas C, Thomas VD, Migden M, MacFarlane D, Thompson E, Shen J, Takata Y, McNiece K, Polansky MA, Abbas HA, Rajapakshe K, Gower A, Spira A, Covington KR, Xiao W, Gunaratne P, Pickering C, Frederick M, Myers JN, Shen L, Yao H, Su X, Rapini RP, Wheeler DA, Hawk ET, Flores ER, Tsai KY. 2016. Cross-species identification of genomic drivers of squamous cell carcinoma development across preneoplastic intermediates. Nat Commun 7:12601. https://doi.org/10.1038/ncomms12601.
10. Weissenborn SJ, Nindl I, Purdie K, Harwood C, Proby C, Breuer J, Majewski S, Pfister H, Wieland U. 2005. Human papillomavirus-DNA loads in actinic keratoses exceed those in non-melanoma skin cancers. J Invest Dermatol 125:93–97. https://doi.org/10.1111/j.0022-202X.2005.23733.x.
11. Howley PM, Pfister HJ. 2015. Beta genus papillomaviruses and skin cancer. Virology 479–480:290–296. https://doi.org/10.1016/j.virol.2015.02.004.
12. Weissenborn SJ, De Koning MNC, Wieland U, Quint WGV, Pfister HJ. 2009. Intrafamilial transmission and family-specific spectra of cutaneous betapapillomaviruses. J Virol 83:811–816. https://doi.org/10.1128/JVI.01338-08.
13. Akgül B, Cooke JC, Storey A. 2006. HPV-associated skin disease. J Pathol 208:165–175. https://doi.org/10.1002/path.1893.
14. Aldabagh B, Angeles JGC, Cardones AR, Arron ST. 2013. Cutaneous squamous cell carcinoma and human papillomavirus: is there an association? Dermatol Surg 39:1–23. https://doi.org/10.1111/j.1524-4725.2012.02558.x.
15. Rosen T, Lebwohl MG. 2013. Prevalence and awareness of actinic keratosis: barriers and opportunities. J Am Acad Dermatol 68:S2–9. https://doi.org/10.1016/j.jaad.2012.09.052.
16. Warino L, Tusa M, Camacho F, Teuschler H, Fleischer AB, Feldman SR. 2006. Frequency and cost of actinic keratosis treatment. Dermatol Surg 32:1045–1049. https://doi.org/10.1111/j.1524-4725.2006.32228.x.
17. Criscione VD, Weinstock MA, Naylor MF, Luque C, Eide MJ, Bingham SF, Department of Veteran Affairs Topical Tretinoin Chemoprevention Trial Group. 2009. Actinic keratoses: natural history and risk of malignant transformation in the Veterans Affairs Topical Tretinoin Chemoprevention Trial. Cancer 115:2523–2530. https://doi.org/10.1002/cncr.24284.
18. Marcuzzi GP, Hufbauer M, Kasper HU, Weißenborn SJ, Smola S, Pfister H. 2009. Spontaneous tumour development in human papillomavirus type 8 E6 transgenic mice and rapid induction by UV-light exposure and wounding. J Gen Virol 90:2855–2864. https://doi.org/10.1099/vir.0.012872-0.
19. Schaper ID, Marcuzzi GP, Weissenborn SJ, Kasper HU, Dries V, Smyth N, Fuchs P, Pfister H. 2005. Development of skin tumors in mice transgenic for early genes of human papillomavirus type 8. Cancer Res 65:1394–1400. https://doi.org/10.1158/0008-5472.CAN-04-3263.
20. Meyers JM, Uberoi A, Grace M, Lambert PF, Munger K. 2017. Cutaneous HPV8 and MmuPV1 E6 proteins target the NOTCH and TGF-β tumor suppressors to inhibit differentiation and sustain keratinocyte proliferation. PLoS Pathog 13:e1006171. https://doi.org/10.1371/journal.ppat.1006171.
21. Underbrink MP, Howie HL, Bedard KM, Koop JI, Galloway DA. 2008. E6 proteins from multiple human betapapillomavirus types degrade Bak and protect keratinocytes from apoptosis after UVB irradiation. J Virol 82:10408–10417. https://doi.org/10.1128/JVI.00902-08.
22. Wallace NA, Robinson K, Howie HL, Galloway DA. 2012. HPV 5 and 8 E6 abrogate ATR activity resulting in increased persistence of UVB induced DNA damage. PLoS Pathog 8:e1002807. https://doi.org/10.1371/journal.ppat.1002807.
23. Viarisio D, Mueller-Decker K, Kloz U, Aengeneyndt B, Kopp-Schneider A, Gröne H-J, Gheit T, Flechtenmacher C, Gissmann L, Tommasino M. 2011. E6 and E7 from beta HPV38 cooperate with ultraviolet light in the development of actinic keratosis-like lesions and squamous cell carcinoma in mice. PLoS Pathog 7:e1002125. https://doi.org/10.1371/journal.ppat.1002125.
24. Deshmukh J, Pofahl R, Pfister H, Haase I. 2016. Deletion of epidermal Rac1 inhibits HPV-8 induced skin papilloma formation and facilitates HPV-8- and UV-light induced skin carcinogenesis. Oncotarget 7:57841–57850. https://doi.org/10.18632/oncotarget.11069.
25. Wallace NA, Robinson K, Galloway DA. 2014. Beta human papillomavirus E6 expression inhibits stabilization of p53 and increases tolerance of genomic instability. J Virol 88:6112–6127. https://doi.org/10.1128/JVI.03808-13.
26. Wallace NA, Gasior SL, Faber ZJ, Howie HL, Deininger PL, Galloway DA. 2013. HPV 5 and 8 E6 expression reduces ATM protein levels and attenuates LINE-1 retrotransposition. Virology 443:69–79. https://doi.org/10.1016/j.virol.2013.04.022.
27. Howie HL, Koop JI, Weese J, Robinson K, Wipf G, Kim L, Galloway DA. 2011. Beta-HPV 5 and 8 E6 promote p300 degradation by blocking AKT/p300 association. PLoS Pathog 7:e1002211. https://doi.org/10.1371/journal.ppat.1002211.
28. Muench P, Probst S, Schuetz J, Leiprecht N, Busch M, Wesselborg S, Stubenrauch F, Iftner T. 2010. Cutaneous papillomavirus E6 proteins must interact with p300 and block p53-mediated apoptosis for cellular immortalization and tumorigenesis. Cancer Res 70:6913–6924. https://doi.org/10.1158/0008-5472.CAN-10-1307.
29. Dancy BM, Cole PA. 2015. Protein lysine acetylation by p300/CBP. Chem Rev 115:2419–2452. https://doi.org/10.1021/cr500452k.

30. Chan HM, Thangue N. 2001. p300/CBP proteins: HATs for transcriptional bridges and scaffolds. J Cell Sci 114:2363–2373.
31. Soto M, García-Santisteban I, Krenning L, Medema RH, Raaijmakers JA. 2018. Chromosomes trapped in micronuclei are liable to segregation errors. J Cell Sci 131:jcs214742. https://doi.org/10.1242/jcs.214742.
32. Ganem NJ, Cornils H, Chiu S-Y, O'Rourke KP, Arnaud J, Yimlamai D, Théry M, Camargo FD, Pellman D. 2014. Cytokinesis failure triggers Hippo tumor suppressor pathway activation. Cell 158:833–848. https://doi.org/10.1016/j.cell.2014.06.029.
33. Stukenberg PT. 2004. Triggering p53 after cytokinesis failure. J Cell Biol 165:607–608. https://doi.org/10.1083/jcb.200405089.
34. Shinmura K, Bennett RA, Tarapore P, Fukasawa K. 2007. Direct evidence for the role of centrosomally localized p53 in the regulation of centrosome duplication. Oncogene 26:2939–2944. https://doi.org/10.1038/sj.onc.1210085.
35. Wallace NA, Robinson K, Howie HL, Galloway DA. 2015. β-HPV 5 and 8 E6 disrupt homology dependent double strand break repair by attenuating BRCA1 and BRCA2 expression and foci formation. PLoS Pathog 11:e1004687. https://doi.org/10.1371/journal.ppat.1004687.
36. Snow JA, Murthy V, Dacus D, Hu C, Wallace NA. 2019. β-HPV 8E6 attenuates ATM and ATR signaling in response to UV damage. Pathogens 8:267. https://doi.org/10.3390/pathogens8040267.
37. Ganem NJ, Storchova Z, Pellman D. 2007. Tetraploidy, aneuploidy and cancer. Curr Opin Genet Dev 17:157–162. https://doi.org/10.1016/j.gde.2007.02.011.
38. Sen S. 2000. Aneuploidy and cancer. Curr Opin Oncol 12:82–88. https://doi.org/10.1016/j.gde.2007.02.011.
39. Meyers JM, Spangle JM, Munger K. 2013. The human papillomavirus type 8 E6 protein interferes with NOTCH activation during keratinocyte differentiation. J Virol 87:4762–4767. https://doi.org/10.1128/JVI.02527-12.
40. Barretina J, Caponigro G, Stransky N, Venkatesan K, Margolin AA, Kim S, Wilson CJ, Lehár J, Kryukov GV, Sonkin D, Reddy A, Liu M, Murray L, Berger MF, Monahan JE, Morais P, Meltzer J, Korejwa A, Jané-Valbuena J, Mapa FA, Thibault J, Bric-Furlong E, Raman P, Shipway A, Engels IH, Cheng J, Yu GK, Yu J, Aspesi P, de Silva M, Jagtap K, Jones MD, Wang L, Hatton C, Palescandolo E, Gupta S, Mahan S, Sougnez C, Onofrio RC, Liefeld T, MacConaill L, Winckler W, Reich M, Li N, Mesirov JP, Gabriel SB, Getz G, Ardlie K, Chan V, Myer VE, et al. 2012. The Cancer Cell Line Encyclopedia enables predictive modelling of anticancer drug sensitivity. Nature 483:603–607. https://doi.org/10.1038/nature11003.
41. Gao J, Aksoy BA, Dogrusoz U, Dresdner G, Gross B, Sumer SO, Sun Y, Jacobsen A, Sinha R, Larsson E, Cerami E, Sander C, Schultz N. 2013. Integrative analysis of complex cancer genomics and clinical profiles using the cBioPortal. Sci Signal 6:pl1. https://doi.org/10.1126/scisignal.2004088.
42. Cerami E, Gao J, Dogrusoz U, Gross BE, Sumer SO, Aksoy BA, Jacobsen A, Byrne CJ, Heuer ML, Larsson E, Antipin Y, Reva B, Goldberg AP, Sander C, Schultz N. 2012. The cBio Cancer Genomics Portal: an open platform for exploring multidimensional cancer genomics data. Cancer Discov 2:401–404. https://doi.org/10.1158/2159-8290.CD-12-0095.
43. Eden E, Navon R, Steinfeld I, Lipson D, Yakhini Z. 2009. GOrilla: a tool for discovery and visualization of enriched GO terms in ranked gene lists. BMC Bioinformatics 10:48. https://doi.org/10.1186/1471-2105-10-48.
44. Eden E, Lipson D, Yogev S, Yakhini Z. 2007. Discovering motifs in ranked lists of DNA sequences. PLoS Comput Biol 3:e39. https://doi.org/10.1371/journal.pcbi.0030039.
45. Stauffer D, Chang B, Huang J, Dunn A, Thayer M. 2007. p300/CREB-binding protein interacts with ATR and is required for the DNA replication checkpoint. J Biol Chem 282:9678–9687. https://doi.org/10.1074/jbc.M609261200.
46. Ogiwara H, Kohno T. 2012. CBP and p300 histone acetyltransferases contribute to homologous recombination by transcriptionally activating the BRCA1 and RAD51 genes. PLoS One 7:e52810. https://doi.org/10.1371/journal.pone.0052810.
47. Iyer NG, Chin S-F, Ozdag H, Daigo Y, Hu D-E, Cariati M, Brindle K, Aparicio S, Caldas C. 2004. p300 regulates p53-dependent apoptosis after DNA damage in colorectal cancer cells by modulation of PUMA/p21 levels. Proc Natl Acad Sci U S A 101:7386–7391. https://doi.org/10.1073/pnas.0401002101.
48. Maness PF, Walsh RC. Jr., 1982. Dihydrocytochalasin B disorganizes actin cytoarchitecture and inhibits initiation of DNA synthesis in 3T3 cells. Cell 30:253–262. https://doi.org/10.1016/0092-8674(82)90031-9.
49. Zhao B, Li L, Tumaneng K, Wang C-Y, Guan K-L. 2010. A coordinated phosphorylation by Lats and CK1 regulates YAP stability through SCFβ-TRCP. Genes Dev 24:72–85. https://doi.org/10.1101/gad.1843810.
50. Cornelissen M, Philippé J, De Sitter S, De Ridder L. 2002. Annexin V expression in apoptotic peripheral blood lymphocytes: an electron microscopic evaluation. Apoptosis 7:41–47. https://doi.org/10.1023/a:1013560828090.
51. Riccardi C, Nicoletti I. 2006. Analysis of apoptosis by propidium iodide staining and flow cytometry. Nat Protoc 1:1458–1461. https://doi.org/10.1038/nprot.2006.238.
52. Senovilla L, Vitale I, Martins I, Tailler M, Pailleret C, Michaud M, Galluzzi L, Adjemian S, Kepp O, Niso-Santano M, Shen S, Marino G, Criollo A, Boileve A, Job B, Ladoire S, Ghiringhelli F, Sistigu A, Yamazaki T, Rello-Varona S, Locher C, Poirier-Colame V, Talbot M, Valent A, Berardinelli F, Antoccia A, Ciccosanti F, Fimia GM, Piacentini M, Fueyo A, Messina NL, Li M, Chan CJ, Sigl V, Pourcher G, Ruckenstuhl C, Carmona-Gutierrez D, Lazar V, Penninger JM, Madeo F, Lopez-Otin C, Smyth MJ, Zitvogel L, Castedo M, Kroemer G. 2012. An immunosurveillance mechanism controls cancer cell ploidy. Science 337:1678–1684. https://doi.org/10.1126/science.1224922.
53. McBride AA. 2008. Replication and Partitioning of Papillomavirus Genomes. Adv Virus Res 72:155–205. https://doi.org/10.1016/S0065-3527(08)00404-1.
54. He C, Mao D, Hua G, Lv X, Chen X, Angeletti PC, Dong J, Remmenga SW, Rodabaugh KJ, Zhou J, Lambert PF, Yang P, Davis JS, Wang C. 2015. The Hippo/YAP pathway interacts with EGFR signaling and HPV oncoproteins to regulate cervical cancer progression. EMBO Mol Med 7:1426–1449. https://doi.org/10.15252/emmm.201404976.
55. Morgan E, Patterson M, Lee SY, Wasson C, Macdonald A. 2018 High-risk human papillomaviruses down-regulate expression of the Ste20 family kinase MST1 to inhibit the Hippo pathway and promote transformation. bioRxiv https://doi.org/10.1101/369447.
56. Cheng J, Jing Y, Kang D, Yang L, Li J, Yu Z, Peng Z, Li X, Wei Y, Gong Q, Miron RJ, Zhang Y, Liu C. 2018. The role of Mstl in lymphocyte homeostasis and function. Front Immunol 9:149. https://doi.org/10.3389/fimmu.2018.00149.
57. Zhang Y, Zhang H, Zhao B. 2018. Hippo signaling in the immune system. Trends Biochem Sci 43:77–80. https://doi.org/10.1016/j.tibs.2017.11.009.
58. Crequer A, Picard C, Patin E, D'Amico A, Abhyankar A, Munzer M, Debré M, Zhang S-Y, Saint-Basile G. d, Fischer A, Abel L, Orth G, Casanova J-L, Jouanguy E. 2012. Inherited MST1 deficiency underlies susceptibility to EV-HPV infections. PLoS One 7:e44010. https://doi.org/10.1371/journal.pone.0044010.
59. Pan D. 2010. The Hippo signaling pathway in development and cancer. Dev Cell 19:491–505. https://doi.org/10.1016/j.devcel.2010.09.011.
60. Li YY, Hanna GJ, Laga AC, Haddad RI, Lorch JH, Hammerman PS. 2015. Genomic analysis of metastatic cutaneous squamous cell carcinoma. Clin Cancer Res off J Am Assoc Cancer Res 21:1447–1456. https://doi.org/10.1158/1078-0432.CCR-14-1773.
61. Pickering CR, Zhou JH, Lee JJ, Drummond JA, Peng SA, Saade RE, Tsai KY, Curry JL, Tetzlaff MT, Lai SY, Yu J, Muzny DM, Doddapaneni H, Shinbrot E, Covington KR, Zhang J, Seth S, Caulin C, Clayman GL, El-Naggar AK, Gibbs RA, Weber RS, Myers JN, Wheeler DA, Frederick MJ. 2014. Mutational landscape of aggressive cutaneous squamous cell carcinoma. Clin Cancer Res off J Am Assoc Cancer Res 20:6582–6592. https://doi.org/10.1158/1078-0432.CCR-14-1768.
62. Murthy V, Dacus D, Gamez M, Hu C, Wendel SO, Snow J, Kahn A, Walterhouse SH, Wallace NA. 2018. Characterizing DNA repair processes at transient and long-lasting double-strand DNA breaks by immunofluorescence microscopy. JoVE e57653. https://doi.org/10.3791/57653.

Virology 549 (2020) 32–38

Contents lists available at ScienceDirect

Virology

journal homepage: www.elsevier.com/locate/virology

β-HPV 8E6 combined with *TERT* expression promotes long-term proliferation and genome instability after cytokinesis failure

Dalton Dacus, Elizabeth Riforgiate, Nicholas A. Wallace*

Division of Biology, Kansas State University, Manhattan, KS, USA

ARTICLE INFO

Keywords:
Aneuploid
Polyploid
Chromosome
Skin cancer
β-HPV
Telomerase

ABSTRACT

Human papillomavirus (HPV) is a family of viruses divided into five genera: alpha, beta, gamma, mu, and nu. There is an ongoing discussion about whether beta genus HPVs (β-HPVs) contribute to cutaneous squamous cell carcinoma (cSCC). The data presented here add to this conversation by determining how a β-HPV E6 protein (β-HPV 8E6) alters the cellular response to cytokinesis failure. Specifically, cells were observed after cytokinesis failure was induced by dihydrocytochalasin B (H2CB). β-HPV 8E6 attenuated the immediate toxicity associated with H2CB but did not promote long-term proliferation after H2CB. Immortalization by telomerase reverse transcriptase (*TERT)* activation also rarely allowed cells to sustain proliferation after H2CB exposure. In contrast, *TERT* expression combined with β-HPV 8E6 expression allowed cells to proliferate for months following cytokinesis failure. However, this continued proliferation comes with genome destabilizing consequences. Cells that survived H2CB-induced cytokinesis failure suffered from changes in ploidy.

1. Introduction

Cutaneous squamous cell carcinoma (cSCC) is one of the most common malignancies worldwide (Lomas et al., 2012; Alam and Ratner, 2001). The annual rate of cSCC has risen for thirty straight years (Hollestein et al., 2014). These malignancies represent a tremendous financial burden, especially in fair-skinned populations. As a result, the United States currently spends $3.8 billion annually on treatments (Deady et al., 2014). UV radiation, light skin color, and immunosuppression are the major risk factors implicated in the development of cSCC (Fahradyan et al., 2017). Additionally, it has been hypothesized that cutaneous human papillomavirus of the beta genus (β-HPV) may be another factor in cSCC progression (Howley and Pfister, 2015a; McLaughlin-Drubin, 2015; Tommasino, 2017).

β-HPV types 5 and 8 were first isolated from sun-exposed skin lesions found in individuals with the rare genetic disorder, epidermodysplasia verruciformis (EV) (Orth, 2008). People with EV are prone to β-HPV infections and cSCC (Orth, 2008; Nunes et al., 2018). A similar association has been observed in people taking immunosuppressive drugs after organ transplants (Genders et al., 2015; Boyle et al., 1984; Boxman et al., 1997). Further, animal and epidemiological studies also suggest β-HPV infections are associated with cSCC (Tommasino, 2017; Chahoud et al., 2016; Patel et al., 2008). Yet β-HPV expression in immunocompetent individuals drops significantly as healthy skin progresses to precancerous actinic keratosis (AK), then onto cSCC (Nunes et al., 2018; Winer et al., 2017; Hampras et al., 2017; Weissenborn et al., 2005, 2009; Howley and Pfister, 2015b). *In vitro* assays suggest that β-HPV proteins, particularly β-HPV E6, alter cell signaling to promote proliferation, impairing genome stability in the process (Wendel and Wallace, 2017; Rollison et al., 2019). These data have led some to hypothesize that β-HPV augments the mutational burden associated with UV, promoting the early stages of malignant conversion. In what has been called the “hit-and-run” model of viral oncogenesis, these mutations result in a tumor that no longer relies on continued viral gene expression (Aldabagh et al., 2013; Hufbauer and Akgül, 2017; de Koning et al., 2007). While this model has merit, other factors seem to dictate the oncogenic potential of β-HPV infections. For example, a recent publication from Strickley et al. helped solidify the growing consensus that immune status is a central determinant of the oncogenic potential associated with β-HPV infections (Strickley et al., 2019). Other factors may also increase or decrease the risk associated with these infections. Given how widespread β-HPV infections are, it remains important to understand the genetic changes that could augment their deleterious characteristics.

The work described here focuses on the maintenance of genome fidelity during cell division. Live cell microscopy and brightfield microscopy demonstrate that failed cytokinesis occurs about 10% of the time that skin cells enter mitosis (Wallace et al., 2014; Dacus et al.,

* Corresponding author.
E-mail address: nwallac@ksu.edu (N.A. Wallace).

https://doi.org/10.1016/j.virol.2020.07.016
Received 6 July 2020; Received in revised form 28 July 2020; Accepted 29 July 2020
Available online 04 August 2020
0042-6822/

2020). When this occurs, if the cells continue proliferating, they will suffer changes in ploidy (Hayashi and Karlseder, 2013; Alonso-Lecue et al., 2017; Lens and Medema, 2019). Responses to failed cytokinesis are often studied after induction by dihydrocytochalasin B (H2CB). H2CB causes cytokinesis failure by inhibiting actin polymerization. One study used this approach to show that the Hippo pathway kinase LATS was responsible for orchestrating the cellular response to failed cytokinesis, by inducing p53 accumulation and preventing further proliferation (Ganem et al., 2014). β-HPV 8E6 expression inhibits this buildup of p53 by attenuating LATS activation in a p300-dependent manner (Dacus et al., 2020). Despite the impairment of relevant signaling events, β-HPV 8E6 only imparted transient protection from failed cytokinesis. While β-HPV 8E6 expressing cells tolerated the immediate impact of failed cytokinesis, they were not capable of sustained proliferation. Mutations that activate telomerase are common in cSCC and are associated with growth advantages (Cheng et al., 2015; Griewank et al., 2013; Pópulo et al., 2014). Like β-HPV 8E6 expression, *TERT* expression had a limited ability to promote proliferation after failed cytokinesis. However, expression of β-HPV 8E6 in cells immortalized by telomerase activation promoted short- and long-term proliferation after failed cytokinesis. The survival of H2CB-induced failed cytokinesis was associated with increased aneuploidy.

2. Results

β-HPV 8E6 expressing HFK cannot sustain proliferation after H2CB-induced failed cytokinesis. β-HPV 8E6 hinders the cellular response to genome destabilizing events, including DNA damage and failed cytokinesis (Wendel and Wallace, 2017; Dacus et al., 2020). This study examines the consequences of β-HPV 8E6's impairment of signaling events stemming from H2CB-induced cytokinesis failure. β-HPV 8E6 reduces H2CB-induced activation of a Hippo tumor suppressor pathway kinase (LATS), p53 stabilization, and the accumulation of apoptotic markers. β-HPV 8E6 also increases the expression of pro-proliferative TEAD-responsive genes. To determine if these alterations allowed cells to survive H2CB-induced failed cytokinesis, we exposed vector control human foreskin keratinocytes (HFK LXSN) and β-HPV 8E6 expressing HFK (HFK β-HPV 8E6) to media containing 4 μM of H2CB for 6 days (Ganem et al., 2014). Cells counted on day 0 are referred to as 'before' H2CB. After 6 days of H2CB exposure, cells were counted and are referred to as 'during'. H2CB was washed out and cells were placed in growth media. Cells were monitored until they reached approximately 90% confluency or stopped proliferating (referred to as 'after'). At this point, viable cultures were counted, passaged, and considered to have recovered (recovered-HFK LXSN or recovered-HFK β-HPV 8E6) from H2CB exposure. Three independent biological replicates found similar results. β-HPV 8E6 attenuated the immediate consequences of H2CB-associated toxicity (compare the number of HFK LXSN and HFK β-HPV 8E6 after 6 days of H2CB exposure in Fig. 1A). However, neither cell line was capable of sustained proliferation after H2CB (Fig. 1A).

β-HPV infections occur in different genetic backgrounds, some of which could act synergistically with β-HPV 8E6 to allow cells to recover from H2CB-induced failed cytokinesis (Martincorena et al., 2015). Given the links between β-HPV and cSCC development, recurrent genetic contributors to cSCC development were examined to identify candidate alterations. Specifically, common mutations from sequencing data of 68 cSCC were ranked by their frequency (Pickering et al., 2014; Li et al., 2015; Gao et al., 2013; Cerami et al., 2012) (Supplemental Data 1). Then, a gene ontology analysis was performed on the top 10% of mutations using the web-based gene ontology software, PANTHER (Mi et al., 2017; The Gene Ontology Resourc, 2019; Ashburner et al., 2000) (Fig. 1B). The biological process "replicative senescence" contained within the "proliferation" node contained commonly mutated genes in cSCC. A complementary gene ontology software also identified "replicative senescence" among the cellular responses enriched within cSCC mutated genes (data not shown). This broad unbiased approach was complimented with a literature-based prioritization of the mutated genes. Among the genes in the "replicative senescence" node, mutations in *TERT* (the gene encoding telomerase reverse transcriptase, a component of telomerase) were notable. Multiple other studies have identified telomerase activating mutations within *TERT* promoter region in cSCC (Cheng et al., 2015; Griewank et al., 2013; Pópulo et al., 2014; Scott et al., 2014). Enhanced telomerase activity can promote proliferation despite damage and stress that would normally remove cells from the cell cycle (Urquidi et al., 2000; Victorelli and Passos, 2017; Davoli et al., 2010). It also allows cells immortalized by telomerase activation to continue growing after exposure to cytochalasin B, an unsaturated derivative of H2CB, which shares the ability to inhibit cell division, but unlike H2CB, it affects sugar transport (31, 48–51). These observations suggest that *TERT* activation is a relevant alteration in cSCC and that it could act on its own or synergize with β-HPV 8E6 to promote growth after cytokinesis failure.

To determine if *TERT* activation could promote survival from H2CB, β-HPV 8E6 expression was examined in HFK immortalized by telomerase activation (*TERT*-HFK). Specifically, the effects of H2CB on long term proliferation were studied in previously characterized HA-tagged β-HPV 8E6 and vector control *TERT*-HFKs (*TERT*-HFK β-HPV 8E6 and *TERT*-HFK LXSN, respectively) (Wang et al., 2016; Dickson et al., 2000). β-HPV 8E6 maintained its previously reported ability to alter the response to H2CB and increase TEAD-responsive gene expression in this genetic background (Supplementary Fig. 1A–C). Further, H2CB exposure was more effective at inducing binucleation and senescence (indicated by senescence-associated β-Galactosidase or SA β-Gal staining) in *TERT*-HFK cells (Supplementary Fig. 1D,E). These data confirmed that both β-HPV 8E6 and H2CB retained their reported activities in *TERT*-HFK cells. Next, the impact of H2CB exposure (6 days of 4 μM H2CB) on long-term proliferation was defined for three biological replicates using the growth conditions described in Fig. 1A. β-HPV 8E6 continued to reduce cell death in *TERT*-HFKs during H2CB exposure (compare cell lines at day 6 in Fig. 2A). However, β-HPV 8E6 was also able to promote recovery from H2CB-induced failed cytokinesis in this genetic background (recovered-*TERT*-HFK β-HPV 8E6). In each of these long-term growth assays, *TERT*-HFK β-HPV 8E6 survived for at least 17 days after H2CB exposure (Fig. 2A). Unfortunately, one repeat was contaminated and could not be expanded after survival. In contrast, none of the attempts to grow *TERT*-HFK LXSN after H2CB exposure were successful (recovered-*TERT*-HFK LXSN).

To obtain recovered-*TERT*-HFK LXSN to compare to recovered-*TERT*-HFK β-HPV 8E6 cells, 6 additional replicates were performed in a format with a larger initial population of cells (expansion from a 6-well to 10-cm plate format). In these conditions, only one of the *TERT*-HFK LXSN cell lines survived (See Fig. 2B). *TERT*-HFK β-HPV 8E6 cells also survived in each of the experiments conducted in 10-cm plates. Representative growth data for these cells can be found in Supplementary Figure 2. Recovered-*TERT*-HFK cells were expanded to determine the genomic consequences of surviving H2CB.

3. β-HPV 8E6 exacerbates aneuploidy in *TERT*-HFKs after recovering from failed cytokinesis

Failed cytokinesis jeopardizes genome integrity, particularly when cells continue to proliferate afterward (Hayashi and Karlseder, 2013; Storchova and Kuffer, 2008; Ganem et al., 2007). To determine if the cells that survived H2CB-induced failed cytokinesis had impaired genomic instability, differential interference contrast microscopy of condensed chromosomes from metaphase spreads was used to compare the ploidy of *TERT*-HFK LXSN to recovered-*TERT*-HFK LXSN cells (Fig. 3A). While most *TERT*-HFK LXSN were diploid before H2CB treatment, many recovered-*TERT*-HFK LXSN cells had aneuploid genomes. A small subset of recovered-*TERT*-HFK LXSN cells had tetraploid genomes (Fig. 3B). Chromosome abnormalities were exacerbated by β-HPV 8E6 in the cell line paired with the only recovered-*TERT*-HFK

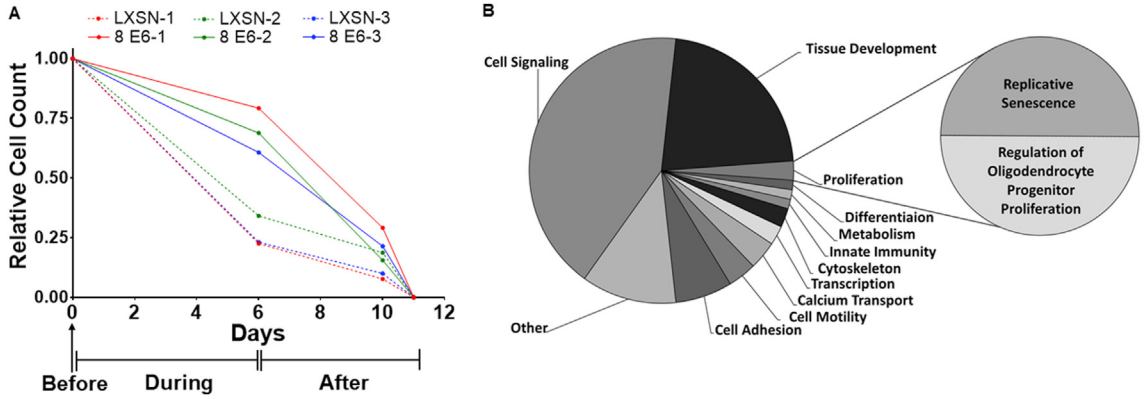

Fig. 1. H2CB-induced failed cytokinesis prevents long-term proliferation. (A) Three growth curves (biological replicates) comparing HFK LXSN and β-HPV 8E6 cells before, during, and after 6 days of H2CB exposure in 6-well tissue culture plates. HFK LXSN (dashed) and β-HPV 8E6 (solid) data with the same color and number (red, 1; green, 2; and blue, 3) were treated in parallel. (B) Two charts representing GO analysis of common mutations in cSCC. The larger chart on the left represents nodes of similar GO: biological process terms. The smaller chart represents the two GO: biological process terms within the "Proliferation" node. *TERT* expression allows β-HPV 8E6 HFKs growth after H2CB-induced failed cytokinesis. (For interpretation of the references to color in this figure legend, the reader is referred to the Web version of this article.)

LXSN cell line. Most *TERT*-HFK β-HPV 8E6 cells had aneuploid genomes before H2CB exposure and all the recovered-*TERT*-HFK β-HPV 8E6 were aneuploid (Fig. 3B, C). The length of time in passage is unlikely to explain these data as the cells were analyzed after a similar time in culture. Further, the results were nearly identical when ploidy was determined immediately after recovery or several passages later (data not shown).

4. Discussion

β-HPVs promote the proliferation of damaged skin cells (Howley and Pfister, 2015a; Tommasino, 2017; Rollison et al., 2019; Wallace et al., 2014; Dacus et al., 2020). β-HPV 8E6 is a critical contributor to this phenotype and acts at least in part by suppressing apoptotic responses (Dacus et al., 2020; Underbrink et al., 2008). As a result, β-HPV infections have been hypothesized to allow the accumulation of potentially tumorigenic mutations. Here, we examine the ability of β-HPV 8E6 to act along with *TERT* expression to facilitate the survival of cells that do not divide after replicating their genomes. We summarize our observations in Fig. 4. When cytokinesis failure was induced by H2CB, HFK were unable to sustain long-term growth (Fig. 4A). β-HPV 8E6 did not change this outcome (Fig. 4B). Immortalization by telomerase activation rarely allowed cells to recover from.

H2CB exposure (Fig. 4C). However, the combination of β-HPV 8E6 expression and *TERT* expression allowed cells to sustain proliferation for months (presumably indefinitely) after cytokinesis failure and augmented genomic instability (Fig. 4D).

When comparing HFK and *TERT*-HFK cell lines some caution should be exercised as they were generated from different donors. However, phenotypes are frequently replicated across.

Keratinocytes from separate persons (White et al., 2012; Howie et al., 2011; Meyers et al., 2017). More specific to this study and these cells, the previously reported attenuation of the Hippo pathway kinase LATS activation by β-HPV 8E6 was conserved between both HFK and *TERT*-HFK cell lines (Supplementary Figure 1 and (Dacus et al., 2020)). These data are consistent with the established idea that telomerase activation promotes carcinogenesis and suggest that β-HPV infections may augment the transformative power of telomerase activation.

Our data also provides other, more specific insights. For instance, we found that β-HPV 8E6 made *TERT*-HFKs approximately 2.5 times more likely to be aneuploid (Fig. 3C). To our knowledge, this is the first report associating changes in ploidy with β-HPV 8E6. The observation is in line with reports from the Tommasino Lab that describe changes in ploidy in β-HPV 38 E6 and E7 immortalized keratinocytes (Gabet et al., 2008). Unlike our report, they demonstrated that ectopic *TERT* expression reduced aneuploidy, likely by reducing the chromosomal rearrangements, anaphase bridges, and multipolar mitoses associated with β-HPV 38 E6/E7 immortalization. This could be the result of differences between β-HPV 38 E6 and β-HPV 8E6 or they might be explained by the presence/absence of the β-HPV E7 protein (Tommasino, 2017; Howley and Pfister, 2015b).

In vitro studies on β-HPVs tend to examine the effects of stimuli over a short time interval (hours to days). However, the average β-HPV infection persists for six to eleven months (de Koning et al., 2007; Hampras et al., 2014). *TERT*-HFK cells provide a system to replicate lengthier conditions and our data demonstrates the utility of such an

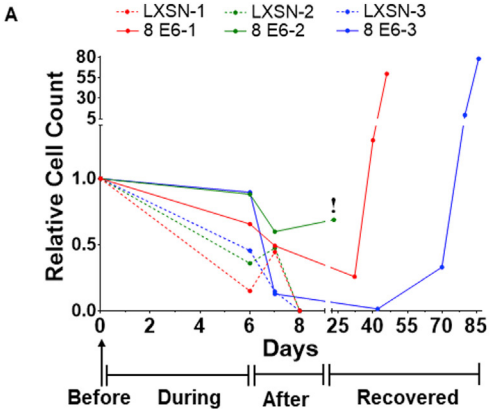

B

Cell Type	% Recovered
LXSN	0% (3/3)
8 E6	0% (3/3)
LXSN + *TERT*	~11% (1/9)
8 E6 + *TERT*	100% (9/9)

Fig. 2. *TERT* expression promotes recovery from failed cytokinesis. (A) Three growth curves (biological replicates) comparing *TERT*-HFK LXSN and β-HPV 8E6 cells before, during, after, and recovered from 6 days of H2CB exposure in 6-well tissue culture plates. LXSN (dashed) and β-HPV 8E6 (solid) data with the same color and number (red, 1; green, 2; and blue, 3) were treated in parallel. **!** signifies the premature end of the long-term cultivation due to bacterial contamination. (B) Percent of HFK and *TERT*-HFK cells capable of long-term growth after 6 days in H2CB. (For interpretation of the references to color in this figure legend, the reader is referred to the Web version of this article.)

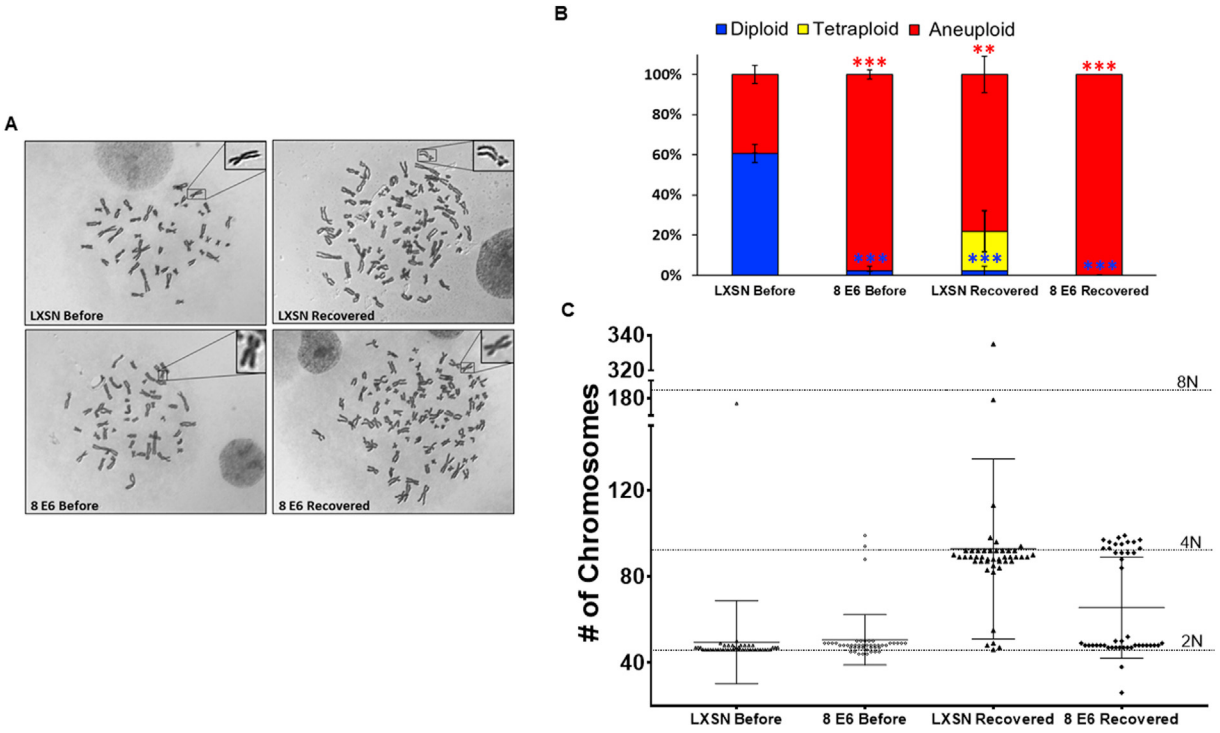

Fig. 3. β-HPV 8E6 and cytokinesis failure induce changes in ploidy. (A) Representative images of metaphase spreads. Insert on the top-right corner shows a magnified chromosome. (B) Relative frequency of diploidy (blue), tetraploidy (yellow), and aneuploidy (red) before H2CB treatment and once cells recovered. Red and blue asterisks denote a significant difference from 'LXSN Before' for aneuploidy and diploidy, respectively. (C) Graphical presentation of the distribution of the number of chromosomes among ≥ 45 cells analyzed by metaphase spreads (before or recovered from 6 days of H2CB exposure). Horizontal-dotted lines represent 46 (2 N), 92 (4 N), or 184 (8 N) chromosomes. ** denotes significant difference between indicated samples $p \leq 0.01$, *** denotes $p \leq 0.001$ (Student's *t*-test). (For interpretation of the references to color in this figure legend, the reader is referred to the Web version of this article.)

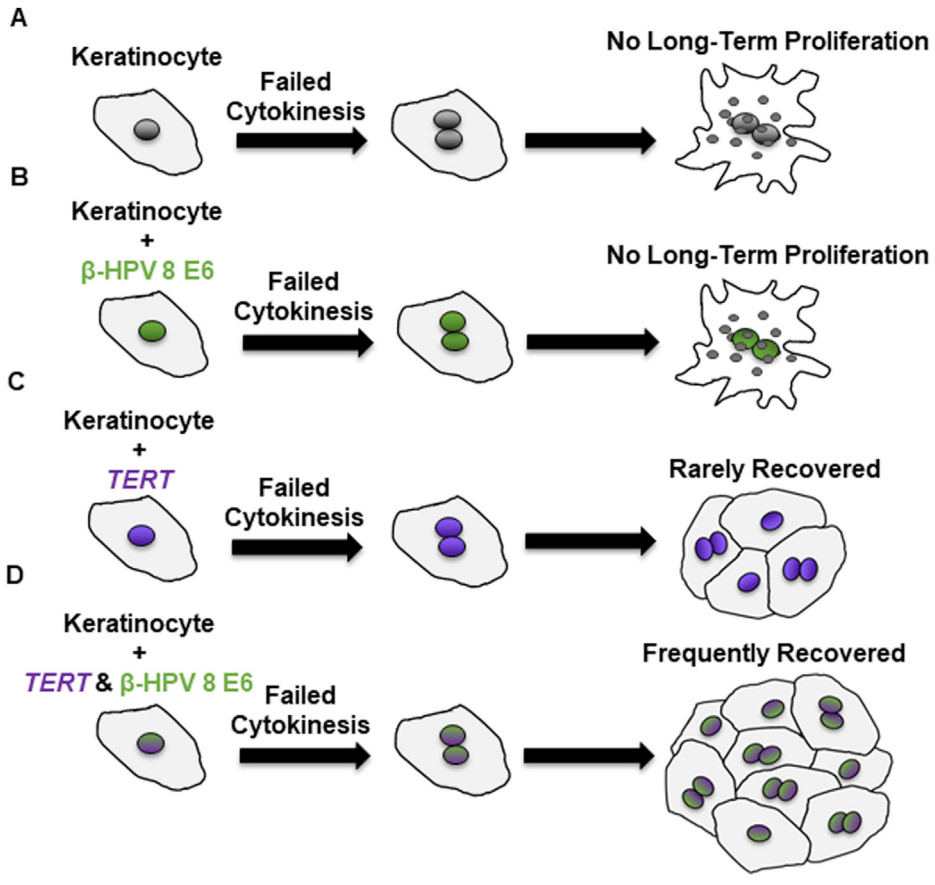

Fig. 4. β-HPV 8E6 and telomerase activation affect cell fate after failed cytokinesis. (A) Keratinocytes that experience H2CB-induced cytokinesis failure become binucleated (indicated by two nuclei inside the cell) resulting in cell death and inhibition of long-term proliferation. (B) β-HPV 8E6 (indicated by green nuclei) reduces the death associated with cytokinesis failure but cells remain unable to sustain long-term proliferation. (C) Keratinocytes immortalized by *TERT* activation (indicated by purple nuclei) experience H2CB-associated binucleation and toxicity, but unlike primary keratinocytes, a small number recover. (D) *TERT* immortalized keratinocytes that co-express β-HPV 8E6 (indicated by green/purple nuclei) regularly survive H2CB-exposure but have high levels of aneuploidy. (For interpretation of the references to color in this figure legend, the reader is referred to the Web version of this article.)

approach. By removing the restrictive nature of primary cell growth, we were able to describe the changes in ploidy stemming from failed cytokinesis. Based on our data, caution should be exercised when examining these systems as *TERT* expression can change the cellular response to genome destabilizing events.

Indeed, our data offers proof of principle that phenotypes associated with β-HPV E6 can change based on the genetic context of viral gene expression. There may be genetic environments where cutaneous papillomavirus infections promote cSCC and others where the same infections prevent cSCC. If this were true, it might help explain conflicting reports that describe these infections as oncogenic and oncopreventative (Howley and Pfister, 2015a; Aldabagh et al., 2013; Strickley et al., 2019; Hasche et al., 2018). Moving forward, it will be interesting to determine the ability of β-HPV E6 to synergize with other common mutations and the mechanism by which β-HPV 8E6 increases aneuploidy.

5. Material and methods

5.1. Cell culture

Primary HFK were derived from neonatal human foreskins. HFK and *TERT*-immortalized-HFK (obtained from Michael Underbrink, University of Texas Medical Branch) were grown in EpiLife medium supplemented with calcium chloride (60 μM), human keratinocyte growth supplement (ThermoFisher Scientific), and penicillin-streptomycin. HPV genes were cloned, transfected, and confirmed as previously described (Wallace et al., 2014). In order not to activate the Hippo pathway via contact inhibition, we carefully monitored the cell density in all experiments. Experiments were aborted if unintended differences in seeding resulted in cell densities that were more than 10% different among cell lines at the beginning of an experiment.

5.2. cBioPortal and gene ontology analysis

Software from (www.cbioportal.org) was used to recognize, analyze, and categorize mutations and transcriptomic data from cutaneous squamous cell carcinomas (Pickering et al., 2014; Li et al., 2015). Analysis of the squamous cell carcinoma samples was done at (http://geneontology.org/) powered by Protein ANalysis THrough Evolutionary Relationships (PANTHER) (The Gene Ontology Resourc, 2019; Ashburner et al., 2000).

5.3. H2CB recovery assay

6-well format: Cells were counted, then either 1.5×10^5 HFK or 5×10^4 *TERT*-HFK cells were seeded on a 6 well tissue culture plate and grown for 24 h. Cells were then treated with 4 μM H2CB, refreshing the H2CB media every 2 days. After 6 days, the cells were washed with PBS and given fresh EpiLife. Once cells reached 90% confluency, they were counted then moved to new 6 wells. This process was continued until cells were no longer able to be passaged or cells could be moved to a 10 cm plate.

10 cm format: Cells were counted, then 3.0×10^5 cells were seeded on a 10 cm tissue culture plate and grown for 24 h. Cells were then treated with 4 μM H2CB, refreshing the H2CB media every 2 days. After 6 days, the cells were washed with PBS and given fresh EpiLife. Once cells reached 90% confluency they were counted, then 9.0×10^4 cells were reseeded. This process was continued until cells were no longer able to be passaged or for 28 days.

5.4. RT-qPCR

Cells were lysed, isolated, reverse transcribed, and then RT-qPCR was performed as previously described (Dacus et al., 2020). The following probes (Thermo Scientific) were used: ACTB (Hs01060665_g1), STK4 (Hs00178979_m1), LATS2 (Referred to as LATS in the text) (Hs01059009_m1), YAP1 (Hs00902712_g1), CTGF (Hs00170014_m1), CYR61 (Hs00155479_m1), TEAD1 (Hs00173359_m1), CCND1 (Hs00765553_m1), AXL (Hs01064444_m1), SERPINE1 (Hs00167155_m1).

5.5. Immunoblotting

Cells were washed and lysed, then lysates were run, transferred, probed, and visualized as previously described (Dacus et al., 2020). The following antibodies were used: GAPDH (Santa Cruz Biotechnologies sc-47724), LATS2 (Referred to as LATS in the text, Cell Signaling Technologies D83D6), Phospho-LATS1/2 (Ser909) (Referred to as pLATS in the text) (Cell Signaling Technologies #9157), YAP (Cell Signaling Technologies 4912S), Phospho-YAP (Ser127) (Referred to pYAP in the text) (Cell Signaling Technologies 4911S), AXL (Cell Signaling Technologies 8661S, p300 (Santa Cruz Biotechnologies sc-584).

5.6. Senescence-associated β-galactosidase staining

Cells were seeded onto three 6-well plates and treated with H2CB then stained as previously described (Dacus et al., 2020).

5.7. Chromosome counts via metaphase spread

'Before' and after cells recovered from H2CB exposure *TERT*-immortalized HFK cells were grown to 80% confluency then chromosomes were detected and counted as previously described (Howe et al., 2014).

5.8. Statistical analysis

Unless otherwise noted, statistical significance was determined by a paired Student *t*-test and was confirmed when appropriate by a two-way analysis of variance (ANOVA) with Turkey's correction. Only *P* values less than 0.05 were reported as significant.

CRediT authorship contribution statement

Dalton Dacus: Conceptualization, Methodology, Validation, Formal analysis, Investigation, Writing - original draft, Writing - review & editing, Visualization, Project administration. **Elizabeth Riforgiate:** Validation, Writing - original draft, Writing - review & editing, Investigation. **Nicholas A. Wallace:** Conceptualization, Methodology, Validation, Investigation, Resources, Writing - original draft, Writing - review & editing, Supervision, Project administration, Funding acquisition.

Declaration of competing interest

The authors declare that they have no conflicts of interests related to the work described in our manuscript.

Acknowledgments:

We thank and acknowledge Jocelyn A. McDonald for assisting with our metaphase spread imaging. Michael Underbrink for providing the *TERT*-immortalized-HFK. Jazmine A. Snow and Emily Burghardt for constructive criticism of the manuscript.

This work was supported by the Department of Defense CMDRP PRCRP CA160224 (NW) and made possible through generous support from the Les Clow family and the Johnson Cancer Research Center at Kansas State University. Declarations of interest: none.

Appendix A. Supplementary data

Supplementary data to this article can be found online at https://doi.org/10.1016/j.virol.2020.07.016.

References

Alam, M., Ratner, D., 2001. Cutaneous squamous-cell carcinoma. N. Engl. J. Med. 344, 975–983.

Aldabagh, B., Angeles, J.G.C., Cardones, A.R., Arron, S.T., 2013. Cutaneous squamous cell carcinoma and human papillomavirus: is there an association? Dermatol. Surg. Off. Publ. Am. Soc. Dermatol. Surg. Al. 39, 1–23.

Alonso-Lecue, P., de Pedro, I., Coulon, V., Molinuevo, R., Lorz, C., Segrelles, C., Ceballos, L., López-Aventín, D., García-Valtuille, A., Bernal, J.M., Mazorra, F., Pujol, R.M., Paramio, J., Ramón Sanz, J., Freije, A., Toll, A., Gandarillas, A., 2017. Inefficient differentiation response to cell cycle stress leads to genomic instability and malignant progression of squamous carcinoma cells. 6. Cell Death Dis. 8, e2901 e2901.

Ashburner, M., Ball, C.A., Blake, J.A., Botstein, D., Butler, H., Cherry, J.M., Davis, A.P., Dolinski, K., Dwight, S.S., Eppig, J.T., Harris, M.A., Hill, D.P., Issel-Tarver, L., Kasarskis, A., Lewis, S., Matese, J.C., Richardson, J.E., Ringwald, M., Rubin, G.M., Sherlock, G., 2000. Gene Ontology: tool for the unification of biology. Nat. Genet. 25, 25–29.

Boxman, I.L.A., Berkhout, R.J.M., Mulder, L.H.C., Wolkers, M.C., Bavinck, J.N.B., Vermeer, B.J., ter Schegget, J., 1997. Detection of human papillomavirus DNA in plucked hairs from renal transplant recipients and healthy volunteers. J. Invest. Dermatol. 108, 712–715.

Boyle, J., Briggs, J.D., RonaM, Mackie, Junor, B.J.R., Aitchison, T.C., 1984. CANCER, warts, and sunshine IN renal transplant patients: a case-control study. Lancet 323, 702–705.

Cerami, E., Gao, J., Dogrusoz, U., Gross, B.E., Sumer, S.O., Aksoy, B.A., Jacobsen, A., Byrne, C.J., Heuer, M.L., Larsson, E., Antipin, Y., Reva, B., Goldberg, A.P., Sander, C., Schultz, N., 2012. The cBio cancer genomics portal: an open platform for exploring multidimensional cancer genomics data. Cancer Discov 2, 401–404.

Chahoud, J., Semaan, A., Chen, Y., Cao, M., Rieber, A.G., Rady, P., Tyring, S.K., 2016. Association between β-genus human papillomavirus and cutaneous squamous cell carcinoma in immunocompetent individuals—a meta-analysis. JAMA Dermatol 152, 1354–1364.

Cheng, K.A., Kurtis, B., Babayeva, S., Zhuge, J., Tantchou, I., Cai, D., Lafaro, R.J., Fallon, J.T., Zhong, M., 2015. Heterogeneity of TERT promoter mutations status in squamous cell carcinomas of different anatomical sites. Ann. Diagn. Pathol. 19, 146–148.

Dacus, D., Cotton, C., McCallister, T.X., Wallace, N.A., 2020. Beta Human Papillomavirus 8E6 Attenuates LATS Phosphorylation after Failed Cytokinesis. Journal of Virology 94. https://doi.org/10.1128/JVI.02184-19.

Davoli, T., Denchi, E.L., de Lange, T., 2010. Persistent telomere damage induces bypass of mitosis and tetraploidy. Cell 141, 81–93.

de Koning, M.N.C., Struijk, L., Bavinck, J.N.B., Kleter, B., ter Schegget, J., Quint, W.G.V., Feltkamp, M.C.W., 2007. Betapapillomaviruses frequently persist in the skin of healthy individuals. J. Gen. Virol. 88, 1489–1495.

Deady, S., Sharp, L., Comber, H., 2014. Increasing skin cancer incidence in young, affluent, urban populations: a challenge for prevention. Br. J. Dermatol. 171, 324–331.

Dickson, M.A., Hahn, W.C., Ino, Y., Ronfard, V., Wu, J.Y., Weinberg, R.A., Louis, D.N., Li, F.P., Rheinwald, J.G., 2000. Human keratinocytes that express hTERT and also bypass a p16INK4a-enforced mechanism that limits life span become immortal yet retain normal growth and differentiation characteristics. Mol. Cell Biol. 20, 1436–1447.

Fahradyan, A., Howell, A.C., Wolfswinkel, E.M., Tsuha, M., Sheth, P., Wong, A.K., 2017. Updates on the management of non-melanoma skin cancer (NMSC). Healthcare 5.

Gabet, A.-S., Accardi, R., Bellopede, A., Popp, S., Boukamp, P., Sylla, B.S., Londoño-Vallejo, J.A., Tommasino, M., 2008. Impairment of the telomere/telomerase system and genomic instability are associated with keratinocyte immortalization induced by the skin human papillomavirus type 38. FASEB J 22, 622–632.

Ganem, N.J., Storchova, Z., Pellman, D., 2007. Tetraploidy, aneuploidy and cancer. Curr. Opin. Genet. Dev. 17, 157–162.

Ganem, N.J., Cornils, H., Chiu, S.-Y., O'Rourke, K.P., Arnaud, J., Yimlamai, D., Théry, M., Camargo, F.D., Pellman, D., 2014. Cytokinesis failure triggers Hippo tumor suppressor pathway activation. Cell 158, 833–848.

Gao, J., Aksoy, B.A., Dogrusoz, U., Dresdner, G., Gross, B., Sumer, S.O., Sun, Y., Jacobsen, A., Sinha, R., Larsson, E., Cerami, E., Sander, C., Schultz, N., 2013. Integrative analysis of complex cancer genomics and clinical profiles using the cBioPortal. Sci. Signal. 6, pl1.

Genders, R.E., Mazlom, H., Michel, A., Plasmeijer, E.I., Quint, K.D., Pawlita, M., van der Meijden, E., Waterboer, T., de Fijter, H., Claas, F.H., Wolterbeek, R., Feltkamp, M.C.W., Bouwes Bavinck, J.N., 2015. The presence of betapapillomavirus antibodies around transplantation predicts the development of keratinocyte carcinoma in organ transplant recipients: a cohort study. J. Invest. Dermatol. 135, 1275–1282.

Griewank, K.G., Murali, R., Schilling, B., Schimming, T., Möller, I., Moll, I., Schwamborn, M., Sucker, A., Zimmer, L., Schadendorf, D., Hillen, U., 2013. TERT promoter mutations are frequent in cutaneous basal cell carcinoma and squamous cell carcinoma. PLoS ONE 8.

Hampras, S.S., Giuliano, A.R., Lin, H.-Y., Fisher, K.J., Abrahamsen, M.E., Sirak, B.A., Iannacone, M.R., Gheit, T., Tommasino, M., Rollison, D.E., 2014. Natural history of cutaneous human papillomavirus (HPV) infection in men: the HIM study. PLOS ONE 9, e104843.

Hampras, S.S., Rollison, D.E., Giuliano, A.R., McKay-Chopin, S., Minoni, L., Sereday, K., Gheit, T., Tommasino, M., 2017. Prevalence and concordance of cutaneous beta human papillomavirus infection at mucosal and cutaneous sites. J. Infect. Dis. 216, 92–96.

Hasche, D., Vinzón, S.E., Rösl, F., 2018. Cutaneous papillomaviruses and non-melanoma skin cancer: causal agents or innocent bystanders? Front. Microbiol. 9.

Hayashi, M.T., Karlseder, J., 2013. DNA damage associated with mitosis and cytokinesis failure. Oncogene 32, 4593–4601.

Hollestein, L.M., de Vries, E., Aarts, M.J., Schroten, C., Nijsten, T.E.C., 2014. Burden of disease caused by keratinocyte cancer has increased in The Netherlands since 1989. J. Am. Acad. Dermatol. 71, 896–903.

Howe, B., Umrigar, A., Tsien, F., 2014. Chromosome preparation from cultured cells. J Vis Exp. https://doi.org/10.3791/50203. e50203.

Howie, H.L., Koop, J.I., Weese, J., Robinson, K., Wipf, G., Kim, L., Galloway, D.A., 2011. Beta-HPV 5 and 8 E6 promote p300 degradation by blocking AKT/p300 association. PLoS Pathog. 7.

Howley, P.M., Pfister, H.J., 2015a. Beta genus papillomaviruses and skin cancer. Virology 290–296 0.

Howley, P.M., Pfister, H.J., 2015b. Beta genus papillomaviruses and skin cancer. Virology 290–296 0.

Hufbauer, M., Akgül, B., 2017. Molecular mechanisms of human papillomavirus induced skin carcinogenesis. Viruses 9.

Lens, S.M.A., Medema, R.H., 2019. Cytokinesis defects and cancer. Nat Rev Cancer 19, 32–45.

Li, Y.Y., Hanna, G.J., Laga, A.C., Haddad, R.I., Lorch, J.H., Hammerman, P.S., 2015. Genomic analysis of metastatic cutaneous squamous cell carcinoma. Clin Cancer Res Off J Am Assoc Cancer Res 21, 1447–1456.

Lomas, A., Leonardi-Bee, J., Bath-Hextall, F., 2012. A systematic review of worldwide incidence of nonmelanoma skin cancer. Br. J. Dermatol. 166, 1069–1080.

Martincorena, I., Roshan, A., Gerstung, M., Ellis, P., Loo, P.V., McLaren, S., Wedge, D.C., Fullam, A., Alexandrov, L.B., Tubio, J.M., Stebbings, L., Menzies, A., Widaa, S., Stratton, M.R., Jones, P.H., Campbell, P.J., 2015. High burden and pervasive positive selection of somatic mutations in normal human skin. Science 348, 880–886.

McLaughlin-Drubin, M.E., 2015. Human papillomaviruses and non-melanoma skin cancer. Semin. Oncol. 42, 284–290.

Meyers, J.M., Uberoi, A., Grace, M., Lambert, P.F., Munger, K., 2017. Cutaneous HPV8 and MmuPV1 E6 proteins target the NOTCH and TGF-β tumor suppressors to inhibit differentiation and sustain keratinocyte proliferation. PLoS Pathog. 13.

Mi, H., Huang, X., Muruganujan, A., Tang, H., Mills, C., Kang, D., Thomas, P.D., 2017. PANTHER version 11: expanded annotation data from Gene Ontology and Reactome pathways, and data analysis tool enhancements. Nucleic Acids Res. 45, D183–D189.

Nunes, E.M., Talpe-Nunes, V., Sichero, L., 2018. Epidemiology and biology of cutaneous human papillomavirus. Clinics 73.

Orth, G., 2008. Host defenses against human papillomaviruses: lessons from epidermodysplasia verruciformis. Curr. Top. Microbiol. Immunol. 321, 59–83.

Patel, A.S., Karagas, M.R., Perry, A.E., Nelson, H.H., 2008. Exposure profiles and human papillomavirus infection in skin cancer: an analysis of 25 genus β-types in a population-based study. J. Invest. Dermatol. 128, 2888–2893.

Pickering, C.R., Zhou, J.H., Lee, J.J., Drummond, J.A., Peng, S.A., Saade, R.E., Tsai, K.Y., Curry, J.L., Tetzlaff, M.T., Lai, S.Y., Yu, J., Muzny, D.M., Doddapaneni, H., Shinbrot, E., Covington, K.R., Zhang, J., Seth, S., Caulin, C., Clayman, G.L., El-Naggar, A.K., Gibbs, R.A., Weber, R.S., Myers, J.N., Wheeler, D.A., Frederick, M.J., 2014. Mutational landscape of aggressive cutaneous squamous cell carcinoma. Clin. Cancer Res. Off. J. Am. Assoc. Cancer Res. 20, 6582–6592.

Pópulo, H., Boaventura, P., Vinagre, J., Batista, R., Mendes, A., Caldas, R., Pardal, J., Azevedo, F., Honavar, M., Guimarães, I., Manuel Lopes, J., Sobrinho-Simões, M., Soares, P., 2014. TERT promoter mutations in skin cancer: the effects of sun exposure and X-irradiation. J. Invest. Dermatol. 134, 2251–2257.

Rollison, D.E., Viarisio, D., Amorrortu, R.P., Gheit, T., Tommasino, M., 2019. An emerging issue in oncogenic virology: the role of beta human papillomavirus types in the development of cutaneous squamous cell carcinoma. J. Virol. 93, e01003–e01018.

Scott, G.A., Laughlin, T.S., Rothberg, P.G., 2014. Mutations of the *TERT* promoter are common in basal cell carcinoma and squamous cell carcinoma. Mod. Pathol. 27, 516–523.

Storchova, Z., Kuffer, C., 2008. The consequences of tetraploidy and aneuploidy. J. Cell Sci. 121, 3859–3866.

Strickley, J.D., Messerschmidt, J.L., Awad, M.E., Li, T., Hasegawa, T., Ha, D.T., Nabeta, H.W., Bevins, P.A., Ngo, K.H., Asgari, M.M., Nazarian, R.M., Neel, V.A., Jenson, A.B., Joh, J., Demehri, S., 2019. Immunity to commensal papillomaviruses protects against skin cancer. Nature 575, 519–522.

The gene ontology resource: 20 years and still GOing strong. Nucleic. Acids Res. 47, D330–D338.

Tommasino, M., 2017. The biology of beta human papillomaviruses. Virus Res. 231, 128–138.

Underbrink, M.P., Howie, H.L., Bedard, K.M., Koop, J.I., Galloway, D.A., 2008. E6 proteins from multiple human betapapillomavirus types degrade Bak and protect keratinocytes from apoptosis after UVB irradiation. J. Virol. 82, 10408–10417.

Urquidi, V., Tarin, D., Goodison, S., 2000. Role of telomerase in cell senescence and oncogenesis. Annu. Rev. Med. 51, 65–79.

Victorelli, S., Passos, J.F., 2017. Telomeres and cell senescence - size matters not. EBioMedicine 21, 14–20.

Wallace, N.A., Robinson, K., Galloway, D.A., 2014. Beta human papillomavirus E6 expression inhibits stabilization of p53 and increases tolerance of genomic instability. J. Virol. 88, 6112–6127.

Wang, J., Dupuis, C., Tyring, S.K., Underbrink, M.P., 2016. Sterile α motif domain containing 9 is a novel cellular interacting partner to low-risk type human papillomavirus E6 proteins. PLoS ONE 11.

Weissenborn, S.J., Nindl, I., Purdie, K., Harwood, C., Proby, C., Breuer, J., Majewski, S.,

Pfister, H., Wieland, U., 2005. Human papillomavirus-DNA loads in actinic keratoses exceed those in non-melanoma skin cancers. J. Invest. Dermatol. 125, 93–97.
Weissenborn, S.J., De Koning, M.N.C., Wieland, U., Quint, W.G.V., Pfister, H.J., 2009. Intrafamilial transmission and family-specific spectra of cutaneous betapapillomaviruses. J. Virol. 83, 811–816.
Wendel, S.O., Wallace, N.A., 2017. Loss of genome fidelity: beta HPVs and the DNA damage response. Front. Microbiol. 8.
White, E.A., Kramer, R.E., Tan, M.J.A., Hayes, S.D., Harper, J.W., Howley, P.M., 2012. Comprehensive analysis of host cellular interactions with human papillomavirus E6 proteins identifies new E6 binding partners and reflects viral diversity. J. Virol. 86, 13174–13186.
Winer, R.L., Gheit, T., Cherne, S., Lin, J., Stern, J.E., Poljak, M., Feng, Q., Tommasino, M., 2017. Prevalence and correlates of beta human papillomavirus detection in fingernail samples from mid-adult women. Papillomavirus Res 5, 1–5.

cancers

MDPI

Article

Beta Human Papillomavirus 8E6 Attenuates Non-Homologous End Joining by Hindering DNA-PKcs Activity

Changkun Hu [1], Taylor Bugbee [1], Monica Gamez [2] and Nicholas A. Wallace [1,*]

[1] Division of Biology, Kansas State University, Manhattan, KS 66506, USA; chu1@ksu.edu (C.H.); tbugbee@ksu.edu (T.B.)

[2] Bristol Medical School, Translational Health Sciences, University of Bristol, Bristol BS1 3NY, UK; mg14606@bristol.ac.uk

* Correspondence: nwallac@ksu.edu

Received: 19 July 2020; Accepted: 18 August 2020; Published: 20 August 2020

Abstract: Cutaneous viral infections occur in a background of near continual exposure to environmental genotoxins, like UV radiation in sunlight. Failure to repair damaged DNA is an established driver of tumorigenesis and substantial cellular resources are devoted to repairing DNA lesions. Beta-human papillomaviruses (β-HPVs) attenuate DNA repair signaling. However, their role in human disease is unclear. Some have proposed that β-HPV promotes tumorigenesis, while others suggest that β-HPV protects against skin cancer. Most of the molecular evidence that β-HPV impairs DNA repair has been gained via characterization of the E6 protein from β-HPV 8 (β-HPV 8E6). Moreover, β-HPV 8E6 hinders DNA repair by binding and destabilizing p300, a transcription factor for multiple DNA repair genes. By reducing p300 availability, β-HPV 8E6 attenuates a major double strand DNA break (DSB) repair pathway, homologous recombination. Here, β-HPV 8E6 impairs another DSB repair pathway, non-homologous end joining (NHEJ). Specifically, β-HPV 8E6 acts by attenuating DNA-dependent protein kinase (DNA-PK) activity, a critical NHEJ kinase. This includes DNA-PK activation and the downstream of steps in the pathway associated with DNA-PK activity. Notably, β-HPV 8E6 inhibits NHEJ through p300 dependent and independent means. Together, these data expand the known genome destabilizing capabilities of β-HPV 8E6.

Keywords: human papillomavirus; HPV; DNA repair; double strand breaks; non-homologous end joining

1. Introduction

Human papillomavirus (HPV) is a small double-stranded DNA virus family that infects mucosal and cutaneous epithelia. Currently, about 400 types of HPV have been identified [1]. This family is classified into five genera (alpha, beta, gamma, mu, and nu), based on the sequence of the L1 capsid gene [2–5]. Of these genera, the alpha genus of HPV has been most thoroughly characterized because members of this genus cause cervical cancer, head and neck cancer, and genital warts [2,4,6]. Despite their widespread presence in the skin, the contribution of members of the beta genus of HPV (β-HPV) to human disease is unclear. Moreover, β-HPVs were first isolated from patients with a rare genetic disorder, epidermodysplasia verruciformis (EV) [5,7]. In these individuals and people receiving immunosuppressive drugs after organ transplants, β-HPVs appear to promote non-melanoma skin cancer (NMSC) [5,8]. An array of in vivo and in vitro studies also support the role of β-HPVs in promoting NMSC [9,10].

However, there are questions about the oncogenic potential of β-HPV in the general population. In most immunocompetent individuals, β-HPV infections are transient [11]. Furthermore, β-HPV genes

are rarely expressed in tumor tissue [12,13]. This ruled out traditional methods of viral oncogenesis where the tumor becomes dependent on continued viral gene expression and led to the so-called "hit and run" hypothesis [13]. This hypothesis proposes that β-HPVs promote early stages of tumorigenesis by destabilizing the host genome, leading to mutations that could drive oncogenesis without continued viral gene expression [14]. Although feasible, the model is difficult to test. As a result, it remains unclear if/how frequently β-HPV infections contribute to NMSC. The "hit and run" model faced further challenges when a recent report suggested β-HPV infections protected against NMSC [15]. The widespread nature of these infections and their contentious role in tumorigenesis are strong motivating factors for ongoing research into the basic biology of the virus and its gene products.

Among β-HPV proteins, the E6 or β-HPV E6 is best characterized. This report focuses on the E6 from β-HPV 8 (β-HPV 8E6), and its ability to disrupt DNA repair [16–19]. Interestingly, β-HPV 8E6 exerts its influence in part by binding and destabilizing the cellular histone acetyltransferase, p300 [20]. Moreover, p300 is a transcription factor necessary for robust expression of key DNA repair proteins (ATM, ATR, BRCA1 and BRCA2) [16–18]. When β-HPV 8E6 is present, the reduced availability of these repair factors makes UV-induced DNA lesions more persistent [17,18]. The inability to resolve these lesions increases the frequency of replication fork collapse and the generation of UV-induced double stranded DNA breaks (DSBs) [18]. These breaks occur during S and G2 phases of the cell cycle, when homologous recombination (HR) is the principle mechanism of DSB repair [21–25]. Despite increasing the need for HR, β-HPV 8E6 impairs the pathway by decreasing BRCA1 and BRCA2 expression and foci formation [16].

When HR fails, non-homologous end joining (NHEJ) serves as a backup repair mechanism. NHEJ is not restricted to any portion of the cell cycle, but tends to occur when HR is not available (i.e., G1 and early S phases) [26–30]. It is an error-prone pathway that initiates with 53BP1 binding to the DSB [31,32]. This simultaneously promotes NHEJ, while restricting HR [32–37]. After 53BP1 binding, a heterodimer of Ku70 and Ku80 is recruited to the damaged site, tethering at the exposed DNA ends [27]. Next, DNA-dependent protein kinase catalytic subunit (DNA-PKcs) binds to the Ku dimer to form a holoenzyme, known as DNA-PK. Then, DNA-PKcs becomes activated by auto-phosphorylation (pDNA-PKcs) [38–40]. Once activated, pDNA-PKcs facilitates NHEJ by phosphorylating/activating downstream targets, including Artemis, XRCC4, and DNA ligase IV (LIG4) [40–44]. Artemis has both exonuclease and endonuclease activity that processes DNA single-strand overhangs into blunt end NHEJ-ready substrates [45–47]. When overhanging DNA ends have been removed, the XRCC4-XLF-Ligase IV complex links the two DNA ends together [48,49].

Since limitations in HR are addressed with increases in NHEJ, it was reasonable to hypothesize that β-HPV 8E6 increased repair by NHEJ. However, this report presents contrary evidence to this idea. Furthermore, β-HPV 8E6 reduced NHEJ repair at a defined genomic location and reduced DNA-PKcs autophosphorylation. This culminated in more persistent DNA-PKcs foci and diminished pDNA-PKcs-dependent signaling events (phosphorylation of Artemis and XRCC4 repair complex formation). Interestingly, β-HPV 8E6 appears to diminish NHEJ activity, through both p300-dependent and -independent mechanisms.

2. Results

2.1. β-HPV 8E6 Decreases NHEJ Efficiency

We have previously shown that β-HPV 8E6 disrupts HR by destabilizing p300, a transcription factor for two HR genes (BRCA1 and BRCA2) [16]. NHEJ competes with HR for access to DSBs [26,50,51], suggesting that NHEJ may occur more frequently in cells expressing β-HPV 8E6. To test this, we measured NHEJ efficiency, using a recently described end-joining assay that uses CD4 expression as a readout [28]. In this assay, CAS9 endonucleases are used to create breaks in the human genome downstream of the GAPDH promoter, and upstream of the CD4 exon. These genes are oriented in the same direction and sit ~0.25 Mb apart. When NHEJ repairs the breaks, it results in a recombination event

where CD4 expression is driven by the GAPDH promoter (Figure 1A). The CD4 promoter is typically inactive in cells outside of the immune system, which provides a low background in many cell types [52]. This assay was verified by measuring NHEJ efficiency in U2OS cells. CD4 expression was detected by immunoblot and normalized to the abundance of FLAG-tagged CAS9, as a control for transfection efficiency (Figure 1B,C). As previously reported, expression of CAS9 endonucleases targeting GAPDH and CD4 lead to CD4 expression. The assay was further verified by treating U2OS cells with 10 μM ATM inhibitor (KU55933) and 10 μM DNA-PKcs inhibitor (NU7441), that are known to increase and decrease NHEJ, respectively [28,38]. As expected, KU55933 increased CD4 expression, while NU7441 decreased it (Figure 1B,C). Next, the impact of β-HPV 8E6 on NHEJ was determined in previously described U2OS cells, expressing β-HPV 8E6 (U2OS β-HPV 8E6) or vector control (U2OS LXSN). Unexpectedly, β-HPV 8E6 significantly decreased CD4 compared to U2OS LXSN cells (Figure 1D,E). The p300-dependence of this phenotype was also probed in U2OS cells, expressing a mutant β-HPV 8E6 (β-HPV Δ8E6), where 5 amino acids responsible for p300 binding (Residues 132–136) were deleted [20]. NHEJ frequency was also decreased in these cells (U2OS β-HPV Δ8E6) (Figure 1D,E). Neither inhibitor nor expression of wild type or mutant β-HPV 8E6 significantly altered transfection efficiency (Figure S1). To determine if these results were reproducible in a more physiological relevant cell line, the assay was repeated in a pair of previously described telomerase immortalized human foreskin keratinocytes (HFK) cell lines [53]. Again, β-HPV 8E6 expressing HFK cells (HFK β-HPV 8E6) had reduced NHEJ efficiency, compared with vector control HFK cells (HFK LXSN, Figure 1F,G). Together, these data indicate that β-HPV 8E6 hinders NHEJ, through p300-independent mechanisms. However, they cannot rule out the possibility that β-HPV 8E6 also acts through a p300-dependent mechanism.

2.2. β-HPV 8E6 Attenuates DNA-PKcs Phosphorylation

β-HPV 8E6 prevents the repair of UV lesions and completion of HR by reducing the abundance of key repair factors (ATM, ATR, BRCA1 and BRCA2) [16–18]. This suggests that β-HPV 8E6 may act through a similar mechanism to impair NHEJ. To assess this possibility, the abundance of canonical NHEJ proteins was determined in HFK. In untreated HFK cells, β-HPV 8E6 did not decrease Ku80, DNA-PKcs, Artemis, XRCC4, or Ligase IV abundance (Figure S2). These data suggest that β-HPV 8E6 exerted its influence in a post-translational manner, so DNA-PKcs activation (via autophosphorylation at S2056) was assessed in cells exposed to Zeocin, a radiomimetic [54,55]. This modification was chosen because phosphorylated DNA-PKcs or pDNA-PKcs is a well characterized and early step in NHEJ [39,56]. Cells were treated with designated Zeocin concentrations for 24 hours (Figure 2). pDNA-PKcs increased in a Zeocin dose-dependent manner in HFK LXSN. However, this response was attenuated in HFK β-HPV 8E6 (Figure 2A,B, Figure S3A). Similar results were observed when the experiment was repeated in U2OS LXSN and U2OS β-HPV 8E6 cells. However, U2OS expressing β-HPV Δ8E6 (U2OS β-HPV Δ8E6) behaved like U2OS LXSN cells, by increasing the proportion of activated DNA-PKcs in response to Zeocin exposure (Figure 2C,D). These data suggest that β-HPV 8E6 impairs DNA-PKcs activation in a p300-dependent manner. pDNA-PKcs and total DNA-PKcs were separately normalized to GAPDH (Figure S3). Consistently, β-HPV 8E6 attenuated DNA-PKcs phosphorylation, in both HFK and U2OS. Zeocin exposure consistently decreased total DNA-PKcs. However, β-HPV 8E6 did not statistically significantly change this decrease (Figure S3B,D).

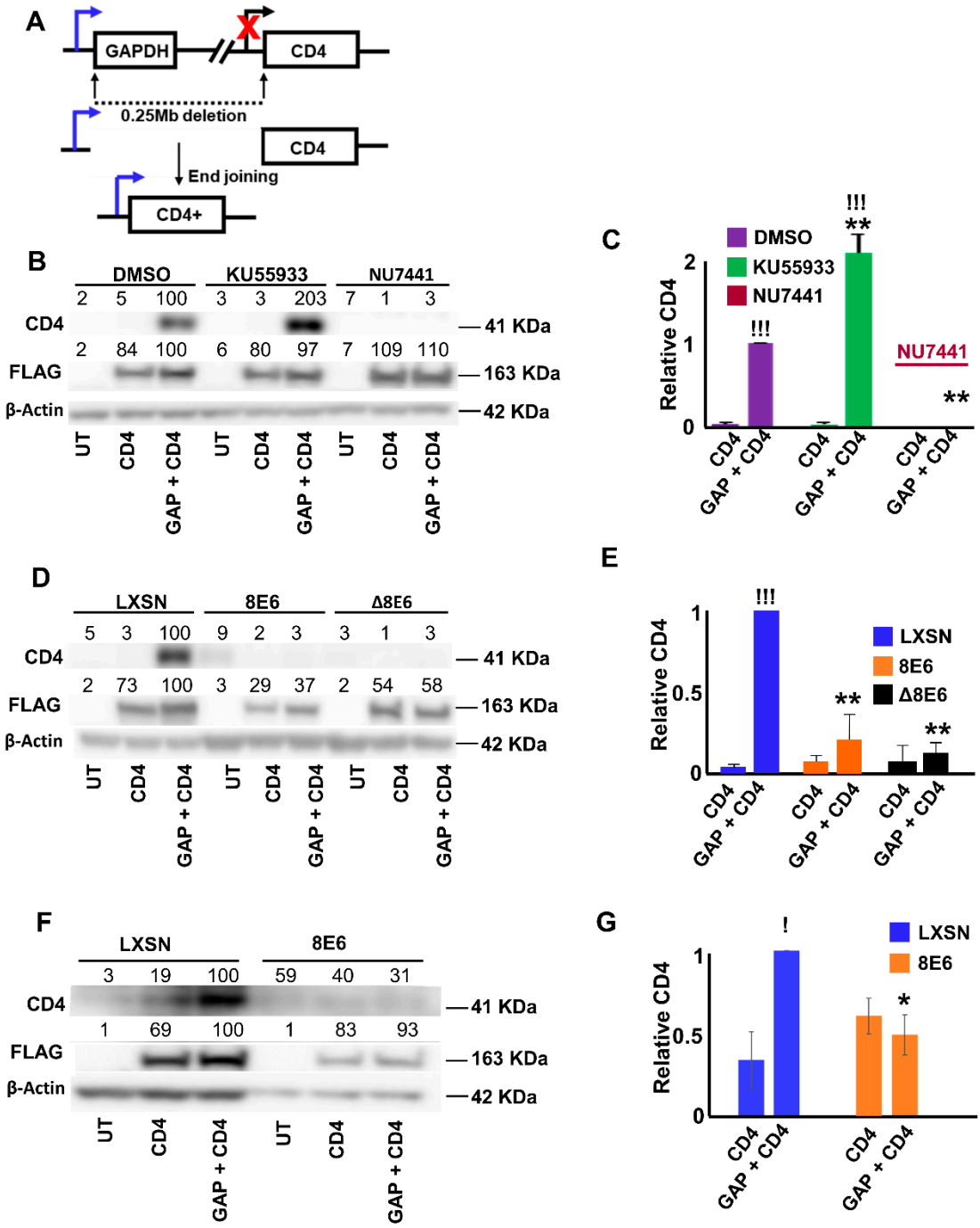

Figure 1. Moreover, beta-human papillomavirus (β-HPV) 8E6 decreases non-homologous end joining (NHEJ) efficiency, using CD4 expression as a readout. (**A**) Schematic of end-joining reporter assay. FLAG-tagged SgRNA-CAS9 induced double strand breaks in GAPDH and CD4 on chromosome 12 in U2OS cells. Rearrangement leads to CD4 expression driven by the promoter of GAPDH. Red "X" represents that CD4 expression is naturally inactivated. (**B**) Representative immunoblots showing CD4 expression in U2OS cells treated with control, ATM inhibitor (KU55933), and DNA-PK inhibitor (NU7441), after transfection with control (UT), FLAG-tagged SgRNA-CAS9 targeting CD4 (CD4), and FLAG-tagged SgRNA-CAS9 targeting GAPDH together with FLAG-tagged SgRNA-CAS9 targeting CD4 (GAP/CD4). (**C**) Densitometry of immunoblots (n = 3) from panel B. CD4 was normalized to β-actin as a loading control. Transfection efficiency was accounted for using FLAG abundance. (**D**) Representative immunoblots showing CD4 expression in U2OS LXSN, β-HPV 8 E6, and β-HPV Δ8E6 after transfection with control (UT), FLAG-tagged SgRNA-CAS9 targeting CD4 (CD4), and FLAG-tagged SgRNA-CAS9

targeting GAPDH and FLAG-tagged SgRNA-CAS9 targeting CD4 (GAP/CD4). (**E**) Densitometry of immunoblots (n = 3) from panel D. CD4 was normalized to β-actin as a loading control. Transfection efficiency was accounted for using FLAG abundance. (**F**) Representative immunoblots showing CD4 expression in HFK LXSN and HFK β-HPV 8 E6, after transfection with control (UT), FLAG-tagged SgRNA-CAS9 targeting CD4 (CD4), and FLAG-tagged SgRNA-CAS9 targeting GAPDH and FLAG-tagged SgRNA-CAS9 targeting CD4 (GAP/CD4). (**G**) Densitometry of immunoblots (n = 3) from panel F. CD4 was normalized to β-actin as a loading control. Transfection efficiency was accounted for using FLAG abundance. All values are represented as mean ± standard error from at least three independent experiments. Statistical differences between groups were measured by using Student's t-test. * indicates $p < 0.05$. ** indicates $p < 0.01$. ! indicates significant difference between transfection with SgRNA-CAS9 targeting CD4 and co-transfection with SgRNA-CAS9 targeting CD4 and GAPDH. !!! indicates significant difference between transfection with SgRNA-CAS9 targeting CD4 and co-transfection with SgRNA-CAS9 targeting CD4 and GAPDH ($p < 0.001$).

To probe the breadth of DNA-PKcs inhibition, another genotoxic reagent (hydrogen peroxide, or H_2O_2) was used to activate NHEJ in U2OS LXSN, U2OS β-HPV 8E6 and U2OS β-HPV Δ8E6 cells. Unlike Zeocin, which induces breaks by intercalating into base pairs and causing cleavage, H_2O_2 generates DSBs by generating reactive oxygen species (ROS) [54,55]. This represents a more physiological type of DSB, as ROS are caused by cell metabolism [57]. β-HPV 8E6 and β-HPV Δ8E6 blunted pDNA-PKcs in response to H_2O_2 (Figure S4A,B).

To facilitate repair, pDNA-PKcs must localize to a DSBs. This localization results in complexes that are detectable as foci by immunofluorescence (IF) microscopy. These foci are indicative of ongoing repair. pDNA-PKcs foci were readily detected in untreated HFK LXSN cells, but less frequent in HFK β-HPV 8E6 cells (Figure 3A,B). Prior reports found that β-HPV 8E6 increased the frequency of DSBs in untreated cells, suggesting that the reduced pDNA-PKcs foci are unlikely to indicate genomic stabilization [16]. An alternative explanation consistent with the data shown in Figure 1 is that β-HPV 8E6 reduced the frequency of NHEJ. When repair complexes are not resolved, the repair proteins spread along nearby chromatin producing larger/brighter foci [58–60]. As a result, foci intensity was used as an indicator of repair efficiency (brighter foci indicate more persistent lesions). Consistent with NHEJ inhibition, β-HPV E6 increased pDNA-PKcs foci intensity in HFKs (Figure 3A,C). Similar results were obtained in U2OS cells (Figure 3D–F). Interestingly, β-HPV Δ8E6 did not alter pDNA-PKcs foci prevalence or intensity (Figure 3D–F). Together, our data suggest that β-HPV 8E6 hinders DNA-PKcs activation in a p300-dependent manner (Figures 1–3), but also can impair NHEJ through a p300-independent mechanism(s) (Figure 1D,E).

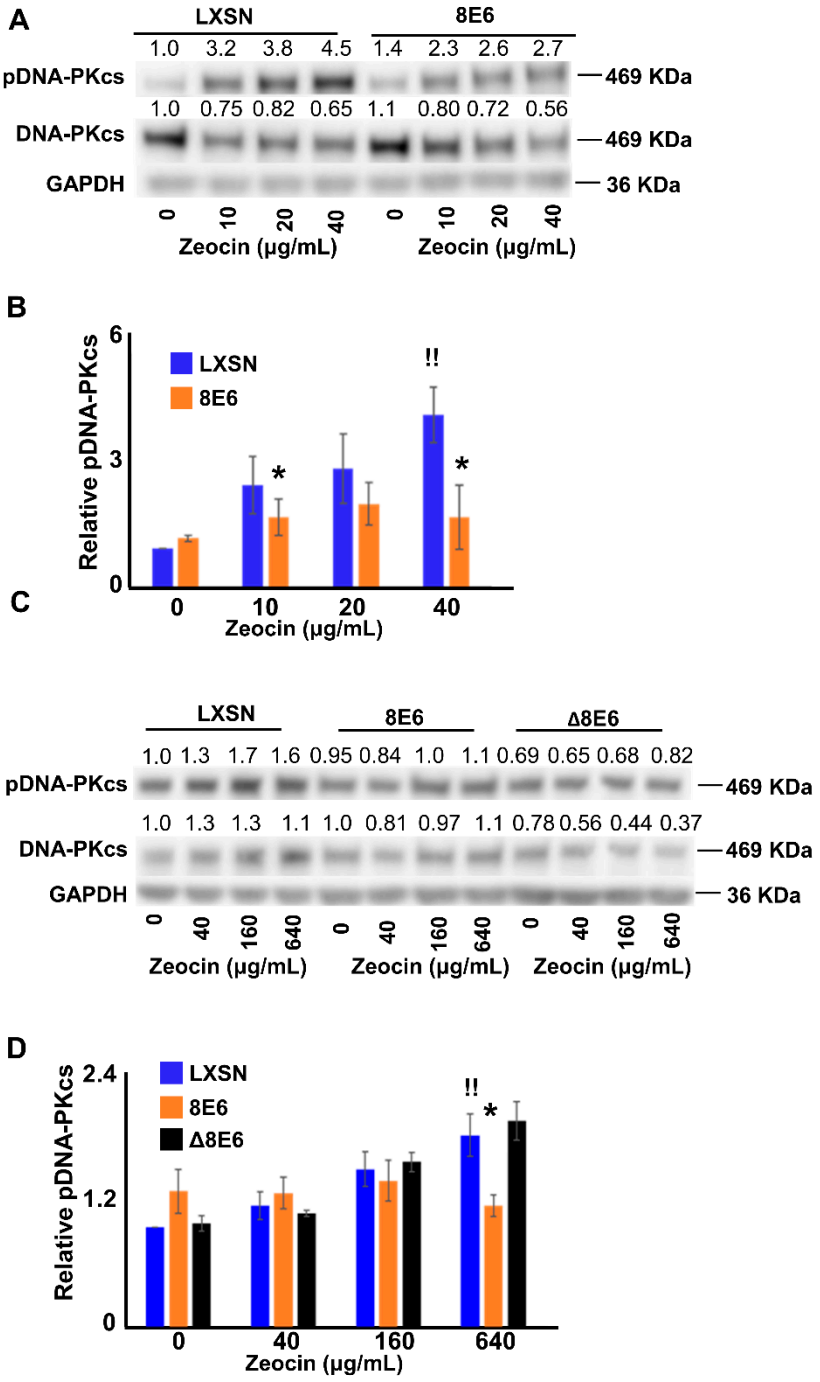

Figure 2. β-HPV 8E6 attenuates DNA-PKcs phosphorylation. (**A**) Representative immunoblot showing phospho-DNA-PKcs (pDNA-PKcs) and total DNA-PKcs in HFK LXSN and HFK β-HPV 8 E6. (**B**) Densitometry of immunoblots of pDNA-PKcs normalized to total DNA-PKcs and GAPDH as a loading control. (**C**) Representative immunoblot showing pDNA-PKcs and DNA-PKcs in U2OS LXSN, U2OS β-HPV 8 E6, and U2OS β-HPV Δ8 E6. (**D**) Densitometry of immunoblots (n = 4) of pDNA-PKcs normalized to total DNA-PKcs and GAPDH as a loading control. All values are represented as mean ± standard error from at least three independent experiments. Statistical differences between groups were measured by using Student's t-test. * indicates $p < 0.05$. !! indicates significant difference between Zeocin treated and untreated group.

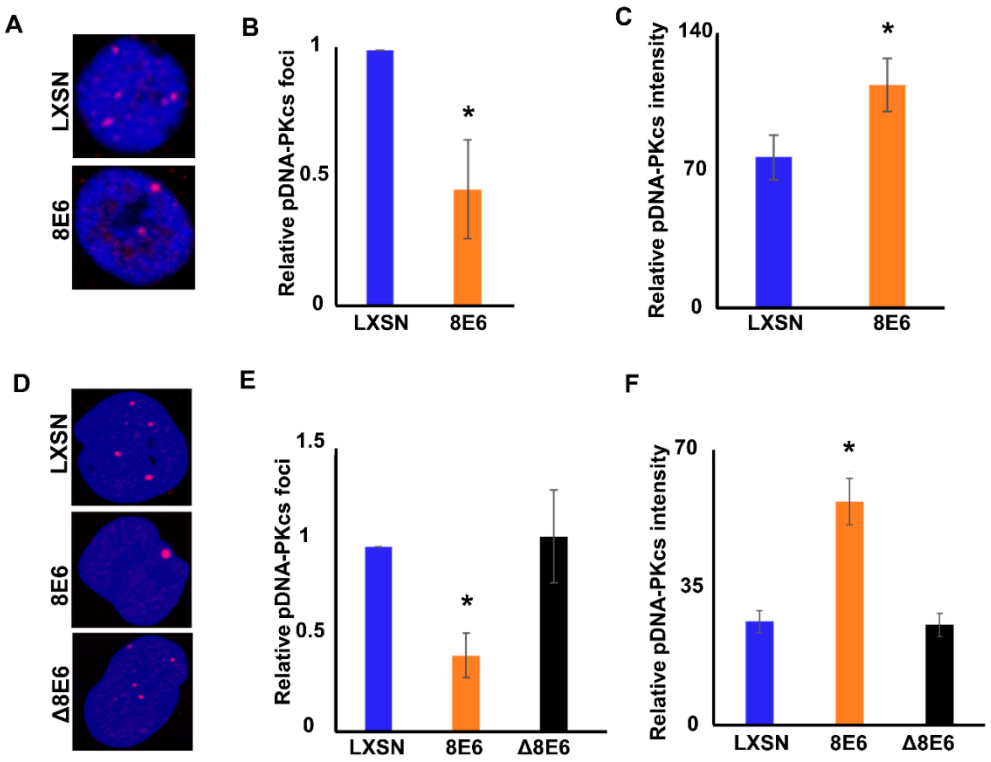

Figure 3. β-HPV 8E6 increases pDNA-PKcs foci size, but decreases frequency in untreated cells. (**A**) Representative images of pDNA-PKcs foci in HFK LXSN and HFK β-HPV 8 E6. (**B**) Percentages of cells with one or more pDNA-PKcs foci. (**C**) Average pDNA-PKcs foci intensity of HFK cells. (**D**) Representative images of pDNA-PKcs foci in U2OS LXSN, U2OS β-HPV 8 E6, and U2OS β-HPV Δ8 E6. (**E**) Percentages of cells with one or more pDNA-PKcs foci. (**F**) Average pDNA-PKcs focus intensity in U2OS cells. All values are represented as mean ± standard error from at least three independent experiments. Statistical differences between groups were measured by using Student's *t*-test. * indicates $p < 0.05$. All microscopy images are 400X magnification.

2.3. β-HPV 8E6 Attenuates DNA-PKcs-Dependent Signaling

To further determine the ability of β-HPV 8E6 to alter pDNA-PKcs signaling, DSBs were induced with Zeocin (10 μg/mL), then observed with immunofluorescence microscopy. pDNA-PKcs foci appeared rapidly in HFK LXSN cells and reached their maxima approximately one hour after Zeocin exposure (Figure 4A,B). Twenty-four hours later, the pDNA-PKcs foci had returned to background levels. β-HPV 8E6 did not alter the initial induction of pDNA-PKcs foci by Zeocin. However, pDNA-PKcs foci were significantly more persistent in HFK β-HPV 8E6 cells. Similar results were obtained in U2OS LXSN and U2OS β-HPV 8E6 cells (Figure 4C,D). Consistent with a p300-dependent mechanism, pDNA-PKcs foci kinetics were similar in U2OS β-HPV Δ8E6 and U2OS LXSN cells after Zeocin exposure (100 μg/mL). Supporting the idea that pDNA-PKcs foci represent active repair complexes, while pDNA-PKcs was detected in damage induced foci, total DNA-PKcs showed pan-nuclear staining in treated and untreated cells (Figure S5).

Having seen β-HPV 8E6 impair DNA-PKcs autophosphorylation and repair complex resolution, the ability of β-HPV 8E6 to hinder other DNA-PKcs-dependent steps in NHEJ was determined. Published reports indicated that Artemis is a DSB-induced target of DNA-PKcs phosphorylation at Serine 516 (pArtemis) [46,47]. This relationship was confirmed using immunoblots to detect pArtemis when DNA-PKcs activity was blocked with a small molecule inhibitor (1 μM NU7441). While pArtemis levels rose in a Zeocin dose-dependent manner in wild type cells, pArtemis abundance was limited by the inhibitor (Figure S6). Having confirmed that Artemis phosphorylation depended on DNA-PKcs activity, the extent that β-HPV 8E6 reduced phosphorylation of Artemis in response to Zeocin was

defined. β-HPV 8E6 blocked Artemis phosphorylation in HFKs (Figure 5A,B, Figure S7A). These results were also reproducible in U2OS (Figure 5C,D, Figure S7C,D). Notably, pArtemis levels rose in U2OS LXSN and U2OS β-HPV △8E6 cells in response to Zeocin. These data indicate that β-HPV 8E6 's p300-dependent attenuation of DNA-PKcs-dependent signaling extended to Artemis activation.

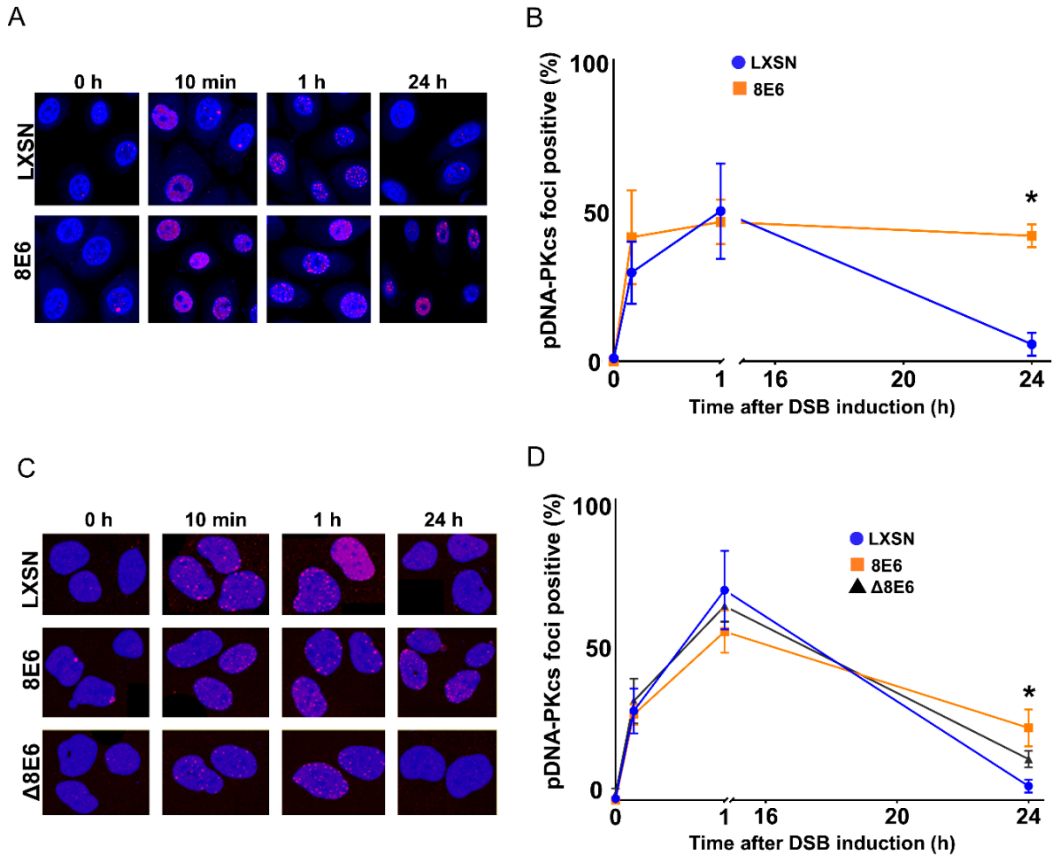

Figure 4. β-HPV 8E6 increases pDNA-PKcs foci persistence. Immunofluorescence microscopy was used to detect pDNA-PKcs foci in cells that were treated with Zeocin. (**A**) Representative images of pDNA-PKcs foci in HFK cell lines, following treatment with Zeocin for 10 min. (**B**) Percentage of pDNA-PKcs foci positive (> 2) cells following Zeocin exposure. (**C**) Representative images of pDNA-PKcs foci in U2OS cell lines treatment with Zeocin for 1 h, then harvested 0 h, 10 min, 1 h, and 24 h after Zeocin treatment. (**D**) Percentage of pDNA-PKcs foci positive (>4) U2OS cells following Zeocin exposure. All values are represented as mean ± standard error from at least three independent experiments. Statistical differences between groups were measured by using Student's *t*-test. * indicates $p < 0.05$. All microscopy images are 400X magnification.

To better understand the extent that NHEJ was impaired by β-HPV 8E6 hindered NHEJ, the ability of XRCC4 to localize to sites of damage was assessed. This occurs downstream of Artemis activation and is required for the DNA ligation step in NHEJ [49,61,62]. Like Artemis, XRCC4 is also a substrate of DNA-PKcs [27,28]. However, the role of that phosphorylation is poorly understood [63,64]. A study showed that DNA ligation fails without XRCC4, because it is required for LIG4 stabilization [65]. In HFK LXSN cells, Zeocin induced XRCC4 foci (detected by IF microscopy) and were readily resolved (Figure 5E,F). However, β-HPV 8E6 prevented an induction of XRCC4 foci in response to Zeocin. These results were repeated in U2OS cells (Figure 5G,H). Interestingly, U2OS β-HPV Δ8E6 also decreased XRCC4 recruitment, which may partially explain the p300-independent mechanism that β-HPV 8E6 diminishes NHEJ efficiency. Together, these data suggest that β-HPV 8E6 impairs XRCC4 recruitment to sites of damage.

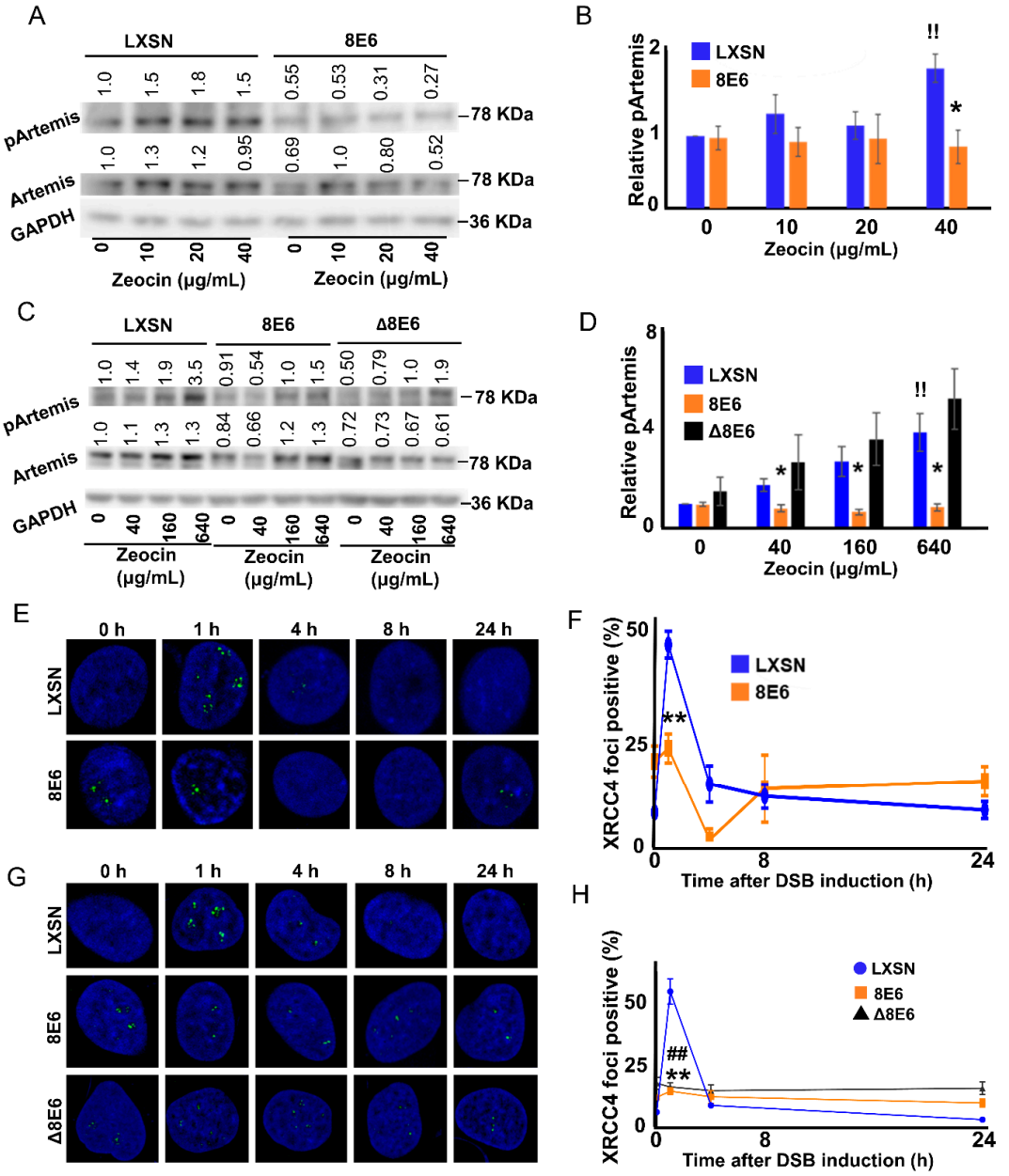

Figure 5. β-HPV 8E6 decreases pDNA-PKcs target proteins pArtemis abundance and XRCC4 foci formation. (**A**) Representative immunoblot showing pArtemis and total Artemis in HFK LXSN and HFK β-HPV 8 E6. (**B**) Densitometry of immunoblots (n = 4) of pArtemis normalized to total Artemis and to GAPDH as a loading control. (**C**) Representative immunoblot showing that pArtemis and total Artemis in U2OS LXSN, U2OS β-HPV 8 E6, or U2OS β-HPV Δ8 E6. (**D**) Densitometry of immunoblots (n = 4) of pArtemis normalized to total Artemis and to GAPDH as a loading control. (**E**) Representative images of XRCC4 foci in HFK cell lines 0–24 h following Zeocin exposure. (**F**) Percentages of XRCC4 foci positive (>2) HFK cells following DSB induction. (**G**) Representative images of XRCC4 foci in U2OS cell lines, 0–24 h following Zeocin exposure. All microscopy images are 400X magnification. (**H**) Percentages of XRCC4 foci positive (> 2) U2OS cells following DSB induction. All values are represented as mean ± standard error from at least three independent experiments. Statistical differences between groups were measured by using Student's t-test. * indicates $p < 0.05$. ** indicates $p < 0.01$. !! indicates significant difference between Zeocin treated and untreated group. ## indicates significant difference between U2OS β-HPV Δ8 E6 and control.

2.4. p300 is Required for Robust DNA-PKcs Signaling

The data above suggest that p300 is required for DNA-PKcs-dependent NHEJ. To confirm this relationship, NHEJ and DNA-PKcs signaling was assessed in previously described p300 competent (p300 WT) and p300 knockout (p300 KO) HCT116 cells [66]. p300 KO HCT116 cells were notably less capable of initiating and completing the pathway. Specifically, the CD4 reporter assay (described in Figure 1A) found reduced NHEJ in p300 KO HCT116 cells (Figure 6A,B). While p300 knockout did not change basal DNA-PKcs phosphorylation (Figure S8), immunoblots indicate that it hindered DNA-PKcs activation (pDNA-PKcs), following Zeocin exposure (Figure 6C,D, Figure S9A,B). Loss of p300 also increased pDNA-PKcs foci persistence (Figure 6E,F). Finally, p300 knockout attenuated Artemis phosphorylation in response to DSB induction (Figure 6G,H, Figure S9C,D). These data demonstrate p300's requirement in NHEJ and DNA-PKcs-dependent signaling.

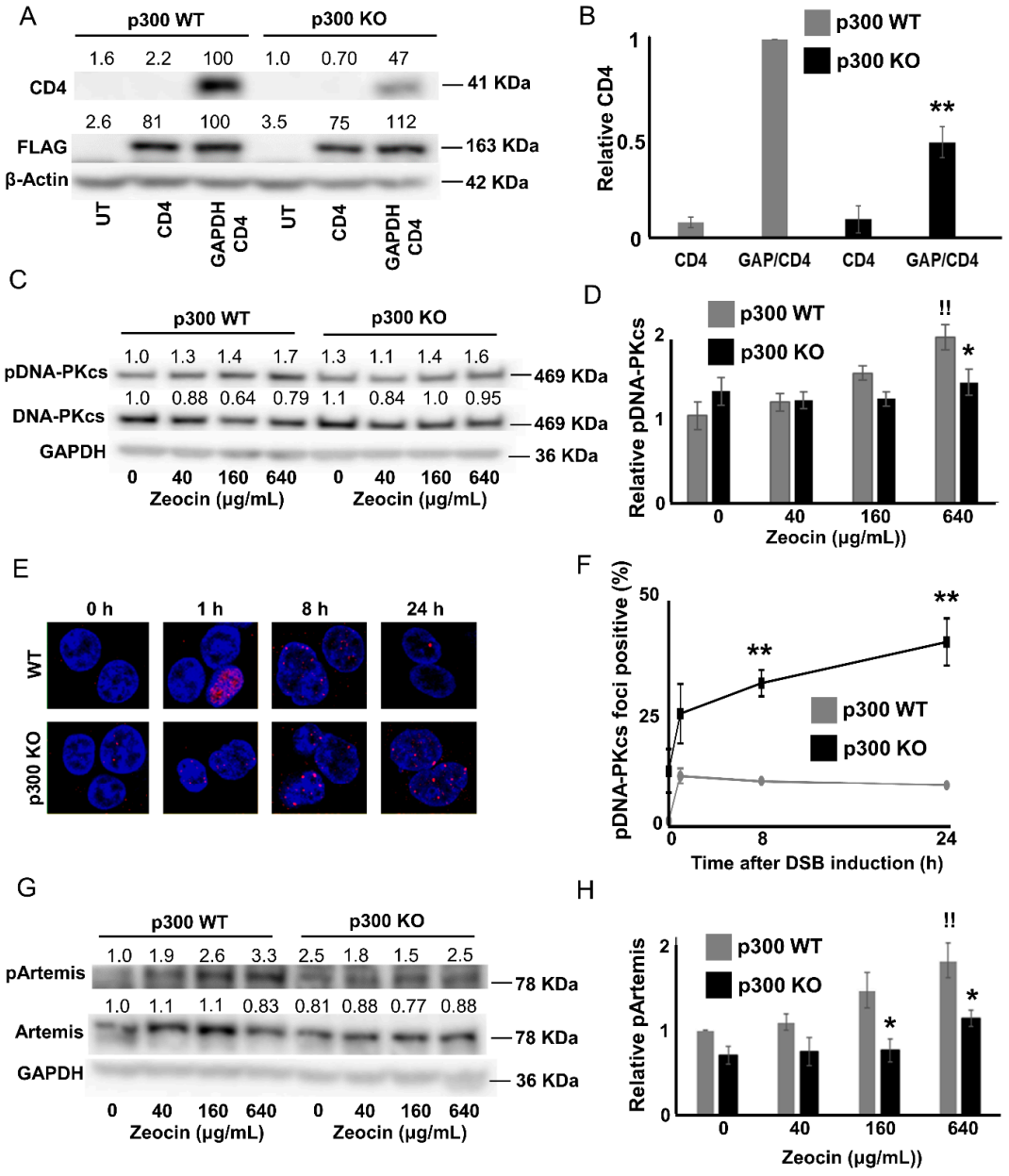

Figure 6. HCT116 P300 knockout decreases NHEJ efficiency. (**A**) Representative immunoblots showing CD4 expression in HCT116 p300 WT and HCT116 p300 KO after transfection with control (UT),

FLAG-tagged SgRNA-CAS9 targeting CD4 (CD4), and FLAG-tagged SgRNA-CAS9 targeting GAPDH and FLAG-tagged SgRNA-CAS9 targeting CD4 (GAP/CD4). (**B**) Densitometry of immunoblots (n = 3) from panel A. CD4 was normalized to β-actin as a loading control. Transfection efficiency was accounted for using FLAG abundance. (**C**) Representative images of immunoblot of pDNA-PKcs and total DNA-PKcs in HCT116 p300 WT and HCT116 p300 KO. (**D**) Densitometry of pDNA-PKcs normalized to total DNA-PKcs and GAPDH as a loading control. Data is shown relative to HCT116 WT control. (**E**) Representative images of pDNA-PKcs foci following Zeocin exposure. (**F**) Percentages of pDNA-PKcs foci positive (>2) HCT116 cells following Zeocin exposure. All microscopy images are 400X magnification. (**G**) Representative immunoblot of pArtemis and total Artemis of HCT116 cells. (**H**). Densitometry of immunoblots (n = 4) of pArtemis normalized to total Artemis, and to GAPDH as a loading control. All values are represented as mean ± standard error, from at least three independent experiments. Statistical differences between groups were measured by using Student's t-test. * indicates $p < 0.05$. ** indicates $p < 0.01$. !! indicates significant difference between Zeocin treated and untreated group.

3. Discussion

Because β-HPV 8E6 attenuated the repair of DSBs by HR [16], we initially hypothesized that this would make cells more likely to use the NHEJ pathway. NHEJ is prone to mutations, because it requires blunt ends as a substrate for repair. Typically, when NHEJ initiates, a Ku70/Ku80/DNA-PKcs trimer localizes to the lesion (Figure 7A). Once becoming activated via autophosphorylation, DNA-PKcs then promotes the pathway's progression via phosphorylating downstream repair components. The phosphorylation of Artemis leads to resection of any overhanging DNA. Finally, XRCC4, XLF and LIG4 form a trimer at the newly blunted ends and ligate them together, fixing the break [48,49,67]. This was not the case in cells expressing β-HPV 8E6 (Figure 7B). β-HPV 8E6 reduced DNA-PKcs autophosphorylation (Figure 2) and increased the persistence of DNA-PKcs localized to DNA damage (Figures 3 and 4). In turn, DNA-PKcs' phosphorylation of Artemis was reduced and XRCC4 was less able to form repair complexes in response to DSB-induction (Figure 5). A reporter assay confirmed that these defects resulted in a reduced ability to repair DSBs via NHEJ.

β-HPV 8E6 hinders NHEJ, at least in part, by binding and destabilizing p300. p300 functions as a transcription factor for repair gene expression [68,69]. By reducing p300 availability, β-HPV 8E6 lowers the abundance of at least four DNA repair factors (BRCA1, BRCA2, ATR, and ATM) [16–18]. This manifests in a limited ability to respond to UV damage, or to utilize the HR pathway. In contrast, p300 does not appear to be a transcription factor for canonical NHEJ genes (Figure S8). Nevertheless, p300 is clearly required for robust NHEJ (Figure 6). Specifically, p300 promotes DNA-PKcs activity. Although the specific mechanistic explanation for our observations are not fully resolved, a prior study showed that p300 is required for the recruitment of Ku70/80 [70]. This may explain our observations, as Ku70/80 form a holoenzyme with DNA-PKcs to facilitate DNA-PKcs-mediated phosphorylation. However, our data rule out the possibility that p300 is needed for DNA-PKcs to localize to sites of damage. Instead, in the absence of p300, DNA-PKcs repair complexes become more persistent. DNA-PKcs activity requires acetylation, but the histone acetyltransferase was not determined [71]. Perhaps p300 is responsible for the post-translational modification. Setting aside these unknowns, our data demonstrate that p300 is required for the completion rather than initiation of NHEJ. Interestingly, the NHEJ reporter assay indicates that β-HPV 8E6 also impairs NHEJ independently of p300 binding or reduced DNA-PKcs activity (Figure 1). Our data suggest a possible mechanism. β-HPV Δ8E6 retains the ability to hinder XRCC4 foci formation (Figure 5G,H) which would limit NHEJ independent of p300 destabilization. Furthermore, these data provide confirmation that the β-HPV Δ8E6 mutant retains some functionality.

The evidence provided here shows that β-HPV 8E6 diminishes essential NHEJ events, including DNA-PKcs phosphorylation at S2056. However, our efforts fall well short of resolving the role of β-HPV in NMSC development. Granted, the reduced DNA repair potential associated with β-HPV

8E6 would not be desirable in cutaneous tissue, as our skin protects against external mutagens. Supporting this assertion, previous studies have shown that pharmacological inhibition of DNA-PKcs increases mutagenesis [72]. Furthermore, DNA-PKcs inhibitors and DNA-PKcs inactivating mutations sensitize in vitro and animal models to radiation [43,73,74]. Given the importance of DNA-PKcs in protecting genome fidelity, β-HPV infections could increase mutations in skin cells after UV exposure. However, given the typically transient nature of β-HPV infections, the increased mutational burden may not be particularly consequential. Furthermore, others have suggested that β-HPV infections prime the immune system, helping to prevent NMSCs [15]. These positions are not mutually exclusive, and should not be interpreted as being in conflict. Perhaps the oncogenic consequences of β-HPV associated repair inhibition are limited to specific circumstances (e.g., immune suppression). One other difference in the two studies is that Strickley and colleagues used a mouse papillomavirus that does not bind p300 [75].

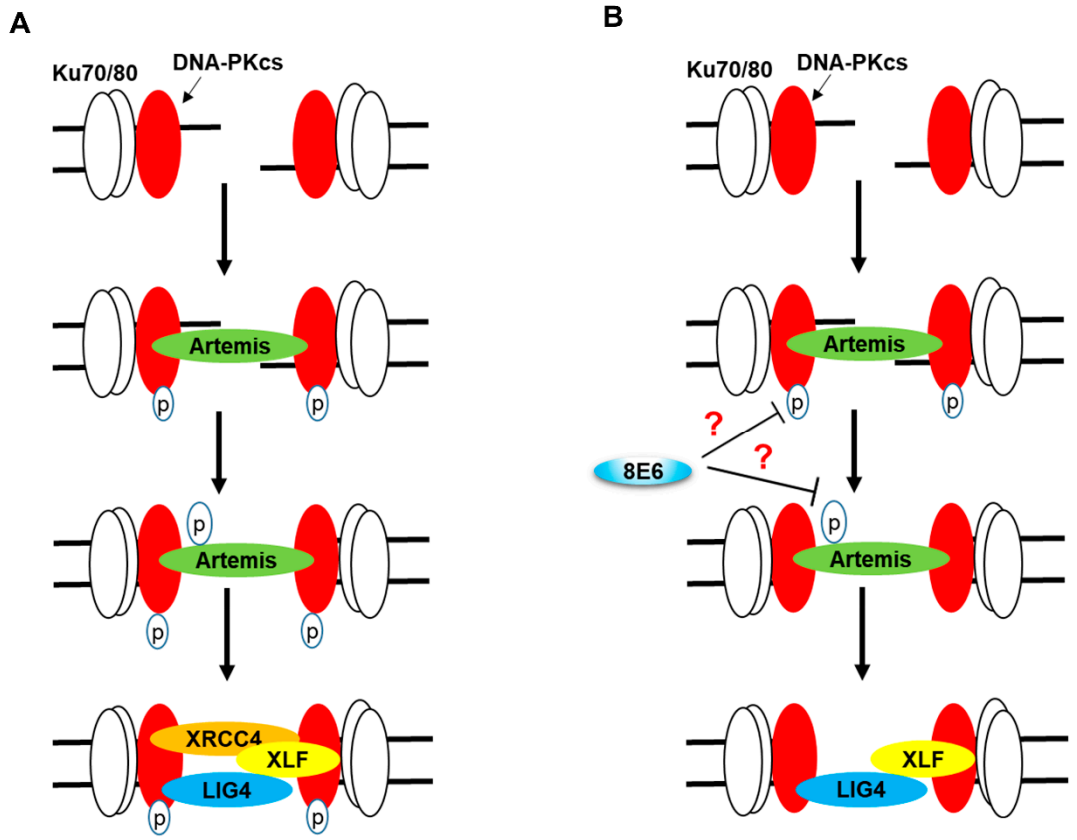

Figure 7. NHEJ in Cells with and without β-HPV 8E6. (**A**) Schematic of canonical NHEJ pathway. DNA-PK holoenzyme (Ku70/80/DNA-PKcs) binds to DSB, leading to DNA-PKcs autophosphorylation. Activated DNA-PK leads to Artemis phosphorylation and DNA end processing. Finally, the XRCC4/XLF/LIG complex repairs the break. (**B**) Schematic of β-HPV 8E6 alterations in canonical NHEJ. β-HPV 8E6 hinders DNA-PKcs autophosphorylation and activation, by which downstream steps, including Artemis phosphorylation and XRCC4 recruitment, were diminished. "?" represents unknown mechanism.

Accumulating evidence shows that β-HPV E6 increases the mutagenic potential of UV. This includes increasing the frequency with which UV causes DSBs and hindering repair of these deleterious lesions. Both error-free HR and error-prone NHEJ are impaired when β-HPV 8E6 is expressed. However, β-HPV 8E6 does not appear to limit their initiation, as evidenced by the formation of both RAD51 [16] and pDNA-PKcs repair complexes (Figure 4). If the initiation of NHEJ and HR were to occur at the same DSB, it would be problematic, as the two pathways are intrinsically incompatible.

HR begins by generating a large single-stranded DNA overhang, while NHEJ starts by removing any overhangs. This could result in large deletions, as repair osculates between the two DSB repair pathways. Furthermore, despite attenuated HR and NHEJ, β-HPV 8E6 expressing cells eventually resolve most DSBs. This suggests that β-HPV 8E6 could force DSB repair, to occur by a less efficient and/or more mutagenic pathway. Our future directions include defining the dominant mechanisms of DSB repair in cells expressing β-HPV 8E6, and determining the mutagenic consequences of β-HPV 8E6 on DSB repair.

4. Materials and Methods

4.1. Cell Culture and Reagents

Immortalized human foreskin keratinocytes (HFK), provided by Michael Underbrink (University of Texas Medical Branch, Galveston, TX, USA), were grown in EpiLife medium (Gibco, Gaithersburg, MD, USA), supplemented with 60 μM calcium chloride (Gibco), human keratinocyte growth supplement (Gibco), and 1% penicillin-streptomycin (Caisson, Smithfield, UT, USA). U2OS and HCT116 cells were maintained in DMEM supplemented with 10% FBS and 1% penicillin-streptomycin. Zeocin (Alfa Aesar, Ward Hill, MA, USA) and H2O2 were used to induce DSBs. NU7441 (Selleckchem) was used to inhibit DNA-PKcs phosphorylation. KU55933 (Selleckchem, Houston, TX, USA) was used to inhibit ATM kinase activity.

4.2. Immunoblotting

After being washed with ice-cold PBS, cells were lysed with RIPA Lysis Buffer (VWR Life Science, Philadelphia, PA, USA), supplemented with Phosphatase Inhibitor Cocktail 2 (Sigma, St. Louis, MO, USA) and Protease Inhibitor Cocktail (Bimake, Houston, TX, USA). The Pierce BCA Protein Assay Kit (Thermo Scientific, Waltham, MA, USA) was used to determine protein concentration. Equal protein lysates were run on Novex 3–8% Tris-acetate 15 Well Mini Gels (Invitrogen, Carlsbad, CA, USA) and transferred to Immobilon-P membranes (Millipore, Burlington, MA, USA). Membranes were then probed with the following primary antibodies: GAPDH (Santa Cruz Biotechnologies, Dallas, TX, USA), DNA-PKcs (abcam, Cambridge, UK), phospho DNA-PKcs S2056 (abcam), Artemis (abcam), phospho Artemis S516 (abcam), XRCC4 (Santa Cruz Biotechnologies), Ligase IV (abcam), CD4 (abcam), and DYKDDDDK (FLAG) Tag (Invitrogen). After exposure to the matching HRP-conjugated secondary antibody, cells were visualized using SuperSignal West Femto Maximum Sensitivity Substrate (Thermo Scientific).

4.3. Immunofluorescence Microscopy

Cells were seeded onto either 96-well glass-bottom plates (Cellvis) or coverslips, and grown overnight. Cells treated with Zeocin for specified time and concentration were fixed with 4% formaldehyde. Then, 0.1% Triton-X solution in PBS was used to permeabilize the cells, followed by blocking with 3% bovine serum albumin in PBS for 30 minutes. Cells were then incubated with the following antibodies: phospho DNA-PKcs S2056 (abcam), XRCC4 (Santa Cruz Biotechnology). The cells were washed and stained with the appropriate secondary antibodies: Alexa Fluor 594 goat anti-rabbit (Thermo Scientific A11012), Alexa Fluor 488 goat anti-mouse (Thermo Scientific A11001). After washing, the cells were stained with 30 μM DAPI in PBS, and visualized with the Zeiss LSM 770 microscope. Images were analyzed using the ImageJ techniques previously described [3].

4.4. End Joining Reporter Assay

The reporter assay used a previously described protocol [38], with the following modifications. Cells were seeded into 6-well plates. After transfection, CD4 expression was measured by immunoblotting.

4.5. Statistical Analysis

All values are represented as mean ± standard error (SE) from at least three independent experiments. Statistical differences between groups were measured by using Student's *t*-test. *p*-values in all experiments were considered significant, at less than 0.05.

5. Conclusions

Accumulating evidence shows that β-HPV 8E6 reduces genome stability by disrupting DNA damage response. Particularly, β-HPV 8E6 disrupts homologous recombination, which is a major DSB repair pathway in the S phase and G2 phase of the cell cycle. The data presented here show that β-HPV 8E6 diminishes NHEJ, which can occur throughout the cell cycle. This expands β-HPV 8E6's influence over DSB repair throughout the cell cycle. Finally, this work demonstrates that β-HPV 8E6 uses p300-dependent and p300-independent mechanisms to disrupt DNA repair. This suggests that there are considerable evolutionary forces driving β-HPV to hinder cellular responses to damaged DNA.

Supplementary Materials: The following are available online at http://www.mdpi.com/2072-6694/12/9/2356/s1, Figure S1: Transfection efficiency represented by FLAG tagged SgRNA-CAS9 targeting CD4 and GAPDH, Figure S2: β-HPV 8 E6 does not decrease NHEJ protein in untreated cells, Figure S3: pDNA-PKcs and total DNA-PKcs normalized to GAPDH in HFK and U2OS, Figure S4: β-HPV 8 E6 decreases H_2O_2 induced DNA-PKcs phosphorylation, Figure S5: Total DNA-PKcs shows pan-nuclear expression in HFK cells, Figure S6: Inhibiting DNA-PK decreases Artemis phosphorylation, Figure S7: pArtemis and total Artemis normalized to GAPDH in HFK and U2OS cells, Figure S8: p300 knockout does not decrease major NHEJ proteins in untreated cells, Figure S9: pDNA-PKcs, total DNA-PKcs, pArtemis, and total Artemis normalized to GAPDH in HCT cells.

Author Contributions: Conceptualization, N.A.W.; methodology, C.H., M.G.; software, C.H.; validation, C.H., T.B.; investigation, C.H., M.G., T.B.; resources, N.A.W.; writing—original draft preparation, C.H., N.A.W.; writing—review and editing, C.H., T.B., N.A.W.; visualization, C.H.; supervision, N.A.W.; funding acquisition, N.A.W. All authors have read and agreed to the published version of the manuscript.

Funding: This study is funded by the U.S. Department of Defense (CMDRP PRCRP CA160224 (NW)) and Kansas State University Johnson Cancer Research Center.

Acknowledgments: We appreciate KSU-CVM Confocal Core for our immunofluorescence microscopy, Michael Underbrink for providing the TERT-immortalized HFKs, and Jeremy M. Stark for providing plasmids of the end-joining reporter assay.

Conflicts of Interest: The authors declare no conflict of interest.

References

1. Bzhalava, D.; Mühr, L.S.A.; Lagheden, C.; Ekström, J.; Forslund, O.; Dillner, J.; Hultin, E. Deep sequencing extends the diversity of human papillomaviruses in human skin. *Sci. Rep.* **2015**, *4*. [CrossRef] [PubMed]
2. Cubie, H.A. Diseases associated with human papillomavirus infection. *Virology* **2013**, *445*, 21–34. [CrossRef] [PubMed]
3. Wendel, S.O.; Wallace, N.A. Loss of Genome Fidelity: Beta HPVs and the DNA Damage Response. *Front. Microbiol.* **2017**, *8*. [CrossRef] [PubMed]
4. Doorbar, J.; Egawa, N.; Griffin, H.; Kranjec, C.; Murakami, I. Human papillomavirus molecular biology and disease association: Human papillomavirus. *Rev. Med. Virol.* **2015**, *25*, 2–23. [CrossRef]
5. Pfister, H.; Nürnberger, F.; Gissmann, L.; Hausen, H.Z. Characterization of a human papillomavirus from epidermodysplasia verruciformis lesions of a patient from upper-volta. *Int. J. Cancer* **1981**, *27*, 645–650. [CrossRef]
6. Mudigonda, T.; Pearce, D.J.; Yentzer, B.A.; Williford, P.; Feldman, S.R. The Economic Impact of Non-Melanoma Skin Cancer: A review. *J. Natl. Compr. Canc. Netw.* **2010**, *8*, 888–896. [CrossRef]
7. Kremsdorf, D.; Jablonska, S.; Favre, M.; Orth, G. Biochemical characterization of two types of human papillomaviruses associated with epidermodysplasia verruciformis. *J. Virol.* **1982**, *43*, 436–447. [CrossRef]
8. Rollison, D.E.; Viarisio, D.; Amorrortu, R.P.; Gheit, T.; Tommasino, M. An Emerging Issue in Oncogenic Virology: The Role of Beta Human Papillomavirus Types in the Development of Cutaneous Squamous Cell Carcinoma. *J. Virol.* **2019**, *93*. [CrossRef]

9. White, E.A.; Walther, J.; Javanbakht, H.; Howley, P.M. Genus Beta Human Papillomavirus E6 Proteins Vary in Their Effects on the Transactivation of p53 Target Genes. *J. Virol.* **2014**, *88*, 8201–8212. [CrossRef]
10. Howley, P.M.; Pfister, H.J. Beta Genus Papillomaviruses and Skin Cancer. *Virology* **2015**, 290–296. [CrossRef]
11. Shanmugasundaram, S.; You, J. Targeting Persistent Human Papillomavirus Infection. *Viruses* **2017**, *9*, 229. [CrossRef] [PubMed]
12. 1Tommasino, M. HPV and skin carcinogenesis. *Papillomavirus Res.* **2019**, *7*, 129–131. [CrossRef] [PubMed]
13. Viarisio, D.; Müller-Decker, K.; Accardi, R.; Robitaille, A.; Dürst, M.; Beer, K.; Jansen, L.; Flechtenmacher, C.; Bozza, M.; Harbottle, R.; et al. Beta HPV38 oncoproteins act with a hit-and-run mechanism in ultraviolet radiation-induced skin carcinogenesis in mice. *PLoS Pathog.* **2018**, *14*. [CrossRef] [PubMed]
14. Hufbauer, M.; Akgül, B. Molecular Mechanisms of Human Papillomavirus Induced Skin Carcinogenesis. *Viruses* **2017**, *9*, 187. [CrossRef] [PubMed]
15. Strickley, J.D.; Messerschmidt, J.L.; Awad, M.E.; Li, T.; Hasegawa, T.; Ha, D.T.; Nabeta, H.W.; Bevins, P.A.; Ngo, K.H.; Asgari, M.M.; et al. Immunity to commensal papillomaviruses protects against skin cancer. *Nature* **2019**, *575*, 519–522. [CrossRef]
16. Wallace, N.A.; Robinson, K.; Howie, H.L.; Galloway, D.A. β-HPV 5 and 8 E6 Disrupt Homology Dependent Double Strand Break Repair by Attenuating BRCA1 and BRCA2 Expression and Foci Formation. *PLoS Pathog.* **2015**, *11*, e1004687. [CrossRef]
17. Wallace, N.A.; Gasior, S.L.; Faber, Z.J.; Howie, H.L.; Deininger, P.L.; Galloway, D.A. HPV 5 and 8 E6 expression reduces ATM protein levels and attenuates LINE-1 retrotransposition. *Virology* **2013**, *443*, 69–79. [CrossRef]
18. Wallace, N.A.; Robinson, K.; Howie, H.L.; Galloway, D.A. HPV 5 and 8 E6 Abrogate ATR Activity Resulting in Increased Persistence of UVB Induced DNA Damage. *PLoS Pathog.* **2012**, *8*, e1002807. [CrossRef]
19. Snow, J.A.; Murthy, V.; Dacus, D.; Hu, C.; Wallace, N.A. β-HPV 8E6 Attenuates ATM and ATR Signaling in Response to UV Damage. *Pathogens* **2019**. [CrossRef]
20. Howie, H.L.; Koop, J.I.; Weese, J.; Robinson, K.; Wipf, G.; Kim, L.; Galloway, D.A. Beta-HPV 5 and 8 E6 Promote p300 Degradation by Blocking AKT/p300 Association. *PLoS Pathog.* **2011**, *7*, e1002211. [CrossRef]
21. Ceccaldi, R.; Rondinelli, B.; D'Andrea, A.D. Repair Pathway Choices and Consequences at the Double-Strand Break. *Trends Cell Biol.* **2016**, *26*, 52–64. [CrossRef]
22. Ahmed, K.M.; Pandita, R.K.; Singh, D.K.; Hunt, C.R.; Pandita, T.K. β1-Integrin Impacts Rad51 Stability and DNA Double-Strand Break Repair by Homologous Recombination. *Mol. Cell Biol.* **2018**, *38*. [CrossRef]
23. Pierce, A.J.; Johnson, R.D.; Thompson, L.H.; Jasin, M. XRCC3 promotes homology-directed repair of DNA damage in mammalian cells. *Genes Dev.* **1999**, *13*, 2633–2638. [CrossRef]
24. Bakr, A.; Oing, C.; Köcher, S.; Borgmann, K.; Dornreiter, I.; Petersen, C.; Dikomey, E.; Mansour, W.Y. Involvement of ATM in homologous recombination after end resection and RAD51 nucleofilament formation. *Nucleic Acids Res.* **2015**, *43*, 3154–3166. [CrossRef]
25. Schwartz, M.; Zlotorynski, E.; Goldberg, M.; Ozeri, E.; Rahat, A.; le Sage, C.; Chen, B.P.C.; Chen, D.J.; Agami, R.; Kerem, B. Homologous recombination and nonhomologous end-joining repair pathways regulate fragile site stability. *Genes Dev.* **2005**, *19*, 2715–2726. [CrossRef]
26. Lieber, M.R. The Mechanism of Double-Strand DNA Break Repair by the Nonhomologous DNA End Joining Pathway. *Annu. Rev. Biochem.* **2010**, *79*, 181–211. [CrossRef]
27. Weterings, E.; van Gent, D.C. The mechanism of non-homologous end-joining: A synopsis of synapsis. *DNA Repair* **2004**, *3*, 1425–1435. [CrossRef]
28. Bhargava, R.; Lopezcolorado, F.W.; Tsai, L.J.; Stark, J.M. The canonical non-homologous end joining factor XLF promotes chromosomal deletion rearrangements in human cells. *J. Biol. Chem.* **2020**, *295*, 125–137. [CrossRef]
29. Zhang, Y.; Hefferin, M.L.; Chen, L.; Shim, E.Y.; Tseng, H.-M.; Kwon, Y.; Sung, P.; Lee, S.E.; Tomkinson, A.E. Role of Dnl4-Lif1 in nonhomologous end-joining repair complex assembly and suppression of homologous recombination. *Nat. Struct. Mol. Biol.* **2007**, *14*, 639–646. [CrossRef]
30. Patel, A.G.; Sarkaria, J.N.; Kaufmann, S.H. Nonhomologous end joining drives poly(ADP-ribose) polymerase (PARP) inhibitor lethality in homologous recombination-deficient cells. *PNAS* **2011**, *108*, 3406–3411. [CrossRef]
31. Gunn, A.; Bennardo, N.; Cheng, A.; Stark, J.M. Correct End Use during End Joining of Multiple Chromosomal Double Strand Breaks Is Influenced by Repair Protein RAD50, DNA-dependent Protein Kinase DNA-PKcs, and Transcription Context. *J. Biol. Chem.* **2011**, *286*, 42470–42482. [CrossRef]

32. Gupta, A.; Hunt, C.R.; Chakraborty, S.; Pandita, R.K.; Yordy, J.; Ramnarain, D.B.; Horikoshi, N.; Pandita, T.K. Role of 53BP1 in the Regulation of DNA Double-Strand Break Repair Pathway Choice. *Radiat. Res.* **2014**, *181*, 1–8. [CrossRef]
33. A Chromatin-Based Signalling Mechanism Directs the Switch from Mutagenic to Error-Free Repair of DNA Double Strand Breaks: Molecular & Cellular Oncology. Available online: https://www.tandfonline.com/doi/full/10.1080/23723556.2019.1605820 (accessed on 27 November 2019).
34. Sollazzo, A.; Brzozowska, B.; Cheng, L.; Lundholm, L.; Scherthan, H.; Wojcik, A. Live Dynamics of 53BP1 Foci Following Simultaneous Induction of Clustered and Dispersed DNA Damage in U2OS Cells. *Int. J. Mol. Sci.* **2018**, *19*, 519. [CrossRef]
35. Daley, J.M.; Sung, P. 53BP1, BRCA1, and the Choice between Recombination and End Joining at DNA Double-Strand Breaks. *Mol. Cell. Biol.* **2014**, *34*, 1380–1388. [CrossRef]
36. Dimitrova, N.; Chen, Y.-C.M.; Spector, D.L.; de Lange, T. 53BP1 promotes non-homologous end joining of telomeres by increasing chromatin mobility. *Nature* **2008**, *456*, 524–528. [CrossRef]
37. Bunting, S.F.; Callén, E.; Wong, N.; Chen, H.-T.; Polato, F.; Gunn, A.; Bothmer, A.; Feldhahn, N.; Fernandez-Capetillo, O.; Cao, L.; et al. 53BP1 Inhibits Homologous Recombination in Brca1-Deficient Cells by Blocking Resection of DNA Breaks. *Cell* **2010**, *141*, 243–254. [CrossRef]
38. Zhen, Y.; Li, S.; Zhu, Y.; Wang, X.; Zhou, X.; Zhu, L. Identification of DNA-PKcs as a primary resistance factor of salinomycin in osteosarcoma cells. *Oncotarget* **2016**, *7*, 79417–79427. [CrossRef]
39. Jiang, W.; Crowe, J.L.; Liu, X.; Nakajima, S.; Wang, Y.; Li, C.; Lee, B.J.; Dubois, R.L.; Liu, C.; Yu, X.; et al. Differential phosphorylation of DNA-PKcs regulates the interplay between end-processing and end-ligation during non-homologous end-joining. *Mol. Cell* **2015**, *58*, 172–185. [CrossRef]
40. Uematsu, N.; Weterings, E.; Yano, K.; Morotomi-Yano, K.; Jakob, B.; Taucher-Scholz, G.; Mari, P.-O.; van Gent, D.C.; Chen, B.P.C.; Chen, D.J. Autophosphorylation of DNA-PKCS regulates its dynamics at DNA double-strand breaks. *J. Cell Biol.* **2007**, *177*, 219–229. [CrossRef]
41. Smith, G.C.M.; Jackson, S.P. The DNA-dependent protein kinase. *Genes Dev.* **1999**, *13*, 916–934. [CrossRef]
42. Veuger, S.J.; Curtin, N.J.; Richardson, C.J.; Smith, G.C.M.; Durkacz, B.W. Radiosensitization and DNA Repair Inhibition by the Combined Use of Novel Inhibitors of DNA-dependent Protein Kinase and Poly(ADP-Ribose) Polymerase-1. *Cancer Res.* **2003**, *63*, 6008–6015.
43. Zhao, Y.; Thomas, H.D.; Batey, M.A.; Cowell, I.G.; Richardson, C.J.; Griffin, R.J.; Calvert, A.H.; Newell, D.R.; Smith, G.C.M.; Curtin, N.J. Preclinical Evaluation of a Potent Novel DNA-Dependent Protein Kinase Inhibitor NU7441. *Cancer Res.* **2006**, *66*, 5354–5362. [CrossRef]
44. Mamo, T.; Mladek, A.C.; Shogren, K.L.; Gustafson, C.; Gupta, S.K.; Riester, S.M.; Maran, A.; Galindo, M.; van Wijnen, A.J.; Sarkaria, J.N.; et al. Inhibiting DNA-PKCS Radiosensitizes Human Osteosarcoma Cells. *Biochem. Biophys. Res. Commun.* **2017**, *486*, 307–313. [CrossRef]
45. Beucher, A.; Birraux, J.; Tchouandong, L.; Barton, O.; Shibata, A.; Conrad, S.; Goodarzi, A.A.; Krempler, A.; Jeggo, P.A.; Löbrich, M. ATM and Artemis promote homologous recombination of radiation-induced DNA double-strand breaks in G2. *EMBO J.* **2009**, *28*, 3413–3427. [CrossRef]
46. Soubeyrand, S.; Pope, L.; De Chasseval, R.; Gosselin, D.; Dong, F.; de Villartay, J.-P.; Haché, R.J.G. Artemis phosphorylated by DNA-dependent protein kinase associates preferentially with discrete regions of chromatin. *J. Mol. Biol.* **2006**, *358*, 1200–1211. [CrossRef]
47. Li, S.; Chang, H.H.; Niewolik, D.; Hedrick, M.P.; Pinkerton, A.B.; Hassig, C.A.; Schwarz, K.; Lieber, M.R. Evidence That the DNA Endonuclease ARTEMIS also Has Intrinsic 5′-Exonuclease Activity. *J. Biol. Chem.* **2014**, *289*, 7825–7834. [CrossRef]
48. Mari, P.-O.; Florea, B.I.; Persengiev, S.P.; Verkaik, N.S.; Bruggenwirth, H.T.; Modesti, M.; Giglia-Mari, G.; Bezstarosti, K.; Demmers, J.A.A.; Luider, T.M.; et al. Dynamic assembly of end-joining complexes requires interaction between Ku70/80 and XRCC4. *Proc. Natl. Acad. Sci. USA* **2006**, *103*, 18597–18602. [CrossRef]
49. Normanno, D.; Négrel, A.; de Melo, A.J.; Betzi, S.; Meek, K.; Modesti, M. Mutational phospho-mimicry reveals a regulatory role for the XRCC4 and XLF C-terminal tails in modulating DNA bridging during classical non-homologous end joining. *ELife* **2017**, *6*, e22900. [CrossRef]
50. Hustedt, N.; Durocher, D. The control of DNA repair by the cell cycle. *Nat. Cell Biol.* **2017**, *19*, 1–9. [CrossRef]
51. Heyer, W.-D.; Ehmsen, K.T.; Liu, J. Regulation of homologous recombination in eukaryotes. *Annu. Rev. Genet.* **2010**, *44*, 113–139. [CrossRef]

52. Salmon, P.; Giovane, A.; Wasylyk, B.; Klatzmann, D. Characterization of the human CD4 gene promoter: Transcription from the CD4 gene core promoter is tissue-specific and is activated by Ets proteins. *Proc. Natl. Acad. Sci. USA* **1993**, *90*, 7739–7743. [CrossRef] [PubMed]
53. Underbrink, M.P.; Howie, H.L.; Bedard, K.M.; Koop, J.I.; Galloway, D.A. E6 proteins from multiple human betapapillomavirus types degrade Bak and protect keratinocytes from apoptosis after UVB irradiation. *J. Virol.* **2008**, *82*, 10408–10417. [CrossRef] [PubMed]
54. Delacôte, F.; Deriano, L.; Lambert, S.; Bertrand, P.; Saintigny, Y.; Lopez, B.S. Chronic exposure to sublethal doses of radiation mimetic ZeocinTM selects for clones deficient in homologous recombination. *Mutat. Res. Fundam. Mol. Mech. Mutagenesis* **2007**, *615*, 125–133. [CrossRef] [PubMed]
55. Tsukuda, M.; Miyazaki, K. DNA fragmentation caused by an overdose of Zeocin. *J. Biosci. Bioeng.* **2013**, *116*, 644–646. [CrossRef]
56. Davis, A.J.; Chi, L.; So, S.; Lee, K.-J.; Mori, E.; Fattah, K.; Yang, J.; Chen, D.J. BRCA1 modulates the autophosphorylation status of DNA-PKcs in S phase of the cell cycle. *Nucleic Acids Res.* **2014**, *42*, 11487–11501. [CrossRef]
57. Greinert, R.; Volkmer, B.; Henning, S.; Breitbart, E.W.; Greulich, K.O.; Cardoso, M.C.; Rapp, A. UVA-induced DNA double-strand breaks result from the repair of clustered oxidative DNA damages. *Nucleic Acids Res.* **2012**, *40*, 10263–10273. [CrossRef]
58. Lee, C.-S.; Lee, K.; Legube, G.; Haber, J.E. Dynamics of yeast histone H2A and H2B phosphorylation in response to a double-strand break. *Nat. Struct. Mol. Biol.* **2014**, *21*, 103–109. [CrossRef]
59. Polo, S.E.; Jackson, S.P. Dynamics of DNA damage response proteins at DNA breaks: A focus on protein modifications. *Genes Dev.* **2011**, *25*, 409–433. [CrossRef]
60. Murthy, V.; Dacus, D.; Gamez, M.; Hu, C.; Wendel, S.O.; Snow, J.; Kahn, A.; Walterhouse, S.H.; Wallace, N.A. Characterizing DNA Repair Processes at Transient and Long-lasting Double-strand DNA Breaks by Immunofluorescence Microscopy. *J. Vis. Exp.* **2018**, e57653. [CrossRef]
61. Drouet, J.; Delteil, C.; Lefrançois, J.; Concannon, P.; Salles, B.; Calsou, P. DNA-dependent Protein Kinase and XRCC4-DNA Ligase IV Mobilization in the Cell in Response to DNA Double Strand Breaks. *J. Biol. Chem.* **2005**, *280*, 7060–7069. [CrossRef]
62. Koike, M.; Yutoku, Y.; Koike, A. Cloning, localization and focus formation at DNA damage sites of canine XRCC4. *J. Vet. Med. Sci.* **2016**, *78*, 1865–1871. [CrossRef] [PubMed]
63. Collis, S.J.; DeWeese, T.L.; Jeggo, P.A.; Parker, A.R. The life and death of DNA-PK. *Oncogene* **2005**, *24*, 949–961. [CrossRef] [PubMed]
64. Davis, A.J.; Chen, B.P.C.; Chen, D.J. DNA-PK: A dynamic enzyme in a versatile DSB repair pathway. *DNA Repair* **2014**, *17*, 21–29. [CrossRef] [PubMed]
65. Ghezraoui, H.; Piganeau, M.; Renouf, B.; Renaud, J.-B.; Sallmyr, A.; Ruis, B.; Oh, S.; Tomkinson, A.; Hendrickson, E.A.; Giovannangeli, C.; et al. Chromosomal translocations in human cells are generated by canonical nonhomologous end-joining. *Mol. Cell* **2014**, *55*, 829–842. [CrossRef] [PubMed]
66. Iyer, N.G.; Chin, S.-F.; Ozdag, H.; Daigo, Y.; Hu, D.-E.; Cariati, M.; Brindle, K.; Aparicio, S.; Caldas, C. p300 regulates p53-dependent apoptosis after DNA damage in colorectal cancer cells by modulation of PUMA/p21 levels. *Proc. Natl. Acad. Sci. USA* **2004**, *101*, 7386–7391. [CrossRef] [PubMed]
67. Francis, D.B.; Kozlov, M.; Chavez, J.; Chu, J.; Malu, S.; Hanna, M.; Cortes, P. DNA Ligase IV regulates XRCC4 nuclear localization. *DNA Repair* **2014**, *21*, 36–42. [CrossRef]
68. Goodman, R.H.; Smolik, S. CBP/p300 in cell growth, transformation, and development. *Genes Dev.* **2000**, *14*, 1553–1577. [CrossRef]
69. Chen, J.; Halappanavar, S.S.; St-Germain, J.R.; Tsang, B.K.; Li, Q. Role of Akt/protein kinase B in the activity of transcriptional coactivator p300. *Cell. Mol. Life Sci.* **2004**, *61*, 1675–1683. [CrossRef]
70. Ogiwara, H.; Ui, A.; Otsuka, A.; Satoh, H.; Yokomi, I.; Nakajima, S.; Yasui, A.; Yokota, J.; Kohno, T. Histone acetylation by CBP and p300 at double-strand break sites facilitates SWI/SNF chromatin remodeling and the recruitment of non-homologous end joining factors. *Oncogene* **2011**, *30*, 2135–2146. [CrossRef]
71. Mori, E.; Davis, A.J.; Hasegawa, M.; Chen, D.J. Lysines 3241 and 3260 of DNA-PKcs are important for genomic stability and radioresistance. *Biochem. Biophys. Res. Commun.* **2016**, *477*, 235–240. [CrossRef]
72. Jette, N.; Lees-Miller, S.P. The DNA-dependent protein kinase: A multifunctional protein kinase with roles in DNA double strand break repair and mitosis. *Prog. Biophys. Mol. Biol.* **2015**, *117*, 194–205. [CrossRef] [PubMed]

73. Eccles, L.J.; Bell, A.C.; Powell, S.N. Inhibition of non-homologous end joining in Fanconi Anemia cells results in rescue of survival after interstrand crosslinks but sensitization to replication associated double-strand breaks. *DNA Repair* **2018**, *64*, 1–9. [CrossRef] [PubMed]
74. Dong, J.; Zhang, T.; Ren, Y.; Wang, Z.; Ling, C.C.; He, F.; Li, G.C.; Wang, C.; Wen, B. Inhibiting DNA-PKcs in a non-homologous end-joining pathway in response to DNA double-strand breaks. *Oncotarget* **2017**, *8*, 22662–22673. [CrossRef] [PubMed]
75. Meyers, J.M.; Uberoi, A.; Grace, M.; Lambert, P.F.; Munger, K. Cutaneous HPV8 and MmuPV1 E6 Proteins Target the NOTCH and TGF-β Tumor Suppressors to Inhibit Differentiation and Sustain Keratinocyte Proliferation. *PLoS Pathog.* **2017**, *13*, e1006171. [CrossRef] [PubMed]